Synthesis and Characterization of Hydrophobic-Hydrophilic Multiblock Copolymers for Proton Exchange Membrane Applications

Yu Chen

Dissertation submitted to the faculty of the Virginia Polytechnic Institute and State University in partial fulfillment of the requirements for the degree of

Doctor of Philosophy

in

Macromolecular Science and Engineering

James E. McGrath, Committee Chair
Judy S. Riffle
Alan R. Esker
Richey M. Davis
Timothy E. Long

September 9, 2011

Blacksburg, VA

Keywords: proton exchange membrane, fuel cell, hydrophobic-hydrophilic, multiblock copolymers, disulfonated poly(arylene ether sulfone), partially fluorinated, semi-crystalline

Synthesis and Characterization of Hydrophobic-Hydrophilic Multiblock Copolymers for Proton Exchange Membrane Applications

Yu Chen

ABSTRACT

Proton exchange membrane fuel cells (PEMFCs) have been extensively studied as clean, sustainable and efficient power sources for electric vehicles, and portable and residential power sources. As one of the key components in PEMFC system, proton exchange membranes (PEMs) act as the electrolyte that transfers protons from the anode to the cathode. The state-of-art commercial PEM materials are typically based on perfluorinated sulfonic acid containing ionomers (PFSAs), represented by DuPont's Nafion®. Despite their good chemical stability and proton conductivity at high relative humidity (RH) and low temperature, several major drawbacks have been observed on PFSAs, such as high cost, high fuel permeability, insufficient thermo-mechanical properties above 80℃, and low proton conductivity at low RH levels. Therefore the challenge lies in developing alternative PEMs which feature associated ionic domains at low hydration levels. Nanophase separated hydrophilic-hydrophobic block copolymer ionomers are believed to be desirable for this purpose

Three series of hydrophobic/hydrophillic, partially fluorinated/sulfonated multiblock copolymers were synthesized and characterized in this thesis. The hydrophilic blocks were based upon the nucleophilic step polymerization of 3, 3′-disulfonated, 4, 4′-dichlorodiphenyl sulfone (SDCDPS) with an excess 4, 4′-biphenol (BP) to afford phenoxide endgroups. The partially fluorinated hydrophobic blocks were largely based on 4, 4′-hexafluoroisopropylidenediphenol (6F-BPA) and various difluoro monomers (excess). These copolymers were obtained through moderate temperature (~130-150 ℃) coupling reactions, which minimize the ether-ether interchanges between hydrophobic and hydrophilic telechelic oligomers via a nucleophilic aromatic substitution mechanism. The copolymers were obtained in high molecular weights and were solvent cast into tough membranes, which had nanophase separated hydrophilic and hydrophobic regions. The performance and structure-property relationships of these materials were studied and compared to random copolymer systems. NMR results supported that the multiblock sequence had been achieved. They displayed superior proton conductivity, due to ionic, proton conducting channels formed through the self-assembly of the sulfonated blocks. The nano-phase separated morphologies of the copolymer membranes were studied and confirmed by transmission electron microscopy (TEM) and small angle X-ray scattering (SAXS). Through control of a variety of parameters, including ion exchange capacity and sequence lengths, performances as high, or even higher than those of the state-of-the-art PEM, Nafion®, were achieved.

Another series of semi-crystalline hydrophobic poly(ether ether ketone)-hydrophilic sulfonated poly(arylene ether sulfone) (PEEK-BPSH100) multiblock copolymers was first synthesized and characterized. However due to their semi-crystalline structure,

PEEK blocks are insoluble in most organic solvents at relatively low reaction temperatures, which prevents the coupling reaction between PEEK and BPS100. In order to facilitate the synthesis and processing, removable bulky ketimine groups were introduced to synthesize amorphous pre-oligomers poly(ether ether ketimine) (PEEKt). The synthetic procedure first involves the synthesis of hydrophobic poly(ether ether ketimine)-hydrophilic sulfonated poly(arylene ether sulfone) (PEEKt-BPS100) multiblock pre-copolymers via coupling reactions between phenoxide terminated hydrophilic BPS100 and fluorine terminated hydrophobic PEEKt blocks. The membranes cast from PEEKt-BPS100 were boiled in 0.5M hydrochloric acid then 0.5M sulfuric acid water solution to hydrolyze the amorphous PEEKt blocks to semi-crystalline PEEK blocks and acidify BPS100 blocks to BPSH100 blocks simultaneously. FT-IR spectra clearly showed the successful hydrolysis and acidification. The proton conductivity, water uptake and other membrane properties of the acidified semi-crystalline PEEK-BPSH100 membranes were then evaluated and compared with those of the state-of-the-art PEM, Nafion®.

Acknowledgements

I would first like to express my sincere gratitude to my advisor, Dr. James E. McGrath, for his guidance, inspiration and encouragement during my Ph.D. study at Virginia Tech. I have greatly benefited not only from his breadth and depth of knowledge, but also from his wonderful personality, which will continue to be a great source of inspiration for me. I would also like to thank the members of my advisory committee, Dr. Judy S. Riffle, Dr. Timothy E. Long, Dr. Richey M. Davis, and Dr. Alan R. Esker for their valuable suggestions and support. I also want to show a special thanks to Dr. S. Richard Turner for agreeing to attend my defense and give me insightful suggestions and comments.

I would like to give a big thanks to our wonderful administrative assistant lady, Mrs. Laurie Good, for her kindness and tremendous assistance during my stay at Virginia Tech.

Many thanks go to my colleagues in our great research group for their selfless assistance and friendship: Dr. Chang Hyun Lee, Ozma Lane, Dr. MyoungBae Lee, Dr. Ruilan Guo, Dr. Zhongbiao Zhang, Dr. Xiang Yu, Dr. Haeseung Lee, Drs. Rachael and Desmond VanHouten, Dr. Mehmet Sankir, Dr. Anand Badami, Dr. Natalie Arnett, and Dr. Guangyu Fang. I especially wish to express my acknowledgments to Dr. Chang Hyun Lee, Dr. Myoungbae Lee and Ozma Lane, for their assistance in PEM properties and morphologies of the membranes measurements.

I am thankful for the love and continued support of my parents, Delong Chen and Jianping Wu. They have motivated me and encouraged me throughout my academic career. This thesis is dedicated to them.

Attribution

Several colleagues facilitated the research described in the chapters included in this dissertation. Their contributions are described below.

James E. McGrath, Ph.D., is currently a university distinguished professor in chemistry at Virginia Tech. He is the author's academic advisor and committee chair. He provided support and guidance on all of the work.

Chang Hyun Lee, Ph.D., is currently a postdoctoral associate in chemistry at Virginia Tech. He aided in proton conductivity measurement and was a co-ahthor of Chapter 3, 4, 5, and 6.

Mingqiang Zhang, is currently a graduate student in chemistry at Virginia Tech. He aided in small angle X-ray scattering measurement and was a co-author of Chapter 3, 4, and 5.

Myoungbae Lee, Ph. D., is currently a research engineer at Dow Corning. He obtained transmission electron microscopy images and was a co-author of Chapter 3, 4 and 5.

Ozma Lane, is currently a graduate student in chemistry at Virginia Tech. She aided in transmission electron microscopy images and was a co-author of Chapter 5.

Desmond VanHouten, Ph.D., is currently a research engineer at Owens Corning. He assisted with thermal analysis and tensile testing and was a co-author of Chapters 5.

Robert B. Moore, Ph.D., is currently a professor in chemistry at Virginia Tech. He contributed the discussion on the results of the small angle X-ray scattering measurement with the author and was a co-author of Chapter 3, 4 and 5.

Table of Contents

Table of Figures

Table of Tables

Chapter 1: Literature Review

1.1 Introduction

1.1.1 Brief History of Fuel Cells

The principle of the fuel cell was discovered by a Swiss scientist, Christian Schönbein, in 1838 [1]. Based on the principle of the reversal of the decomposition of water by electric current, the first fuel cell device in the world, called "gas voltaic battery", was developed by an English scientist, Sir William Grove in 1839. This device was a forerunner of the modern fuel cell. Yet it was not until 1932 that a modern fuel cell device, the alkali fuel cell, was first successfully developed by a British engineer, Francis Bacon. Later, in 1959, Bacon and his colleagues demonstrated a practical 5 kW unicapable of powering a welding machine.

Based on Bacon's concept, the National Aeronautics and Space Administration (NASA) developed polymer electrolyte fuel cells, which were displaced by alkaline fuel cells in the Gemini space mission and Apollo program to supply electricity and drinking water. The demands for very pure hydrogen and oxygen, extremely expensive materials and intolerance of high operating temperature limited the applications of the earlier fuel cells. However, the future shortage of fossil fuels, the high energy efficiency of H_2/O_2, and the expectation of reduced CO_2 emissions and other negative environmental impacts associated with current power sources have triggered the extensive research to reduce the cost and make size effective fuel cells available for stationary and mobile applications. Industrial and academic researchers have focused on the commercialization and

technological improvement of proton exchange membrane (PEM) fuel cells.

1.1.2 Principles of Fuel Cells

Fuel cells are electrochemical conversion devices that generate direct current (DC) electricity by isothermally converting the chemical energy to electrical energy. Figure 1.1 [2] shows the basic compartments and operation mechanism of the fuel cells. A fundamental fuel cell is composed of an anode, a cathode and an electrolyte. When a fuel cell works, fuel is oxidized at the anode, while the oxidant is reduced at the cathode. The protons travel through the electrolyte from anode to cathode and the electrons transfer from anode to cathode through an external circuit to generate electricity power. Water and heat are released during this procedure.

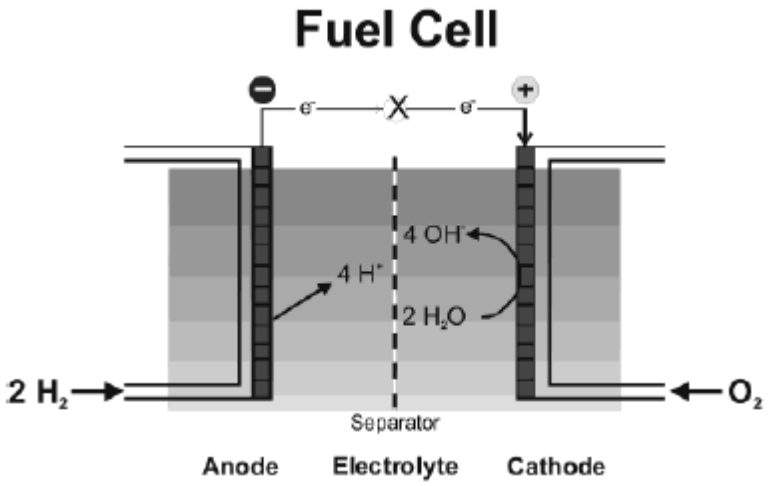

Figure 1. 1. Schematic of a Typical Fuel Cell

Although fuel cells are similar to the dry-cell batteries, there are many differences between fuel cells and dry-cell batteries. Dry-cell batteries, which are more like energy

storage devices, use sealed case fuel and oxidants as one unit. Furthermore, batteries will eventually run out of energy. On the other hand, fuel cells can theoretically produce continuous electricity as long as the external fuels are supplied. The environmentally friendly energy conversion, high energy efficiency, design variability, and flexibility of fuel types, make fuel cells very attractive in a variety of areas both in the low power applications such as notebook computers, cell phones, and in the high power applications such as stationary power and automobiles. Based on the different types of electrolytes, fuel cells can be classified into alkaline, phosphoric acid, sulfuric acid, molten carbonate, solid oxide, and proton exchange membrane fuel cells. The proton exchange membranes are classified as pre-sulfonated, post-sulfonated and non-sulfonated polymer membranes. Our group has focused on developing proton exchange membranes (PEM) and understanding the structural and electrochemical properties of the PEMs in fuel cells.

1.1.3 Types of Fuel Cells

Fuel cells are mainly classified according to the type of electrolyte used in them. In general, five different types of fuel cells produce electricity through specific operation conditions and electrochemical reactions. Alkaline fuel cells, phosphoric acid fuel cells, solid oxide fuel cells, molten carbonate fuel cells, and proton exchange membrane fuel cells are the five main types.

Table 1. 1. Five main types of fuel cells

Name	Electrolyte	Ions	Working Temperature	Fuel	Oxidant	Power Range	Application
Alkaline Fuel Cells (AFC)[3-5]	KOH	H^+	50-200 ^oC	Pure H_2	Pure O_2	5-150 KW	Space craft
Phosphoric Acid Fuel Cells (PAFC)[6]	H_3PO_4	H^+	150-200 ^oC	Reformed Gas	Air	5-20 MW	Stationary power
Solid Oxide Fuel Cells (SOFC) [4, 7]	Y_2O_3 stabilized Z_rO_2	O^{2-}	900-1000 ^oC	Hydrogen, natural gas, diesel fuel, alcohols	Air	1KW-5MW	Stationary power
Molten Carbonate Fuel Cells (MCFC) [8, 9]	Molten carbonate salt	CO_3^{2-}	650-700 ^oC	Purified coal gas, nature gas	Air	5KW-20MW	Stationary power
Proton Exchange Membrane Fuel Cell (PEMFC)	polymer electrolyte membrane	H^+	60-90 ^oC	H_2, methanol	Air	1-300KW	Vehicles, cell phone, laptop computer

1.1.4 Proton Exchange Membrane Fuel Cells (PEMFCs)

Proton exchange membrane fuel cells, also known as polymer electrolyte membrane fuel cells (PEMFCs), use proton exchange membranes, which contain ionic groups for the protons transport from the anode to the cathode, as the solid electrolyte. PEMFCs can be applied in many fields, from stationary power to laptop computers, from automobiles

to cell phones.

Numerous advantages of PEMFCs [10-14] make them preferable to other types of fuel cells. These advantages include high power density, high efficiency, relatively quick start-up, insensitivity to differential pressures, and the ease of design and adaptable size. However, there are still some disadvantages of PEMFCs, such as the need for expensive catalysts, intolerance to impurities, water management difficulties and lifetime limitations due to polymeric membrane degradation.

The operating temperature of PEMFC is relatively low, mostly from 60-90 ^{o}C, Figure 1.2 and Figure 1.3 show the anode and cathode half-cell reactions and the overall cell reaction of hydrogen and methanol PEMFCs.

Anode : $H_2 \longrightarrow 2H^+ + 2e^-$

Cathode : $1/2\ O_2 + 2H^+ + 2e^- \longrightarrow H_2O$

Overall : $H_2 + 1/2\ O_2 \longrightarrow H_2O$

Figure 1. 2. Anode, Cathode and Overall Cell Reaction in a Hydrogen Gas Powered PEMFC

Anode : $CH_3OH + H_2O \longrightarrow CO_2 + 6H^+ + 6e^-$

Cathode : $3/2\ O_2 + 6H^+ + 6e^- \longrightarrow 3H_2O$

Overall : $CH_3OH + 3/2\ O_2 \longrightarrow CO_2 + 2H_2O$

Figure 1. 3. Anode, Cathode and Overall Cell Reaction in a Methanol Powered PEMFC

The state-of-the-art proton exchange membrane (PEM) is Nafion®, a product of DuPont, which is a poly(perfluorosulfonic acid) copolymer as shown in Figure 1.4 [15]. Nafion® has a semi-crystalline tetrafluoroethylene backbone containing pendant side chains of perfluorinated vinyl ethers terminated by perfluorosulfonic acid groups. Nafion® is believed to be synthesized by free radical polymerization. The semicrystalline backbone provides excellent chemical and electrochemical stability while highly acidic perfluorosulfonic acid groups lead to high proton conductivity under both fully hydrated and partially hydrated conditions. However, Nafion® has some disadvantages including high cost, limited operating temperature (80 ℃), and high fuel permeability. Recently significant efforts have been made to develop alternative proton exchange membrane materials.

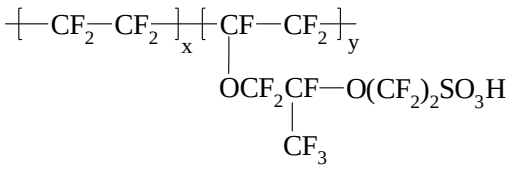

Figure 1. 4. Chemical structure of Nafion® produced by DuPont

1.1.5 Proton Exchange Membranes (PEM) Materials

The solid proton exchange membrane is a critical component of a PEMFC. The electrolyte membrane transfers protons from the anode to the cathode and separate the fuel (hydrogen or methanol) from the oxidants (oxygen, or air). The desirable properties of PEMs have been discussed elsewhere [16-19]. McGrath et al. have proposed critical issues for the development of high performance PEMs: (1) high proton conductivities, (2) low electronic conductivity, (3) low permeability to fuel and oxidants, (4) low water

transport through diffusion and electro-osmosis, (5) oxidative and hydrolytic stability, (6) good mechanical properties both in the dry and hydrated states, (7) cost, and (8) capability for fabrication into membrane electrode assemblies (MEAs) [20].

Proton conductivities are produced by interactions between acid groups attached to the PEM and water absorbed by the PEM. Water transport and mechanical properties of the PEM after water absorption affects the performance of the PEMFC. High proton conductivity with minimal amounts of absorbed water of a PEM may be the greatest challenge that researchers face. The fuel can also cross through the membrane and react with the oxidants at the cathode thus lowering the efficiency of a fuel cell. Accordingly, water management and the control of permeability of fuel to oxidants are main concerns in the design of the PEM. The combination of the anode, PEM and cathode is known as a membrane electrode assembly (MEA). Better MEA design is desirable to produce smaller, lighter and less expensive fuel cell stacks with higher power density [4]. Figure 1.5 [20] shows a typical membrane electrode assembly. To prevent platinum aggregation, the platinum catalyst is adsorbed onto carbon black and the platinum loaded carbon black is dispersed in a polymer matrix to provide higher mechanical strength and adhesion to the membrane.

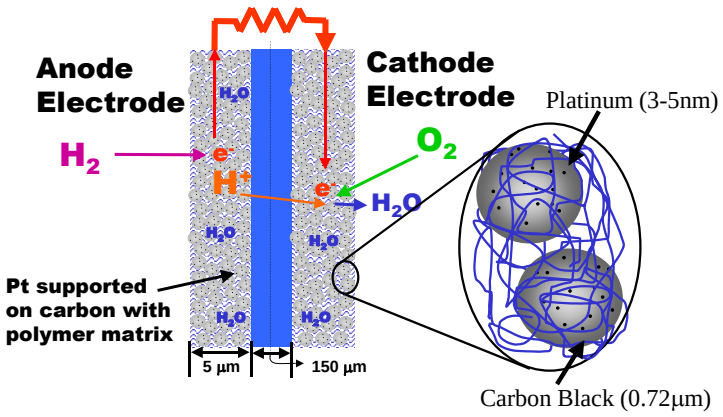

Figure 1. 5. Typical demonstration of a MEA

Over the past 20 years, many research groups around the world have been focusing on developing membranes that could replace the expensive perfluoro sulfonated copolymers, Nafion®. This review will discuss some proposed polymers that may be better candidates as PEMs for fuel cells.

1.2 PEMs Based on Sulfonated Aliphatic Backbone Polymers

1.2.1 Perfluorinated Copolymers

Perfluorinated copolymers are derived by free radical copolymerization of tetrafluoroethylene and a perfluorinated comonomer with around 13 mole percent of vinyl ethers with sulfonated fluoride functionality [12, 15, 20]. High chemical and thermal stabilities of fluorine-containing copolymers have been confirmed in the presence of strong acids, strong oxidants and strong reducants [5, 21]. Perfluorinated polymers are stable in the oxidative environment of fuel cells, which enhances confidence in the PEM fuel cell for alternative energy sources.

Nafion® (DuPont), Flemion (Asahi Glass), Aciplex (Asahi Chemical), GoreSelect (W. L. Gore& Associates) and the Dow membrane (Dow Chemical) are several successful commercially available perfluorinated ionomer membranes. Nafion® is the most common one among them. Figure 1.6 shows general structures of several perfluorinated membrane materials [17]. The perfluorosulfonic acid groups provide proton conductivity, while fluorinated backbones provide better mechanical and chemical stability, as well as a good water management.

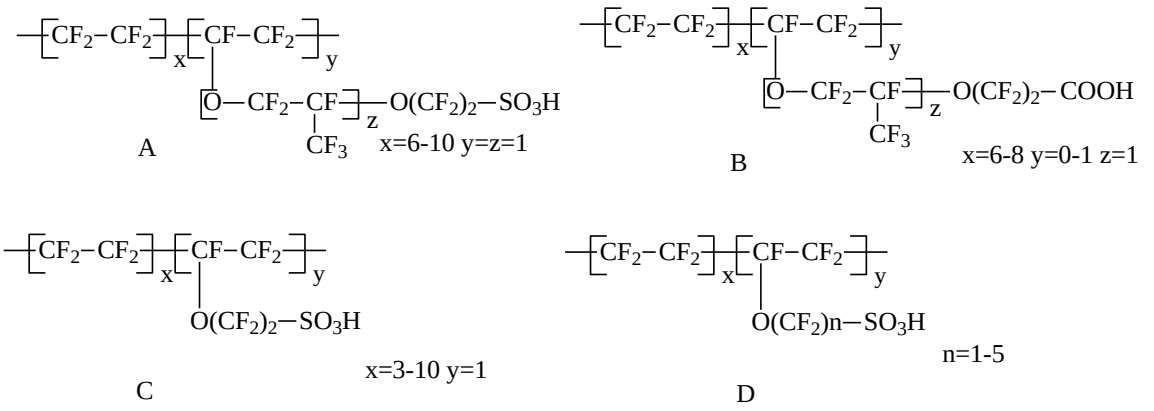

Figure 1. 6. General structure of (A) Nafion®, (B) Aciplex, (C) Dow membrane and (D) Flemion

Commercial Nafion® membranes are often labeled as Nafion® 112, 115 and 1100. The designation of 112, 115, and 1100 means these films have 1100 equivalent weights (EW), which is the number of grams of dry Nafion® per mole of sulfonic acid groups when the material is in the acid form with nominal thicknesses of 2, 5, or 10 mil, respectively [15]. Maximum proton conductivities of the Nafion® 1100 series at 25°C have been reported to be from 0.07-0.23 S/cm [22]. The lifetime of the Nafion® membranes at 10W cell potential has been reported to last as long as 60,000 hours in a

fuel cell operated at 80 °C, but this figure is unrealistic [23].

Yang and Rajendran synthesized copolymers of ethylene, tetrafluoroethylene, and olefin-containing fluorosulfonyl fluoride, which has a structure similar to Nafion® but reportedly less expensive [24]. The fuel cell performance of the copolymer membranes is allegedly comparable to Nafion®. Thomas and his colleagues reported the synthesis of bis[(perfluoroalkyl)sulfonyl]imide ionomers (PFSI) by copolymerization of sodium 3,6-dioxa-Δ-4-trifluoromethyl perfluorooctyl trifluoromethyl sulfonimide with tetrafluoroethylene (TFE) through a emulsion polymerization [25]. The new ion exchange copolymer had a similar backbone structure to Nafion®, which suggested its potential application as PEMs.

The Dow membrane, a perfluorinated copolymer (Figure 1.6 C), is no longer produced. The only difference between the Dow membrane and Nafion® is that the side chains of the Dow membrane are shorter than Nafion®. Obviously, the EW of the Dow membrane is lower than that of Nafion®, which means the Dow membrane possesses higher concentrations of proton exchange sites in a thinner membrane. A better performance in hydrogen/air fuel cells with 10,000 hour durability was achieved with the Dow membrane [26, 27]. A major problem with the Dow membrane was its even higher cost than Nafion®.

There are several disadvantages of Nafion®-type membranes. The first one is the cost, which is about $600-700 per square meter. Secondly, the fuel cell performance degrades at lower humidity or temperatures above 100 ℃. The high methanol and water permeability and relatively low mechanical strength at operating temperature also create serious problems for the application of Nafion® in PEMFCs. Furthermore, the safety

concerns of tetrafluoroethylene in the synthesis of the perfluorinated copolymers have inevitably led to the search for new alternative membranes to Nafion®.

1.2.2 Sulfonated Polystyrene Copolymers

Crosslinked polystyrene sulfonic acid membranes were first used as the electrolyte in the fuel cell of the Gemini space program. Durability of the sulfonated polystyrene became an issue due to the fact that fuel cell performance decreased as the operating times increased. Furthermore, the degraded products contaminated the water produced by the fuel cells, which meant the water could not be recycled or consumed by the astronauts. The durability and degradation problems of crosslinked polystyrene sulfonic acid membranes led NASA to employ alkaline fuel cells in their subsequent missions.

Figure 1.7 shows a series of sulfonated copolymers of substituted α,ß,ß-trifluorostyrene, BAM, developed by Ballard Advanced Materials Corporation [28]. This sulfonated polystyrene analogue exhibited good stability and superior performance compared to Nafion®. The third generation Ballard Advanced Material (BAM3G) has been reported to exhibit good protonic conductivity (0.08 S/cm) and long durability over 100,000 hours [28].

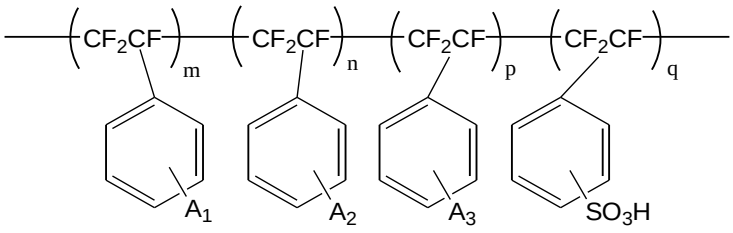

At least 2 of m, n, p, q are integers>0
A_1, A_2, A_3=alkyls, halogens, O-R, $CF=CF_2$, CN, NO_2, OH

Figure 1. 7. Chemical structure of BAM PEMs

Dais Analytic Corporation introduced new PEMs by sulfonating styrene/ethylene-butene/styrene copolymers (PSEBS) which are better known as the commercially available block copolymers Kraton [29]. The chemical structure of the Dais Analytic PEMs is shown in Figure 1.8. When fully hydrated, the conductivity of the PEMs vary from 0.08 to 0.1 S/cm [30-32]. Although the Dais Analytic PEMs possess the price advantage and desirable rich array of microphase-separated morphologies [33], the main drawback of these PEMs are oxidatively unstable due to partially aliphatic backbones [34].

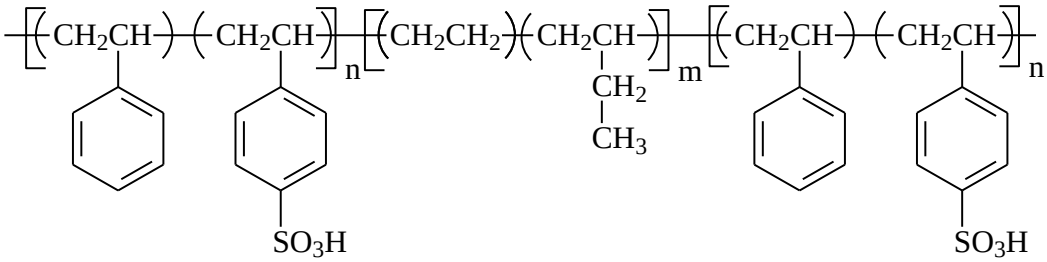

Figure 1. 8. Chemical structure of styrene/ethylene-butene/styrene triblock copolymers

To improve upon the mechanical properties of PSEBS, crosslinking of styrene-ethylene-butylene has been attempted. Crosslinked PSEBS via sulfonamide linkages was reported [35], but no ion exchange capacity (IEC) and proton conductivity test had been conducted by the authors. Chen et al. reported photo-crosslinked sulfonated styrene-ethylene-butylene [36]. After crosslinking the IEC and proton conductivity decreased slightly, but these values were still higher than Nafion® 115. However, the durability of the photo-crosslinked sulfonated PSEBS in the fuel cell environment is significantly improved compared to the non-crosslinked PSEBS. Shi et al. developed partially sulfonated poly([vinylidene difluoride-*co*-hexafluoropropylene]-*b*-styrene)

[P(VDF-*co*-HFP)-*b*-SPS]. The proton conductivity of sulfonated P(VDF-*co*-HFP)-*b*-SPS is greater than that of sulfonated nonfluorous block copolymer membranes [37]. Fluoropolymer segments induced an enhanced nanophase separation and well-connected channel networks to improve the proton transport.

Another approach is to radition graft sulfonated poly(styrene sulfonic acid) onto a fluorinated polymer backbone such as poly(tetrafluoroethylene-*co*-hexafluoropropylene) [38], poly(ethylene-*alt*-tetrafluoroethylene) [39, 40] or poly(vinylidene fluoride) [41]. Figure 1.9 shows some structures of radiation grafted copolymers.

The degree of grafting, which determines the membrane properties, can be controlled by irradiation intensity, temperature and time, and a Lewis acid catalyst [42]. Sometimes the grafted polymer membranes were crosslinked with divinylbenzene to improve the mechanical properties and water management [43-45]. The grafted membranes show comparable fuel cell performance to Nafion®. The methanol permeability of grafted membranes is reduced compared to Nafion®, while the cost of grafted membranes is much less than that of Nafion®. However, free radicals degrade the polystyrene grafts and lead to the loss of poly(styrenesulfonic acid) groups, which induces the loss of IEC [46].

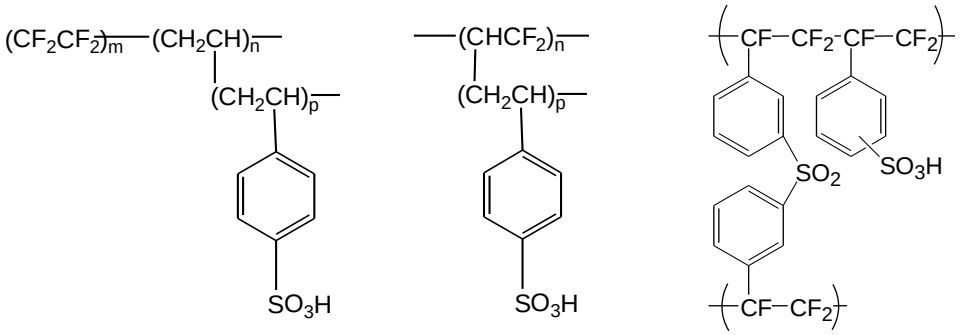

Figure 1. 9. Some radiation grafted copolymers

1.3 PEMs Based on High Performance Engineering Materials

1.3.1 Poly (arylene ether)s

Wholly aromatic polymers have many advantages such as their availability, processability, wide variety of chemical composition and anticipated stability in the fuel cell environment [20]. Proper molecular design can achieve different poly(arylene ether) with specific chemical structures. As shown in Figure 1.10, the polymer can be a poly(arylene ether sulfone), a poly(arylene ether ketone), or a poly(arylene ether phosphine oxide); depending on Z, which can be either a sulfone group, a ketone group, or a phenyl phosphine oxide group. Y, also could be a bond, a sulfone group, or an isopropylidene linkage, etc.

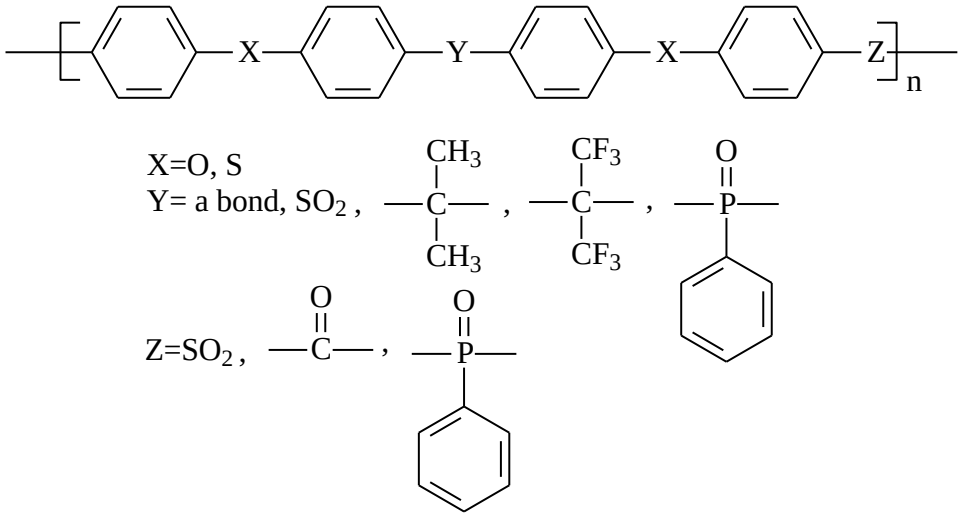

Figure 1.10. Chemical structure of poly(arylene ether sulfone)s : various random copolymers are possible by a one-step copolymerization reaction

The most practical method to synthesize poly(arylene ether)s is nucleophilic aromatic substitution [47-50]. The mechanism of S_NAr nucleophilic aromatic substitution is shown in Figure 1.11. In the rate-determining step, the nucleophile attacks the carbon atom of the activated C-X bond, and forms a resonance-stabilized Meisenheimer complex. The leaving group, X, is kicked off in the second step.

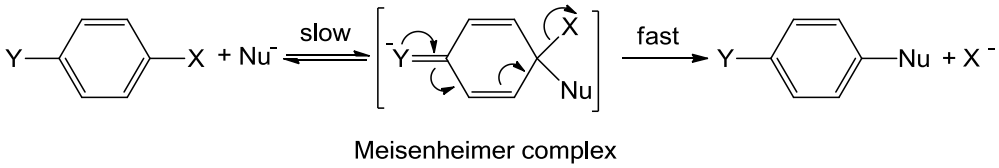

Figure 1. 11. Mechanism of S_NAr nucleophilic aromatic substitution

The preparation of poly(arylene ether)s is usually conducted through the step polymerization of aromatic dihalide and bisphenolate salt, which is produced in situ by bisphenol and alkali metal carbonate or hydroxide. Although aromatic halides are generally not reactive to nucleophilic substitution, the electron-withdrawing sulfone and carbonyl groups significantly facilitate the polymerization. For example, A bisphenol A polysulfone (Udel®) can be synthesized by 4,4´-dichlorodiphenyl sulfone (DCDPS) and 4,4′-isopropylidenediphenol (bisphenol-A) with sodium hydroxide as the base to produce the reactive phenolate [49, 50]. The reaction scheme is shown in Figure 1.12.

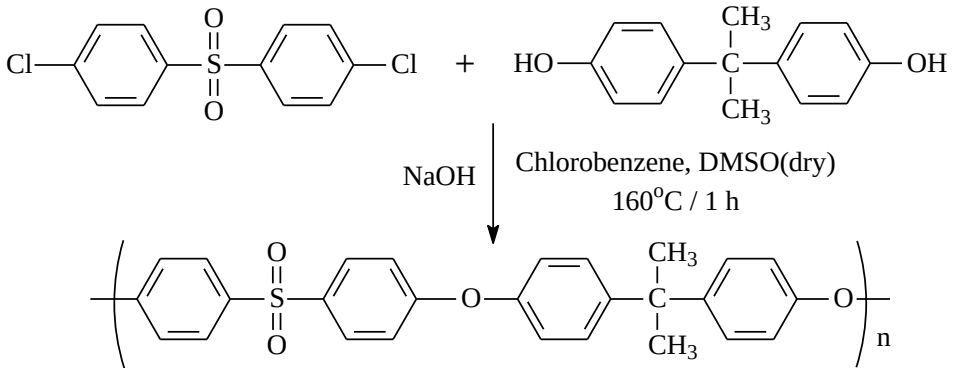

Figure 1. 12. Synthesis of bisphenol-A polysulfone

High boiling point polar aprotic solvents, such as dimethyl sulfoxide (DMSO), *N*-methyl pyrrolidone (NMP) and *N*,*N*-dimethyl acetamide (DMAc), are usually required in this type of polymerization. Polymerzation should also be carried out in the absence oxygen and water to prevent oxidation and hydrolysis of phenolate [51].

The mechanism of the synthesis of poly(arylene ether ketone) is similar to that of poly(arlene ether sulfone). Poly(arylene ether ketone)s using hydroquene are partially crystalline (approximately 35%), which results in very poor solubility. It is difficult to directly synthesize high molecular weight poly(arylene ether ketone)s from dihalide benzophenone monomers and bisphenol monomers, because the resulting polymers will precipitate during the reaction and limit the molecular weight of the poly(ether ketone)s [52]. High temperatures of 200-350 ^{o}C and aromatic difluorides are normally required in synthesis of poly(arylene ether ketone)s. However, higher polymerization temperatures may induce undesirable side reactions [53].

Poly(arylene ether) remains stable even after introducing the proton conductive sites, which make this class of polymers attractive for applications in fuel cells. Two methods

of introducing proton conductive sites to poly(arylene ether) are post sulfonation and direct copolymerization of sulfonated monomers.

1.3.1.1 Post Sulfonated Poly(arylene ether)s

Post sulfonation of poly(arylene ether) are often carried out in sulfonation reagents such as concentrated sulfuric acid, fuming sulfuric acid, chlorosulfonic acid, or sulfur trioxide via an electrophilic aromatic substitution reaction. Poly(aryl ether sulfone) (UDEL), polysulfone, poly(ether sulfone) (Victrex) are several common commercialized poly(arylene ether) which are often post sulfonated [54, 55].

Noshay and Robeson were some of the first to synthesize sulfonated poly(arylene ether sulfone) [56]. They developed a mild sulfonation procedure where a complex of sulfur trioxide and triethyl phosphate were used to sulfonate a commercially available bisphenol-A- based poly(ether sulfone), as shown in Figure 1.13. Due to the mild reaction condition, the sulfonic site is usually restricted to only one per activated unit. Although the employment of mild sulfonation reagents can prevent the crosslinking or main chains degradation in the sulfonation reaction, the mild sulfonation reagents also lower the efficiency of the sulfonation reaction.

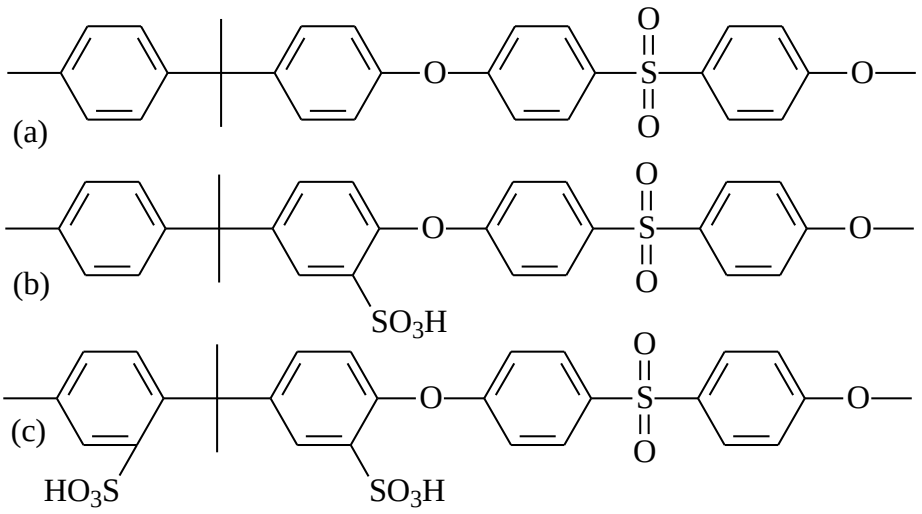

Figure 1.13. Post sulfonation of poly(arylene ether sulfone)s: (a) back bone of poly (arylene ether sulfone), and the most probable sulfonic acid attachment to a poly(arylene ether sulfone), (b) and (c)

Poly(ether ether ketone) (PEEK) exhibits good thermal stability, chemical resistance, and electrical and mechanical properties. Post-sulfonation of PEEK to produce a film for fuel cells has sparked great interest [57]. Concentrated sulfuric acid has been reported as the best sulfonation agent for PEEK [58]. Figure 1.14 shows the structure of sulfonated PEEK. The sulfonic acid moieties on the polymer backbone decrease the crystallinity and increase solubility of the polymer, which allows further characterization of sulfonated PEEK. The degree of sulfonation can be controlled over a range of 30-100% by adjusting the reaction time, temperature, and the concentration of the sulfonating reagent [59].

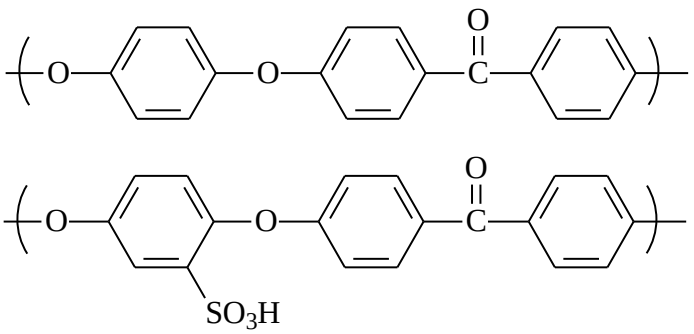

Figure 1. 14. Chemical structure of sulfonated and nonsulfonated poly(ether ether ketone) PEEK.

Synthesis of post-sulfonated PEEK and PEEK derivatives are widely reported [60-64]. Shang and his colleagues synthesized sulfonated fluorene-containing PEEK; and the conductivity of this polymer membranes is comparable to Nafion® 117 at temperatures around 100 ^{o}C [60]. High temperature PEMs made by post sulfonated poly(oxa-*p*-phenylene-3,3-phtalido-*p*-phenylenxoxa-*p*-phenylenexoxy-*p*-phenylene) (SPEEK-WC) were reported by Patuzo et al [61]. Compared to Nafion® 117, SPEEK-WC membranes showed slightly higher power density at 120 ^{o}C in H_2/Air fuel cell operations.

Another interesting sulfonation procedure, based on several steps including metalation, was developed by Kerres et al [65]. This route is more complex and expensive than using concentrated sulfuric acid. One problem in this route is the control of crosslinking and chain degradation. Crosslinking decreases the IEC of membranes, while chain degradation produces poor mechanical properties. On the other hand, the crosslinking facilitates the control of water uptake and gas permeability. Figure 1.15 shows the metalation route of the sulfonation of polysulfones [66, 67].

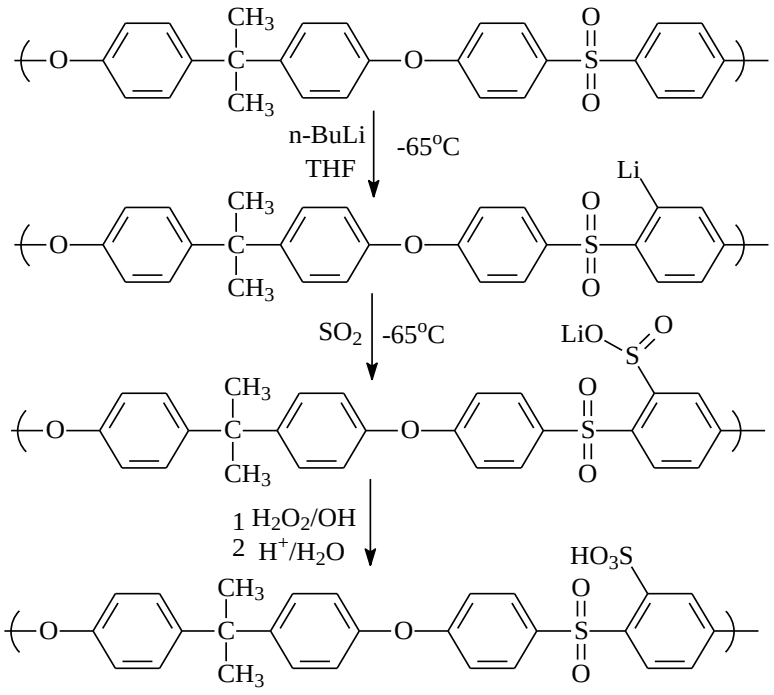

Figure 1. 15. The metalation route to sulfonated polysulfone

Post sulfonation is a convenient method to modify the chemical structure and properties of the polymers. However, the limitations are also obvious: (1) lack of precise control of the degree of sulfonation; (2) lack of precise control over the location of the sulfonic acid groups; and (3) high electron density leads to relatively easy desulfonation.

1.3.1.2 Direct Copolymerization of Sulfonated Poly(arylene ether)s

Direct copolymerization of sulfonated monomers can be adopted to precisely control the degree of sulfonation and the position of sulfonate groups. There are several advantages of direct sulfonation over the post polymerization sulfonation: (1) precise control of degree of sulfonation, including exact control of the amount of disulfonation with adjustable molecular weights; (2) disulfonation on deactivated rings, enhanced

stability and acidity; (3) one step controlled copolymerization with no side reactions that can cause backbone degradation; and (4) very high molecular weight copolymers are possibly achieved.

Robeson and Matzner first reported sulfonation of 4,4´-dichloro diphenyl sulfone (DCDPS) for the purpose of producing flame retardant materials [68]. Ueda et al. used this sulfonated 4,4´-dichlorodiphenyl sulfone, the unsulfonated monomer and bisphenol A to synthesize a disulfonated poly(arylene ether sulfone) copolymer [69]. Although the research on sulfonated monomers has been conducted for years, these types of materials did not have many specific applications until the McGrath group introduced disulfonated monomers to the application of PEMs in fuel cells. The synthesis procedure of the sulfonated monomers was further improved in McGrath's lab to obtain high yield, high degrees of disulfonation [70, 71]. Recently Sankir developed a novel procedure for the synthesis and characterization of 3,3´-disulfonated 4,4´- dichlorodiphenyl sulfone (SDCDPS) with high conversions on a kilogram scale [72]. Li et al. developed a new method to determine the purity of SDCDPS by UV-visible (UV-vis) spectroscopy [73]. The UV-vis spectroscopy has been proven to be a fast and convenient method to determine the purity of SDCDPS for the following synthesis of high molecular weight polymers. Similarly, disulfonated monomer 3,3´-disulfonated 4,4´-difluorodiphenyl sulfone (SDFDPS) was synthesized using 4,4´-difluorodiphenyl sulfone. SDFDPS is more reactive than SDCDPS, which enables the copolymerization to be conducted at a relatively low temperature [74]. Another sulfonated monomer, 5,5´-carbonylbis-(2-fluorobenzenesulfonate), has been developed to prepare ketone based copolymers [75].

Sulfonated poly(arylene ether sulfone) (BPSH) random copolymers have been synthesized and characterized. The membrane properties of the sulfonated poly(arylene ether sulfone) such as water uptake, proton conductivity, and IEC have been studied. The water uptake and proton conductivity increase as the degree of sulfonatation increases. However, the mechanical properties of the membranes became worse with an increasing water uptake. A balance between the proton conductivity and the mechanical properties is very important in the design and synthesis of new sulfonated poly(arylene ether sulfone). Wang et al. synthesized a series of random sulfonated poly(arylene ether sulfone) with different ratios of disulfonated to non-sulfonated repeating units [76]. Figure 1.16 shows the synthetic scheme. It was reported that the water uptake of the membrane increased significantly when the molar ratio of disulfonated to nonsulfonated repeat unit is higher than 1:1 in the copolymer. After acidification, the membranes remain stable up to 220 ^{o}C in air, with the proton conductivity of 0.11 S/cm (SDCDPS/DCDPS=40/60) and 0.17 S/cm (SDCDPS/DCDPS=60/40), respectively.

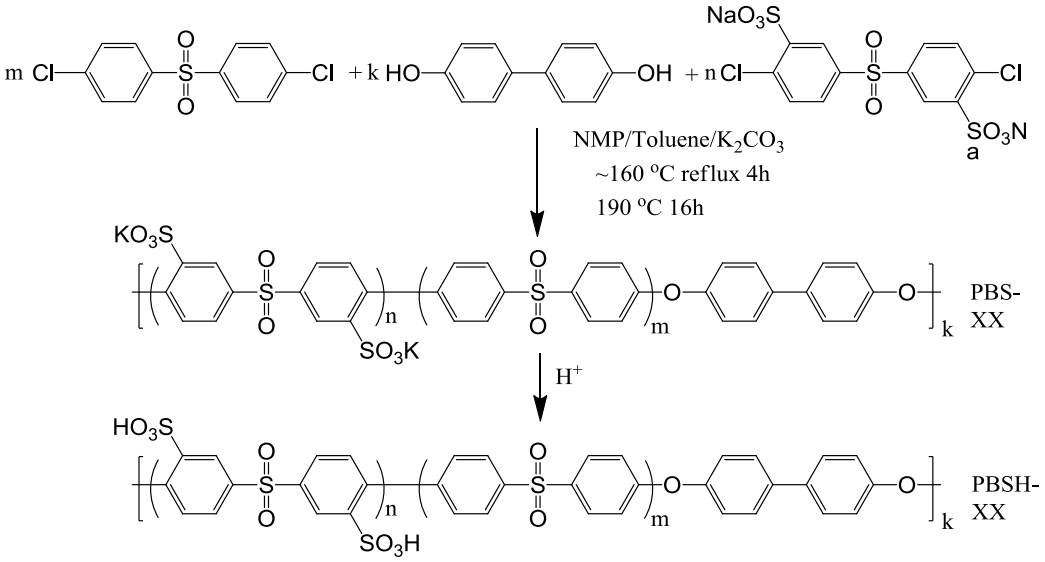

Figure 1. 16. Synthesis of random sulfonated poly(arylene ether sulfone)s

Direct copolymerization of sulfonated poly(arylene sulfide sulfone)s

Poly(phenylene sulfide sulfone) and poly(phenylene sulfide) are high performance engineering thermoplastic materials with high glass transition temperatures, good mechanical and electrical properties, and good chemical resistance. Sulfonated poly(arylene sulfide sulfone)s have been reported by Wang and his colleagues, as shown in Figure 1.17 [71]. 3,3´-Disulfonated 4,4´-diflorodiphenylsulfone (SDFDPS), bis-(4-mercaptophenyl sulfone) and 4,4´-diflorodiphenylsulfone (DFDPS) were used as monomers in the polymerization. The sulfonated poly(arylene sulfide sulfone)s are potential membrane materials for PEM fuel cells.

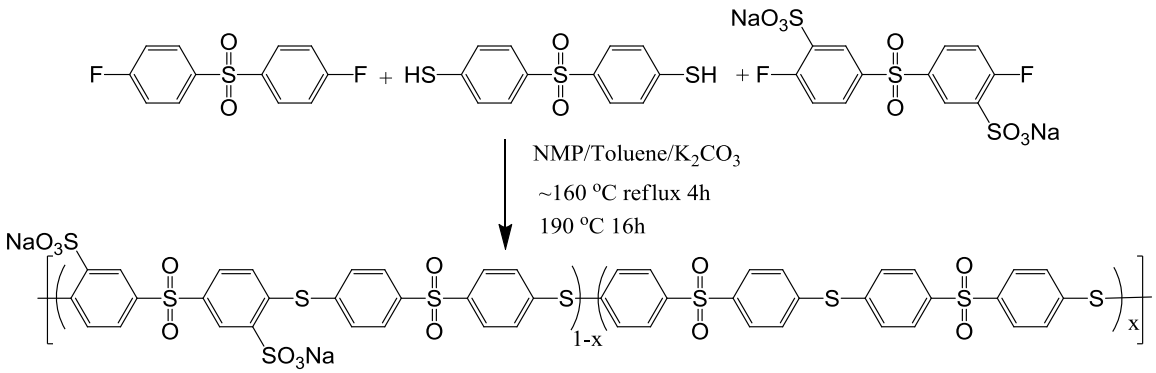

Figure 1. 17. Directly copolymerized sulfonated poly(arylene sulfide sulfone)

More recently, Wiles et al.[77] used 4,4´-thiobisbenzenethiol (TBBT) instead of bis-(4-mercaptophenyl sulfone) to synthesize a series of novel sulfonated poly(arylene thioether sulfone) copolymers (PATS) for application as PEM materials following the scheme of Wang et al. [76]. Properties of these copolymer membranes and fuel cell performances have been extensively studied.

Direct copolymerization of sulfonated poly(arylene ether benzonitrile)s

Figure 1.18 shows the direct polymerization of sulfonated poly(arylene ether benzonitrile)s (SPAEB). A series of sulfonated poly(arylene ether benzonitrile)s were synthesized via copolymerization of 3,3´-disulfonated 4,4´-dichlorodiphenylsulfone (SDCDPS), 2,6-dichlorobenzonitrile (DCBN) and 4,4´-dichlorodiphenylsulfone (DCDPS) [78]. SPAEB membranes showed equivalent IEC to BPSH membranes. Proton conductivity of SPAEB with 35 mol% of the disulfonated comonomer was slightly higher than 0.10 S/cm at 30 ^{o}C in liquid water.

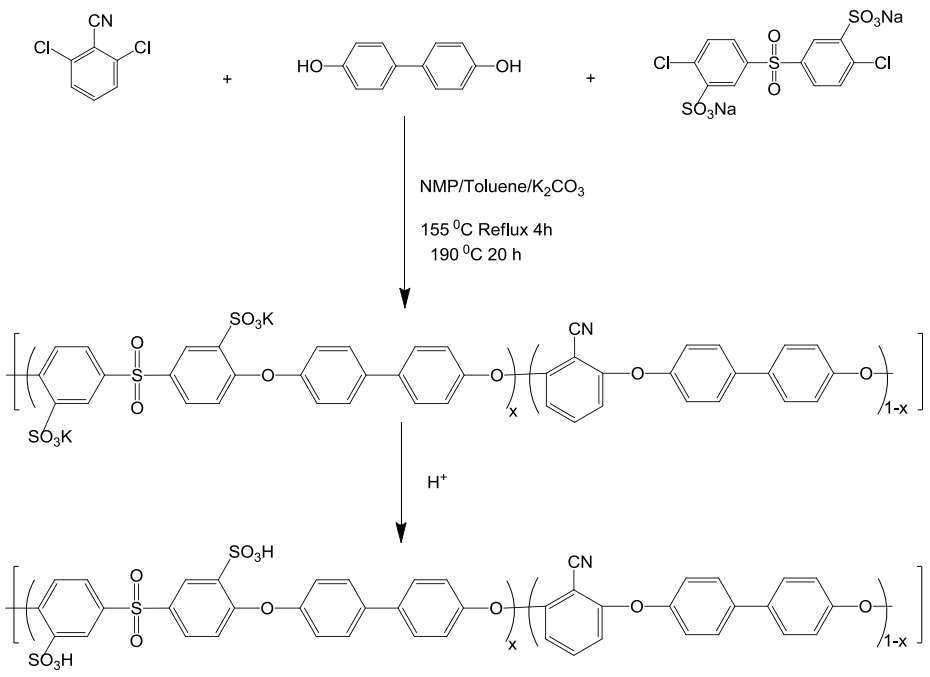

Figure 1. 18. Directly copolymerized sulfonated poly(arylene ether benzonitrile)

Direct copolymerization of sulfonated poly(arylene phosphine oxide)s

As fire retardant materials, poly(arylene phosphine oxide)s were reported to have high thermal stability at high temperature. 4,4´-bis(fluorophenyl)phenylphosphine oxide (BFPPO) was sulfonated by fuming sulfuric acid to produce the mono sulfonated monomers. Recystallization was necessary to remove the byproducts, di- and tri-sulfonated monomers [79]. The direct copolymerization reaction of BFPPO, biphenol and monosulfonated BFPPO is shown in Figure 1.19. Compared to the sulfonated poly(arylene ether sulfone) and poly(arylene ether ketone), the proton conductivity of sulfonated poly(arylene phosphine oxide)s is relatively low, which is due to the lower degree of sulfonation in per repeat units and the hydrogen bonds between the sulfonic acid groups and phosphine oxide groups.

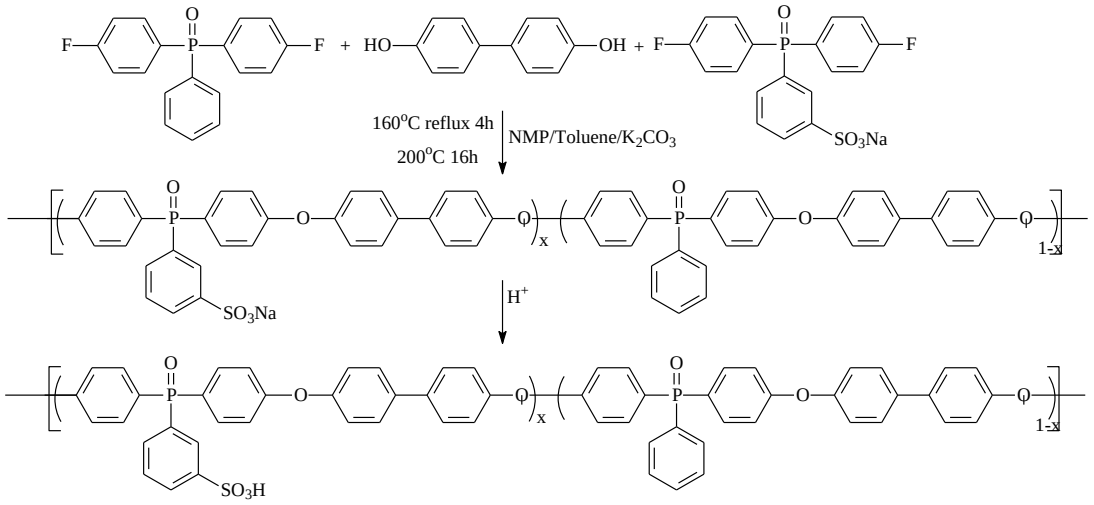

Figure 1. 19. Directly copolymerized sulfonated poly(arylene ether phosphine oxide)

Direct copolymerization of sulfonated poly(arylene ether ketone)s

Wang et al. first developed direct copolymerization of sulfonated poly(arylene ether ketone)s [75, 80]. Unlike post sulfonated PEEK, the degree of sulfonation can be precisely controlled in direct copolymerization. 5,5´-Carbonylbis-(2-fluorobenzenesulfonate) was used as the sulfonated monomer. Thermally stable sulfonated polymers with high molecular weight were produced as shown in Figure 1.20. Similarly, Chen et al. developed a novel synthesis of sulfonated poly(phthalazinone ether ketone) by an N-C coupling reaction for potential PEM applications [81]. Li and his colleagues synthesized sulfonated poly(ether ether ketone ketone)s (SPEEKK) and found the SPEEKK membranes showed proton conductivity as high as 0.1 S/cm [82]. Xiang et al. also prepared series of sulfonated poly(arylene ether ketone)s (SPAEKs) by aromatic nucleophilic polycondensation of 2,6-dihydroxynaphthalene with 5,5´-carbonyl-bis(2-fluorobenzenesulfonate) and

4,4´-difluorobenzophenone in different ratios [83]. After acidification, the SPEAK membranes still remained stable up to 240 ℃. The proton conductivity of SPEAK membranes increased as the degree of sulfonation increases. A temperatue dependence of proton conductivity in liquid water was also observed; SPEAK membranes with a degree of sulfonation of 1.6 showed proton conductivity of 0.042 S/cm and 0.11 S/cm at room temperature and 80 ℃, respectively.

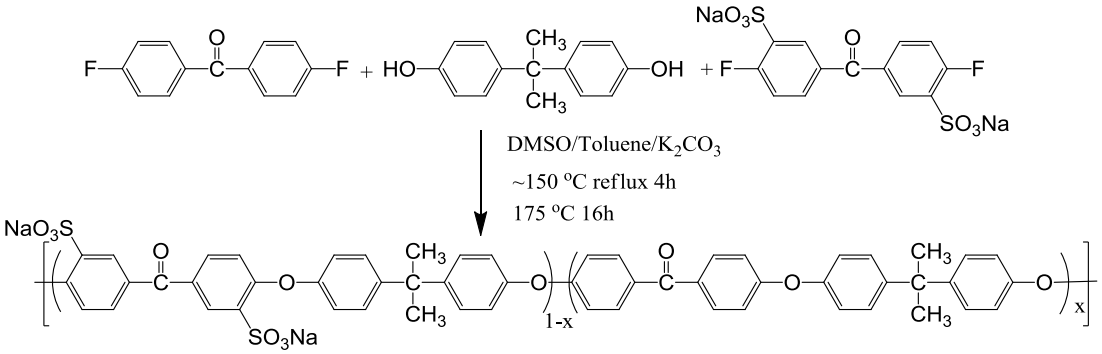

Figure 1. 20. Directly copolymerized sulfonated poly(arylene ether ketone)

1.3.2 Poly(imide)s

Since DuPont introduced the first commercial poly(imide) Kapton® in the 1960's, Polyimides have played important roles in the advanced materials industry due to their excellent thermal stability along with good chemical, mechanical and electrical properties. Aromatic poly(imide)s are generally prepared through the reaction of dianhydrides and diamines [84, 85] by a two-stage procedure due to the resulting poly(imide)s with common structures are insoluble in polar organic solvents [51], as shown in Figure 1.21. In the first stage, pyromellitic dianhydride reacted with oxydianiline to form soluble poly(amic acid) at relatively low temperatures. In the second-stage, temperature was increased to 300 °C for the solid-state cyclization reaction to produce the final

poly(imide)s.

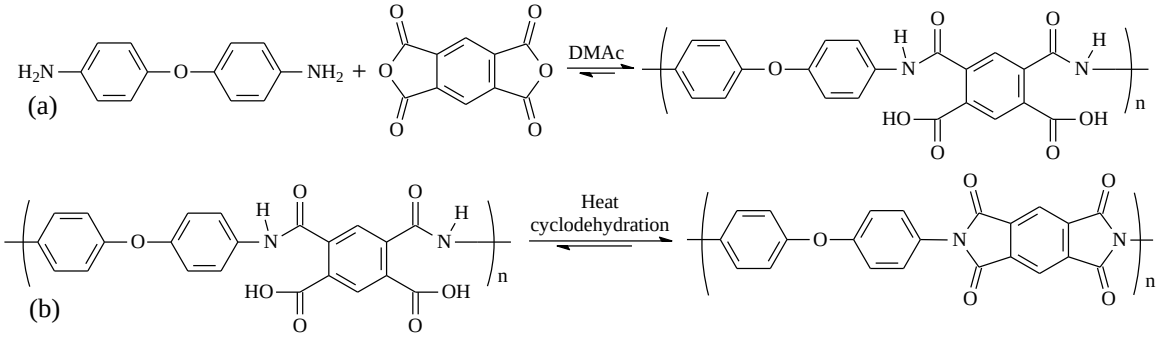

Figure 1. 21. Two-stage synthesis of poly(imide)

1.3.2.1 Sulfonated Poly(imide)s (SPIs):

Because the phthal imide groups under the post sulfonation conditions are unstable, sulfonated poly(imide)s are generally synthesized by direct polymerization from sulfonated diamine monomers and nonsulfonated dianhydrides. However, the hydrolytic stability of sulfonated poly(imide)s in fuel cell environments depends on the structure of the dianhydride during polymerization. It has been found that the rapid degradation of phthalic poly(imide)s with five-membered ring structures under acidic conditions leads to chain scission and causes the membrane to become brittle [18]. It was suggested that six-membered ring sulfonated poly(imide)s from napthalenic dianhydrides are much more stable to hydrolysis. However, the validity of this hypothesis is still debatable [86]. Genies et al. successfully synthesized six-membered ring sulfonated poly(imide), as shown in Figure 1.22 [87].

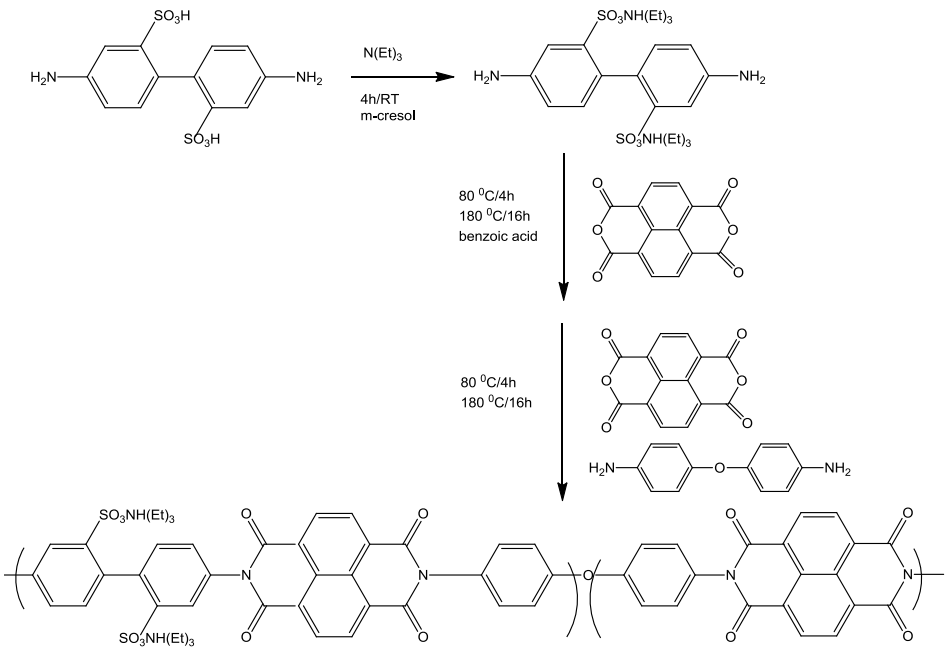

Figure 1. 22. Synthesis of naphthalenic sulfonated poly(imide) random copolymers

In the first step, 4,4´-diamino-2,2'-biphenyl disulfonic acid (BDA) reacted with 1,4,5,8-tetracarboxylic dianhydride (NDA). By control of the stoichiometry of the monomers, sulfonated poly(imide)s with different chain lengths can be synthesized. Then calculated amounts of NDA and 4,4´-oxydianiline (ODA) were added to control the degree of sulfonation in a second step. In order to improve solubility, the sulfonated diamine was usually converted to the triamine salt prior to copolymerization.

In addition to the commercially available 4,4´-diamino-2,2´-biphenyl disulfonic acid (BDA), McGrath et al. [88-90] and Okamoto et al. [91-94] have prepared several novel disulfonated diamines. The solubility of the sulfonated poly(imide)s in organic solvent can be improved by introducing nonsulfonated diamines containing flexible linkages or bulky groups [88]. Figure 1.23 and Figure 1.24 show some disulfonated diamines and

nonsulfonated diamines monomers which have been used in the polymerzaion of SPIs.

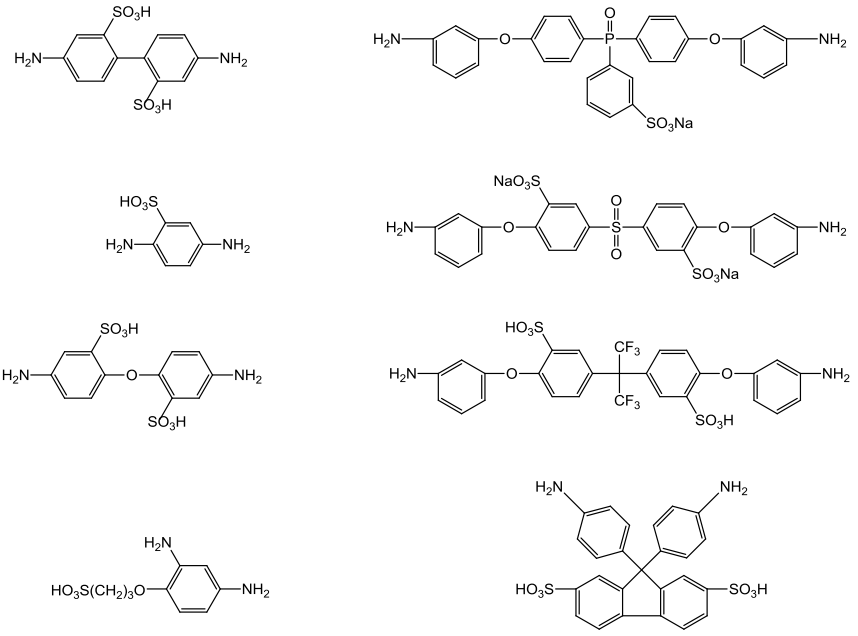

Figure 1. 23. Structures of sulfonated diamine monomers

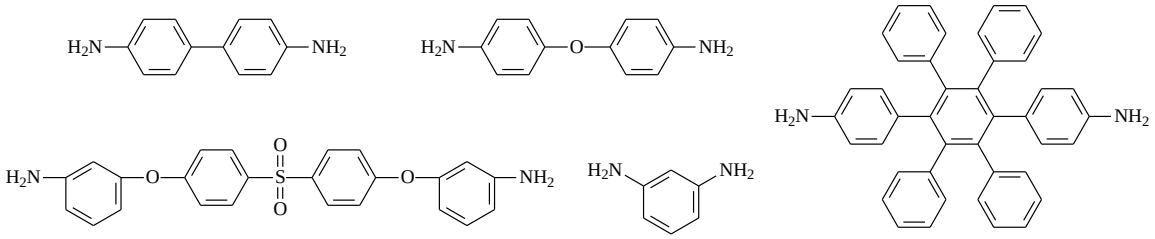

Figure 1. 24. Structures of nonsulfonated diamine monomers

Watanabe et al. synthesized diamines with pendant side chains of perfluorosulfonic acid terminated vinyl ethers [95]. On the basis of these diamines, they developed proton conductive aliphatic/aromatic polyimide ionomers. Without sacrificing proton conductivity, oxidative and mechanical stability, the hydrolytic stability of poly(imide) ionomers were significantly improved by introducing the aliphatic segments both in the

main and side chains. One of the poly(imide) ionomers with 70 mol% of the sulfonated component possessed an IEC value as high as 2.31 mequiv/g and only 21 wt% water uptake. Under harsh hydrolytic conditions (140 ^{o}C and 100% RH) the poly(imide) ionomers were still stable. Figure 1.25 shows the synthesis of the aliphatic/aromatic polyimide ionomers.

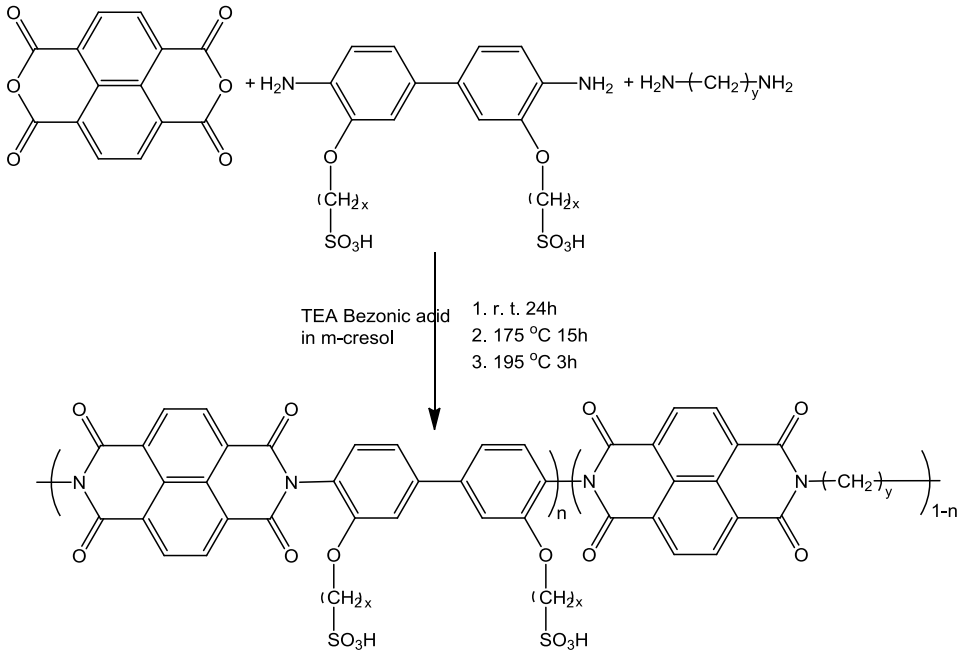

Figure 1. 25. Synthesis of the aliphatic/aromatic polyimide ionomers

Okamoto et al. recently developed novel diamines with sulfonated aromatic pendant groups, 3,5-diamino-3´-sulfo-4´-(4-sulfophenoxy) benzophenone (DASSPB) and 3,5-diamino-3´-sulfo-4´-(2,4-disulfophenoxy) benzophenone (DASDSPB) [96]. New side-chain-type sulfonated poly(imide)s were synthesized from these two diamines, NDA and unsulfonated aromatic diamines such as 4,4´-bis(3-aminophenoxy) phenyl sulfone (BAPPS). At 120 ^{o}C, the NDA-DASDSPB/BAPPS(1:1) based poly(imide) membrane

showed conductivity values of 0.05 S/cm and 0.3 S/cm at 50 and 100 RH, respectively, which suggested this kind of SPIs were potentially feasible for PEM applications at high temperature. The structures of DASSPB and DASDSPB are shown in Figure 1.26.

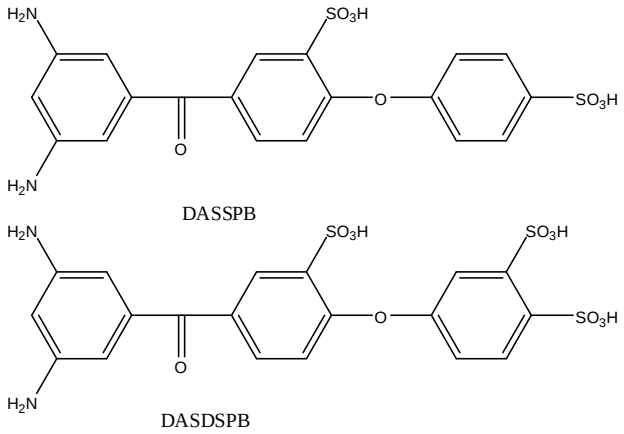

Figure 1. 26. Structures of DASSPB and DASDSPB

1.3.3 Aromatic 5-membered-ring Heterocyclic Polymers

Aromatic heterocyclic polymers are high performance materials which are characterized by their excellent thermal and mechanical properties. As shown in Figure 1.27, poly(benzimidazole), poly(benzoxazole) and poly(benzthiazole) are the polycondensation products of a dicarboxyl (or phenyl ester) with a tetramine, a bis-*o*-aminophenol, or a bis-*o*-aminothiophenol, respectively [97-101].

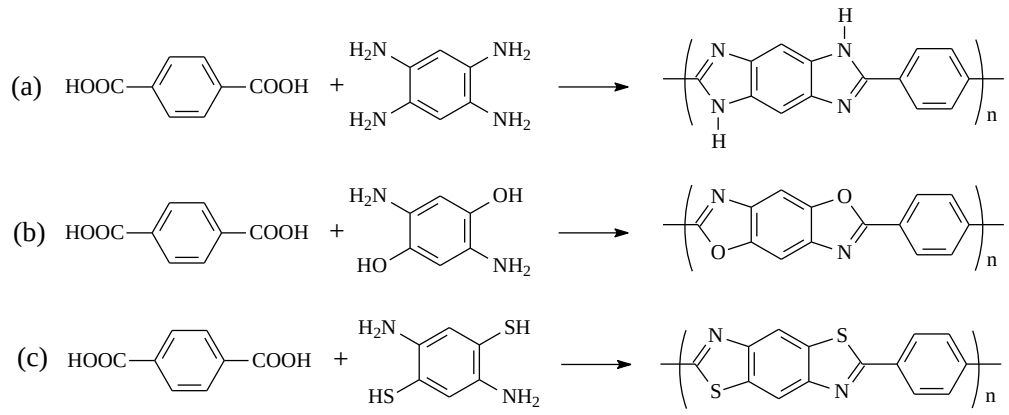

Figure 1. 27. General scheme for the synthesis of (a): poly(benzimidazole)s, (b): poly(benzoxazole)s and (c): poly(benzthiazole)s

1.3.3.1 Post Sulfonation of Poly(benzimidazole)s (PBI)s

Post sulfonation of poly(benzimidazole)s can be accomplished by immersing the PBI or AB-PBI membranes in sulfuric acid, and heating to around 400 ^{o}C, as Figure 1.28 shows [102-104]. Due to protonation of the nitrogen in the imidazolium ring, post sulfonated PBIs show low proton conductivity. Therefore, post sulfonated PBI membranes are not directly suitable for PEM applications.

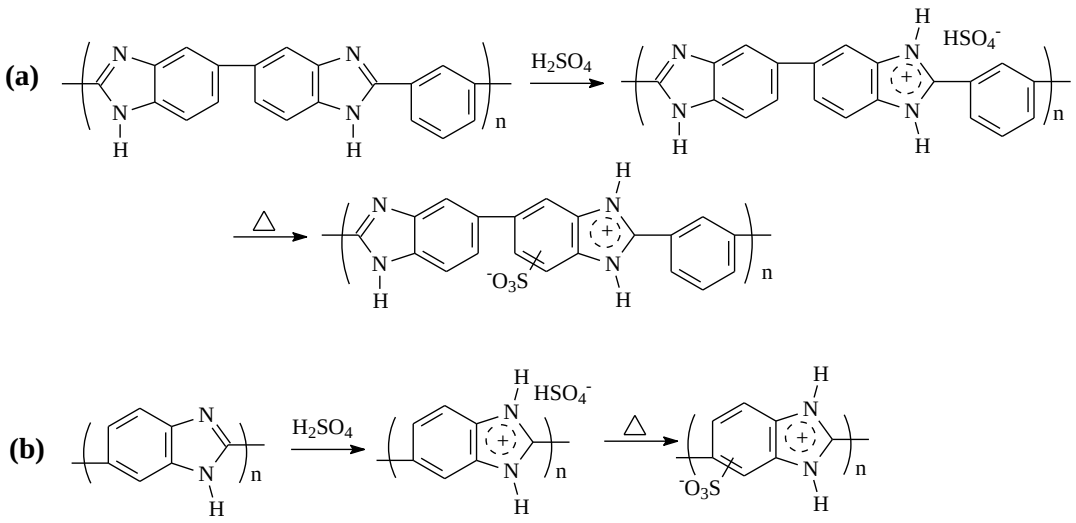

Figure 1. 28. Sulfonation of (a) PBI and (b) ABPBI

However, post sulfonation of poly(benzimidazole)s received a lot of attention as hosts for phosphoric acid doping. Under the same acid doping condition, sulfonated PBIs show much higher proton conductivities than nonsufonated ones. Gómez-Romero et al [103]. found the presence of sulfonic acid groups in the sulfonated AB-PBIs might facilitate the phosphoric acid doping. In their earlier work, the sulfonated PBI showed a conductivity up to two orders of magnitude higher than its nonsulfonated counterpart under the same circumstances [105]. This suggested that the sulfonic acid groups themselves might also contribute to the proton conductivity.

Another approach of post sulfonating poly(benzimidazole)s is proton abstraction with an alkali metal hydride, followed by reaction with sodium (4-bromomethyl)benzenesulfonate [106, 107]. The degree of sulfonation, which is critical to study of the PEM properties, can be controlled by this method.

1.3.3.2 Direct Copolymerization of Sulfonated Aromatic 5-membered-ring

Heterocyclic Polymers

Sulfonated aromatic 5-membered-ring heterocyclic polymers such as poly(benzimidazole), poly(benzoxazole) and poly(benzothiazole) homopolymers have been synthesized by the direct polymerization of sulfonated diacid monomers, which are shown in Figure 1.29 [105, 108-110].

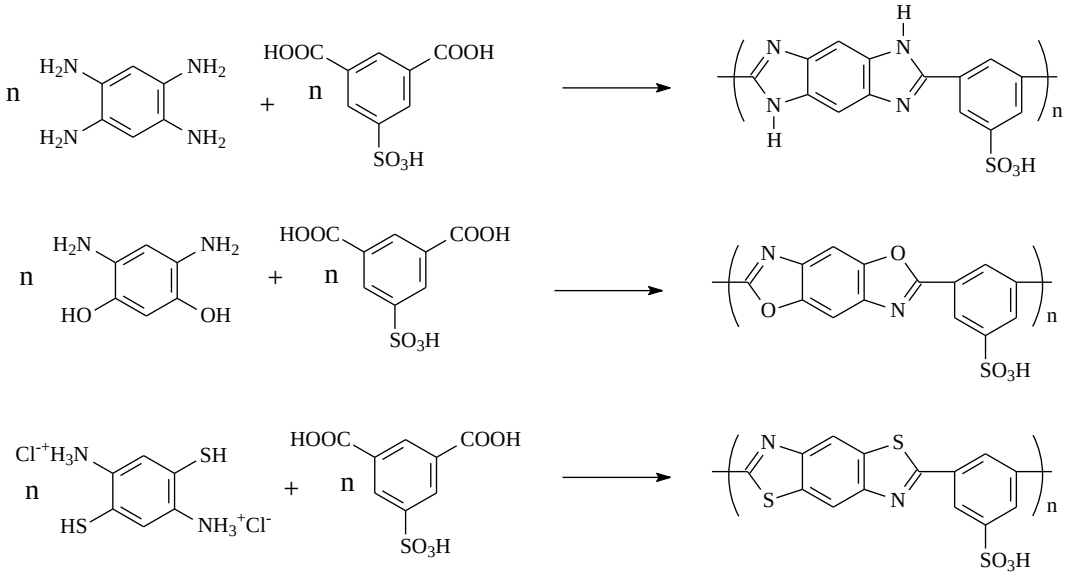

Figure 1. 29. Synthesis of sulfonated heterocyclic homopolymers

Yan et al. reported the detailed synthesis of partially sulfonated poly(benzimidazole) random copolymers. However, they did not systemically study the PEM properties of the polymers [111, 112]. Figure 1.30 shows the synthetic scheme of partially sulfonated poly(benzimidazole).

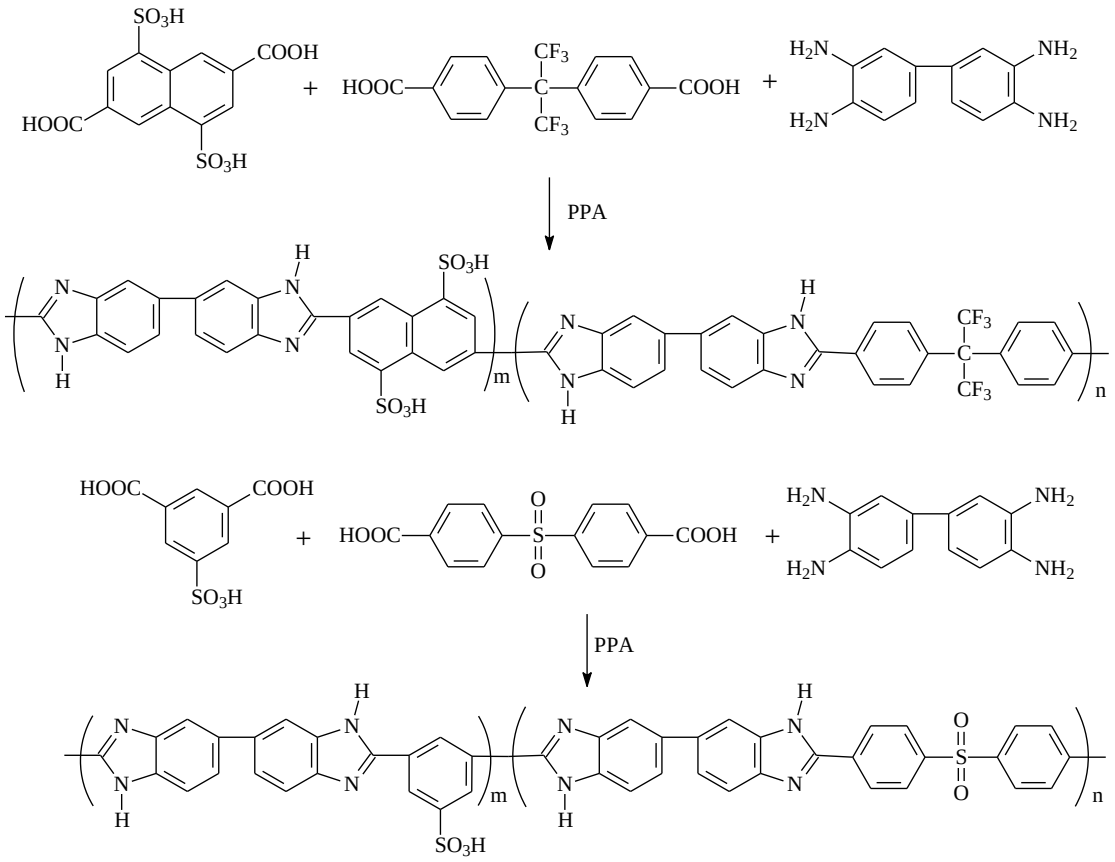

Figure 1. 30. Synthesis of sulfonated poly(benzimidazole) random copolymers

1.3.4 Poly(*p*-phenylene) Derivatives

Substituted poly(2,5-benzophenone)s (PBP)s are important poly(*p*-phenylene)s derivatives which are well known for their high degree of polymerization, good solubility in dipolar, aprotic solvents, as well as excellent thermal and oxidative stability and mechanical properties. Furthermore, the pendent phenyl rings enable modifications with various functional groups. As Figure 1.31 shows, the monomers are synthesized via Friedel-Crafts acylation of substituted benzene with 2,5-dichlorobenzoyl chloride. PBPs are prepared by the nickel-catalyzed polymerization [113, 114].

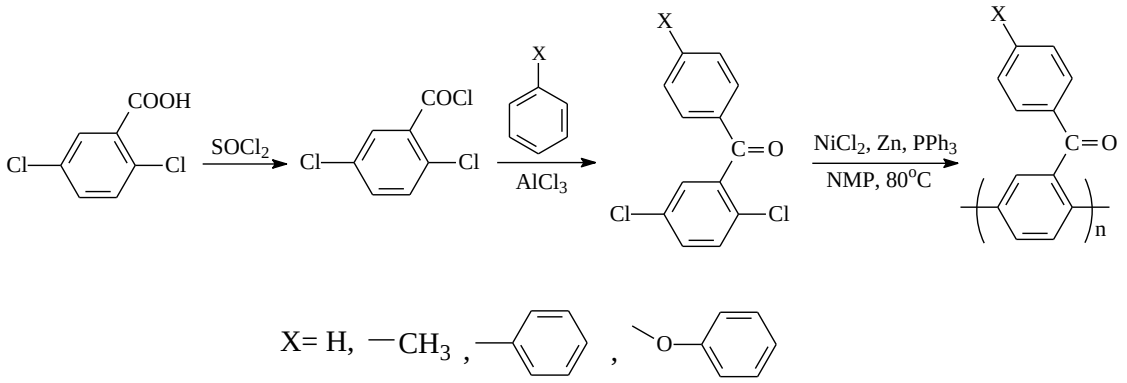

Figure 1. 31. Synthesis and polymerization of 2,5-dichlorobenzophenone monomers

1.3.4.1 Post Sulfonation of Poly(p-phenylene) (PPP) Derivatives

Generally, post sulfonation of poly(*p*-phenylene) derivatives is carried out at room temperature with fuming sulfuric acid or chlorosulfonic acid as sulfonation reagents. The degree of sulfonation can be controlled by the feed ratio of sulfonation reagent to the poly(*p*-phenylene) derivatives, or the sulfonation time. Okamoto et al. reported sulfonation of unsubstituted poly(2,5-benzophenone)s [115]. They believed the phenyl rings in the main chains, rather than the pendant phenyl rings, were susceptible to sulfonation. However, this interpretation is still a source of contention. Figure 1.32 shows the structures of partially sulfonated poly(2,5-benzophenone).

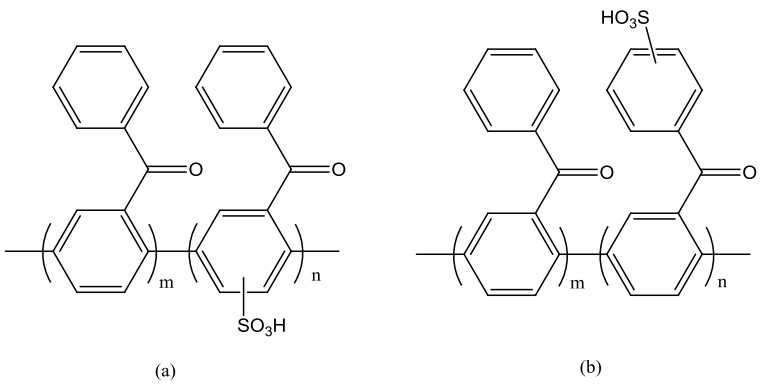

Figure 1. 32. Structures of sulfonated poly(2,5-benzophenone)s; (a): main chain sulfonated, (b): side chain sulfonated

Fujimoto et al. developed a series of poly(phenylene)s (DAPPs) from 1,4-bis(2,4,5-triphenylcyclopentadienone) benzene and 1,4-diethynylbenzene via Diels-Alder polymerization [116]. DAPPs were sulfonated with chlorosulfonic acid at room temperature. Figure 1.33 shows the synthesis of DAPPs and SDAPPs.

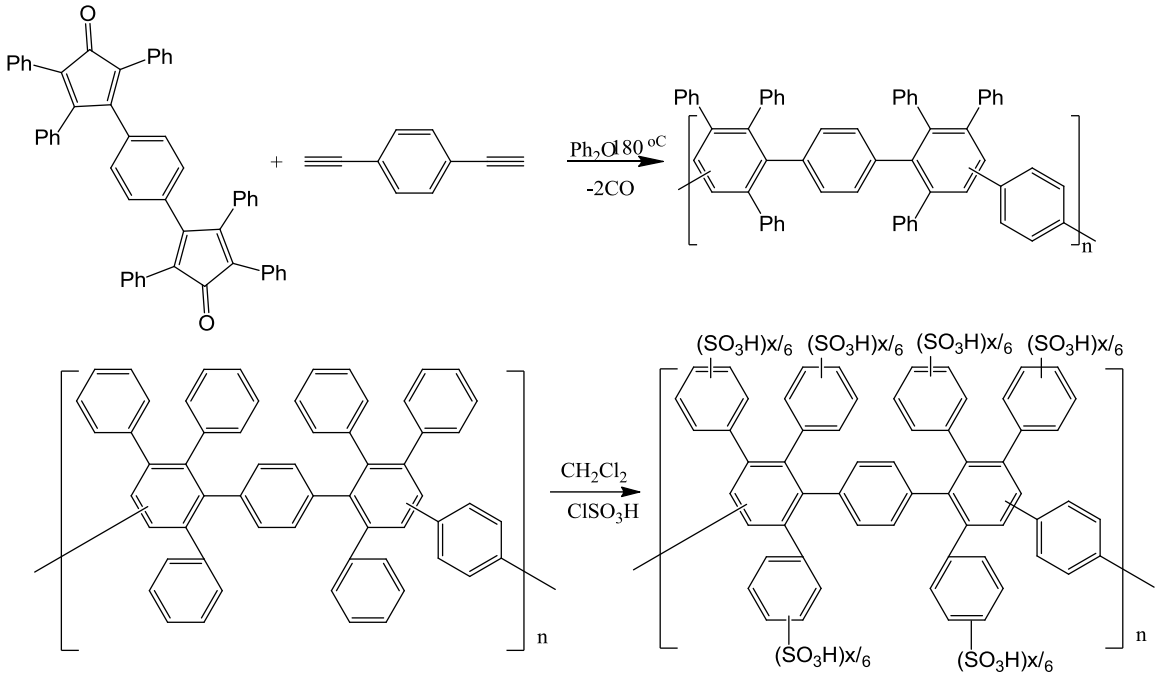

Figure 1. 33. Synthesis and sulfonation of DA poly(phenylene)

Fuel cell relevant properties such as high proton conductivity and high IEC were observed. Although the Young's modulus of the sulfonated DAPP (SDAPP) was as high as 1.2×10^9 Pa, the elongation of the SDAPP membrane was low. SDAPP membrane would break at 12% elongation in the dry state.

1.3.4.2 Direct Synthesis of Sulfonated Poly(p-phenylene) Derivatives

Ghassemi and McGrath reported the synthesis of sulfonated poly(4-phenoxybenzoyl-1,4-phenylene) by condensation of poly(4-fluoro-2,5-benzophenone) with 4-hydroxybenzenesulfonic acid [114], as shown in Figure 1.34.

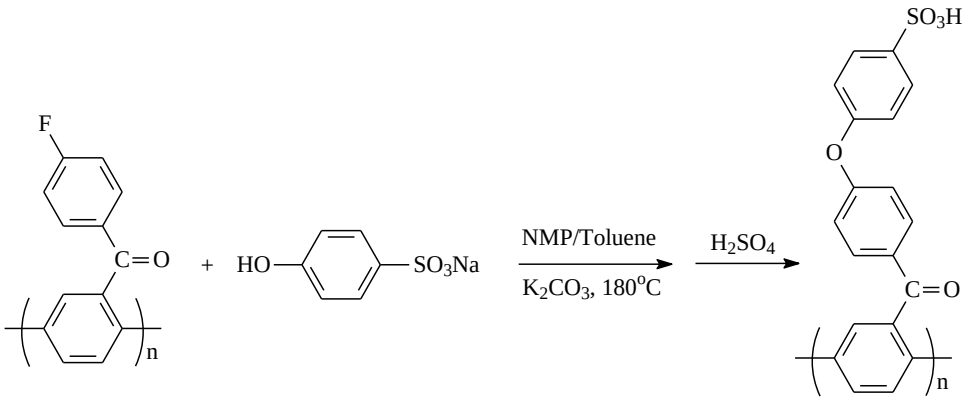

Figure 1. 34. Sulfonation of poly(4-fluoro-2,5-benzophenone)

Zhang and his colleagues reported direct synthesis of sulfonated poly(*p*-phenylene)s (SPPs) by Ni(0) catalytic coupling of sodium 3-(2,5-dichlorobenzoyl) benzenesulfonate and 2,5-dichlorobenzophenone [117], as shown in Figure 1.35.

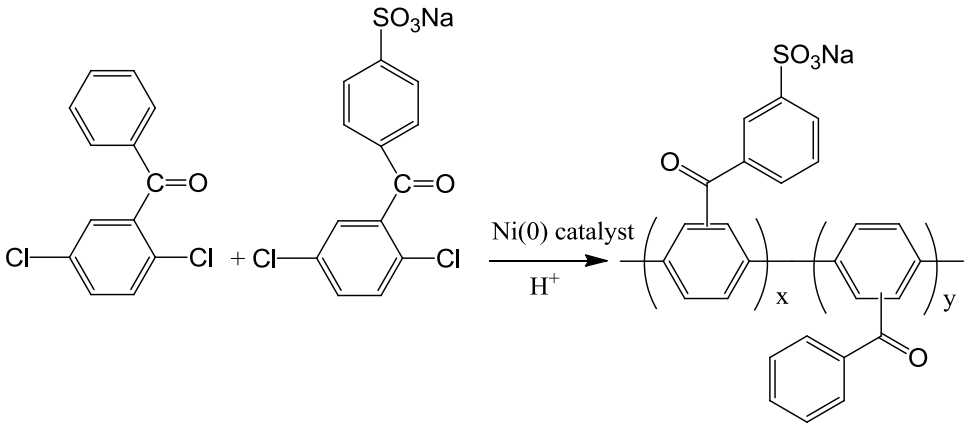

Figure 1. 35. Directy synthesis of sulfonated poly(2,5-benzophenone)

At 120 ^{o}C, the proton conductivity of the SPPs increased to as high as 0.34 S/cm with the degree of the sulfonation increased, which was almost 3 times higher than

Nafion 117 under the same condition. However, the SPP with a 50% degree of sulfonation tended to break at 12% elongation in the dry state, which indicated that SPPs behaved more like engineering thermoplastics rather than rubbery materials.

Similar to nonsulfonated poly(*p*-phenylene)s (PPPs), the membrane-forming performance of sulfonated PPP derivatives were poor, which limited the applications of sulfonated PPP as PEMs. Although the pendant substituted groups improved the solubility of the sulfonated PPPs, only brittle films with poor mechanical properties were obtained due to the very rigid backbone of sulfonated PPPs.

1.4 Fluorinated Aromatic High Performance Copolymers for PEMs

1.4.1 Moderately Fluorinated Copolymers Containing Hexafluoroisopropylidene units

Fluorinated polymers possess high thermal stability, excellent chemical resistance as well as outstanding mechanical strength. Fluorinated polymer backbone PEMs have been intensively studied by many research groups [74, 78, 118-122]. Low water uptake and water transport, along with the capability for fabrication into membrane electrode assemblies (MEAs), are two important critical issues for PEMs. The fluoro groups in the polymers are strongly hydrophobic which could reduce water uptake of the PEMs. Furthermore, the presence of the fluorine units leads to better compatibility with the Nafion®-based electrodes. 4,4′-hexafluoroisopropylidene diphenol (6F-BPA) has been widely used in the synthesis of sulfonated poly(arylene ether)s to introduce fluorine units.

Due to the electron-withdrawing property of the hexafluoroisopropylidene linkage,

6F-BPA has relatively low reactivity with aryl dichloride comonomers. Longer polymerization time, higher temperature and higher reaction solution concentration or difluoride arly comonomers may bring about partial success in the synthesis of high molecular weight hexafluoroisopropylidene-containing copolymers.

Harrison et al. synthesized a series of partially fluorinated, partially disulfonated poly(arylene ether sulfone)s [74], as shown in Figure 1.36. Thermogravimetric analysis (TGA) data showed that thermal stabilities of the partially fluorinated poly(arylene ether sulfone)s were improved compared to the non-fluorinated polymers. At the same degree of disulfonation, the partially fluorinated membranes showed lower water uptake and lower IEC which would greatly affect the proton conductivity of the membranes.

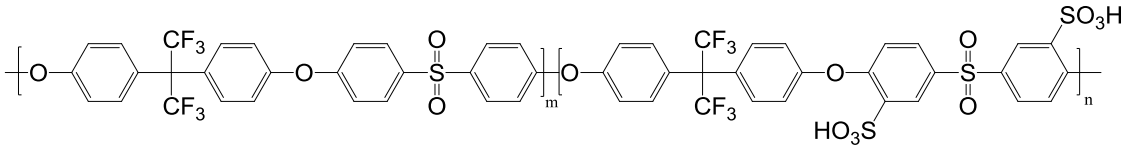

Figure 1. 36. Structures of partially sulfonated, partially fluorinated poly(arylene ether sulfone)s

Wiles et al. investigated the fuel cell behavior of partially fluorinated sulfonated poly(arylene ether sulfone)s with a 45% degree of disulfonation [123], as shown in Figure 1.37. The components of hexafluoroisopropylidene were varied from 0 to 100 mol% by adjusting 6F-BPA and the correct stoichiometric amount of 4,4 ′-biphenol. At room temperature, the IEC and proton conductivities of the membranes decreased as the mol fraction of 6F-BPA increased.

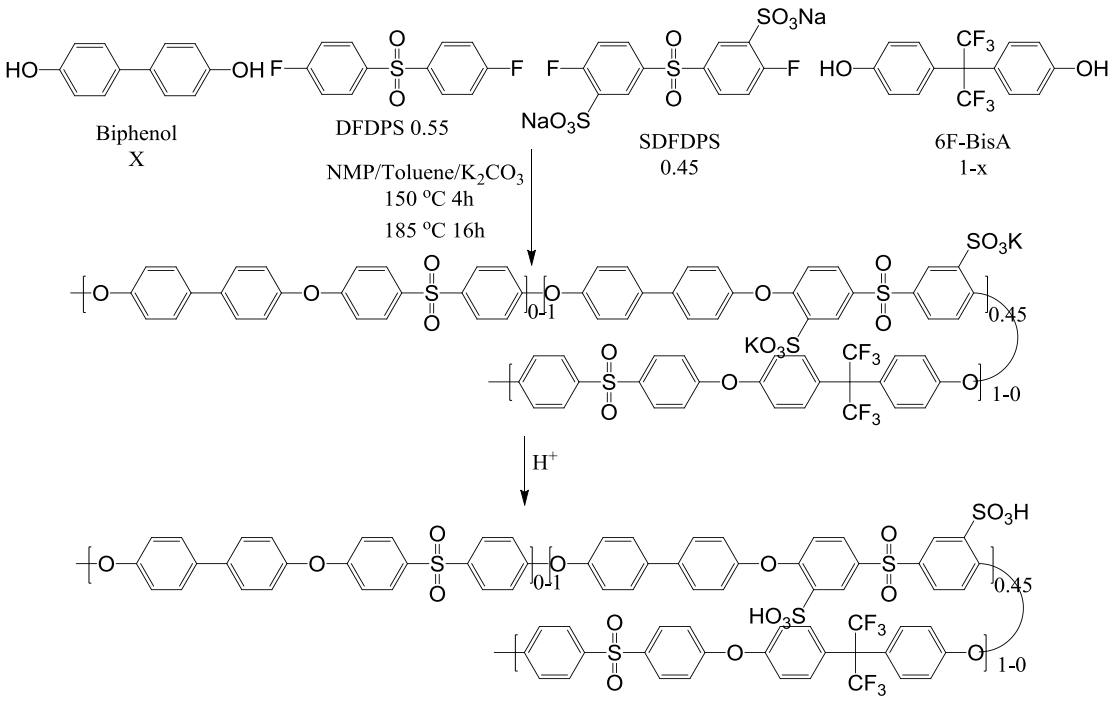

Figure 1. 37. Synthesis of 45 mol% disulfonated partially fluorinated poly(arylene ether sulfone) random co- and terpolymers

Partially fluorinated poly(arylenethioethersulfone) copolymers containing pendant sulfonic acid groups for PEM wers reported by Dang et al [124]. Those coplymers, as shown in Figure 1.38, were synthesized by 4,4 ´-(Hexafluoroisopropylidene)-diphenylthiol, 4,4 ´-Difluorodiphenylsulfone, and 3,3 ´-disulfonate-4,4 ´-difluorodiphenylsulfone. At 85% RH and 85 ^{o}C the proton conductivity was obtained as high as 0.12 S/cm for 6FSPTES-50, where 50 is the degree of sulfonation. The water uptake of 6FSPTES-50 increased with temperature increased in liquid water. At 95 ^{o}C, the water uptake of 6FSPTES-50 still did not reach 40 wt%.

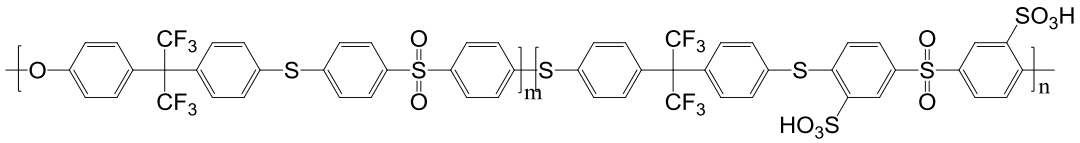

Figure 1. 38. Structures of partially fluorinated suflonated poly(arylenethioethersulfone)s

A series of partially fluorinated sulfonated poly(arylene ether benzonitrile)s (6FPAEBs) were synthesized with SDCDPS, 6F-BPA and 4,4´-dichlorobenzonitrile (DCBN) by Sumner et al. [78]. Acidified 6FPAEB membranes showed a relatively low water uptake relative to membranes made from non-fluorinated sulfonated poly(arylene ether sulfone). The proton conductivity of the copolymer with 35 mol% of the disulfonated comonomer was slightly higher than 0.10 S/cm at 110 °C and 100% relative humidity. The synthetic scheme is shown in Figure 1.39.

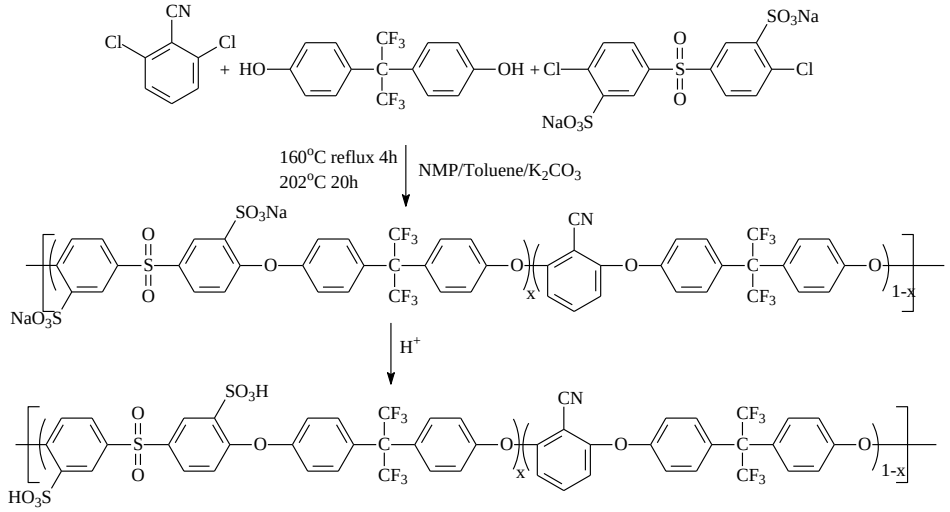

Figure 1. 39. Directly copolymerization of partially fluorinated sulfonated poly(arylene ether benzonitrile)

Li et al. synthesized three series of random copolymers with 6F-BPA; 3 ketone-type

monomers: 4,4´-difluorobenzophenone (DFK), 1,4-bis(p-fluorobenzoyl)benzene (PBFB), and 1,3-bis(p-fluorobenzoyl)benzene (MBFB); and their corresponding sulfonated monomers [125], as shown in Figure 1.40. At similar IEC levels, copolymers containing sulfonated and nonsulfonated *meta* diketone repeat units showed the highest water uptake and proton conductivities. The 'DFK' series membranes also showed lower methanol permeability compared to Nafion®. Other researchers also adopted 6F-BPA in preparing sulfonated poly(arylene ether ketone)s for PEMs to reduce water uptake of the membranes [126, 127].

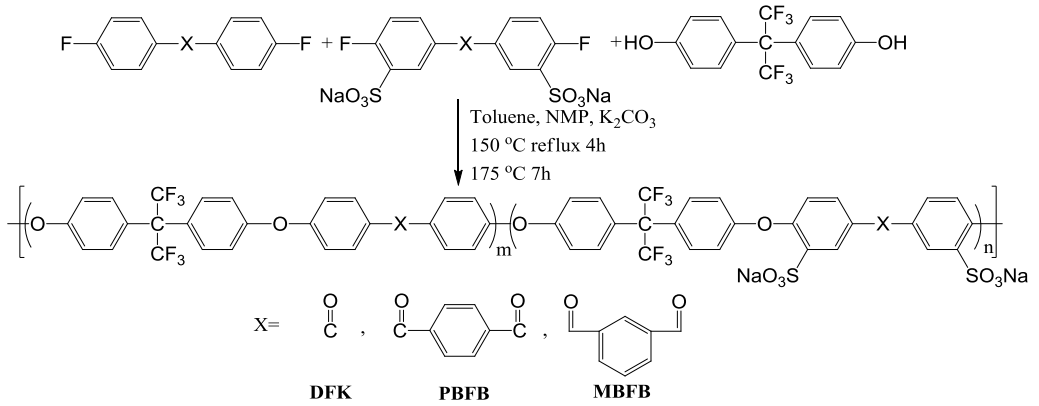

Figure 1. 40. Synthesis of three series of disulfonated poly(arylene ether ketone) copolymers

1.4.2 Highly Fluorinated Copolymers Containing Perfluorophenylene Units

Poly(arylene ether)s containing perfluorophenylene groups were initially developed as optical wave guide materials for potential telecommunication applications due to their thermal and chemical stability, low dielectric constant, small refractive index, less optical loss, and low moisture absorption [128-132]. The most widely used perfluorinated

monomer is decafluorobiphenyl. Figure 1.41 shows the step growth polymerization of poly(arylene ether)s containing perfluorophenylene groups.

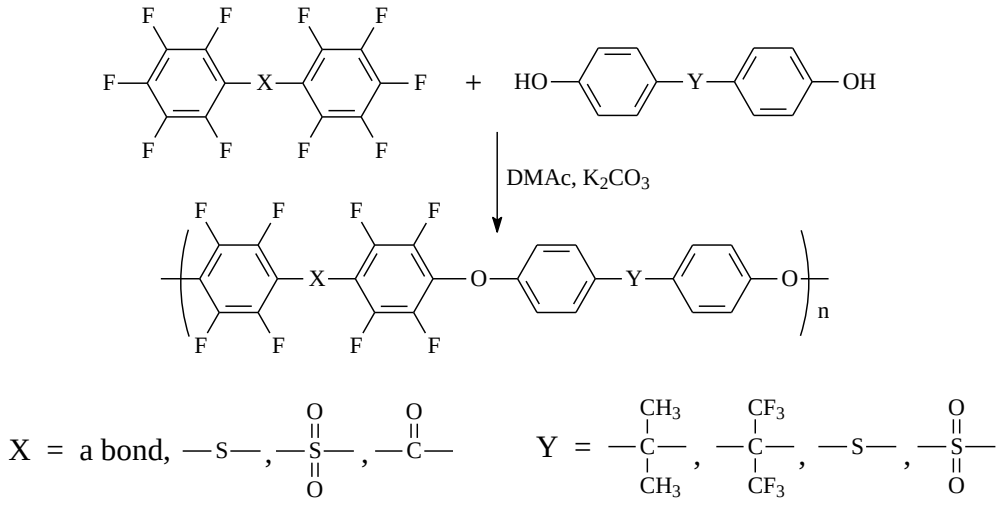

Figure 1. 41. Synthesis of poly(arylene ether)s containing perfluorophenylene units

Due to the high reactivity of fluorine substituents on the phenyl rings, fluorines at *ortho*-positions may also participate in the reaction and produce branched or even crosslinked structures as shown in Figure 1.42 [132, 133]. Therefore, low polymerization temperature is necessary to reduce undesirable side reactions.

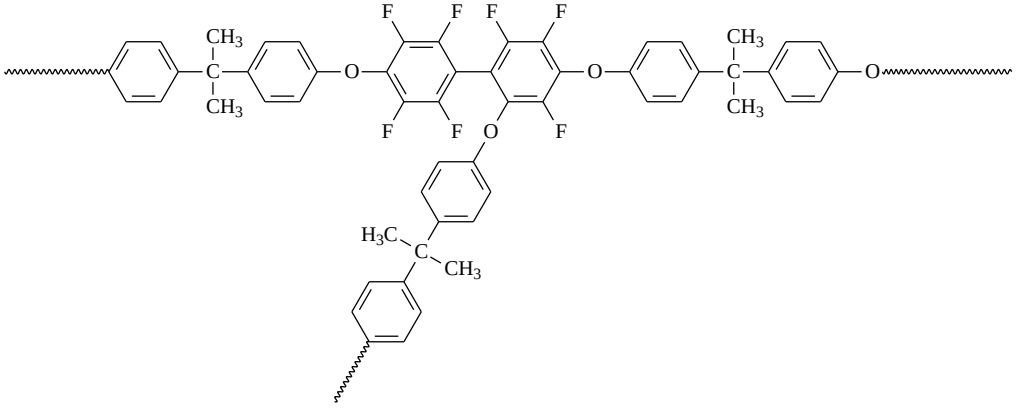

Figure 1. 42. Reactions of *ortho*-position fluorine leading to branching or corsslinking

Lee et al. synthesized two types of highly fluorinated poly(arylene ether)s with

DFBP and 6F-BPA or Bis-A, respectively[121]. Then the highly fluorinated poly(arylene ether)s were sulfonated with fuming sulfuric acid (30% SO_3), as shown in Figure 1.43. The degree of sulfonation was controlled by the amount of fuming sulfuric acid and/or the sulfonation time. At similar IEC levels, these post-sulfonated highly fluorinated poly(arylene ether)s showed higher water uptake and lower proton conductivities relative to Nafion® 117. Moreover, sulfonated DFBP-6F-BPA copolymers showed much lower water uptake than sulfonated DFBP-BisA copolymers but maintained comparable proton conductivities.

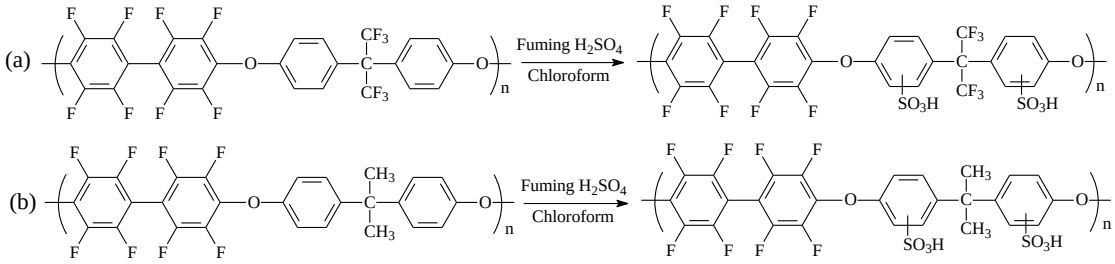

Figure 1. 43. Post sulfonation of highly fluorinated poly(arylene ether)s

Hay et al. synthesized highly fluorinated random copolymers with DFBP and bulk bisphenol comonomers [119, 120]. The copolymers were sulfonated with chlorosulfonic acid. Figure 1.44 shows the synthetic and sulfonation scheme. The sulfonation occured only at the *para* positions on the pendant phenyl rings due to the designed structure of the bisphenols. Furthermore, the sulfonation reaction with chlorosulfonic acid was quantitative, so the degree of sulfonation could be controlled by the molar feed ratio of the comonomers.

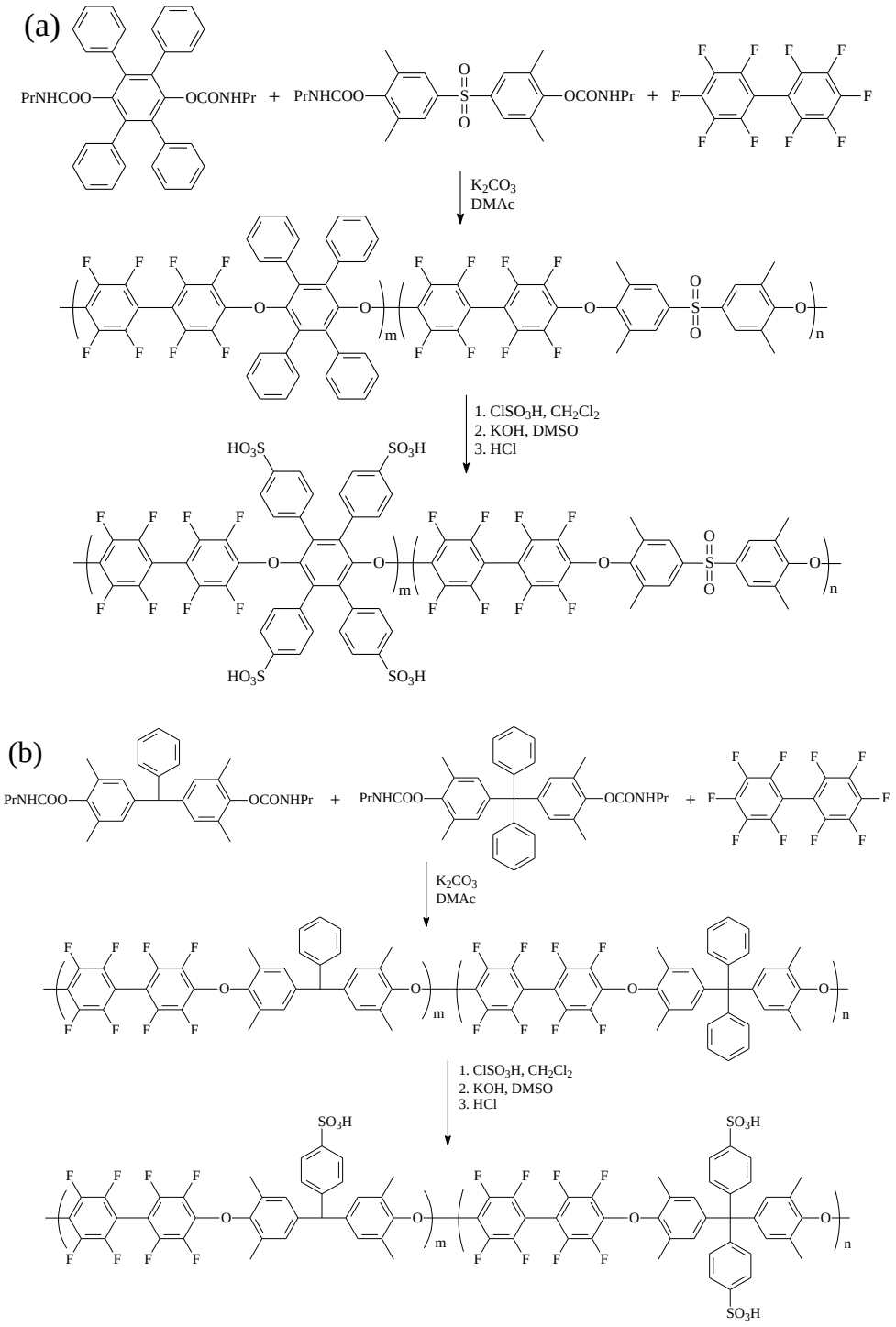

Figure 1. 44. Synthesis and sulfonation of fluorinated poly(arylene ether sulfone) random copolymers

Kim and coworkers reported the synthesis of sulfonated random copolymers for PEMs with 2,8-dihydroxynaphthalene-6-sulfonated sodium salt (2,8-DHNS-6), 6F-BPA and DFBP [122]. The synthetic scheme is shown in Figure 1.45.

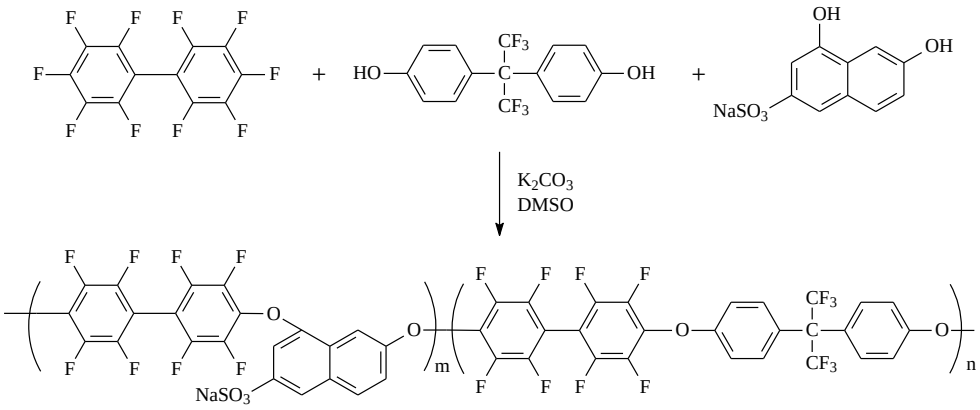

Figure 1. 45. Direct dynthesis of sulfonated perfluorinated poly(arylene ether) random copolymers

1.5 Hydrophilic-Hydrophobic Block Copolymer Systems as PEMs

Proton conductivity of statistical sulfonated copolymers such as BPSH strongly depend upon the relative humidity. Although BPSH and other copolymers show comparable proton conductivity to Nafion® in fully hydrated states, proton conductivity of those statistical copolymers decrease significantly as the relative humidity decreases. The loss of proton conductivity at lower humidity might be due to narrow proton channels, less phase separation, more dead-ended channels as well as larger SO_3^-/ SO_3^- separation in BPSH and other statistical copolymers [134]. To develop alternative PEM materials with better hydrophilic domain connectivity is a challenge for researchers.

Fortunately, hydrophilic/hydrophobic block copolymers might meet the criteria

discussed above. Figure 1.46 shows several architectures of copolymers. It can clearly be seen that in hydrophilic/hydrophobic block copolymers, the SO_3^- groups are selectively incorporated in one or more hydrophilic blocks. At the same time, these hydrophilic blocks array in ordered sequences. The incorporation and association of the SO_3^- groups along hydrophilic blocks might create wide and continuous proton channels as well as enhanced aggregation of ionic group.

Another important issue for PEM performance at low humidity is phase separation. It has been reported that the semi-crystalline copolymer Nafion® showed a nanophase separated morphology in the low humidity state, the ionic clusters interconnected to form ion channels for water and ion transportation [15]. This unique nanophase separation provided good proton transport at low water contents and/or high temperatures. If alternative PEM materials with hydrophilic-hydrophobic blocks could form the nanophase morphology like some diblock copolymers, such as the poly(styrene-*b*-butadiene) shown in Figure 1.47 [135], the diffusion coefficient and the transport processes would be greatly enhanced by the continuous hydrophilic phase. The mechanical stability and reduction of swelling would also be improved by the continuous hydrophobic phase. Copolymers with separated continuous nanophases might be beneficial for higher proton conductivity at lower humidities [136].

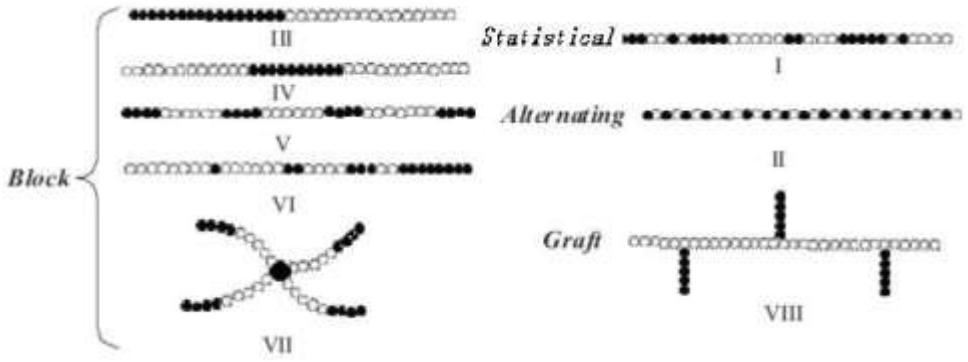

Figure 1. 46. Illustration of copolymer architectures

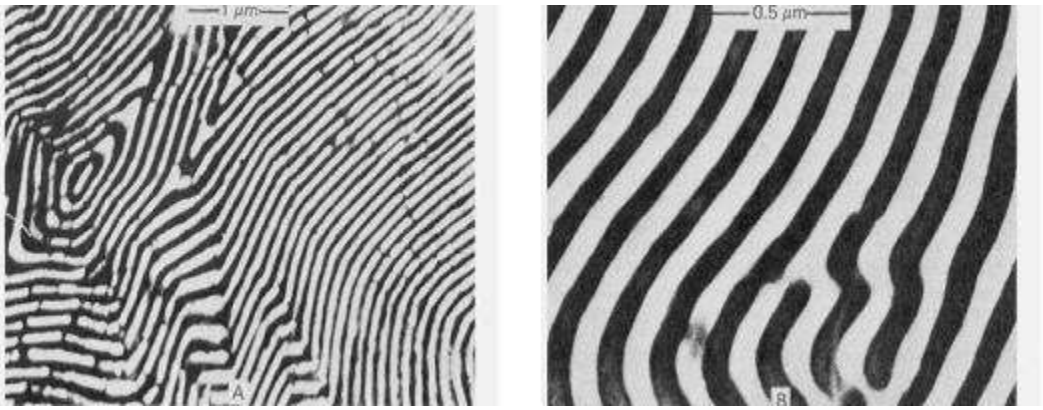

Figure 1. 47. Nanophase separation morphology in poly(styrene-*b*-butadiene)

1.5.1 Aliphatic Backbone Block Copolymers for PEMs

Dais Analytic Corporation introduced new PEMs of sulfonated styrene/ethylene-butene/styrene tri-block copolymers (PSEBS) [137]. The nonsulfonated precursor is better known as the commercially available block copolymers Kraton. Figure 1.48 shows the chemical structure of the Dais Analytic PEMs. The unsulfonated PSEBS was dissolved in dichloroethane/cyclohexane solvent mixture. Then the sulfur

trioxide/triethylphosphate sulfonating reagents were added. Sulfonation temperature was controlled between –5 ℃ and 0 ℃. Wnek et al. reported the properties of sulfonated PSEBS PEMs with 18 mol% polystyrene and 55 % sulfonation degree of the PS blocks [32, 137, 138]. When fully hydrated, proton conductivity of the membrane was 0.085 S/cm, which was comparable to Nafion® 117's 0.079 S/cm. However, the water uptake of sulfonated SEBS membrane was 3 times higher than that of Nafion®.

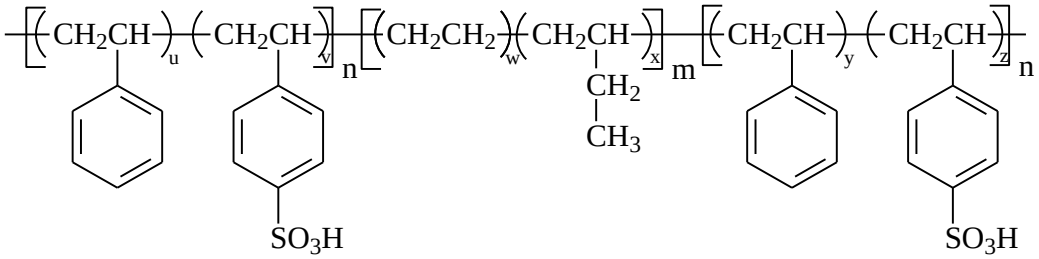

Figure 1. 48. Chemical structure of sulfonated SEBS triblock copolymers

Transmission electron microscopy (TEM) studies of the membranes indicated distinct nanophase separated structures. X-ray and neutron scattering studies also revealed co-continuous hydrophobic/hydrophilic domains. The properties of sulfonated SEBS with 20-30 mol% of styrene were also studied [139, 140]. With the increase of the sulfonation degree, the water absorption and the proton conductivity both increased.

There are some drawbacks of sulfonated SEBS, such as higher volume water uptake, higher methanol permeability, and poorer oxidative stability compared to Nafion®, because of its aliphatic backbone.

Just like SEBS, another kind of commercially available block copolymer, poly(styrene-isobutylene-styrene) (SIBS) was sulfonated with acetyl sulfate in methyl chloride by Elabd et al. [141, 142]. Figure 1.49 shows the structure of sulfonated SIBS

(S-SIBS) block copolymers. The IEC of S-SIBS increased from 0.12 meq/g to 0.97 meq/g as the degree of sulfonation increased.

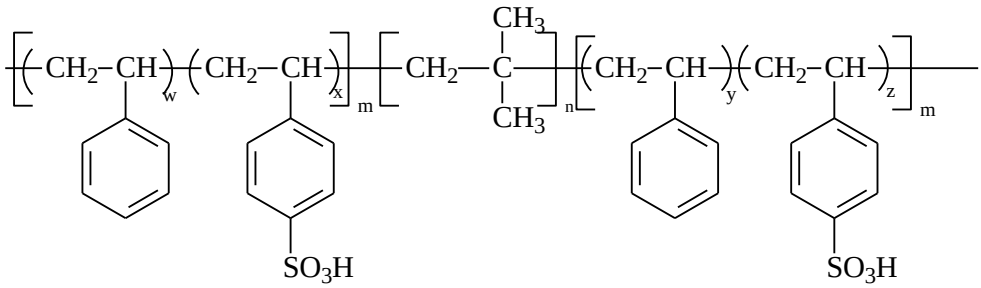

Figure 1. 49. Structure of S-SIBS block copolymers

The membranes were tested via two different geometric configurations, one is '*in the plane'* and the other is '*normal to the plane'*, which are shown in Figure 1.50. When the conductivity of Nafion® was measured through those two directions, the proton conductivity only showed a 2.5-fold difference. In contrast to Nafion®, the conductivity of S-SIBS series membranes decreased by a factor of 9 to12 between '*in the plane'* and '*normal to the plane'* measurements in the range of IECs from 0.6 to 1.0 meq/g. When '*in the plane'* measurements were applied, the methanol permeability of S-SIBS-1.0 meq/g was 10 times less than Nafion® 117, while the conductivity was only 2 times less than Nafion® 117. But when '*normal to the plane'* measurements were applied, the methanol permeability of S-SIBS-1.0 meq/g was 15 times less than Nafion® 117, while the conductivity was over 10 times less than Nafion® 117. This difference revealed that nanophase separated morphology in S-SIBS possessed a better orientation '*in the plane'*, which was also confirmed by small angle X-ray scattering (SAXS) studies.

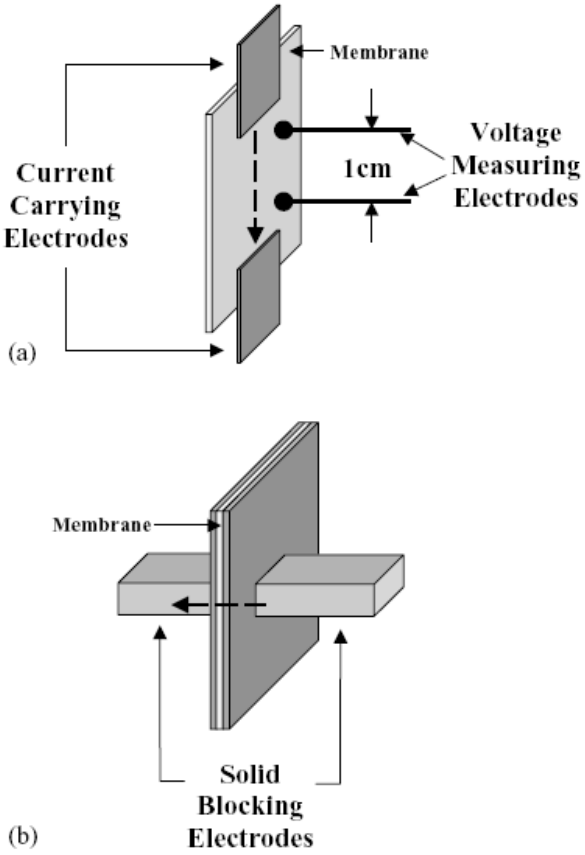

Figure 1. 50. (a) Four-electrode cell (in the plane of the membrane) and (b) two-electrode cell (normal to the plane of the membrane)

There are several disadvantages of hydrocarbon backbone PEM materials, such as poorer oxidative stability, less phase separation and more water uptake. Shi et al. synthesized partially fluorinated block copolymers for PEMs [37, 143]. First, poly(vinylidene difluoride-co-hexafluoropropylene) (PVDF-*co*-PHFP) macroinitiators with terminal chloride groups were synthesized via emulsion polymerization of vinylidene difluoride (VDF) and hexafluoropropylene (HFP) in the presence of chloroform. Then via atom transfer radical polymerization (ATRP), the PVDF-*co*-PHFP

-*b*-PS block copolymers were prepared as shown in Figure 1.51. The chain length of each block could be adjusted. Sulfonation of the block coplymers was carried out in 1,2-dichloroethane by acetyl sulfate to achieve ionmers with degrees of sulfonation up to 50%.

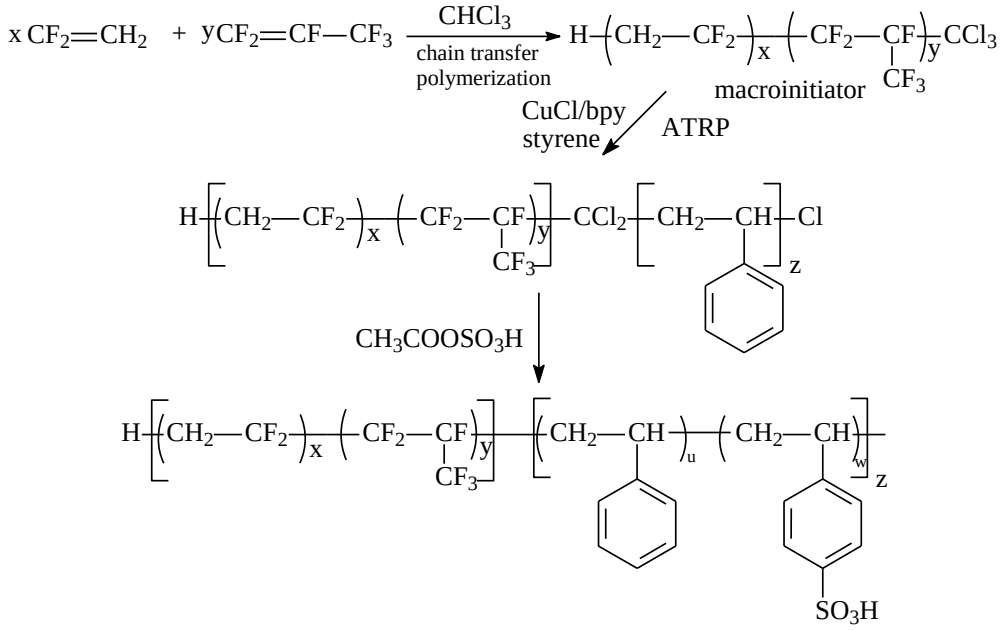

Figure 1. 51. Synthesis of partially sulfonated (PVDF-*co*-PHFP)-*b*-PS Copolymer

Proton conductivity of sulfonated (PVDF-*co*-PHFP)-*b*-PS reached a maximum at 40 % degree of sulfonation of the PS block. Further increases of the degree of sulfonation for sulfonated (PVDF-*co*-PHFP)-*b*-PS significantly increased water uptake. At a degree of sulfonation of 49% of the PS block, water uptake by the membrane reached 388%, which resulted in a significant drop of the proton concentration and induced low proton conductivity.

1.5.2 Partially Aromatic Multiblock Copolymers

Recently, Zhang et al. reported a new block copolymer for PEMs [144, 145]. The authors synthesized poly(arylene ether sulfone)-b-polybutadiene (PAES-b-PB) and then sulfonated the polymer to obtain the sulfonated block copolymer as shown in Figure 1.52. The proton conductivity of the sulfonated block copolymer exhibited as high as 0.0303 S/cm at a low degree of sulfonation (11.5%). However the water uptake of the membrane was high even at such low degrees of sulfonation. The unsaturated section (double bond in polybutadiene) was easily attacked by the oxidants and radicals produced in fuel cells. On the other hand, the unsaturated sections were good places for crosslinking reactions, which might help to control water uptake.

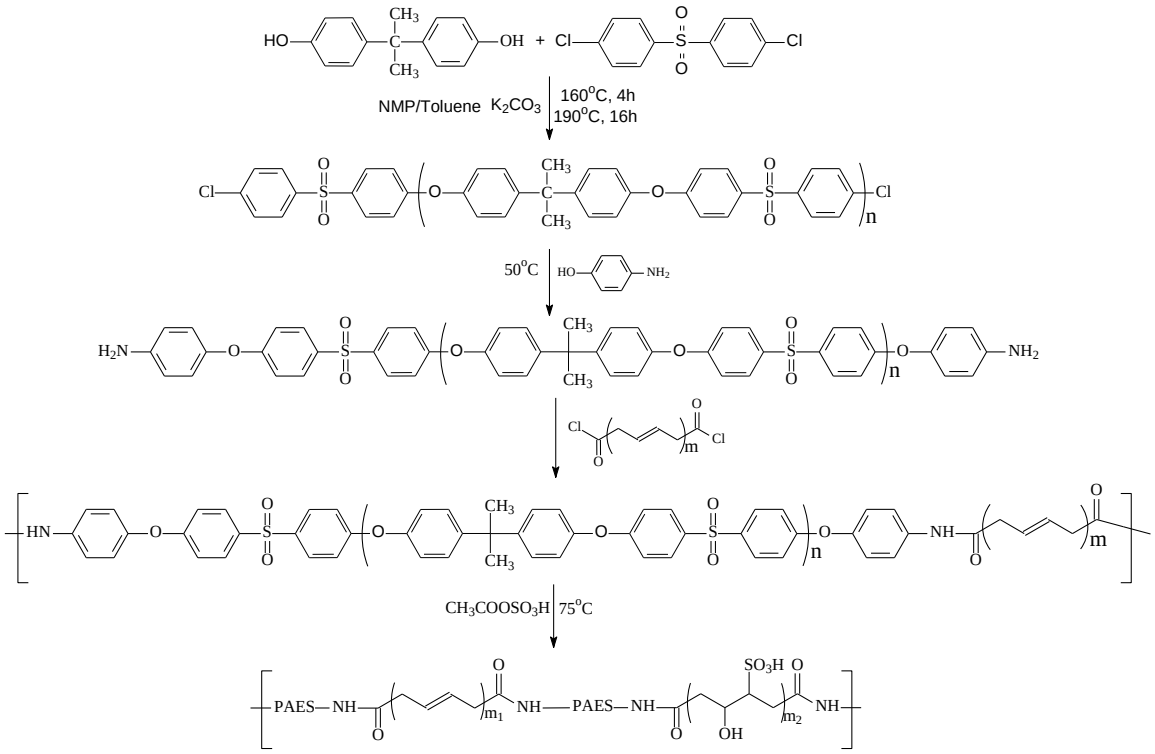

Figure 1. 52. Scheme of SPAES-b-PB synthesis

Later, to improve the thermal oxidative stability of their PAES-b-PB multiblock copolymers, Zhang and coworkers modified their SPAES-b-PB polymers [146]. They

epoxidated PB blocks of the copolymer by an ***in situ*** generated peracid method, as shown in Figure 1.53. Mechanical properties and thermal stability of the modified SPAES-b-PB series of polymers were slightly improved after epoxidation. However the proton conductivity of the epoxidated SPAES-b-PB did not show significant improvement. Only one membrane with a degree of sulfonation of 15.7% showed increased proton conductivity relative to its nonepoxidated membrane counterpart. Water uptake of all epoxidated membranes increased slightly, but the changes were insignificant with respect to performance.

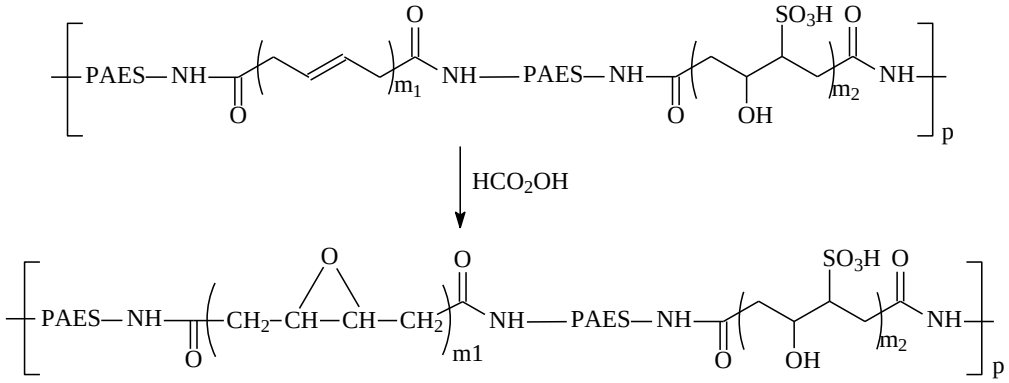

Figure 1. 53. Modification of SPAES-b-PB

Yang et al. reported the synthesis and characterization of sulfonated PAES-PVDF multiblock ionomer membranes [147, 148], which are shown in Figure 1.54. PAES-b-PVDF block copolymers were synthesized by a coupling reaction of hydroxy-terminated PAES oligomers and α,ω−dibromo PVDF oligomers with controlled molecular weight. The block copolymers were sulfonated with $(CH_3)_3SiSO_3Cl$ in $CHCl_3$. The degree of sulfonation can be controlled by the ratio of $(CH_3)_3SiSO_3Cl$ to the PAES repeat unit. As the degree of sulfonation increased, the IEC of the sulfonated

PAES-b-PVDF increased from 0.78 to 2.18 meq./g. Both proton conductivity and water uptake increased with IEC. For low IEC, the sulfonated PAES-b-PVDF showed higher proton conductivity than partially sulfonated PAES. It might be explained by the distinct separation of hydrophilic and hydrophobic domains. TEM pictures showed phase separation in sulfonated PAES-b-PVDF membranes but further experiments such as SAXS are needed to gather more information about the morphology.

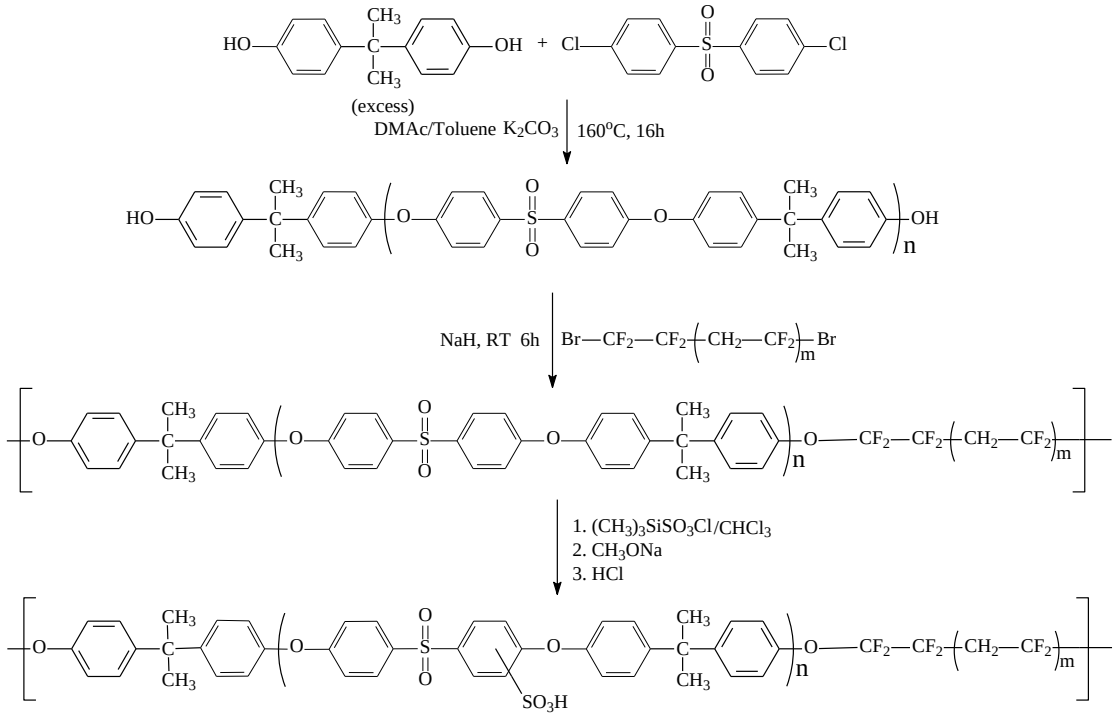

Figure 1. 54. Synthesis of sulfonated PAES-PVDF multiblock copolymers

1.5.3 Wholely Aromatic Multiblock Copolymers

Wholely aromatic copolymers synthesized via step growth polymerizations have many advantages, such as thermal stability, chemical resistance and excellent mechanical properties. The synthesis of wholely aromatic hydrophobic-hydrophilic multiblock

copolymers can be carried out in polar solvents such as dimethyl sulfoxide (DMSO) or *N*-methyl-2-pyrrolidinone (NMP) with hydrophobic and hydrophilic telechelic oligomers via a nucleophilic aromatic substitution mechanism.

Ghassemi et al. synthesized a series of new multiblock copolymers of sulfonated poly(4 ´-phenyl-2,5-benzophenone) and poly(arylene ether sulfone) for PEM applications [149]. The authors first synthesized poly(4 ´-phenyl-2,5-benzophenone) telechelic oligomers by Ni(0) catalytic coupling of 2,5-dichloro-4 ´-phenylbenzophenone and the end-capping agent 4-chloro-4 ´-fluorobenzophenone. The oligomers were then sulfonated in concentrated sulfuric acid at 50 ^{o}C. Next the hydroxyl-terminated poly(arylene ethersulfone) (PAES) was synthesized from 4,4 ´-dichlorodiphenylsulfone and 4,4 ´-biphenol. Finally, the multiblock copolymers were prepared by coupling the two types of oligomers, as shown in Figure 1.55.

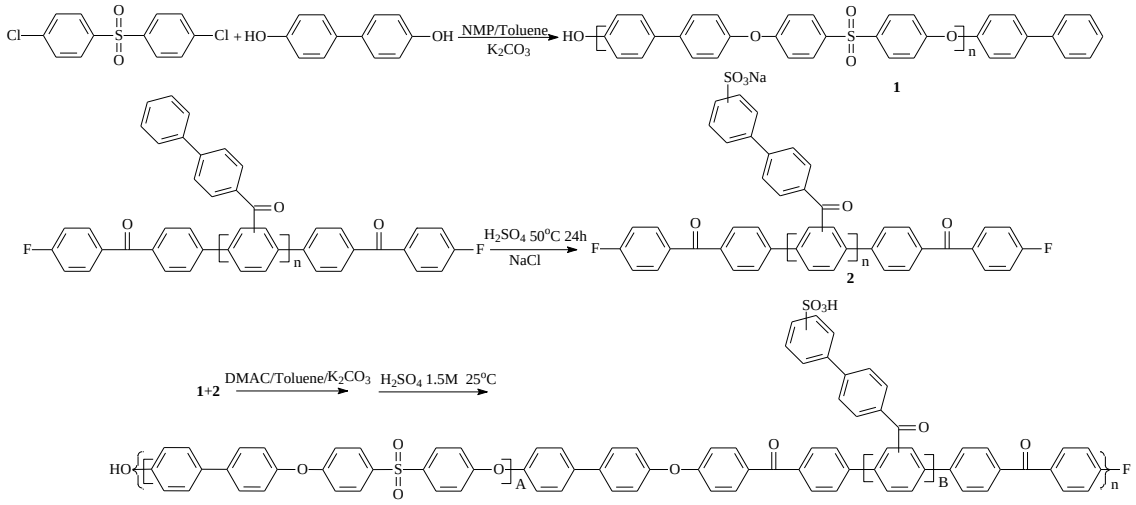

Figure 1. 55. Synthesis of Sulfonated PPP-PAES Multiblock Copolymer

The IEC and proton conductivity of this multiblock copolymer increased with the number of acid groups attached to the repeat units. The highest IEC and proton

conductivity of the multiblock copolymer were reported to be 1.2 meq./g and 0.036 S/cm respectively. Although the IEC value was comparable to Nafion® 117, the proton conductivity of this multiblock copolymer was still much lower. The authors also reported that the multiblock copolymers could form strong and flexible membranes even at low molecular weight (M_n <17,300 g/mol from size-exclusion chromatography (SEC)).

Shin et al. and Na et al. synthesized and characterized a series of poly(arylene ether ketone) multiblock copolymers [150, 151]. Figure 1.56 and Figure 1.57 show the synthetic schemes of sulfonated poly(arylene ether ketone) multiblock copolymers.

In Shin's and Na's work, hydrophobic oligomers with desired M_n were synthesized first. Because hydrophobic and hydrophilic oilgomers did not dissolve well synchronously in common solvents such as DMSO or NMP, the hydrophilic blocks were generated ***in-situ***, which meant the monomers of the hydrophilic block were added into the reaction flask of the hydrophobic oligomers to generate block copolymers. The main problem of so called ***in-situ*** generated block copolymers was that the block length of hydrophilic blocks varied substuntially, even though the M_n weight of hydrophobic blocks was fixed.

For block copolymers BC1a-BC2e (Figure 1.56), Shin found when the M_n of hydrophobic block was larger than that of the hydrophilic block, the acidified membranes were more flexible. Otherwise the membranes were more brittle. For block copolymer BC3a-BC3g, the mechanical properties were better than BC1a-Bc2e, since there was one $–SO_3H$ group in each hydrophilic repeat unit. BC3a displayed high conductivity and low water uptake (0.081 S/cm and 15%, respectively) at room temperature. The Young's modulus, yield stress and elongation at break of BC3a were 1.58 GPa, 88 MPa and 114%,

respectively.

Na reported the synthesis and characterization of 3 different sulfonated block poly(ether ether ketone)s (S-PEEKs) with degrees of sulfonation of 0.36 (Block-1), 0.32 (Block-2) and 0.27 (Block-3). The block S-PEEK membranes showed comparable mechanical properties to random S-PEEK membranes. Only Block-3 membrane showed better conductivity performance than the random S-PEEK membrane at different temperatures, even the IEC value of block-3 was just 0.488 meq./g compared to random SPEEK's 0.712 meq./g. Block-1 and Block-2 had higher degrees of sulfonation and IEC than Block-3, but the conductivity of Block-1 and Block-2 were lower than Blocks-3, which might be explained by the different morphology of those membranes. Small angle X-ray scattering (SAXS) confirmed that in the membranes of Block-3, the hydrophilic segments aggregated into larger ionic clusters which induced increased separation between hydrophilic and hydrophobic domains.

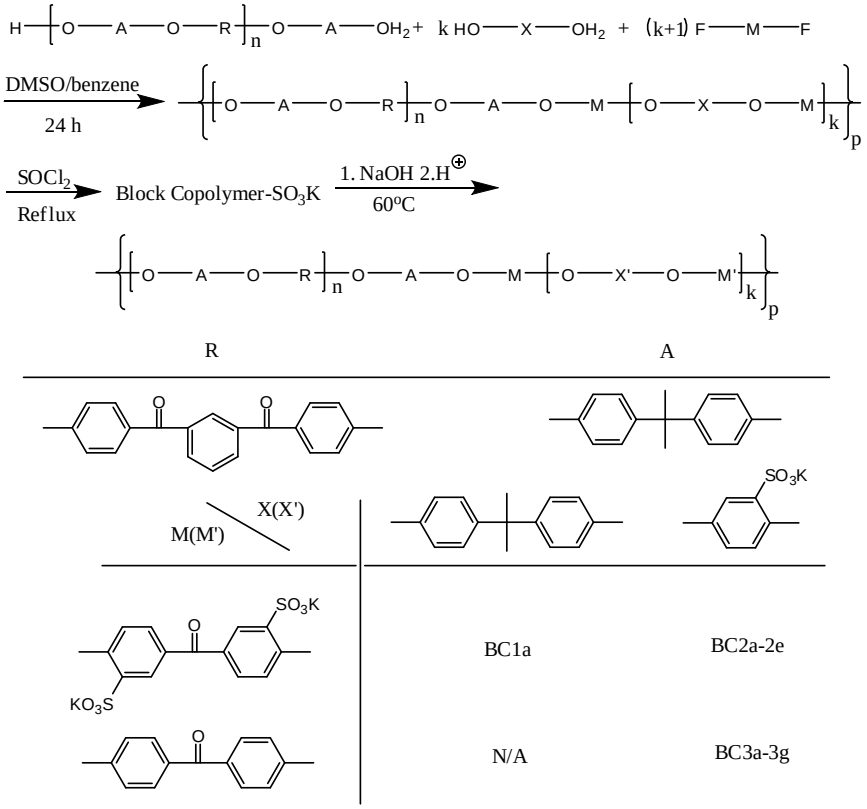

Figure 1. 56. Synthesis of sulfonated poly(arylene ether ketone) multiblock copolymer

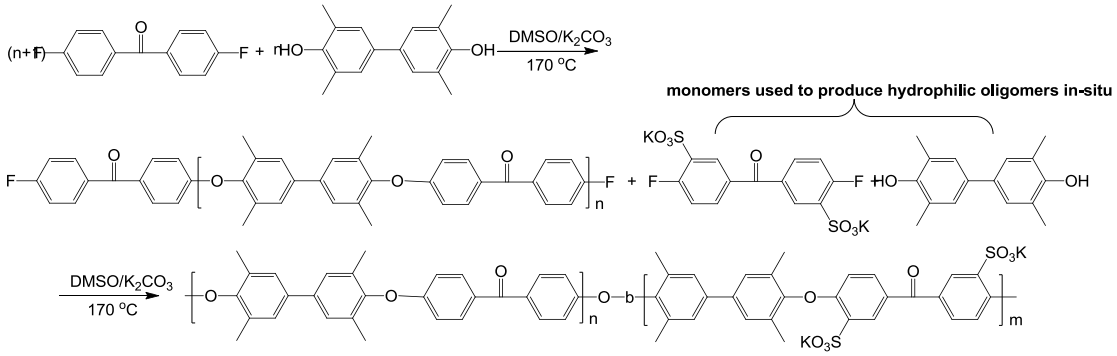

Figure 1. 57. Synthesis of sulfonated poly(ether ether ketone) multiblock copolymer

Recently, McGrath's group has achieved significant progress in developing multiblock copolymer membranes based on 100% disulfonated poly(arylene ether

sulfone)s (BPSH-100) [152-154]. BPSH-100 telechelic oligomers can be directly synthesized From 3,3´-disulfonated-4,4´-dichlorodiphenylsulfone (SDCDPS) and 4,4´-biphenol (BP). The molecular weight of hydrophilic oligomers can be controlled by adjusting the stoichiometry of SDCDPS and BP. Sometimes the end-groups of hydrophilic oligomers can be controlled by adding an end-capper. Figure 1.58 shows different synthetic routes for BPSH-100.

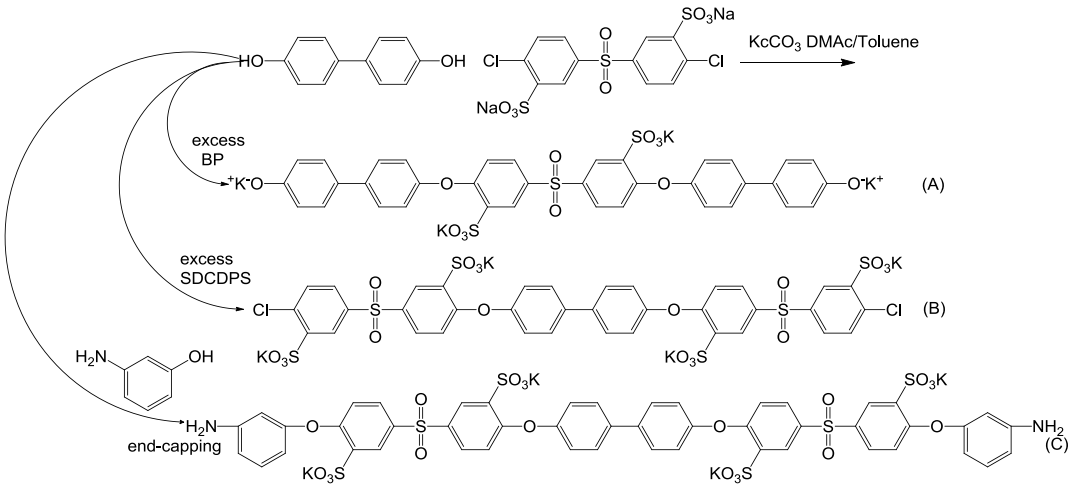

Figure 1. 58. Synthesis of (A) phenoxide-teminal; (B) Cl-terminal; (C) NH_2-endcapped BPSH-100 oligomers

Theoretically, chloro-terminated BPSH-100 can be synthesized and used for coupling reactions. However, there are several disadvantages of Cl-terminated BPSH-100. For example, it is hard to determine the exact molecular weight by NMR or SEC which makes it impossible to calculate the stoichiometry in the polymerization of multiblock copolymers. Furthermore, sulfonic groups near Cl will deactivate the nucleophilic aromatic substitution, which is unfavorable for the growth of polymer chains. Thus only phenoxide-terminated BPSH-100 or functional group endcapped BPSH-100 are widely

used in the synthesis of multiblock copolymers for PEMs.

Wang et al. prepared fluorine terminated poly(2,5-benzophenone) oligomers with different molecular weights, and then coupled them with phenoxide-terminated BPSH-100 oligomers to synthesize multiblock copolymers [153], as shown in Figure 1.59. Following Ghassemi et al.'s procedure, fluoro terminated poly(2,5-benzophenone) oligomers were synthesized via Ni(0) catalytic coupling of 2,5-dichloro-4´-phenylbenzophenone and the end-capping agent 4-chloro-4´-fluorobenzophenone. The properties of the final multiblock copolymers did not achieve the anticipated targets. The IEC and proton conductivity results were much lower than theoretical values. It might be due to insufficient control of stoichiometry during the coupling reaction. In addition, the membranes were generally brittle and the mechanical strength was poor. This is reasonable because the poor IEC values showed that the rigid, rod-like poly(2,5-benzophenone) parts led to poor membrane flexibility.

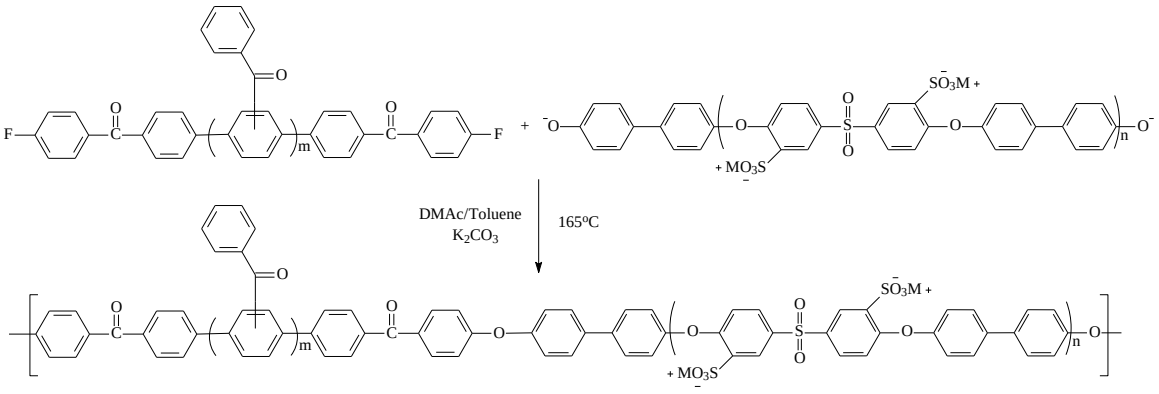

Figure 1. 59. Synthesis of PPP-BPSH100 multiblock copolymer

Lee et al. synthesized and characterized a series of multiblock copolymers for PEMs based on amine-terminated BPSH-100 telechelics (Figure 1.58 c) and NDA-terminated polyimide oligomers [155-157]. The NDA-terminated polyimide oligomers with different

molecular weight were synthesized via the polymerization of 1,4,5,8-naphthalene tetracarboxylic dianhydride (NDA) with bis[4-(3-aminophenoxy)phenyl]sulfone] (DADPS) in *m*-cresol. Synthesis of BPSH100-*b*-polyimide (BPSH-PI) was carried out in NMP or a mixture of NMP and m-cresol. Although NMP was a good solvent for both the hydrophobic and hydrophilic oligomers, the conversion of the coupling reaction was not high enough to make high molecular weight multiblock copolymers. Figure 1.60 shows the complete synthetic scheme of BPSH-PI. High molecular weight multiblock copolymers were obtained in the mixed solvent of NMP and m-cresol; the intrinsic viscosity of the copolymers varied from 0.5 dL/g to 1.0 dL/g. The proton conductivity of the membranes was relatively high with moderate water uptake. The multiblock copolymer BPS20-PI20 possessed proton conductivity as high as 0.11 S/cm with 56% water uptake and a low IEC value of 1.2 meq./g. Taping mode atomic force microscopy (TM-AFM) confirmed a nanophase separated morphology. With the increase of the block length, the morphology of the multiblock copolymers changed from small round domains to long co-continuous lamellar structures, as shown in Figure 1.61.

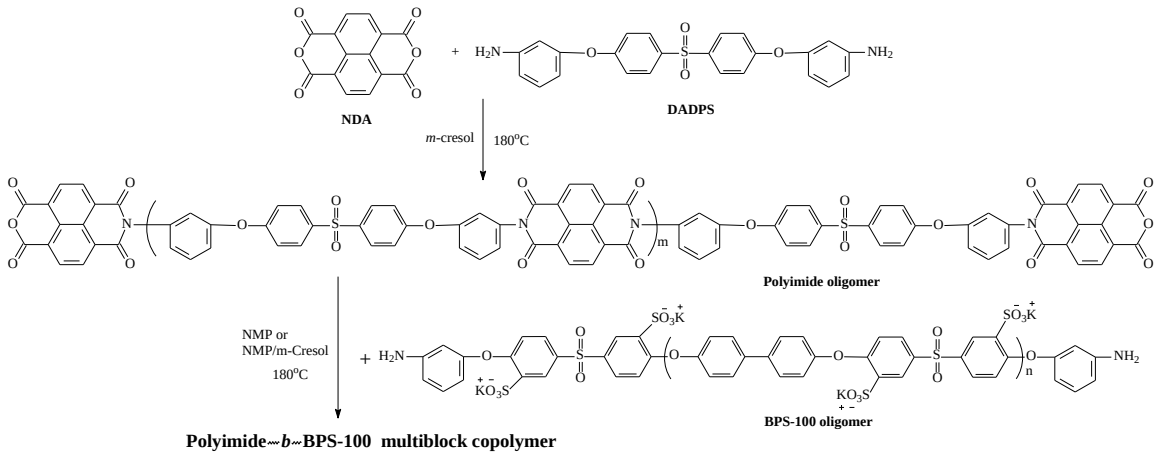

Figure 1. 60. Synthesis of BPSH-PI multiblock copolymer

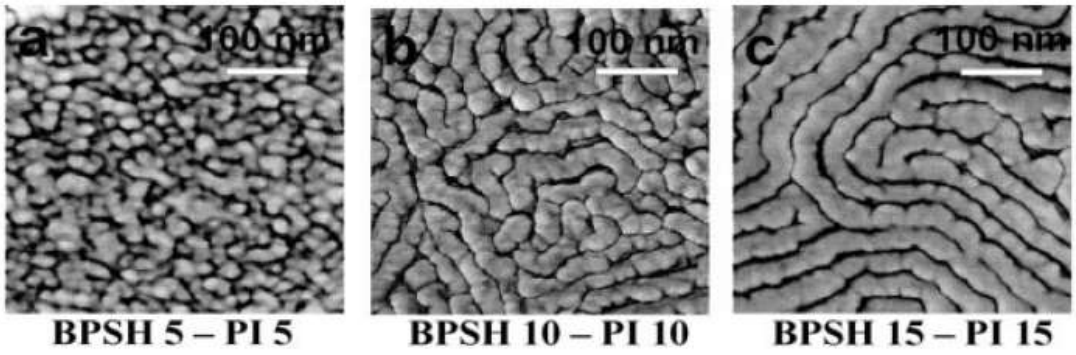

Figure 1. 61. TM-AFM Images of BPSH-PI multiblock copolymers with different block lengths

Hydrolytic stability is a critical issue for PEMs in long-term fuel cell operation. For the BPSH-PI multiblock copolymers, the hydrolysis of the imido ring in acidic environments often induces degradation. This problem not only decreases the life-time of the membranes but also lowers the conductivity of the membranes. Hydrolytic stability experiments with BPSH-PI multiblock copolymer membranes showed that after 1000

hours in 80 ^{o}C liquid water, the intrinsic viscosity of the membranes decreased by 15-25%, and IEC decreased by 5-15%. These results were much better than the BPSH-PI random copolymers with similar composition but still could not fully satisfy long-term fuel cell operation target.

Li et al. reported the synthesis of a 4K-4K multiblock copolymer (6FK-BPSH100) containing poly(arylene ether ketone) hydrophobic blocks (6FK) and BPSH100 hydrophilic blocks [158], as shown in Figure 1.62. ^{13}C NMR confirmed the minimization of ether-ether exchange reactions, which could have induced the loss of order due to randomization of the hydrophilic-hydrophobic sequences. The proton conductivity of this 4K-4K 6FK-BPSH100 multiblock copolymer was 0.08 S/cm at 30 ^{o}C in liquid water. Studies of the proton conductivity as a function of relative humidity confirmed that the 4K-4K 6FK-BPSH100 multiblock copolymer showed decent performance even at low RH, which could be explained by the presence of long, co-continuous proton channels in the multiblock copolymer. Unfortunately, the 4K-4K 6FB-BPSH100 was the only multiblock copolymer synthesized by Li et al. Further systematic studies on the 6FK-BPSH100 series with different block lengths should be investigated.

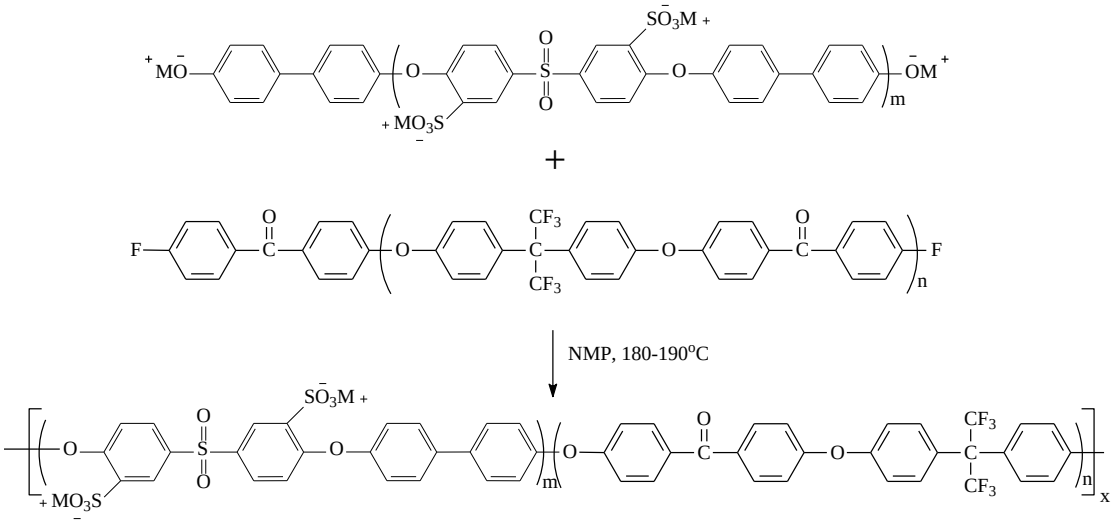

Figure 1. 62. Synthesis of sulfonated 6FK-BPSH100 multiblock copolymer

Based on the work of Ghassemi et al. [159], Xiang et al. developed another two series of multiblock copolymers for PEMs called BisAF-BPSH and BisSF-BPSH [152, 160], as shown in Figures 1.63 and 1.64.

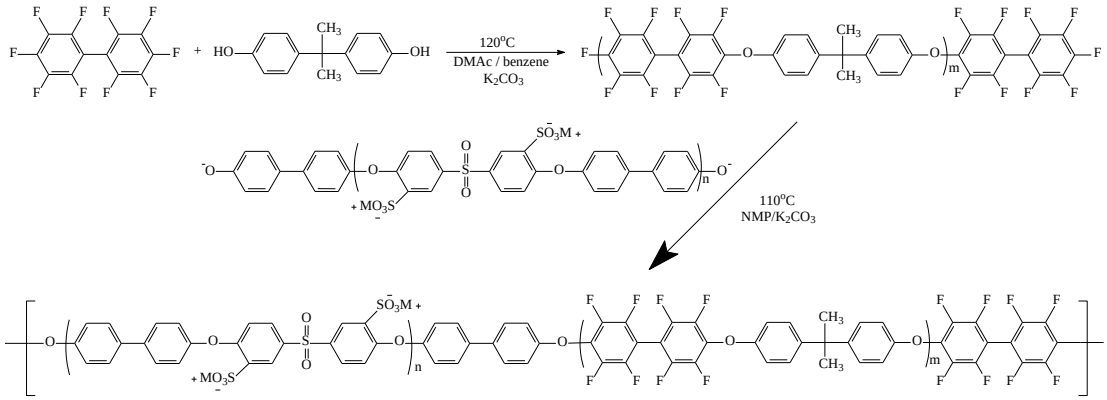

Figure 1. 63. Synthesis of BisAF-BPS100 multiblock copolymer

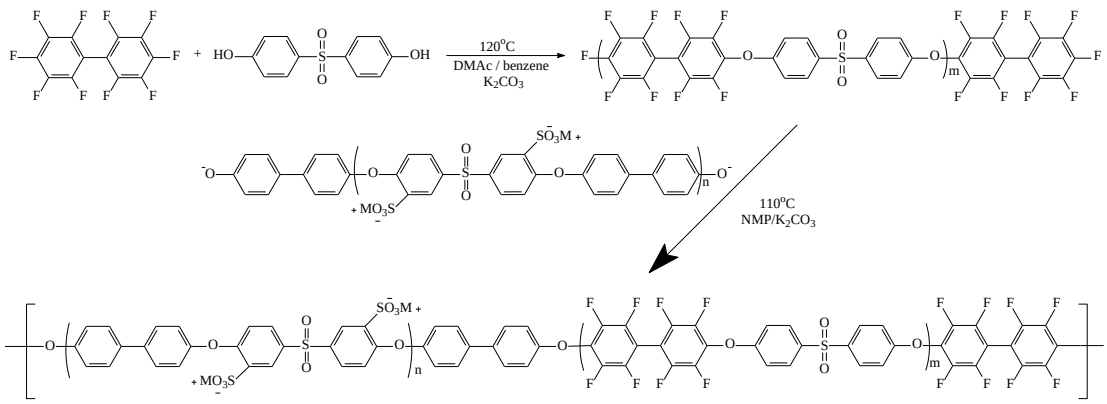

Figure 1. 64. Synthesis of BisSF-BPS100 multiblock copolymer

For the BisAF-BPSH series, the hydrophobic blocks were synthesized via polymerization of decafluorobiphenyl and bisphenol-A. A series of BisAF-BPSH with different block lengths from 3K-3K to 8K-8K showed higher proton conductivity in liquid water and relatively lower water uptake compared to the fluorinated multiblock copolymers synthesized by Ghassemi et al. [159] Exposure of the isopropylidene group of the hydrophobic blocks to acidic conditions often induced the degradation via hydrolysis, which was a significant disadvantage for PEM applications.

For the BisSF-BPSH series, the hydrophobic blocks were synthesized via polymerization of decafluorobiphenyl and 4,4'-dihydroxydiphenyl sulfone. A series of controlled IEC BisAF-BPSH with different block lengths from 5K-5K to 20K-20K were investigated. The entire series exhibited higher proton conductivity than Nafion® and BPSH35 in liquid water. Even under partially hydrated conditions, several BisSF-BPSH multiblock copolymers with IEC values of 1.3 meq./g outperformed Nafion® by as much as 15mS/cm. By careful control of the composition and architecture of the multiblock copolymers, the water uptake of the BisAF-BPSH series had been reduced by 20 wt.%

without losing performance.

In conventional coupling reactions to prepare multiblock copolymers, high reaction temperature was necessary. But high temperature could induce the ether-ether interchange reactions, which could lead to the loss of order due to the randomization of the hydrophilic-hydrophobic sequences. In recent studies by Lee et al. [161], decafluorobiphenyl (DFBP) and hexafluorobenzene (HFB) were used as end-capping agents to produce fluoro-terminal hydrophobic poly(arylene ether sulfone) (BPS0) oligomers, as shown in Figure 1.65. High reactivity of DFBP and HFB in nucleophilic aromatic substitution reactions made the low reaction temperature possible, which help minimize the chance of ether-ether interchange side reactions. One issue that must be considered in the end-caping reaction was that DFBP or HFB should be present in large excess. Otherwise DFBP or HFB would act as linkage reagents to produce longer hydrophobic blocks.

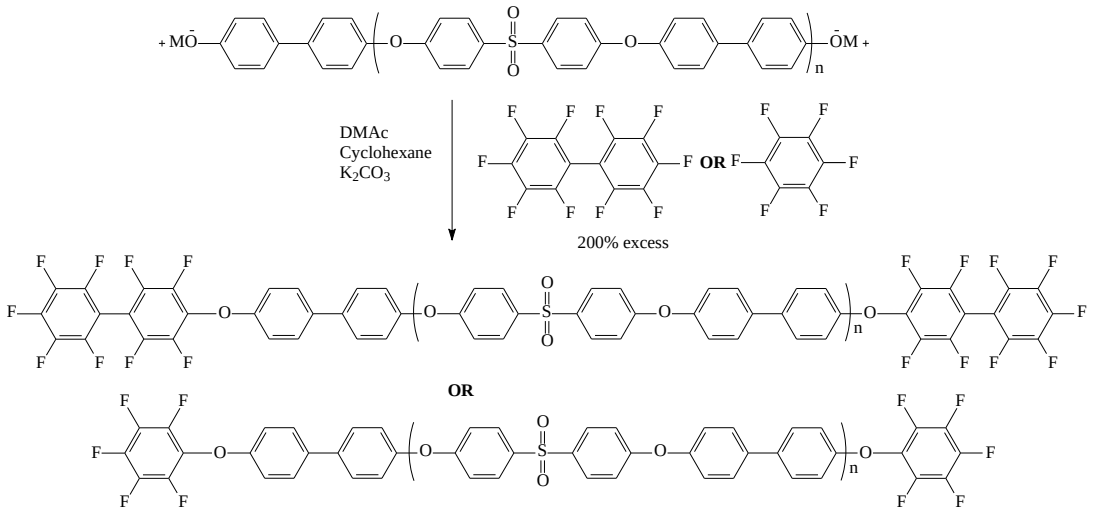

Figure 1. 65. Synthesis of fluorine-terminal BPS0 oligomer

The coupling reactions between fluoro-terminated BPS0 and phenoxide terminated

BPSH100 were accomplished under mild reaction conditions. Two series of BPS0-BPSH100 multiblock copolymers with different linkages were synthesized. The scheme of the coupling reaction is shown in Figure 1.66. ^{13}C NMR confirmed the multiblock copolymers showed ordered sequences. During the coupling reaction, reaction temperature must be precisely controlled at a relative low level to prevent possible cross-linking reactions on the highly reactive DFBP or HFB linkages.

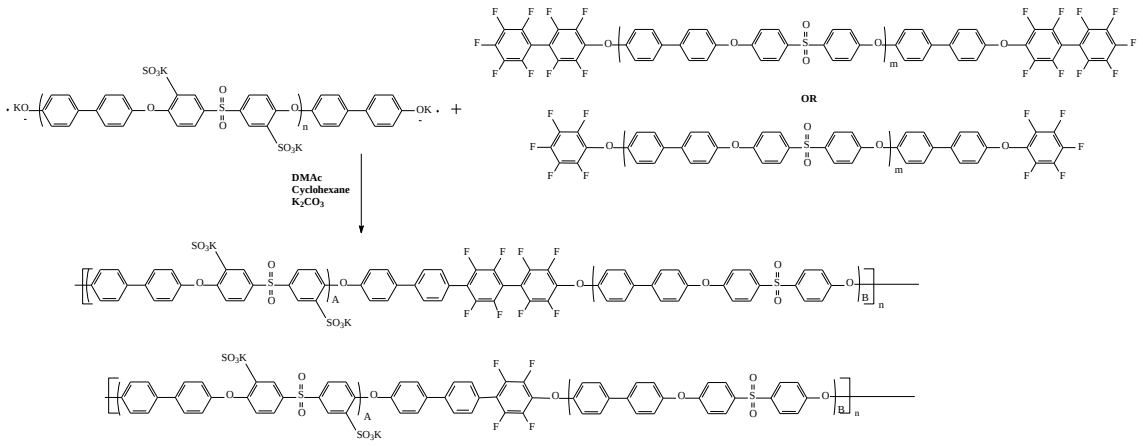

Figure 1. 66. Synthesis of BPS0-BPSH100 with different linkages

At similar IEC values, the proton conductivity and water uptake increased as the hydrophilic block length increased. The BPSH100-BPS0 10K-5K showed proton conductivity as high as 0.16 S/cm with 100 wt% water uptake.

The phase separated morphologies of BPSH100 – BPS0 multiblock copolymers were influenced by different linkages (DFBP and HFB). From TEMs micrograph, the degree of phase separation in the bulk morphologies of all the series appeared to increase as block length increased. However, atomic force microscopy (AFM) micrographs failed

to reveal similar trends for the surface morphologies. The amount of fluorine on the HFB linkage was not sufficient to change the surface morphologies of the BPSH100-BPS0 series in contrast to DFBP [162].

The distinct phase separated morphology of the BPSH100-BPS0 with DFBP linkages improved the proton conductivity under partially hydrated conditions. As the block lengths increased, the proton conductivity of the multiblock copolymers under partially hydrated conditions improved. The performance of BPSH100-BPS0-10k-10k was comparable to that of Nafion® 112 [163].

Nakabayashi et al. synthesized partially fluorinated poly(arylene ether sulfone) (6F-BPS0) oligomers and end-caped the oligomers with DFBP [164]. Then the fluoro-terminated 6F-BPS0 was coupled with phenoxide-terminated BPSH100 to produce multiblock copolymers for PEMs. The membranes with high IEC values showed relatively low water uptake and maintained relatively high proton conductivity (6 mS/cm) under 50% relative humidity.

Takamuku et al. synthesized phenoxide terminated poly (ether sulfone) oligomers with bis(4-hydroxyphenyl) sulfone (BHPS) and 4,4′-dichlorodiphenyl sulfone (DCDPS) and introduced DFBP as an end-capping reagent to produce 10F-terminated poly(ether sulfone) oligomers (10F-PES) [165]. A diblock copolymer was then synthesized by the 10F-PES and phenoxide terminated poly (ether ether sulfone) oligomer (PEES) through a coupling reaction. The synthetic scheme is shown in Figure 1.67. After post-sulfonation in concentrated sulfuric acid, ^{1}H NMR confirmed that sulfonation occurred almost perfectly on PEES block. Although the conductivity of the sulfonated 10F-PES-*b*-PEES increased as the IEC values increased, the highest conductivity only reached 40mS/cm.

Perhaps a better sulfonation procedure could improve proton conductivity.

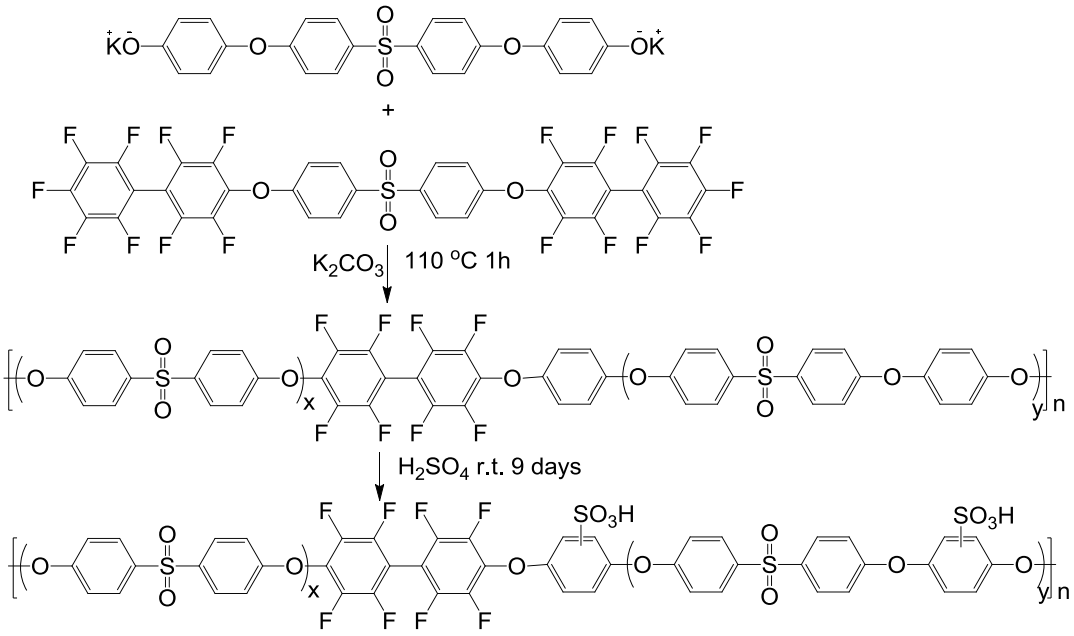

Figure 1. 67. Synthesis of sulfonated 10F-PES-PEES diblock copolymer

The high reactivity of DFBP and/or HFB in nucleophilic aromatic substitution reactions might lower the reaction temperature of the coupling reaction. On the other hand, the multi-functionality of DFBP and/or HFB could induce side-reactions such as cross-linking. To avoid this problem, Chen et al. synthesized difluoro-terminated poly(arylene ether nitrile) (6FPAEB) hydrophobic oligomers with different molecular weights, which were coupled with hydrophilic BPSH100 oligomers to obtain multiblock copolymers [166], as shown in Figure 1.68.

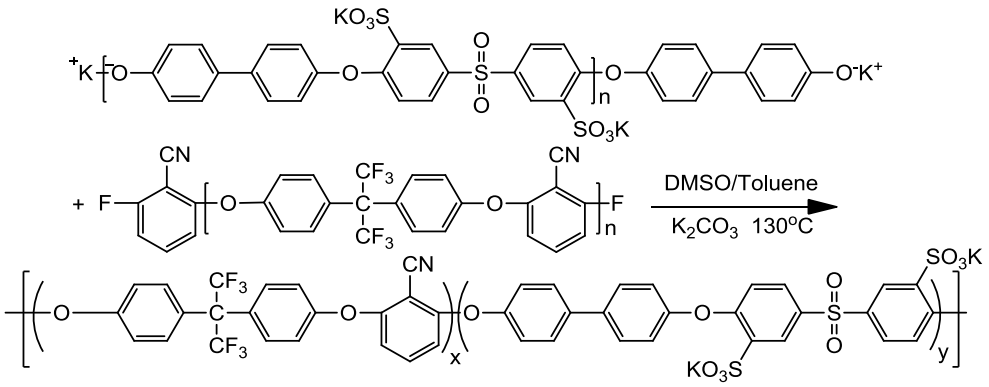

Figure 1. 68. Synthesis of 6FPAEB-BPSH100 multiblock copolymers

Some properties of the 6FPAEB-BPSH100 multiblock copolymers with block lengths from 4 kg/mol up to 15 kg/mol are listed in Table 1. All the copolymers had high proton conductivity in liquid water. At a similar IEC value, the water uptake of block copolymers increased with an increase in block length, which was believed to be related to a better defined nanophase separation. The proton conductivity of 15k-15k decreased slightly compared to those of the 4k-4k and 7k-7k systems. This decrease may have been caused by the increased water uptake, and a dilution of the proton concentration in the membranes.

Table 1. 2**. Properties of 6FPAEB-BPSH100 multiblock copolymers**

6FPAEB-BPSH100	IV (dL/g)[a]	IEC (meq/g)[b]	Water Uptake (wt%)	Proton Conductivity[c] (S/cm)
4k-4k	0.61	1.60	113	0.13
7k-7k	0.81	1.70	136	0.17
15k-15k	1.25	1.70	235	0.11

a: Measured by SEC with 0.05M LiBr/NMP as mobile phase at 60 ^{o}C
b: Measured from ^{1}H NMR
c: Measured in liquid water at 30 ^{o}C

Bai et al. developed multiblock sulfonated poly(arylene thioether suflone)

copolymers for PEMs [167]. Fluorine-terminated hydrophobic poly(arylene thioether suflone) (PTES) and hydrophilic sulfonated poly(arylene thioether suflone) (SPTES) oligomers were synthesized via polycondensation. Multiblock copolymers were then synthesized with PTES and SPTES oligomers via coupling reactions, as shown in Figure 1.69. The reaction temperature was higher than the synthesis of multiblock sulfonated poly(arylene ether sulfone)s, due to the relative poor nucleophilicity of the sulfide group. The authors did not mention how to determine the number average molecular weight of each oligomer, which were critical issues in the next step coupling reaction.

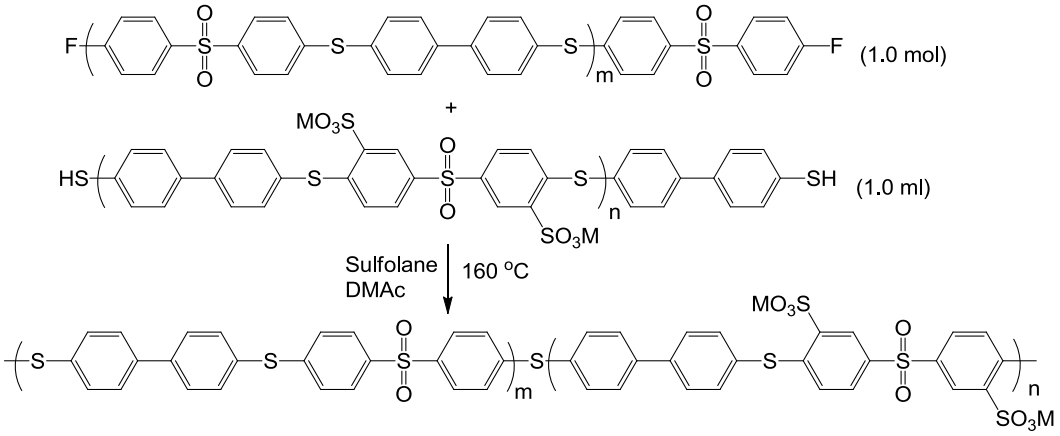

Figure 1. 69. Chemical and reaction scheme of SPTES-50 multiblock copolymer

AFM and TEM images showed well-defined phase separation on the surface and in the bulk of the SPTES-50 membrane, which suggested the existence of well connected hydrophilic domains. The proton conductivity of SPTES-50 multiblock copolymer was as high as 256 mS/cm at 65 ℃ and 85% relative humidity. However, the authors did not equilibrate SPTES-50 membranes in deionized water after acidification, which meant some residual sulfuric acid in the membrane could have affected the proton conductivity result.

1.5.4 Comparisons between Random and Multiblock Copolymer PEMs

Compared with random copolymers, multiblock copolymers contain long sequences of sulfonic acid groups, which may associate to form wider proton channels and afford better proton transport. The structures of the random and block coopolymers are shown in Figure 1.70. Roy et al. compared the transport properties of highly fluorinated block copolymers and random copolymers [168].

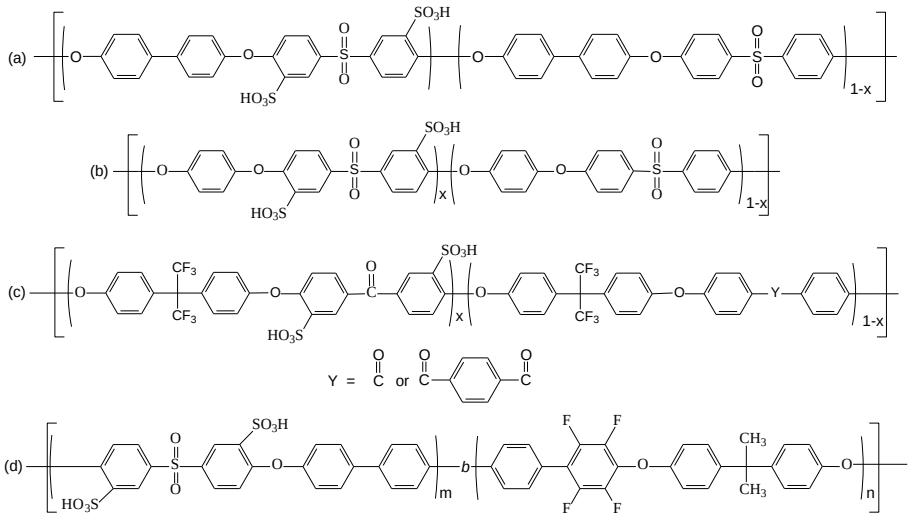

Figure 1. 70. (a-d) Copolymers chemical structures: (a) BPSHxx, (b) HQSH-xx, (c) B-ketone-xx and PB-diketone-xx, (d) Block BisAF-BPSH(x:y)K

Figures 1.71 and 1.72 show plots of proton conductivity vs. relative humidity (RH) for random and block copolymers, respectively. In Figure 1.71, the conductivity of random copolymer membranes at high RH is comparable to that of Nafion® 117. However, with the decreasing RH, the conductivity of random copolymer membranes decreases more rapidly than Nafion® 117. At 30% RH, the proton conductivity performance of random copolymers is much worse than Nafion® 117. In Figure 1.72, the

BisAF-BPSH multiblock copolymers show increasing proton conductivity with increasing block length from 3k:3k to 8k:8k, even though the copolymer has the lowest IEC and water uptake value. Furthermore, the conductivity of the copolymer BisAF-BPSH 8k:8k is comparable to that of Nafion® 117 over the entire RH range. The high performance of the BisAF-BPSH copolymers may be attributed to distinct nano-phase separation caused by highly hydrophobic fluorinated segments.

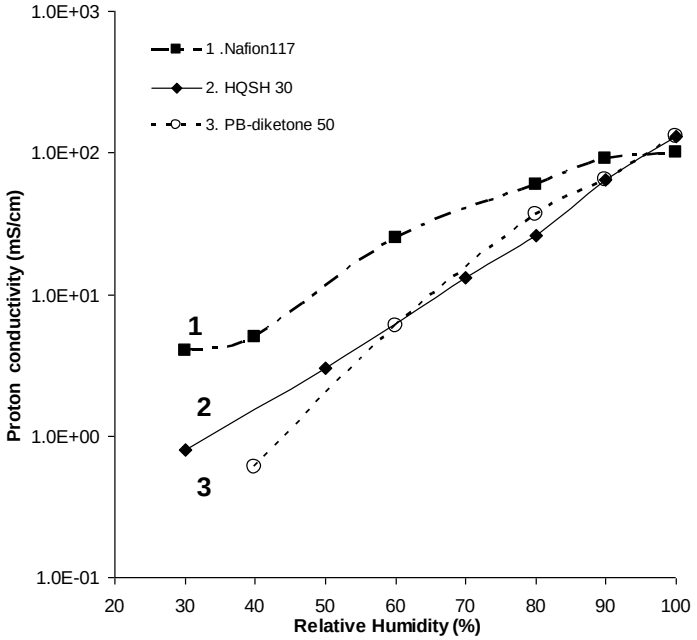

Figure 1. 71. Proton conductivity vs. relative humidity plots for Nafion® 117, poly(ether sulfone) random copolymer (HQSH 30), and poly(ether ketone) random copolymer (PB-diketone 50)

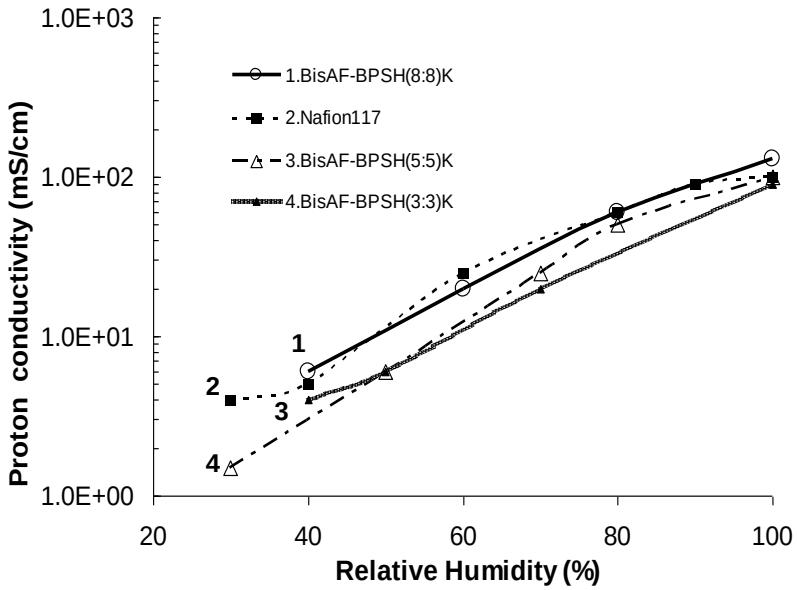

Figure 1. 72. Proton conductivity vs. relative humidity plots for Nafion® 117 and BisAF-BPSH multiblock copolymers

1.6 References:

1. <http://www.efcf.com/media/ep010813.shtml>.
2. Winter M and Brodd RJ. Chem. Rev. 2004;104(10):4245.
3. Gülzow E. Fuel Cells 2004;4(4).
4. Hoogers G. Fuel cell technology handbook. Boca Raton, Fla.: CRC Press, 2003.
5. Liebhafsky HA and Cairns EJ. Fuel cells and fuel batteries. Guide to their research and development. United States: John Wiley and Sons, Inc.,New York, 1968.
6. Brenscheidt T, Janowitz K, Salge HJ, Wendt H, and Brammer F. Int. J. Hydrogen Energy 1998;23(1):53.
7. Bruijn Fd. Green Chemistry 2005;7(3):132.
8. Minh NQ. CHEMTECH ; Vol/Issue: 21:2 1991:Pages: 120.
9. Prabhu G, Solaiyan C, Dheenadayalan S, Chandrasekaran R, and Pattabiraman R. Proceedings of the Indian National Science Academy - Part A: Physical Sciences 2004;70(3):489.
10. Dhathathreyan KS, Sridhar P, Sasikumar G, Ghosh KK, Velayutham G, Rajalakshmi N, Subramaniam CK, Raja M, and Ramya K. Int. J. Hydrogen Energy 1999;24(11):1107.
11. Hickner MA. Transport and Structure in Fuel Cell Proton Exchange Membranes. Chemical Engineering, vol. Ph. D. Blacksburg: Virginia Tech, 2003.
12. Kordesch K and Simader G. Fuel cells and their applications. Weinheim ; New York: VCH, 1996.
13. Mehta V and Cooper JS. J. Power Sources 2003;114(1):32.
14. Passalacqua E, Lufrano F, Squadrito G, Patti A, and Giorgi L. Electrochim. Acta

2001;46(6):799.
15. Mauritz KA and Moore RB. Chem. Rev. 2004;104(10):4535.
16. Hickner MA and Pivovar BS. Fuel Cells 2005;5(2):213.
17. Meier-Haack J, Taeger A, Vogel C, Schlenstedt K, Lenk W, and Lehmann D. Sep. Purif. Technol. 2005;41(3):207.
18. Savadogo O. J. New Mater. Electrochem. Syst. 1998;1(1):47.
19. Rozière J and Jones DJ. Annual Review of Materials Research 2003;33.
20. Hickner MA, Ghassemi H, Kim YS, Einsla BR, and McGrath JE. Chem. Rev. 2004;104(10):4587.
21. Kerr JA. Chem. Rev. 1966;66(5):465.
22. Slade S, Campbell SA, Ralph TR, and Walsh FC. J. Electrochem. Soc. 2002;149(12):A1556.
23. Steck AE. Proceedings of the First International Symposium on New Materials for Fuel Cell Systems. Montreal, 1995. pp. 74.
24. Yang ZY and Rajendran RG. Angewandte Chemie-International Edition 2005;44(4):564.
25. Thomas BH, Shafer G, Ma JI, Tu MH, and Desmarteau DD. J. Fluorine Chem. 2004;125(8):1231.
26. Eisman GA. J. Power Sources 1990;29(3-4):389.
27. Tant MR, Darst KP, Lee KD, and Martin CW. ACS Symp. Ser. 1989;395:370.
28. Wei J, Stone C, and Steck AE. U. S. Patent 5422411. In: Patent US, editor. United States, 1993.
29. Basura VI, Chuy C, Beattie PD, and Holdcroft S. J. Electroanal. Chem. 2001;501(1-2):77.
30. Kim J, Kim B, and Jung B. J. Membr. Sci. 2002;207(1):129.
31. Wnek G. Abstr Pap Am Chem S 2001;222:U308.
32. Wnek GE, Sheikh-Ali BM, Serpico JM, Ehrenberg SG, Tangredi TN, Kruppaiah C, and Ye Y. Abstr Pap Am Chem S 1998;215:U352.
33. Wnek GE, Rider JN, Serpico JM, Einset AG, Ehrenberg SG, and Raboin LA. Proton Conducting Membrane Fuel Cells I, PV 95-23, The Electrochemical Society Proceedings Series. 1995. pp. 247.
34. Russell B. Hodgdon Jr. Journal of Polymer Science Part A-1: Polymer Chemistry 1968;6(1):171.
35. Kaur S, Florio G, and Michalak D. Polymer 2002;43(19):5163.
36. Chen S-L, Benziger JB, Bocarsly AB, and Zhang T. Industrial & Engineering Chemistry Research 2005;44(20):7701.
37. Shi Z and Holdcroft S. Macromolecules 2005;38(10):4193.
38. Büchi FN, Gupta B, Haas O, and Scherer GG. Electrochim. Acta 1995;40(3):345.
39. Holmberg S, Lehtinen T, Nasman J, Ostrovskii D, Paronen M, Serimaa R, Sundholm F, Sundholm G, Torell L, and Torkkeli M. J. Mater. Chem. 1996;6(8):1309.
40. Gubler L, Gürsel SA, and Scherer GG. Fuel Cells 2005;5(3):317.
41. Flint SD and Slade RCT. Solid State Ionics 1997;97(1-4):299.
42. Chen JH, Asano M, Yamaki T, and Yoshida M. J. Membr. Sci. 2005;256(1-2):38.
43. Gupta B, Buchi FN, and Scherer GG. Journal of Polymer Science Part a-Polymer Chemistry 1994;32(10):1931.
44. Gupta B and Scherer GG. Chimia 1994;48(5):127.

45. Li JY, Ichizuri S, Asano S, Mutou F, Ikeda S, Iida M, Miura T, Oshima A, Tabata Y, and Washio M. Appl. Surf. Sci. 2005;245(1-4):260.
46. Hubner G and Roduner E. J. Mater. Chem. 1999;9(2):409.
47. Attwood TE, Barr DA, King T, Newton AB, and Rose JB. Polymer 1977;18(4):359.
48. Attwood TE, Newton AB, and Rose JB. British Polymer Journal 1972;4(5):391.
49. Johnson RN, Farnham AG, Clendinning RA, Hale WF, and Merriam CN. Journal of Polymer Science Part A-1: Polymer Chemistry 1967;5(9):2375.
50. Kroschwitz JI and Mark HF. Encyclopedia of polymer science and technology, 3rd ed. Hoboken, N.J.: Wiley-Interscience, 2003.
51. Odian GG. Principles of polymerization, 4th ed. Hoboken, N.J.: Wiley-Interscience, 2004.
52. Attwood TE, Dawson PC, Freeman JL, Hoy LRJ, Rose JB, and Staniland PA. Polymer 1981;22(8):1096.
53. Mohanty DK, Sachdeva Y, Hedrick JL, Wolfe JF, and Mcgrath JE. Abstr Pap Am Chem S 1984;188(Aug):49.
54. Kerres J, Cui W, and Reichle S. Journal of Polymer Science Part a-Polymer Chemistry 1996;34(12):2421.
55. Nolte R, Ledjeff K, Bauer M, and Mulhaupt R. J. Membr. Sci. 1993;83(2):211.
56. Noshay A and Robeson LM. J. Appl. Polym. Sci. 1976;20(7):1885.
57. Bonnet B, Jones DJ, Rozière J, Tchicaya L, Alberti G, Casciola M, Massinelli LB, B. , Peraio A, and Ramunni E. J. New Mater. Electrochem. Syst. 2000;3(2).
58. Bishop MT, Karasz FE, Russo PS, and Langley KH. Macromolecules 1985;18(1):86.
59. Huang RYM, Shao PH, Burns CM, and Feng X. J. Appl. Polym. Sci. 2001;82(11):2651.
60. Shang XY, Tian SH, Kong LH, and Meng YZ. J. Membr. Sci. 2005;266(1-2):94.
61. Paturzo L, Basile A, Iulianelli A, Jansen JC, Gatto I, and Passalacqua E. Catal. Today 2005;104(2-4):213.
62. Sun YM, Wu TC, Lee HC, Jung GB, Guiver MD, Gao Y, Liu YL, and Lai JY. J. Membr. Sci. 2005;265(1-2):108.
63. Zhang HB, Pang JH, Wang D, Li AZ, Li XF, and Jiang ZH. J. Membr. Sci. 2005;264(1-2):56.
64. Swier S, Chun YS, Gasa J, Shaw MT, and Weiss RA. Polymer Engineering & Science 2005;45(8):1081.
65. Kerres J, Cui W, Eigenberger G, Beavers D, Schnurnberger W, Fischer A, and Wendt H. In: Veziroglu TN, Winter CJ, Baselt JP, and Kreysa G, editors. Proceedings of the 11th World Hydrogen Energy Conference. Stutgart, Germany, 1996. pp. 1951.
66. Kerres J, Cui W, and Junginger M. J. Membr. Sci. 1998;139(2):227.
67. Kerres J, Zhang W, and Cui W. Journal of Polymer Science Part A-Polymer Chemistry 1998;36(9):1441.
68. Robeson LM and Matzner M. U.S. Patent 4,380,598. In: Patent US, editor.: United States 1983.
69. Ueda M, Toyota H, Ouchi T, Sugiyama JI, Yonetake K, Masuko T, and Teramoto T. Journal of Polymer Science Part A-Polymer Chemistry 1993;31(4):853.
70. Wang F, Hickner M, Ji Q, Harrison W, Mecham J, Zawodzinski TA, and McGrath JE. Macromolecular Symposia 2001;175:387.
71. Wang F, Mecham JB, Harrison W, and McGrath JE. Abstr Pap Am Chem S

2000;220:U316.
72. Sankir M, Bhanu VA, Ghassemi H, Wiles KB, Hill ML, Harrison W, Sumner M, Glass TE, Riffle J, and McGrath JE. Abstr Pap Am Chem S 2003;225:U640.
73. Li Y, VanHouten RA, Brink AE, and McGrath JE. Polymer 2008;49(13-14):3014.
74. Harrison WL, Wang F, Mecham JB, Bhanu VA, Hill M, Kim YS, and McGrath JE. Journal of Polymer Science Part a-Polymer Chemistry 2003;41(14):2264.
75. Wang F, Chen TL, and Xu JP. Macromol. Chem. Phys. 1998;199(7):1421.
76. Wang F, Hickner M, Kim YS, Zawodzinski TA, and McGrath JE. J. Membr. Sci. 2002;197(1-2):231.
77. Wiles KB, Bhanu VA, Wang F, Hickner MA, and McGrath JE. Abstr Pap Am Chem S 2003;225:U640.
78. Summer MJ, Harrison WL, Weyers RM, Kim YS, McGrath JE, Riffle JS, Brink A, and Brink MH. J. Membr. Sci. 2004;239(2):199.
79. Shobha HK, Smalley GE, Sankarapandian M, and McGrath JE. Abstr Pap Am Chem S 2000;219:U373.
80. Wang F, Li JK, Chen TL, and Xu JP. Polymer 1999;40(3):795.
81. Chen YL, Meng YZ, and Hay AS. Macromolecules 2005;38(9):3564.
82. Li XF, Zhao CJ, Lu H, Wang Z, and Na H. Polymer 2005;46(15):5820.
83. Xing PX, Robertson GP, Guiver MD, Mikhailenko SD, and Kaliaguine S. Journal of Polymer Science Part A-Polymer Chemistry 2004;42(12):2866.
84. de Abajo J. Makromolekulare Chemie-Macromolecular Symposia 1988;22:141.
85. Johnston JC, Meador MAB, and Alston WB. Journal of Polymer Science Part a-Polymer Chemistry 1987;25(8):2175.
86. Einsla BR, Kim YS, Hickner MA, Hong YT, Hill ML, Pivovar BS, and McGrath JE. J. Membr. Sci. 2005;255(1-2):141.
87. Genies C, Mercier R, Sillion B, Petiaud R, Cornet N, Gebel G, and Pineri M. Polymer 2001;42(12):5097.
88. Einsla BR, Hong YT, Kim YS, Wang F, Gunduz N, and Mcgrath JE. Journal of Polymer Science Part A-Polymer Chemistry 2004;42(4):862.
89. Gunduz N and McGrath JE. Abstr Pap Am Chem S 2000;219:U373.
90. Gunduz N and McGrath JE. Abstr Pap Am Chem S 2000;220:U307.
91. Zhou W, Watari T, Kita H, and Okamoto K-i. Chem. Lett. 2002;31(5):534.
92. Fang JH, Guo XX, Harada S, Watari T, Tanaka K, Kita H, and Okamoto K. Macromolecules 2002;35(24):9022.
93. Guo XX, Fang JH, Watari T, Tanaka K, Kita H, and Okamoto KI. Macromolecules 2002;35(17):6707.
94. Yin Y, Fang J, Cui Y, Tanaka K, Kita H, and Okamoto K-i. Polymer 2003;44(16):4509.
95. Asano N, Aoki M, Suzuki S, Miyatake K, Uchida H, and Watanabe M. J. Am. Chem. Soc. 2006;128(5):1762.
96. Hu ZX, Yin Y, Chen SW, Yamada O, Tanaka K, Kita H, and Okamoto K. Journal of Polymer Science Part a-Polymer Chemistry 2006;44(9):2862.
97. Ueda M, Sato M, and Mochizuki A. Macromolecules 1985;18(12):2723.
98. Chow AW, Bitler SP, Penwell PE, Osborne DJ, and Wolfe JF. Macromolecules 1989;22(9):3514.
99. Evers RC, Arnold FE, and Helminiak TE. Macromolecules 1981;14(4):925.

100. Krause SJ, Haddock TB, Vezie DL, Lenhert PG, Hwang WF, Price GE, Helminiak TE, Obrien JF, and Adams WW. Polymer 1988;29(8):1354.
101. So YH, Heeschen JP, Bell B, Bonk P, Briggs M, and DeCaire R. Macromolecules 1998;31(16):5229.
102. Asensio JA, Borros S, and Gomez-Romero P. J. Membr. Sci. 2004;241(1):89.
103. Asensio JA, Borros S, and Gomez-Romero P. Electrochim. Acta 2004;49(25):4461.
104. Staiti P, Lufrano F, Arico AS, Passalacqua E, and Antonucci V. J. Membr. Sci. 2001;188(1):71.
105. Asensio JA, Borros S, and Gomez-Romero P. Journal of Polymer Science Part a-Polymer Chemistry 2002;40(21):3703.
106. Gieselman MB and Reynolds JR. Macromolecules 1992;25(18):4832.
107. Glipa X, ElHaddad M, Jones DJ, and Roziere J. Solid State Ionics 1997;97(1-4):323.
108. Dang TD, Bai SJ, Heberer DP, Arnold FE, and Spry RJ. Journal of Polymer Science Part B-Polymer Physics 1993;31(13):1941.
109. Einsla B, Tchatchoua CN, Kim YJ, and McGrath JE. Abstr Pap Am Chem S 2003;226:U391.
110. Kim SG, Cameron DA, Lee YK, Reynolds JR, and Savage CR. Journal of Polymer Science Part A-Polymer Chemistry 1996;34(3):481.
111. Qing S, Huang W, and Yan D. Eur. Polym. J. 2005;41(7):1589.
112. Qing S, Huang W, and Yan D. React. Funct. Polym. 2006;66(2):219.
113. Bloom PD, Jones CA, and Sheares VV. Macromolecules 2005;38(6):2159.
114. Ghassemi H and McGrath JE. Polymer 2004;45(17):5847.
115. Fu H, Yun H, Kwei TK, and Okamoto Y. J. Polym. Sci., Part A: Polym. Chem. 1998;36(9):1425.
116. Fujimoto CH, Hicknert MA, Cornelius CJ, and Loy DA. Macromolecules 2005;38(12):5010.
117. Wu S, Qiu Z, Zhang S, Yang X, Yang F, and Li Z. Polymer 2006;47(20):6993.
118. Sankir M, Kim YS, Harrison WL, Badami AS, and McGrath JE. Abstr Pap Am Chem S 2005;230:U1657.
119. Miyatake K and Hay AS. J. Polym. Sci., Part A: Polym. Chem. 2001;39(19):3211.
120. Wang L, Meng YZ, Wang SJ, Shang XY, Li L, and Hay AS. Macromolecules 2004;37(9):3151.
121. Lee HC, Hong HS, Kim YM, Choi SH, Hong MZ, Lee HS, and Kim K. Electrochim. Acta 2004;49(14):2315.
122. Kim DS, Robertson GP, Guiver MD, and Lee YM. J. Membr. Sci. 2006;281(1-2):111.
123. Wiles KB, de Diego CM, de Abajo J, and McGrath JE. J. Membr. Sci. 2007;294(1-2):22.
124. Bai Z, Shumaker JA, Houtz MD, Mirau PA, and Dang TD. Polymer 2009;50(6):1463.
125. Li Y. The Influence of Aromatic Disulfonated Random and Block Copolymers' Molecular Weight, Composition,and Microstructure on the Properties of Proton Exchange Membranes for Fuel Cells. Macromolecular and Science Engineering, vol. Ph. D. Blacksburg: Virginia Tech, 2007.

126. Kim DS, Liu B, and Guiver MD. Polymer 2006;47(23):7871.
127. Xing PX, Robertson GP, Guiver MD, Mikhailenko SD, and Kaliaguine S. Polymer 2005;46(10):3257.
128. Lee H-J, Lee E-M, Lee M-H, Oh M-C, Ahn J-H, Han SG, and Kim HG. J. Polym. Sci., Part A: Polym. Chem. 1998;36(16):2881.
129. Kim JP, Lee WY, Kang JW, Kwon SK, Kim JJ, and Lee JS. Macromolecules 2001;34(22):7817.
130. Lee H-J, Lee M-H, Oh M-C, Ahn J-H, and Han SG. J. Polym. Sci., Part A: Polym. Chem. 1999;37(14):2355.
131. Kim J-P, Kang J-W, Kim J-J, and Lee J-S. J. Polym. Sci., Part A: Polym. Chem. 2003;41(10):1497.
132. Ding J, Liu F, Li M, Day M, and Zhou M. J. Polym. Sci., Part A: Polym. Chem. 2002;40(23):4205.
133. Kimura K, Tabuchi Y, Yamashita Y, Cassidy PE, Fitch JW, and Okumura Y. Polym. Adv. Technol. 2000;11(8-12):757.
134. Kreuer KD. J. Membr. Sci. 2001;185(1):29.
135. Noshay A and McGrath JE. Block copolymers : overview and critical survey. New York: Academic Press, 1977.
136. McGrath JE and Barid DG. *Proposal to Nissan Motor Co. Ltd.*, 2005.
137. Edmondson CA, Fontanella JJ, Chung SH, Greenbaum SG, and Wnek GE. Electrochim. Acta 2001;46(10-11):1623.
138. Serpico JM, Ehrenberg SG, Fontanella JJ, Jiao X, Perahia D, McGrady KA, Sanders EH, Kellogg GE, and Wnek GE. Macromolecules 2002;35(15):5916.
139. Kim B, Kim J, and Jung B. J. Membr. Sci. 2005;250(1-2):175.
140. Sangeetha D. Eur. Polym. J. 2005;41(11):2644.
141. Elabd YA, Napadensky E, Sloan JM, Crawford DM, and Walker CW. J. Membr. Sci. 2003;217(1-2):227.
142. Elabd YA, Walker CW, and Beyer FL. J. Membr. Sci. 2004;231(1-2):181.
143. Shi Z and Holdcroft S. Macromolecules 2004;37(6):2084.
144. Zhang X, Liu S, Liu L, and Yin J. Polymer 2005;46(6):1719.
145. Zhang X, Liu S, and Yin J. J. Membr. Sci. 2005;258(1-2):78.
146. Zhang X, Liu S, and Yin J. J. Membr. Sci. 2006;275(1-2):119.
147. Yang YS, Shi ZQ, and Holdcroft S. Macromolecules 2004;37(5):1678.
148. Yang YS, Shi ZQ, and Holdcroft S. Eur. Polym. J. 2004;40(3):531.
149. Ghassemi H, Ndip G, and McGrath JE. Polymer 2004;45(17):5855.
150. Shin CK, Maier G, Andreaus B, and Scherer GG. J. Membr. Sci. 2004;245(1-2):147.
151. Zhao C, Li X, Wang Z, Dou Z, Zhong S, and Na H. J. Membr. Sci. 2006;280(1-2):643.
152. Yu X, Roy A, Dunn S, Yang J, and McGrath JE. Macromolecular Symposia 2006;245:439.
153. Wang H, Badami AS, Roy A, and McGrath JE. Journal of Polymer Science Part a-Polymer Chemistry 2007;45(2):284.
154. Ghassemi H, Harrison W, Zawodzinski T, and McGrath JE. Abstr Pap Am Chem S 2004;227:U428.
155. Lee HS, Badami AS, Roy A, and McGrath JE. J. Polym. Sci., Part A: Polym.

Chem. 2007;45(21):4879.
156. Lee HS, Einsla B, and McGrath JE. Abstr Pap Am Chem S 2005;230:U1660.
157. Lee HS, Roy A, Badami AS, and McGrath JE. Macromolecular Research 2007;15(2):160.
158. Li YX, Roy A, Badami AS, Hill M, Yang J, Dunn S, and McGrath JE. J. Power Sources 2007;172(1):30.
159. Ghassemi H, McGrath JE, and Zawodzinski TA. Polymer 2006;47(11):4132.
160. Yu X, Roy A, and McGrath JE. Abstr Pap Am Chem S 2005;230:U1659.
161. Lee HS, Roy A, Lane O, Dunn S, and McGrath JE. Polymer 2008;49(3):715.
162. Badami AS, Lane O, Lee H-S, Roy A, and McGrath JE. J. Membr. Sci. 2009;333(1-2):1.
163. Roy A, Lee H-S, and McGrath JE. Polymer 2008;49(23):5037.
164. Nakabayashi K, Matsumoto K, and Ueda M. J. Polym. Sci., Part A: Polym. Chem. 2008;46(12):3947.
165. Takamuku S, Akizuki K, Abe M, and Kanesaka H. J. Polym. Sci., Part A: Polym. Chem. 2009;47(3):700.
166. Chen Y, Lane O, and McGrath JE. Preprints of Symposia - American Chemical Society, Division of Fuel Chemistry 2008;53(2):762.
167. Bai Z, Yoonessi M, Juhl SB, Drummy LF, Durstock MF, and Dang TD. Macromolecules 2008;41(23):9483.
168. Roy A, Hickner MA, Yu X, Li YX, Glass TE, and McGrath JE. J. Polym. Sci., Part B: Polym. Phys. 2006;44(16):2226.

Chapter 2: Overview of The Research

Partially fluorinated hydrophobic-disulfonated hydrophilic multiblock copolymers have been synthesized successfully via coupling reactions of hydrophobic and hydrophilic telechelic oligomers. Such materials contain partially fluorinated poly(arylene ether) blocks and fully disulfonated poly(arylene ether sulfone) (BPSH-100) blocks. The generalized structure of the copolymers studied is shown in Figure 2.1, where Arly can be a nitirle group, a diphenylketone group, or a diphenylsulfone group. Accordingly, the multiblock copolymers are termed 6FPAEB-BPS100, 6FK-BPS100, and 6FBPS0-BPS100, respectively. The weight percentage of hexafluoroisopropylidene group in a given molecular weight of hydrophobic block decreases from 6FPAEB to 6FBPS0, which may induce the difference in the results of nano-phase separation, fuel permeability and etc. The T_g of 6FK hydrophobic block is relatively lower than those of 6FPAEB and 6FBPS0, which may facilitate the self-assembly of 6FK-BPS100 during the annealing procedure. In the Chapters 3-5, the synthesis and characterization of these multiblock copolymer materials will be discussed in detail.

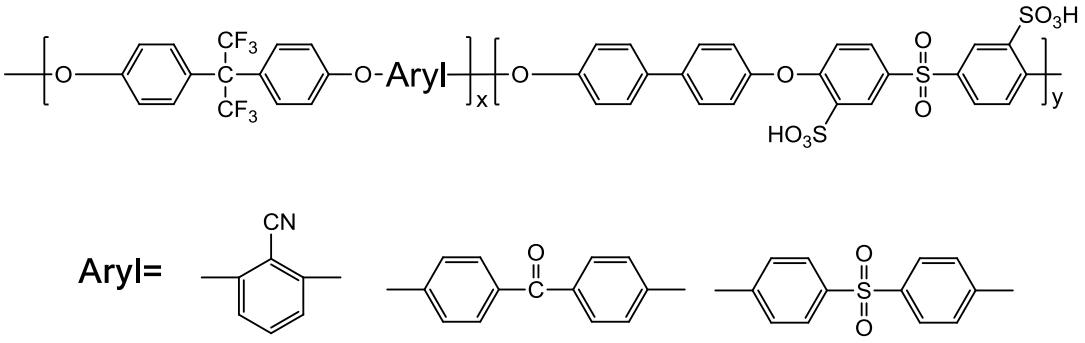

Figure 2. 1. Structure of partially fluorinated hydrophobic-disulfonated hydrophilic multiblock copolymers

We first report the synthesis and characterization of semi-crystalline hydrophobic poly(ether ether ketone)-hydrophilic sulfonated poly(arylene ether sulfone) (PEEK-BPSH100) multiblock copolymers in Chapters 6. However, PEEK blocks are insoluble in most organic solvents at relative lower reaction temperature due to their semi-crystalline structure, which prevents the coupling reaction between PEEK and BPS100. In order to facilitate the synthesis and processing, removable bulky ketimine groups were introduced to synthesize amorphous PEEKt pre-oligomers. The synthetic procedure first involves the synthesis of hydrophobic poly(ether ether ketimine)-hydrophilic sulfonated poly(arylene ether sulfone) (PEEKt-BPS100) multiblock pre-copolymers via coupling reactions. The membranes cast from PEEKt-BPS100 were boiled in 0.5M sulfuric acid solution to hydrolyze the amorphous PEEKt blocks to semi-crystalline PEEK blocks and acidify BPS100 blocks to BPSH100 blocks simultaneously, as shown in Figure 2.2. The membrane properties of the acidified semi-crystalline PEEK-BPSH100 membranes were evaluated.

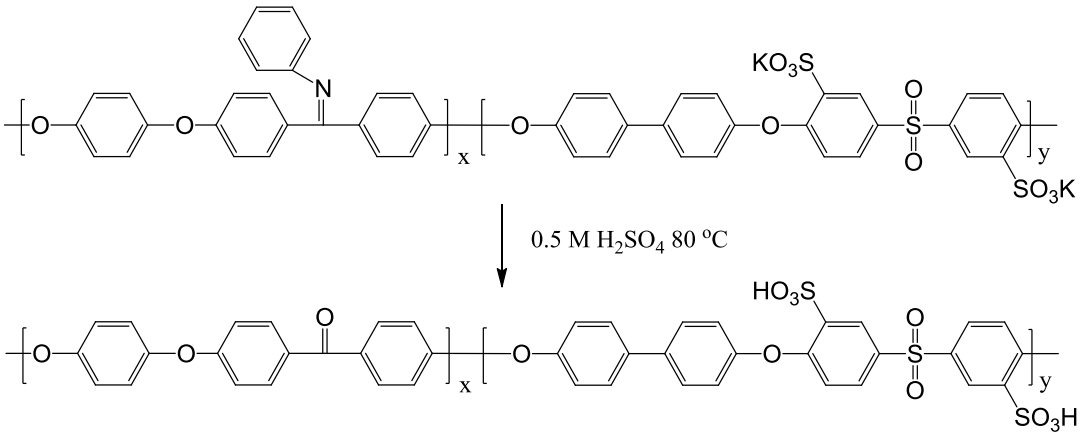

Figure 2. 2. Hydrolysis and acidification to convert amorphous PEEKt-BPS100 to semi-crystalline PEEK-BPSH100

Chapter 3: Synthesis and Characterization of Multiblock Hydrophobic Partially Fluorinated Poly(arylene ether ketone)–Hydrophilic Disulfonated Poly(arylene ether sulfone) Copolymers for Proton Exchange Membranes

Yu Chen, Chang Hyun Lee, Myoungbae Lee, Miangqiang Zhang, Robert B. Moore and James E. McGrath*

Macromolecular Science and Engineering Program, Macromolecules and Interfaces Institute, Virginia Polytechnic Institute and State University, Blacksburg, Virginia 24061

Abstract

Hydrophobic partially fluorinated poly(arylene ether ketone)–hydrophilic disulfonated poly(arylene ether sulfone) multiblock copolymers, 6FK-BPSH100, were prepared by the synthesis and coupling of partly fluorinated hydrophobic poly(arylene ether ketone) oligomers (6FK) and disulfonated hydrophilic poly(arylene ether sulfone) telechelic oligomers (BPSH100). By precisely controlling the molecular weight and composition of the telechelic oligomers, a series of multiblock copolymers were prepared varying in block length and fixed ion exchange capacity (IEC) for a comparative study. The resulting copolymers afforded tough and ductile membranes by solution casting from dimenthylacetamide (DMAc). Membrane properties of these copolymers were characterized with regard to intrinsic viscosity, thermal stabilities, morphology, water uptake, and proton conductivity. The results were compared to those of Nafion® and random copolymer BPSH35 membranes used as controls. The nanophase separated morphology developed in the membranes was illustrated by transmission electron microscopy (TEM) and small angle X-Ray scattering (SAXS), which account for enhanced proton conductivity at reduced relative humidity (RH). More importantly, film processing studies have demonstrated that a major advance in proton conductivity versus

RH behavior and greatly reduced water uptake could be achieved via precise annealing experiments.

Keywords: sulfonated poly(arylene ether ketone sulfone); multiblock copolymer; partly fluorinated polymer; proton exchange membrane; annealing

3.1 Introduction

Proton exchange membrane fuel cells (PEMFCs) have been extensively studied as clean, sustainable and efficient power sources for electric vehicles, as well as portable and stationary power sources. The key component of a PEMFC is the proton exchange membrane (PEM), which act as the electrolyte that transfers protons from the anode to the cathode in a fuel cell [1, 2]. A successful PEM material should have high proton conductivity, good mechanical strength, high oxidative and hydrolytic stability, low fuel and oxidant permeability, ease of fabrication, and controlled swelling-deswelling behavior under wet-dry cycling [3, 4]. The state-of-art commercial PEM material, Nafion®, is a perfluorinated sulfonic acid-containing ionomer (PFSA). Despite its good chemical stability and proton conductivity at high relative humidity (RH) and low temperature, there are several major drawbacks of Nafion®, such as high cost, high fuel permeability, and insufficient thermo-mechanical properties over 80 ℃. Therefore challenge lies in developing alternative PEMs which feature associated ionic domains at low hydration levels. Nanophase separated hydrophobic-hydrophilic block copolymer ionomers are desirable as alternative candidates for PEMs [5-12]. In contrast to the random copolymers, the ionic groups in block copolymers are selectively incorporated

into one or more blocks with a regularly sequenced structure. Thus continuous proton conducting channels are formed and maintained even at low humidity levels, which is critical to sustain high proton conductivity of the membranes under partially hydrated conditions.

Wholly aromatic multiblock copolymers synthesized by coupling fully disulfonated poly(arylene ether sulfone) hydrophilic blocks (BPSH100) with different types of hydrophobic blocks were largely developed in our research group [13-25]. Among these structures, fully or partially fluorinated hydrophobic-hydrophilic multiblock copolymer ionomers are of particular interests since the fluorination of the hydrophobic segment is expected to enhance the nanophase separation between hydrophobic and hydrophilic domains, which could result in an improvement of proton transport. Additionally, partially fluorinated segments may provide better compatibility with Nafion-bonded electrodes than hydrocarbon oligomers. In this work, we will discuss the synthesis of 6FK-BPSH100 multiblock copolymers and some characterization results relating to their potential as alternative proton exchange membranes.

3.2 Experimental

3.2.1 Materials

Monomer grade 4,4'-biphenol (BP) was provided by Solvay Advanced Polymers, and dried in *vacuo* at 110 ℃ for 24 hours prior to use. 3,3'-disulfonated-4,4'-dichlorodiphenylsulfone (SDCDPS) was synthesized and vacuum dried at 150 ℃ for 24 hours prior to use. 4,4'-Hexafluoroisopropylidene diphenol (6F-BPA), received from Ciba, was purified by sublimation and recrystallization in

toluene before use. 4,4'-Difluorobenzophenone (DFK) and potassium carbonate (K_2CO_3), purchased from Sigma-Aldrich, were dried in *vacuo* before use. *N*-methylpyrrolidinone (NMP) and *N,N'*-dimethylacetamide (DMAc) were vacuum-distilled from calcium hydride onto molecular sieves. Toluene, cyclohexane, methanol and 2-propanol were purchased from Fisher Scientific and used as received.

3.2.2 Monomer Synthesis

3,3'-Disulfonated-4,4'-dichlorodiphenyl sulfone (SDCDPS)

To a three necked flask equipped with a mechanical stirrer a nitrogen inlet and a gas outlet 125 g of DCDPS and 250 mL 30% fuming sulfuric acid were added. The solution was heated to 120 ^{o}C for 8 hours. The reaction mixture was allowed to cool to room temperature and added into 800 mL of ice water. Then NaCl was added to salt out the white powder product, which was then filtered and re-dissolved into 800 mL of deionized water. The solution was titrated with 2 M NaOH aqueous solution to a pH of 7. Finally an excess amount of NaCl was added again to precipitate the sodium form of the sulfonated monomer. The crude product was filtered and recrystallized from a mixture of IPA/water. Before use, the monomer was dried under vacuum at 180 ^{o}C for 3 days [26].

3.2.3 Polymer Synthesis

Partially fluorinated hydrophobic oligomers (6FK)

The synthesis of a fluorine terminated 6FK oligomer with 10 Kg/mol number average molecular weight (M_n), for example, was carried out as follows: 6F-BPA (3.500 g, 10.41 mmol) was added to a three-neck 100mL round bottom flask equipped with a

mechanical stirrer, a condenser, a nitrogen inlet and a Dean-Stark trap. DMAc (24 mL) was added to the flask and the mixture was stirred to obtain a clear solution. Then K_2CO_3 (1.655 g, 11.96 mmol) was added, followed by toluene (12 mL). The reaction bath was first set to 140 ^oC and kept at this temperature for 4 h to azeotrope water. The bath temperature was raised to 160 ^oC to remove most of the toluene. The reaction was cooled to 80 ^oC and DFK (2.391g, 11.00mmol) was added. The bath temperature was raised to 135 ^oC for 10 hours, then cooled to room temperature and filtered to remove the salt, and precipitated into methanol (1000 mL). The oligomer was stirred overnight in methanol and then dried in *vacuo* at 110 ^oC for 48 h before use.

Fully disulfonated BPS-100 oligomers (BPS100)

A sample synthesis of pheonxide terminated 10 Kg/mol BPS100 is as follows: A three neck round bottom flask, equipped with a mechanical stirrer, a condenser, a nitrogen inlet and a Dean-Stark trap, was charged with BP (1.590 g, 8.54 mmol), SDCDPS (4.435g, 9.03 mmol), and DMAc (28 mL). The mixture was stirred until dissolved, then K_2CO_3 (1.36g, 9.85mmol) and toluene (14 mL) were added. The reaction bath was heated to 145 ^oC for 4 h in order to azeotropically remove water from the system. The bath temperature was slowly raised to 180 ^oC by the controlled removal of toluene. The reaction was allowed to proceed at 180 ^oC for 72 h. The mixture was cooled to room temperature and filtered to remove most of the salt, then coagulated in acetone (1000 mL). The precipitated oligomer was stirred overnight in acetone for 24 h and then dried in *vacuo* at 140 ^oC for 48 h.

6FK-BPS100 hydrophobic-hydrophilic multiblock copolymers

A typical coupling reaction was conducted as follows: BPSH100 (4.500g, 0.300mmol), K_2CO_3 (0.150g, 1.087mmol), NMP (44 mL) and cyclohexane (15 mL) were added to a three-necked 100-mL flask equipped with a mechanical stirrer, a condenser, a nitrogen inlet and a Dean-Stark trap. The reaction bath was heated to 120 ^oC for 6 hours to remove water from the system. After removing cyclohexane, the reaction bath was cooled to 90 ^oC, and 6FK oligomer (4.500 g, 0.300 mmol) was added. The bath temperature was raised to 150 ^oC and kept at this temperature for 48 h. The reaction mixture was precipitated into acetone (1000 mL), affording a fibrous polymer. The product was stirred in acetone for 12 h and in deionized water at 90 ^oC for 12 hours, and dried in *vacuo* at 120 ^oC for 24 h.

3.2.4 Membrane Preparation

The copolymers in salt form were dissolved in DMAc (~7% w/v) and filtered through a 0.45 μm Teflon syringe filter. The filtered solution was then cast onto dry, clean glass substrate and dried for 24 h under an infrared lamp at ~45 ℃. The membranes were treated via 2 methods. In Method 1, the membranes were annealed under vacuum at 195 ℃, which is about 30 ℃ higher than the T_g of 6FK blocks. In Method 2, the membranes were further dried in a vacuum oven at 110 ℃ for 24 h. The membranes in the salt form were converted to acid form by boiling in 0.5 M sulfuric acid solution for 2 h, followed by boiling in deionized water for 2 h as reported earlier [27].

3.2.5 NMR Spectroscopy, Size Exclusion Chromatography (SEC), Small Angle X-ray Scattering (SAXS) and Transmission Electron Microscopy (TEM) Characterization

^{1}H, ^{13}C and ^{19}F NMR analysis were conducted on a Varian INOVA 400 MHz spectrometer. The spectra of BPS100 oligomers and 6FK-BPS100 multiblock copolymers were obtained from a 10% solution (w/v) in a DMSO-*d*6 solution at room temperature. The spectra of 6FK hydrophobic oligomers were obtained from a solution in $CDCl_3$.

Size exclusion chromatography (SEC) experiments for 6FK-BPS100 multiblock copolymers were performed on a liquid chromatography equipped with a Waters 1515 isocratic HPLC pump, Waters Autosampler, Waters 2414 refractive index detector, and Viscotek 270 RALLS/ viscometric dual detector. NMP (containing 0.05M LiBr) was used as the mobile phase [28]. The column temperature was maintained at 60 ^{o}C because of the viscous nature of NMP. Intrinsic viscosities of 6FK oligomers were obtained from an Alliance Waters 2690 Separations Module with a Viscotek T60A dual viscosity detector and laser refractometer equipped with a Waters HR 0.5 + HR 2 + HR 3 + HR 4 styragel column set. Chloroform was used as the mobile phase at 30 ℃. Both the mobile phase solvent and sample solution were filtered before introduction to the SEC system.

SAXS was performed using a Riguka S-Max 300 3 pinhole SAXS system. X-ray source is the Cu Kα radiation, and the wavelength is 0.154 nm. The sample-to-detector distance is 1600 mm. SAXS two-dimensional images were obtained using a fully integrated 2D multiwire proportional counting gas-filled detector, with an exposure time of 1 hour. All he membranes were characterized in salt form. The measured intensity

values were corrected for sample thickness, sample transmission and background scattering.

The bulk morphologies of the membranes were characterized by transmission electron microscopy (TEM). The electron density contrast between the hydrophilic and hydrophobic segments within the membrane samples was enhanced by quantitatively exchanging the acidic protons on the sulfonic acid moieties with cesium ion. Acidified membranes were immersed in DI water and were titrated with aqueous CsOH solution until the solution became neutral. The cesium stained membranes were then embedded in epoxy and ultramicrotomed into 50–70 nm thin sections with a diamond knife. Transmission electron micrographs were obtained using a Philips EM 420 transmission electron microscope (TEM) operating at an accelerating voltage of 47 kV.

3.2.6 Thermo Properties Analyses

Thermogravimetric analyses (TGA) of the 6FK-BPSH100 membranes (acid form) were determined by using a TA Instrument TGA Q500. Prior to TGA characterization, all the samples were vacuum-dried and kept in the TGA furnace at 150 ^{o}C for 30 min to remove residual solvent and moisture. The samples were then evaluated over the range of 50-650 ^{o}C at a heating rate of 10 ^{o}C/min under an air atmosphere. Glass transition temperatures (T_gs) of 6FK-BPS100 membranes (salt from) were determined by differential scanning calorimetry (DSC) using a TA Instruments DSC Q-1000 at a heating rate of 10 ^{o}C/min under a stream of nitrogen. Prior to DSC characterization, all the samples were thermally treated with Method 1.

3.2.7 Dynamic Mechanical Analysis

Dynamic mechanical analysis (DMA) was performed using a TA Instruments 2890 Dynamic Mechanical Analyzer. Salt-form rectangular membrane films measuring 0.35 mm x 4 mm x 25 mm were used for the test. Multi-frequency tension tests were conducted on the membranes, with an amplitude of 25 μm and a pre-load force of 0.025 N in a nitrogen atmosphere.

3.2.8 Characterization of Fuel Cell-Related Properties

Proton conductivity

The proton conductivity of the membrane was determined from the geometry of the cell and resistance of the film, which was measured at the frequency that produced the minimum imaginary response. Proton conductivity at 30 ^{o}C at full hydration (in liquid water) was determined in a window cell geometry using a Solartron 1252 + 1287 Impedance/Gain-Phase Analyzer over the frequency range of 10 Hz to 1 MHz following procedures reported in the literature. In determining proton conductivity in liquid water, membranes were equilibrated at 30 ^{o}C in DI water for 24 h prior to testing. For determining proton conductivity under partially hydrated conditions, membranes were equilibrated in a humidity-temperature oven (ESPEC, SH-240) at the specified relative humidity (RH) and 80 ^{o}C for 1 h before each measurement. The conductivity was calculated by the following equation (Equation 3.1):

$$\sigma = \frac{L}{R \cdot S} \quad \text{(Equation 3.1)}$$

Where σ (S/cm) is proton conductivity, L (cm) is the distance between two electrodes, R (Ω) is the resistance of the membrane and S (cm^2) is the surface area that protons transport though the membrane.

Water uptake

The water uptake of all membranes was determined gravimetrically and was taken as the wet-to-dry-weight ratio, expressed as a percentage. First, the acidified membranes were soaked in water at room temperature for 2 days. Wet membranes were removed from the liquid water, blotted dry to remove surface droplets, and quickly weighed. The membranes were then vacuum-dried at 120 ℃ for at least 24 h to a constant weight and weighed again. The water uptake of the membranes was calculated according to Equation 3.2 where $mass_{dry}$ and $mass_{wet}$ refer to the mass of the dry membrane and the wet membrane, respectively.

$$water\ uptake\% = \frac{mass_{wet} - mass_{dry}}{mass_{dry}} \times 100 \text{ (Equation 3.2)}$$

Determination of swelling ratio

The volume swelling ratios of the membranes were determined from the dimensional changes from wet to dry state. Both in-plane and through-plane dimensional changes were measured. Membranes were equilibrated in deionized water, and dimensions in the wet state were measured. The dried dimensions were obtained after drying the wet membrane at 80 ^{o}C in a convection oven for 2 h.

3.3 Results and Discussion

3.3.1 Synthesis and Characterization

Synthesis of partially fluorinated Oligomers

The telechelic oligomers bearing appropriate end-groups and molecular weights were synthesized via step growth polymerization. Figure 3.1 shows the synthesis of fluorine terminated hydrophobic 6FK oligomers by polymerizing 6F-BPA with excess DFK. The molecular weight and end group functionality of the oligomers was precisely controlled by off-setting the molar feeding ratios of monomers according to Carothers equation. In all cases, the molar feed ratios of DFK over 6F-BPA were greater than 1 to give fluorine telechelic functionality and target number-average molecular weights ranging from 3 to 17 kg/mol.

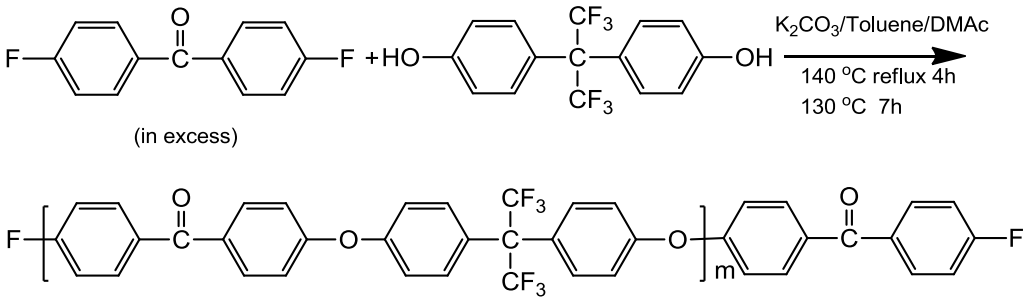

Figure 3. 1. Synthesis of fluorine terminated poly(arylene ether ketone) (6FK) hydrophobic oligomer

Figure 3.2 shows the ^{1}H NMR spectrum of a 6FK oligomer. The peak at 7.23 ppm is the solvent $CDCl_3$.

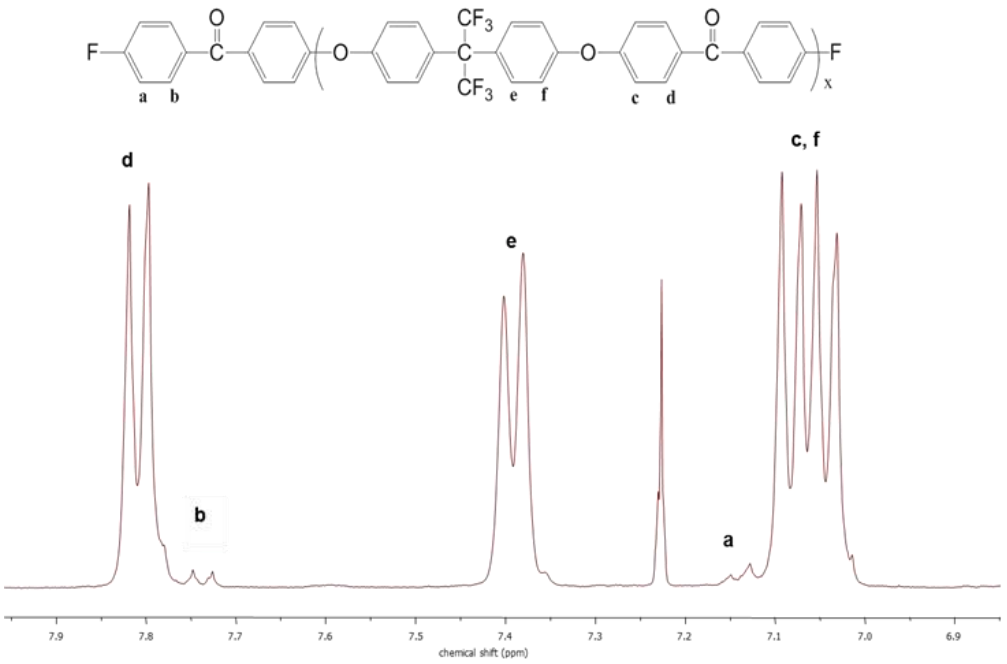

Figure 3. 2. ^{1}H NMR of 6FK 10 kg/mol oligomer

The number-average molecular weight (M_n) of 6FK oligomer can be determined by ^{19}F NMR end group analysis. There are two peaks in the ^{19}F NMR spectrum of a 6FK oligomer, as shown in Figure 3.3, one is attributed to the fluorine of the hexafluoroisopropylidene group in the main chain (−64.0 ppm), and the other is assigned to the end group aromatic fluorine peak (−106.1 ppm). The experimental M_n of the oligomers were calculated based on the integrations of these two peaks assigned to main chains and end-groups fluorines, and were found to be well agree with the target values.

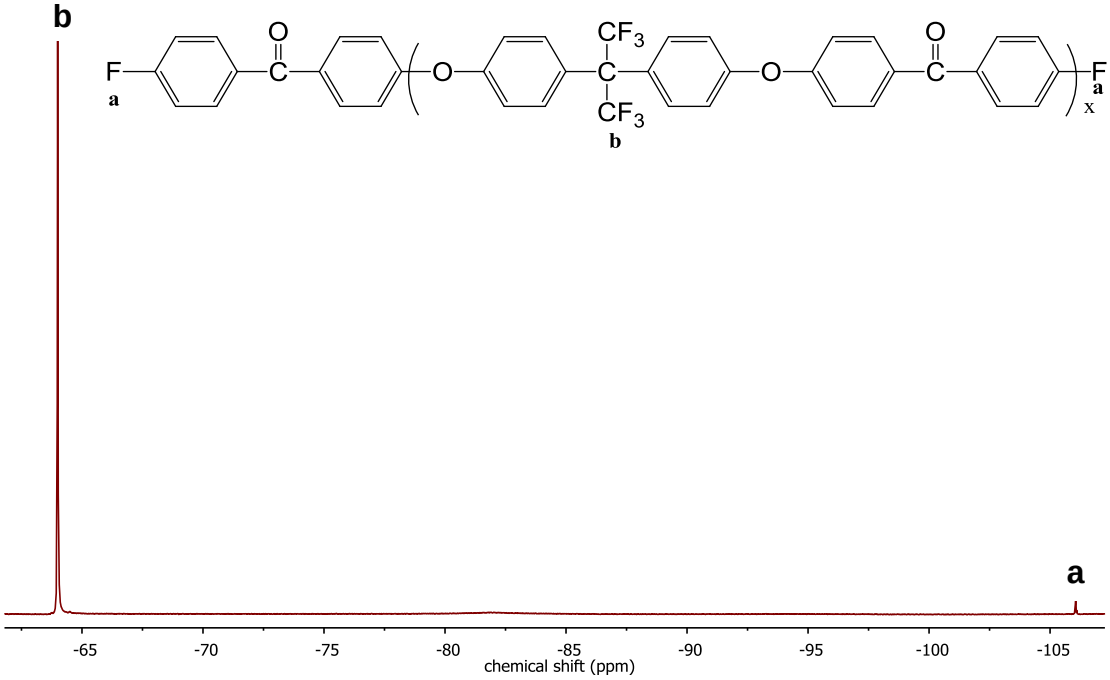

Figure 3. 3. ^{19}F NMR of 6FK 10 Kg/mol oligomer

The determined number average molecular weights from ^{19}F NMR and measured intrinsic viscosity (IV) from SEC of the 6FK hydrophobic oligomers are summarized in Table 3.1. In Figure 3.4, the log-log plot of the intrinsic viscosities and the number-average molecular weights displays a linear relationship and confirms successful control of molecular weight for hydrophobic block series.

Table 3. 1. Molecular weight characterization of 6FK oligomers

Target M_n (kg/mol)	M_n from NMR (g/mol)	IV (dL/g)
5	5200	0.08
7	7100	0.10
10	10300	0.12
12	12100	0.14
14	13600	0.15

* IV values were obtained from SEC in $CHCl_3$ at 30 ^oC

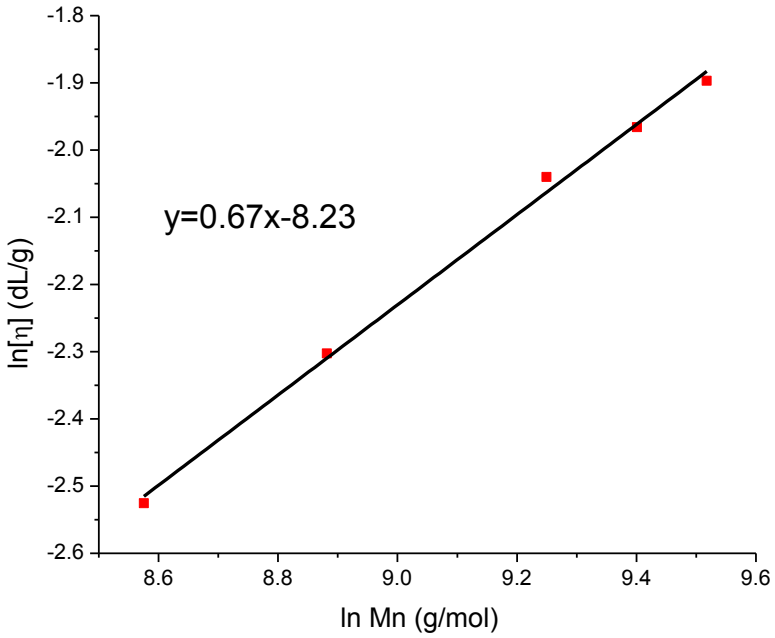

Figure 3. 4. ln η vs. ln M_n plot of 6FK oligomer

Synthesis of fully disulfonated hydrophilic oligomers

As in the synthesis of partially disulfonated BPSH-xx random copolymers, the sulfonated monomer, SDCDPS, was used in the synthesis of the fully disulfonated oligomers. Fully disulfonated poly(arylene ether sulfone) (BPS100) hydrophilic oligomers with phenoxide telechelic functionality were synthesized by copolymerization of SDCDPS and excess BP monomers, as Figure 3.5 shown.

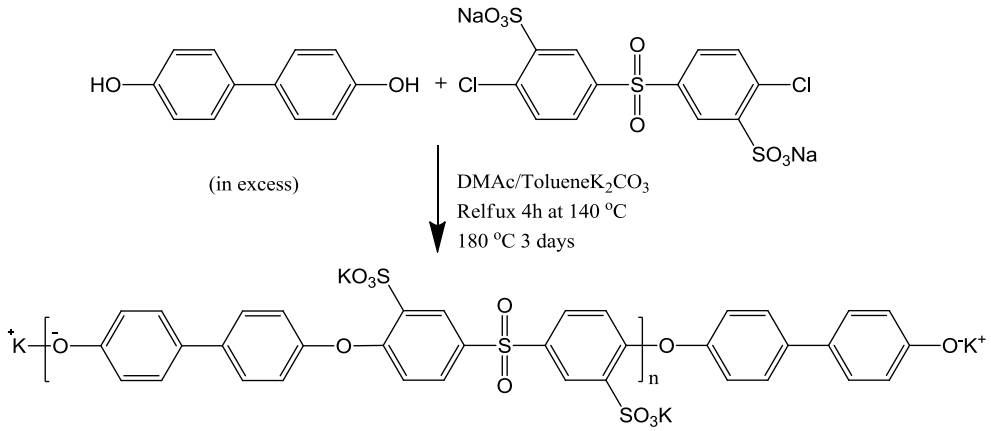

Figure 3. 5. Synthesis of phenoxide terminated fully disulfonated hydrophilic oligomer (BPS100)

The M_n of the hydrophilic oligomer can be determined by ^1H NMR. In the spectrum of a BPS100 oligomer, the four small peaks at 6.80, 7.05, 7.40, and 7.55 ppm are assigned to the protons on the BP moieties located at each end of the oligomer, while the peaks at 7.10 and 7.65 ppm are assigned to the protons on the BP moieties in the middle of BPS100 oligomer backbone, as Figure 3.6 shown. By comparing the integrations of the protons on the end-group BP and of the protons on the SDCDPS moieties, the M_n of BPS100 oligomer can be determined.

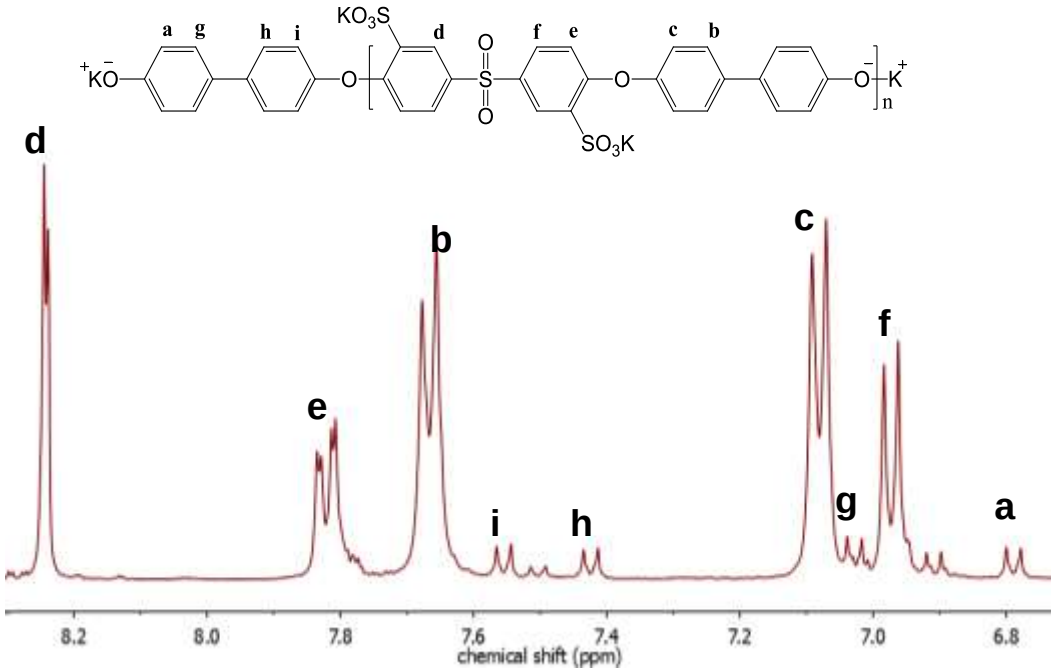

Figure 3. 6. ^{1}H NMR of phenoxide terminated BPS100 Oligomer

The molecular weights measured from NMR and intrinsic viscosities obtained from SEC of BPS100 oligomers are summarized in Table 3.2. In Figure 3.7, there is a linear relationship between the log number average molecular weights and log intrinsic viscosities, indicating that the control of the molecular weights for BPS100 hydrophilic oligomers was successful.

Table 3. 2. Molecular weight characterizations of BPS100 oligomers

Target Mn (g/mol)	Mn from ^{1}H NMR (g/mol)	IV* (dL/g)
5k	5200	0.13
7k	7100	0.18
10k	10300	0.23
12k	12200	0.28
14k	14200	0.30

* IV values were obtained from SEC in 0.05M LiBr/NMP at 60 ^{o}C

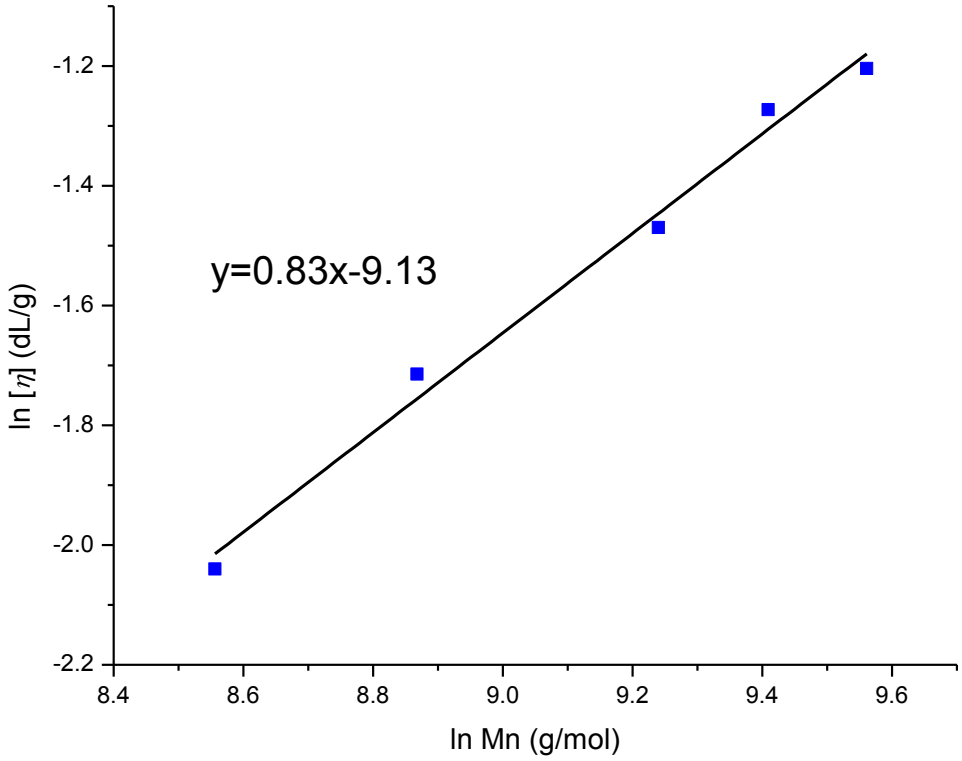

Figure 3. 7. ln η vs. ln M_n plot of BPS100 oligomer

Synthesis of 6FK-BPS100 multiblock copolymers

Multiblock copolymers were synthesized by coupling the telechelic oligomers with appropriate end-groups and molecular weights, as shown in Figure 3.8. The fluorine telechelic functionality in hydrophobic oligomers and phenoxide end group in hydrophilic oligomers enable the block copolymerization to be conducted. The viscosity of the reaction solution increased slowly during the polymerization.

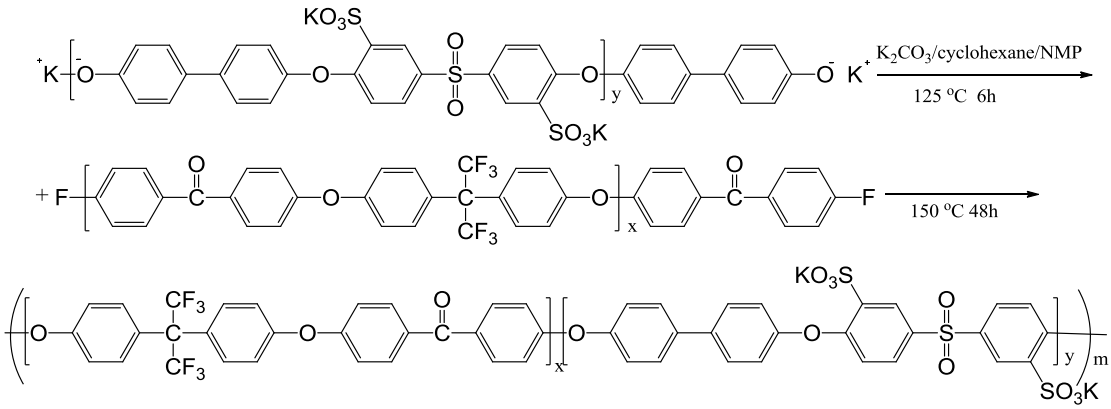

Figure 3. 8. Synthesis of 6FK-BPS100 multiblock copolymers via coupling reaction

The synthesis of the 6FK-BPS100 multiblock copolymers was monitored by ^{1}H NMR. The fully coupled hydrophobic-hydrophilic multiblock structure was confirmed by the disappearance of the peaks due to end-groups of BPS100 oligomers in the ^{1}H NMR spectrum of resulting copolymer, as Figure 3.9 shown. Thus high conversion of the coupling reaction should have been achieved. In this coupling reaction, the ether–ether chain interchange reaction is a concern, which may result in a randomized chain structure. Only narrow, sharp, non-split peaks were observed in the ^{13}C NMR spectrum of 6FK-BPS100 10k-10k, as shown in Figure 3.10, confirming the presence of long ordered

hydrophobic and hydrophilic segments and the minimization of ether-ether chain interchange reaction.

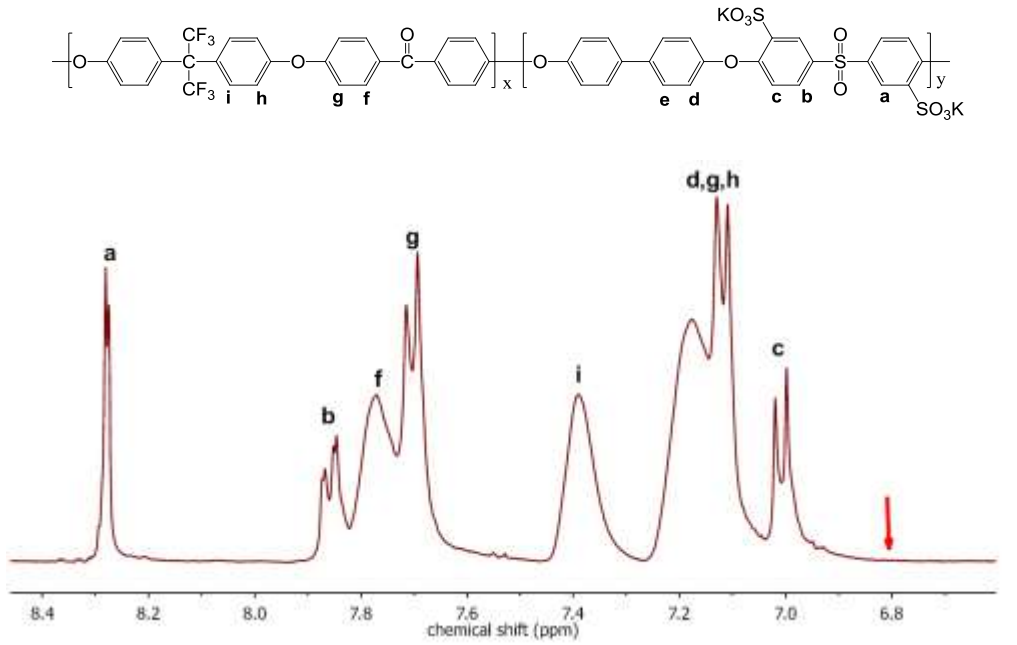

Figure 3. 9. ^{1}H NMR of 6FK-BPS100 10k-10k multiblock copolymer

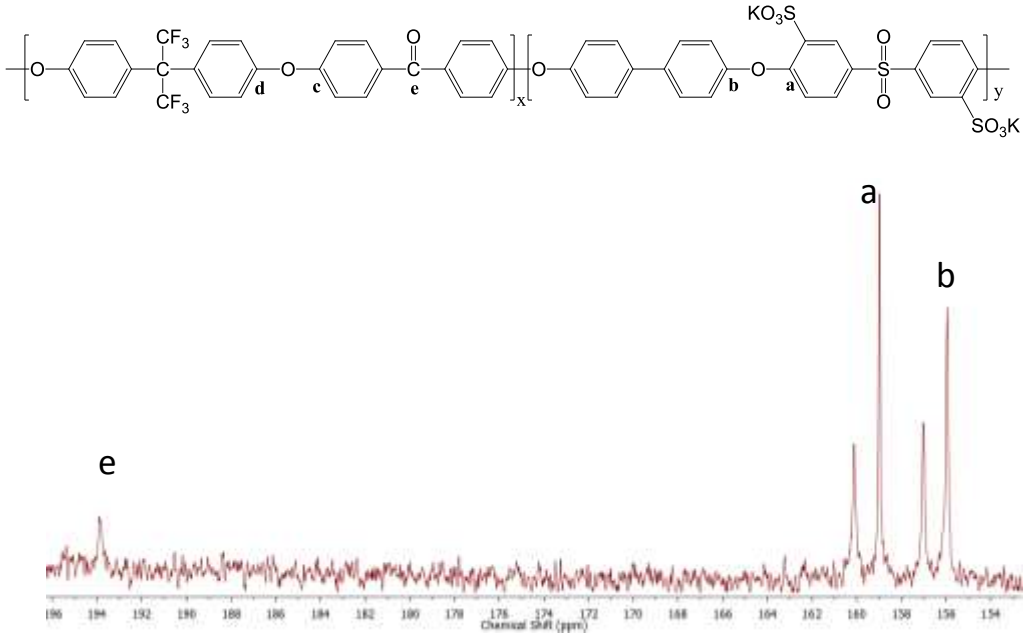

Figure 3. 10. ^{13}C NMR of 6FK-BPS100 10k-10k multiblock copolymer

Characterization data for a series of 6FK-BPS100 multiblock copolymers are listed in Table 3.3. It is worth noting that the IEC values of the multiblock copolymers can be controlled by adjusting the molar charge ratios of the hydrophobic oligomers to the hydrophilic oligomers. Although the feed ratios are generally higher than 1:1, all the copolymers yield high intrinsic viscosities which make they are capable of being cast into tough membranes. Thus, unlike random polymerizations of smaller monomers, a perfect stoichiometry is not necessary in coupling reactions of telechelic oligomers.

Table 3. 3. Characterization of 6FK-BPS100 multiblock copolymers

Hydrophobic-Hydrophilic Block Length (g mol^{-1})	5k-5k	7k-7k	9k-9k	12k-12k	14k-14k	17k-17k
Molar Feed Ratio	1.1:1	1.1:1	1.1:1	1.1:1	1.1:1	1.1:1
Intrinsic Viscosity[a] (dL g^{-1})	1.25	1.34	1.15	1.08	1.10	1.14
IEC[b] (meq g^{-1})	1.50	1.55	1.55	1.50	1.50	1.55

[a] Measured using SEC in NMP with 0.05M LiBr at 60 ℃
[b] Measured by ^{1}H NMR

The DSC trace of a 6FK-BPS100 14k-14k multiblock copolymer is shown in Figure 3.11. Two thermal transitions, one at 165 ^{o}C and the other at 245 ^{o}C, are observed and assigned to the glass transitions for the hydrophobic 6FK and hydrophilic BPS100 oligomers, respectively. The two distinguished T_gs indicate the existence of nanophase separated block structures. The two T_g phenomenon was also found in the DSC trace of 6FK-BPS100 12k-12k and 17-17k. But in the DSC trace of the 6FK-BPS100 5k-5k block copolymer, only one T_g was observed. Longer blocks increase the immiscibility between 2 different blocks and enhance the nanophase separation in the multiblock systems.

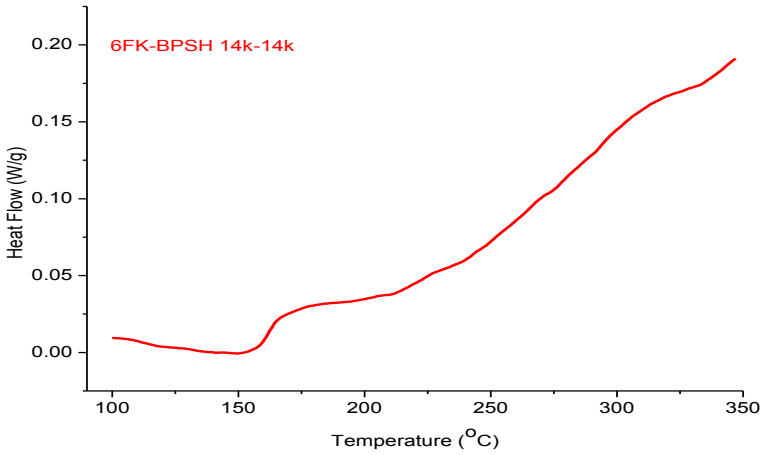

Figure 3. 11. DSC thermogram of a 6FK-BPS100 14k-14k multiblock copolymer

3.3.2 Characterization of Membrane Properties of 6FK-BPS100 Multiblock Copolymers

Membrane properties of the 6FK-BPS(H)100 multiblock copolymers varying in block lengths were characterized on the basis of water uptakes, dynamic mechanical properties, morphology, thermogravimetric properties and proton conductivities (both under fully and partially hydrated conditions) to determine their potential fuel cell applications. Nafion® 212 and random copolymer BPSH35 are represented as controls.

Water uptake of the 6FK-BPSH100 membranes

For proton exchange membranes, one of the most important properties is the water uptake. Water residing in the hydrophilic domains is known to play a critical role in proton transport. It has been shown in our previous research that water uptake generally increases with an increase in block length and/or increase in ion exchange capacity (IEC). Proton conductivity showed some improvement at very long hydrophilic block lengths.

However, the accompanying high water uptake and high swelling ratio deteriorated the mechanical properties of the membrane. To address this dilemma, we adopted in this research various thermal treatments on the salt-form membranes to tailor the morphology development during film formation, aiming at reducing the water sorption without compromising IEC and high proton conductivity. As shown in Table 3.4, the non-annealed membranes (Method 2) showed the typical trend of water uptake increase with longer hydrophilic block lengths. However, upon annealing at 30 ^{o}C higher than the T_g of 6FK block, all the membranes (Method 1) showed greatly reduced water sorption. The reduction in wt% of water sorption was as high as nearly 6 times after annealing treatment. More interestingly, the water uptake of the annealed samples showed no dependence on the block length of copolymers, which seems to suggest that annealing treatment would be a feasible and efficient approach to overcome the loss of mechanical and dimensional stabilities for the membranes with very long hydrophilic blocks in the fully hydrated state.

Table 3. 4. Effect of annealing on the water uptake of 6FK-BPSH100 block copolymers

	Water Uptake				
6FK-BPSH100	5K-5K	7K-7K	9K-9K	12K-12K	14K-14K
Method 1	60%	54%	55%	50%	55%
Method 2	60%	70%	140%	274%	320%

Small angle X-ray scattering (SAXS) profiles of 6FK-BPS100 membranes

Small sngle X-ray scattering (SAXS) can be applied to determine the lamellar structure in semicrystalline polymers, dimensions of phase-separation in block

copolymers and heterogeneities in ionomers. The morphology information of the long-range ordered periodic microdomain structure in a block copolymer can be obtained from the relative positions of the scattering peaks in the SAXS profiles [29]. For a lamellar structure, the SAXS profile shows a series of peaks with the q value at q_{max}, $2q_{max}$ $3q_{max}$……where q_{max} is the scattering wave vector of the first order scattering maximum. The SAXS profiles of the 6FK-BPS100 multiblock copolymer membranes cast with DMAc and thermal treated with Method 1 are presented in Figure 3.12. In the investigated range of scattering wave vectors (q), the profiles of 6FK-BPS100 multiblock copolymer membranes exhibit scattering maxima, while the SAXS profile of BPS35 random copolymer membrane is featureless [30]. The observed scattering maxima in the profiles of 6FK-BPS100 series membranes are attributed to the aggregated ionic domains. The SAXS profiles of 6FK-BPS100 multiblock copolymer membranes also confirm the presence of the ordered periodic microstructures and the dependence of ordered periodic microstructures on the block length of the oligomers. For the 6FK-BPS100 17k-17k and 9k-9k, there are 2 peaks can be clearly observed in each SAXS profile, the first order peak is at q_{max} and the second order one is at 2 q_{max}, which suggests the presence of the highly ordered lamellar structure. The second order peak of 6FK-BPS100 3k-3k is relatively weaker than those of 9k-9k and 17k-17k. The SAXS profile of 6FK-BPS100 3k-3k indicates the short block length, although induces the aggregation of ionic domain, prevents the formation of well-order lamellar structure. It is also observed that with the block length increases of 6FK-BPS100 series, the main scattering peak shifts to the lower q values. This behavior indicates the interdomain distance increases with the block length increases.

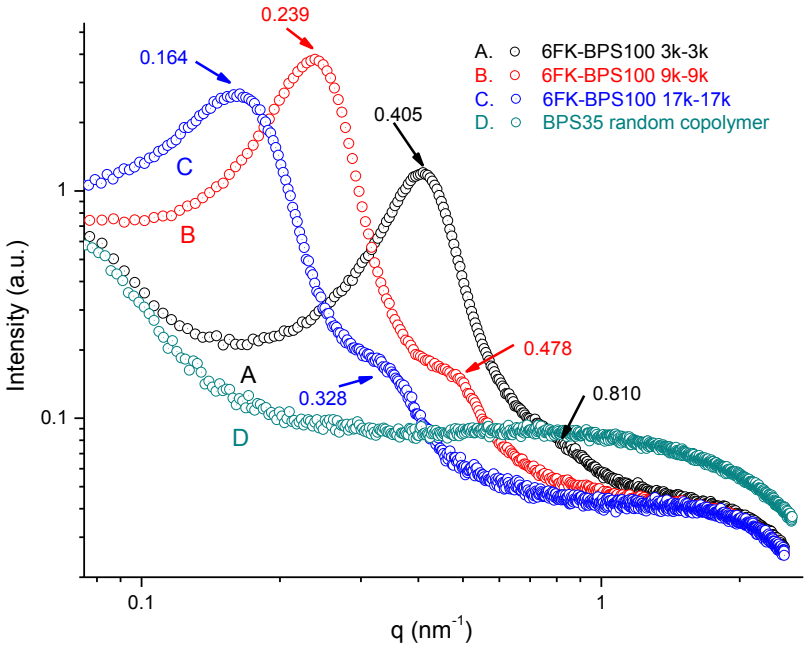

Figure 3. 12. SAXS profiles of 6FK-BPS100 membranes cast from DMAc and treated with Method 1

It is worth noting that the difference of SAXS profiles of 6FK-BPS100 multiblock copolymer membranes thermally treated with 2 different methods. Figure 3.13 shows the SAXS profiles of 6FK-BPS100 17k-17k treated with Method 1 and Method 2. The SAXS profile of 17k-17k treated by Method 2 exhibits 3 peaks at $q(2)_{max}$, $2q(2)_{max}$, and $3q(2)_{max}$, while that of 17k-17k treated by Method 1 only exhibits 2 peaks at $q(1)_{max}$ and $2q(1)_{max}$. The intensity of the scattering peak at 2^{nd}-order peak of 17k-17k treated by Method 1 is weaker than that of 17k-17k treated by Method 2. The 17k-17k membrane treated by Method 2 shows a more ordered lamellar structure with longer-range periodicity, which allows for higher water uptake values and higher swelling ratios. However, the *q* value with the maxima scattered intensity of 17k-17k treated by Method 1 is smaller than that

of 17k-17k treated by Method 2, which indicated an interdomain distance increase in the 17k-17k sample after annealing at 195 ^{o}C.

The thermal treatment also shows a dependence on the block length. The SAXS profiles of the 6FK-BPS100 14k-14k and 9k-9k membranes also show the same tendency as the 17k-17k membrane after annealing. However, the SAXS profiles of 6FK-BPS100 3k-3k membranes treated with 2 methods show no significant difference, as shown in Figure 3.14. The increase of the interdomain distances of 6FK-BPS100 with longer block length after annealed at 195 ^{o}C may induce enhanced ionic domain aggregation and facilitate the proton transport in the membranes.

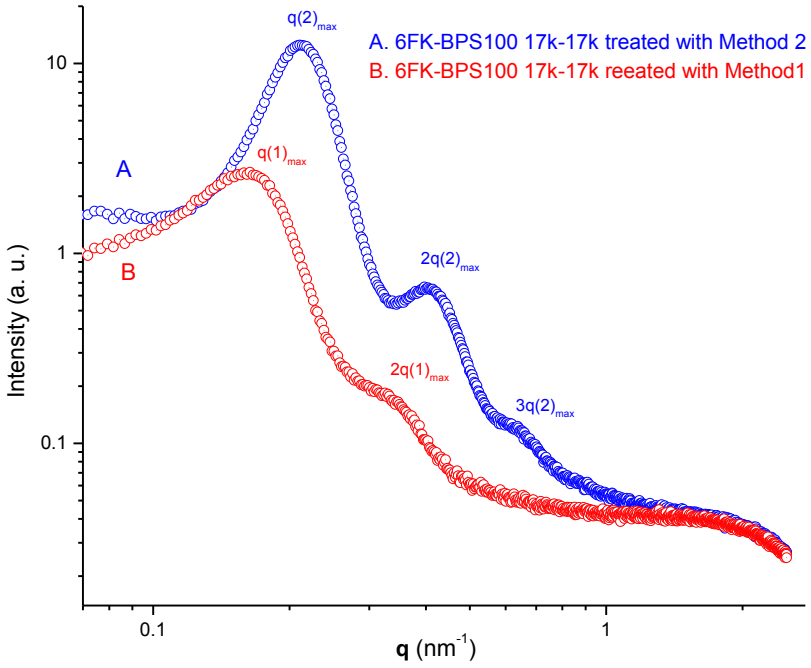

Figure 3. 13. SAXS profiles of 6FK-BPS100 17k-17k membranes cast from DMAc and treated with 2 methods

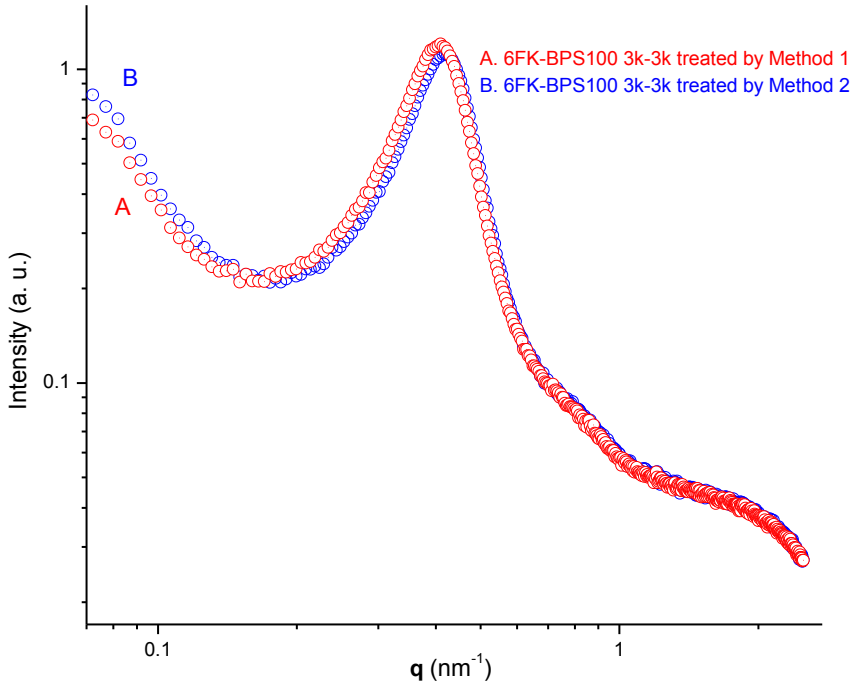

Figure 3. 14. SAXS profiles of 6FK-BPS100 3k-3k membranes cast from DMAc and treated with 2 methods

Dynamic mechanical analysis (DMA) of 6FK-BPS100 14k-14k membranes

Preliminary studies on the dynamic mechanical behavior of these membranes treated by 2 methods were conducted on 6FK-BPS100 14k-14k multiblock copolymer membranes, as shown in Figure 3.15. It is observed that upon annealing at 30 ^{o}C higher than the T_g of 6FK hydrophobic oligomers, the membrane shows an increased initial storage modulus in dynamic tests. The significant difference in dynamic mechanical behavior between the annealed and non-annealed samples, along with the greatly reduced water uptake upon annealing, seem to suggest that a preferable co-continuous nanophase separated morphology was fully developed in the annealed membranes, which is in

agreement with the observed increase of the interdomain distance from the SAXS profiles. The formation of preferable co-continuous nanophase separated morphology may be beneficial in rendering decent proton conductivities under both fully and partially hydrated conditions.

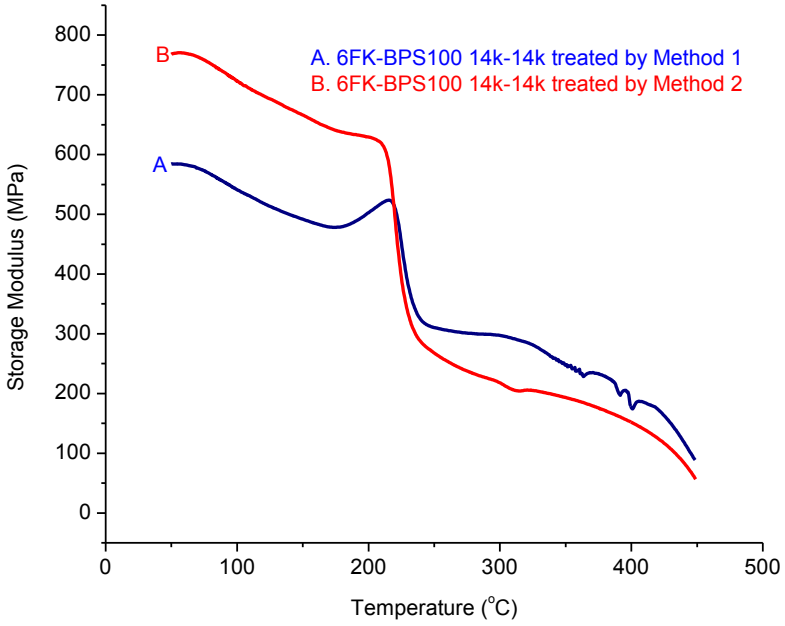

Figure 3. 15. Effect of annealing on the dynamic mechanical behavior of 6FK-BPS100-14K-14K

Membrane properties of 6FK-BPSH100 multiblock copolymers

The fundamental properties of the 6FK-BPSH100 multiblock copolymer membranes thermally treated by Method 1 are summarized in Table 3.5. A BPSH35 random copolymer and a Nafion® 212 were also included as controls. The intrinsic viscosity (IV) data confirmed that high molecular weight multiblock copolymers were achieved. Tough, ductile, transparent membranes were also cast from the copolymers, indicating that high

molecular weight was achieved. The IEC values of the 6FK-BPSH100 multiblock copolymers were well controlled around 1.5 meq/g by adjusting molar charge ratios for the hydrophobic:hydrophilic oligomers at 1.1:1. As a general observation, all of the 6FK-BPSH100 mulitblock copolymer membranes showed superior or comparable proton conductivity compared to Nafion® 212 and BPSH35. The dependence of liquid water proton conductivity on the block length was also observed. With the block length increase, improved proton conductivity was observed in liquid water. This observation is in agreement with our studies on other poly(arylene ether sulfone) multiblock copolymer systems [16].

Table 3. 5. Properties of the 6FK-BPSH100 multiblock copolymers

Polymer (6FK-BPSH100)[a] (1.1:1)	IV (dL/g)[b]	IEC (meq/g)[c]	Water uptake[d] (%)	Proton Conductivity[e] (S/cm)
5k-5k	1.25	1.50	60	0.11
7k-7k	1.34	1.55	54	0.14
9k-9k	1.15	1.55	60	0.15
12k-12k	1.08	1.50	50	0.14
14k-14k	1.10	1.50	55	0.17
17k-17k	0.76	1.55	65	0.17
Nafion® 212	N/A	1.00	22	0.11
BPSH35	0.85	1.52	35	0.07

a: Membranes were treated by Method 1 then acidfied
b: Measured by SEC with 0.05M LiBr/NMP as mobile phase at 60 ℃
c: Measured from ^{1}H NMR
d: Measured in acid form
e: Conductivities were measured in liquid water at 30 ^{o}C

In the practical operation of PEMFC, proton exchange membranes that have high proton conductivity in partially hydrated state are desirable. The thermal treatment dependence on the 6FK-BPS100 membranes of the proton conductivities under 30-95% RH range has been studied. Figure 3.16 shows the proton conductivity at 80 ℃ as a function of RH for 6FK-BPSH100 14K-14K membranes thermal treated by 2 methods. Like Nafion® 212 (curve A), a quick drop of proton conductivity with reduced humidity was observed for 6FK-BPSH100 14k-14k treated by Method 2 (curve B), which was ascribed to the increase in the morphological barrier to proton transport at low RH levels. However, it is not surprising to observe again the beneficial impact of annealing (thermally treated via Method 1) on the proton conductivity under partially hydrated conditions. The annealed membrane (curve C) showed a reduced humidity dependence of proton conductivity. The annealed 6FK-BPSH100 14K-14K outperformed Nafion® 212 across the full RH range, particularly at the low humidity levels from 60% to 30%. Combined with the aforementioned beneficial effects of annealing in reducing water uptake and improving dynamic mechanical behavior, this observation further confirmed the importance of film processing conditions in providing PEM materials with excellent performance.

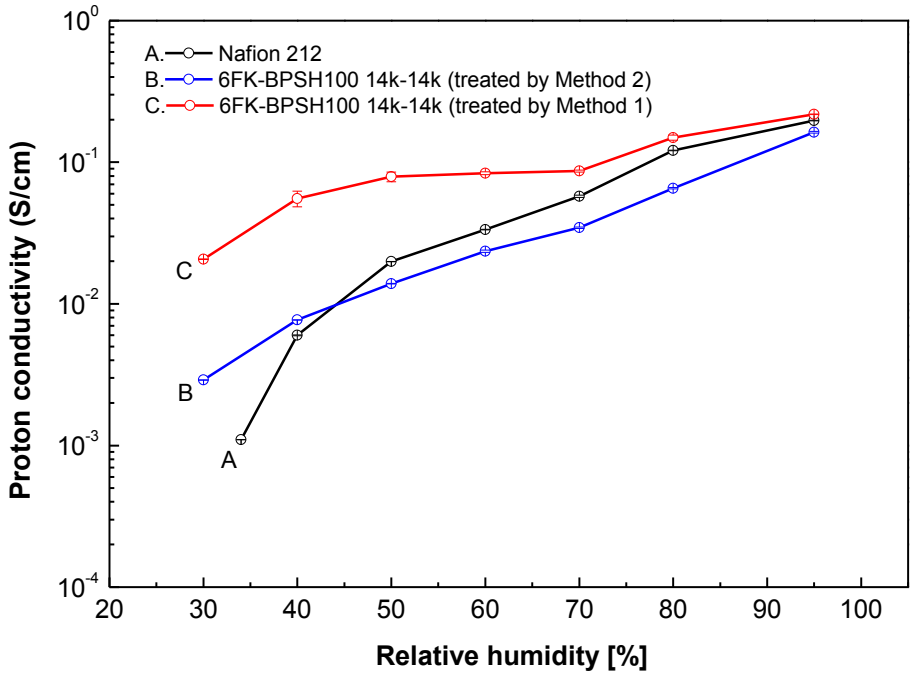

Figure 3. 16. Effect of annealing on the proton conductivity of 6FK-BPSH100 14K-14K multiblock copolymer under partially hydrated conditions (measured at 80 ℃)

It is also interesting to investigate the effect of the block length of 6FK-BPSH100 multiblock copolymers on the proton conductivity dependence of humidity. Figure 3.17 shows the plots of proton conductivity as a function of relative humidity (RH) at 80 ℃ for 6FK-BPSH100 copolymer membranes with difference block lengths. All the 6FK-BPSH100 block copolymer membranes treated by Method 1 outperform Nafion® 212 across the full RH range. As the block length of 6FK-BPSH100 multiblock copolymer increases, the performance under partially hydrated conditions also improves. It is worth noting that in the RH range from 70% to 50%, the conductivity curves for all three 6FK-BPSH100 membranes are relatively flat, which indicates the RH range from 50%-70% may be the optimal operation window for the conductivity performance of

6FK-BPSH100 membranes. These results again suggest the presence of enhanced, co-continuous proton transport channels in the 6FK-BPSH100 multiblock copolymer membranes. Under the partially hydrated conditions, protons still can be transported through enhanced, continuous proton transport channels along the sulfonic acid groups and water molecules.

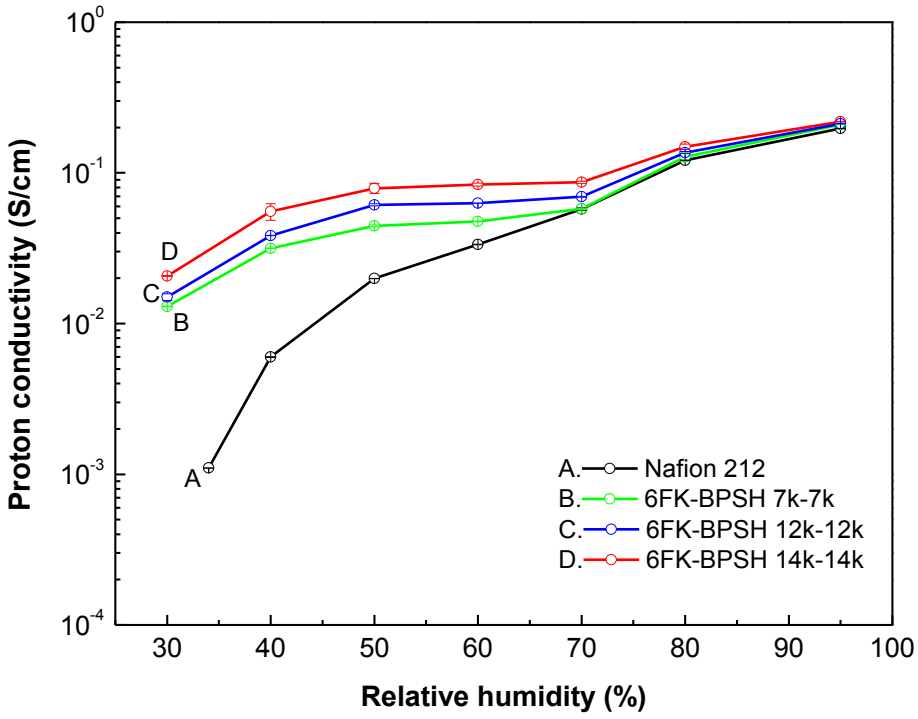

Figure 3. 17. Effect of block length on the proton conductivity of 6FK-BPSH 100 multiblock copolymers (measured at 80 ℃)

Transmission Electron Microscopy (TEM) of 6FK-BPS100

It was observed that hydrophilic-hydrophobic mulitblock copolymers exhibited well ordered nanophase separation [19]. The extent of this nanophase separation is recognized

to provide continuous hydrophilic proton transport channels and facilitate the proton transport. Figure 3.18 shows the TEM images of the 6FK-BPSH multiblock copolymer membranes with different block lengths treated by Method 1. The bright and dark regions in the images correspond to un-stained hydrophobic domains and cesium stained hydrophilic domains, respectively. Distinguished nanophase separated morphologies were developed in the 6FK-BPSH multiblock copolymer membranes. The longer block length multiblock system, 6FK-BPSH100 14k-14k, shows an enhanced connectivity of both bydrophilic and hydrophobic domains and more clear lamellar structure compared to 7k-7k. This observation of well-connected hydrophilic proton transporting channels developed in the annealed membranes reveals the underlying morphological dependence of proton conductivity, and provides a clear explanation of the excellent conductivity performance under partially hydrated conditions for the longer block length 6FK-BPSH1000 multiblock copolymers, as shown in Figure 3.18.

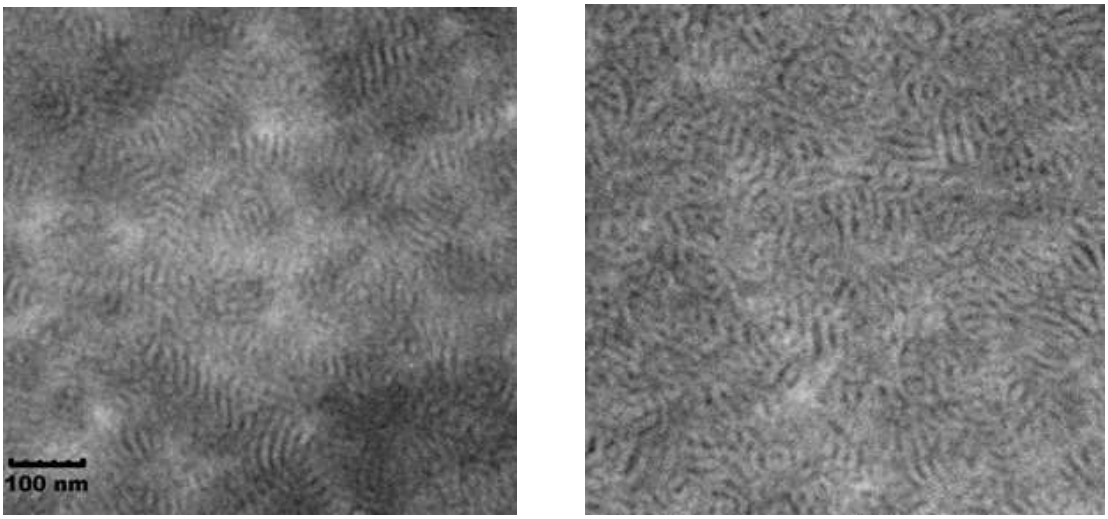

Figure 3. 18. TEM images of 6FK-BPSH multiblock copolymer membranes treated by Method 1 (left: 6FK-BPSH100 7K-7K, right: 6FK-BPSH100 14K-14K)

Dimensional swelling behavior of 6FK-BPSH100 multiblock copolymer membranes

Dimensional swelling testing was performed on the 6FK-BPSH100 series of copolymers. The results for multiblock copolymers treated by Method 1 were also compared to a random copolymer (BPSH35) and Nafion® 112 in Figure 3.19. The multiblock copolymers exhibit anisotropic swelling behavior in contrast to the isotropic swelling of the random copolymer and recast Nafion® 112. With the increase in block length, through-plane (z-direction) swelling increases, while in-plane swelling (x- and y-directions) stays the same or decreases. This behavior indicates the development of enhanced ordered morphology as block length increases. The low in-plane swelling of 6FK-BPSH100 multiblock copolymer membranes should result in much lower stress at the interface and better stability of the MEA to prevent the membrane electrode failure.

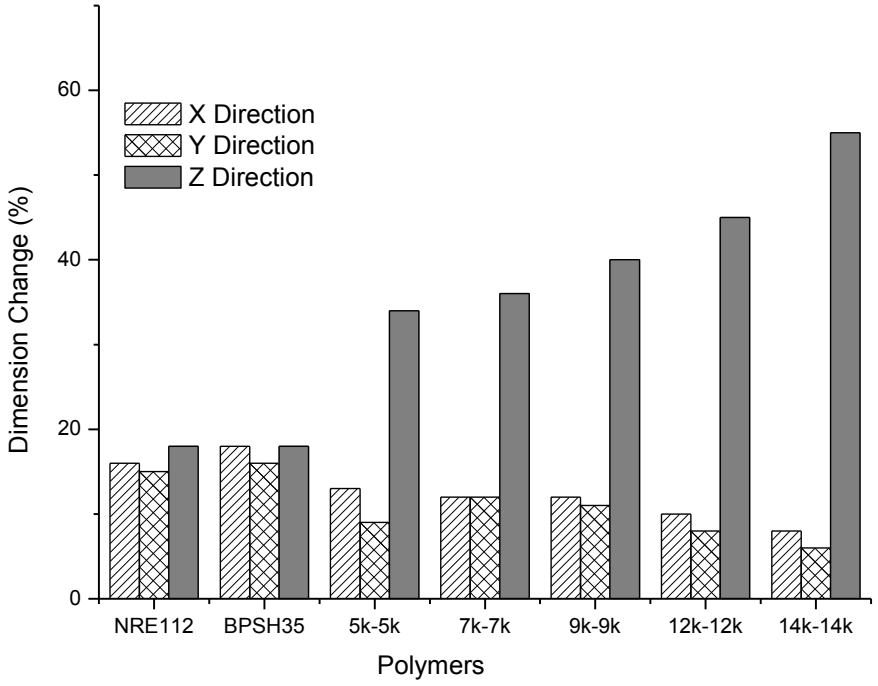

Figure 3. 19. Comparison of dimensional swelling data for 6FK-BPSH100 multiblock, copolymers, BPSH35 and Nafion® 112

3.4 Conclusions

A series of 6FK-BPS100 hydrophobic-hydrophilic multiblock copolymers have been successfully synthesized based on the coupling of a fluorine terminated poly(arylene ether ketone) (6FK) hydrophobic oligomer and a phenoxide terminated disulfonated poly(arylene ether sulfone) (BPS100) hydrophilic oligomer. The regularly sequenced srtructure of 6FK-BPS100 multiblock copolymers were confirmed by ^{13}C NMR. The ether-ether interchange side reactions had been minimized by utilization of a relatively mild reaction temperature. DSC traces of 6FK-BPS100 multiblock copolymers show 2 T_gs and suggest phase separation in copolymers. Intrinsic viscosities of 6FK-BPS100 copolymers confirmed that high molecular weight copolymers were obtained which afforded tough and ductile membranes via DMAc solution casting. For non-annealed samples, water uptake of the membranes in acid form increased with the increase of block lengths. However, water uptake was significantly reduced upon annealing at temperatures greater than the T_g of the 6FK block and the water uptake dependence of block length diminished. Annealing also resulted in the improvement of dynamic mechanical properties of the membranes as demonstrated by the increase in the storage modulus. The block lengths of the annealed copolymers seemed to affect their proton conductivity both in liquid water and under partially hydrated conditions. Multiblock copolymers with higher block lengths showed better performance with regard to proton conductivity, presumably due to their more distinct nanophase separation and better connectivity among the ionic domains, as evidenced by morphology characterizations from TEM and SAXS profiles. Resulting water uptake and superior proton conductivity measurements revealed that the proper combination of hydrophilic and hydrophobic

sequence lengths and film processing conditions (annealing) could yield materials that are more selective than Nafion® 212 by forming distinct nanophase separated morphologies with long and well-connected hydrophilic proton transport channels.

3.5 References:

1. Whittingham MS and Zawodzinski T. Chem. Rev. 2004;104(10):4243.
2. Winter M and Brodd RJ. Chem. Rev. 2004;104(10):4245.
3. Hickner MA, Ghassemi H, Kim YS, Einsla BR, and McGrath JE. Chem. Rev. 2004;104(10):4587.
4. Kerres JA. J. Membr. Sci. 2001;185(1):3.
5. Nakabayashi K, Matsumoto K, and Ueda M. J. Polym. Sci., Part A: Polym. Chem. 2008;46(12):3947.
6. Harrison WL, Hickner MA, Kim YS, and McGrath JE. Fuel Cells 2005;5(2):201.
7. Higashihara T, Matsumoto K, and Ueda M. Polymer 2009;50(23):5341.
8. Smitha B, Sridhar S, and Khan AA. J. Membr. Sci. 2005;259(1-2):10.
9. Nakabayashi K, Matsumoto K, Higashihara T, and Ueda M. J. Polym. Sci., Part A: Polym. Chem. 2008;46(22):7332.
10. Bi H, Chen S, Chen X, Chen K, Endo N, Higa M, Okamoto K, and Wang L. Macromol. Rapid Commun. 2009;30(21):1852.
11. Hu Z, Yin Y, Yaguchi K, Endo N, Higa M, and Okamoto K-i. Polymer 2009;50(13):2933.
12. Uehara H, Kakiage M, Sekiya M, Yamagishi T, Yamanobe T, Nakajima K, Watanabe T, Nomura K, Hase K, and Matsuda M. Macromolecules 2009;42(20):7627.
13. Li YX, Roy A, Badami AS, Hill M, Yang J, Dunn S, and McGrath JE. J. Power Sources 2007;172(1):30.
14. Lee HS, Badami AS, Roy A, and McGrath JE. J. Polym. Sci., Part A: Polym. Chem. 2007;45(21):4879.
15. Lee HS, Roy A, Badami AS, and McGrath JE. Macromolecular Research 2007;15(2):160.
16. Lee HS, Roy A, Lane O, Dunn S, and McGrath JE. Polymer 2008;49(3):715.
17. Lee H-S, Roy A, Lane O, Lee M, and McGrath JE. J. Polym. Sci., Part A: Polym. Chem. 2010;48(1):214.
18. Lee H-S, Roy A, Lane O, and McGrath JE. Polymer 2008;49(25):5387.
19. Badami AS, Roy A, Lee H-S, Li Y, and McGrath JE. J. Membr. Sci. 2009;328(1-2):156.
20. Badami AS, Lane O, Lee H-S, Roy A, and McGrath JE. J. Membr. Sci. 2009;333(1-2):1.
21. Wang H, Badami AS, Roy A, and McGrath JE. Journal of Polymer Science Part a-Polymer Chemistry 2007;45(2):284.

22. Yu X, Roy A, Dunn S, Badami AS, Yang J, Good AS, and McGrath JE. J. Polym. Sci., Part A: Polym. Chem. 2009;47(4):1038.
23. Yu X, Roy A, Dunn S, Yang J, and McGrath JE. Macromolecular Symposia 2006;245-246(1):439.
24. Ghassemi H, McGrath JE, and Zawodzinski TA. Polymer 2006;47(11):4132.
25. Ghassemi H, Ndip G, and McGrath JE. Polymer 2004;45(17):5855.
26. Li Y, VanHouten RA, Brink AE, and McGrath JE. Polymer 2008;49(13-14):3014.
27. Kim YS, Wang F, Hickner M, McCartney S, Hong YT, Harrison W, Zawodzinski TA, and McGrath JE. Journal of Polymer Science Part B-Polymer Physics 2003;41(22):2816.
28. Yang J, Li YX, Roy A, and McGrath JE. Polymer 2008;49(24):5300.
29. Chu B and Hsiao BS. Chem. Rev. 2001;101(6):1727.
30. Lee M, Park JK, Lee H-S, Lane O, Moore RB, McGrath JE, and Baird DG. Polymer 2009;50(25):6129.

Chapter 4: Synthesis and Characterization of Multiblock Partially Fluorinated Hydrophobic Poly(arylene ether nitrile) Hydrophilic Disulfonated Poly(arylene ether sulfone) Copolymers for Proton Exchange Membranes

Yu Chen, Chang Hyun Lee, Myoungbae Lee, Miangqiang Zhang, Robert B. Moore and James E. McGrath*

Macromolecular Science and Engineering Program, Macromolecules and Interfaces Institute, Virginia Polytechnic Institute and State University, Blacksburg, Virginia 24061

Abstract

A series of multiblock copolymers with various block lengths and ion exchange capacities (IECs), based on alternating segments of phenoxide terminated fully disulfonated poly(arylene ether sulfone) (BPS100) and fluorine-terminated poly(arylene ether benzonitrile) (6FPAEB) were synthesized via coupling reaction. By utilizing mild reaction conditions, the ether-ether interchange side reactions were minimized. Tough ductile transparent membranes were cast from the copolymers, indicating that high molecular weight was achieved. Membrane properties of these multiblock copolymers were characterized with regard to intrinsic viscosity, thermal stabilities, morphology, water uptake, and proton conductivity. The results were compared to those of Nafion® and random copolymer 6FPAEB35. The block length dependence on nanophase separated morphology, confirmed by transmission electron microscopy (TEM) and small angle X-Ray scattering (SAXS), accounts for enhanced proton conductivity at reduced relative humidity (RH) with longer block length. In addition, 6FPAEB-BPSH100 multiblock exhibited an improved thermooxide stability compare to BPSH35 and other multiblock copolymers with different chemical structures.

Keywords: multiblock copolymer; partially fluorinated polymer; proton exchange membrane

4.1 Introduction

Fuel cells are electrochemical devices that can directly convert chemical energy into electricity [1, 2]. Due to their high efficiency, high energy density, quiet operation and lack of carbon dioxide emissions, proton exchange membrane fuel cells (PEMFCs) are potentially one of the best candidates for environmentally friendly automotive and stationary power sources [3]. In the PEMFCs, proton exchange membranes (PEMs) are core components, which transport the protons from the anode to the cathode and act as barriers preventing the fuel from mixing with the oxidant. A successful PEM material should have high proton conductivity, good mechanical strength, high oxidative and hydrolytic stability, low fuel and oxidant permeability, ease of fabrication into MEA, and controlled swelling-deswelling behavior under low relative humidity (RH) cycling [3].

The state-of-art commercial PEM materials are typically based on perfluorinated sulfonic acid containing ionomers (PFSAs), such as Nafion® produced by DuPont. Nafion® has high chemical stability, good mechanical stability and high proton conductivity under moderate operating conditions [4]. However, Nafion® is also known to have undesirable drawbacks such as high cost, high methanol permeability, and poor thermomechanical properties over 80 ^{o}C [5, 6].

Sulfonated aromatic statistical copolymers, such as sulfonated poly(arylene ether sulfone)s (BPSHs), poly(ether ether ketone)s (SPEEKs), poly(arylene ether nitrile)s (SPAEBs), polyimides (SPIs) and polybenzimidazoles have been investigated as potential

alternatives to Nafion® [7-14]. High proton conductivities were obtained for some of these polymers, such as BPSH, under well hydrated conditions [15]. However, randomly distributed sulfonic acid groups will lead to isolated morphological domains, which limit the protons transport performance at low relatively humidity (RH). Therefore, the proton conductivities of sulfonated statistical copolymers decreased significantly at low RH.

To improve upon the statistical sulfonated copolymers, hydrophilic-hydrophobic multiblock copolymers based on fully sulfonated poly(arylene ether sulfone) (BPS100) and different types of hydrophobic blocks have been introduced as new PEM materials by McGrath et al. [16-19]. The multiblock copolymer membranes exhibited hydrophilic/hydrophobic nanophase separated morphologies in the presence of water [20]. The sulfonic acid groups formed well-connected hydrophilic channels and resulted a significantly enhanced proton transport even under partially hydrated conditions [21, 22], while well-networked hydrophobic domains provided the mechanical strength of the membranes. Partially fluorinated hydrophobic blocks may enhance the hydrophilic/hydrophobic nanophase separation as well as provide a better adhesion of PEM with Nafion-bonded electrode [23].

In this chapter we report the synthesis and characterization of partially fluorinated hydrophobic poly(arylene ether benzonitrile)-hydrophilic sulfonated poly(arylene ether sulfone) (6FPAEB-BPSH100) multiblock copolymers. A series of 6FPAEB-BPSH100 multiblock copolymers were directly synthesized based on fluorine-terminated partially fluorinated hydrophobic poly(arylene ether benzonitrile) (6FPAEB) telechelic oligomers and phenoxide-terminated hydrophilic sulfonated poly(arylene ether sulfone) telechelic oligomers (BPS100) via coupling reactions. ^{13}C NMR confirmed that the mild coupling

conditions minimized possible ether-ether exchange reactions. A series of characterization using proton conductivity, water uptake, dimensional swelling behavior, SAXS, TEM, differential scanning calorimetry (DSC) and thermal gravimetric analysis (TGA) are also presented.

4.2 Experimental

4.2.1 Materials.

2,6-Difluorobenzonitrile (DFBN) was purchased from Aldrich, and purified by vacuum distillation. 4, 4′-hexafluoroisopropylidenediphenol (6F-BPA), received from Ciba, was sublimated then recrystallized twice from toluene. Monomer grade 4,4′-biphenol (BP) were provided by Eastman Chemical Company, and dried under vacuum at 100 ^{o}C prior to use. 3,3'-Disulfonated-4,4'-dichlorodiphenylsulfone (SDCDPS) was synthesized from DCDPS and purified according to a procedure reported elsewhere [24]. *N*-Methyl-2-pyrrolidinone (NMP), *N*,*N*-dimethylacetamide (DMAc), cyclohexane, and toluene were purchased from Aldrich and distilled from calcium hydride before use. Potassium carbonate (K_2CO_3) was purchased from Aldrich and dried under vacuum at 180 ^{o}C prior to use. Acetone and methanol were purchased from Fisher Scientific and used without further purification.

4.2.2 Synthesis of The 6FPAEB Hydrophobic Oligomer

A typical polymerization procedure for the hydrophobic 9,000g/mol 6FPAEB oligomer is as follows: 6F-BPA (3.500 g, 10.41 mmol) was added to a three-neck 100mL round bottom flask equipped with a mechanical stirrer, a condenser, a nitrogen inlet and a

Dean-Stark trap. DMAc (24 mL) was added to the flask and the mixture was stirred to obtain a clear solution. Then K_2CO_3 (1.655 g, 11.96 mmol) was added, followed by toluene (12 mL). The reaction bath was first set to 140 ^oC and kept at this temperature for 4 h to dehydrate the system. The bath temperature was cooled to 160 ^oC to remove most of the toluene. The reaction was cooled to 80 ^oC and DFBN (1.520g, 11.00mmol) was added. The bath temperature was raised to 125 ^oC for 8 hours, then cooled to room temperature and filtered to remove the salt, and finally precipitated into methanol (1000 mL). The oligomer was stirred overnight in methanol and then dried in *vacuo* at 110 ^oC for at least 48 h.

4.2.3 Synthesis of The BPS100 Hydrophilic Oligomer

A sample synthesis of 9,000 g/mol BPS100 is as follows: A three neck round bottom flask, equipped with a mechanical stirrer, a condenser, a nitrogen inlet and a Dean-Stark trap, was charged with BP (1.788 g, 9.60 mmol), SDCDPS (4.435 g, 9.03 mmol), and DMAc (28 mL). The mixture was stirred until dissolved, then K_2CO_3 (1.53 g, 11.09 mmol) and toluene (14 mL) were added. The reaction bath was heated to 145 ^oC for 4 h in order to azeotropically remove water from the system. The bath temperature was slowly raised to 180 ^oC by the controlled removal of toluene. The reaction was allowed to proceed at 180 ^oC for 72 h. The mixture was cooled to room temperature and filtered to remove the salt, then coagulated in acetone (1000 mL). The precipitated oligomer was stirred overnight in acetone and then dried in *vacuo* at 160 ^oC for 48 h.

4.2.4 Synthesis of The Multiblock Copolymer

A typical coupling reaction was conducted as follows: BPS100 (4.500g, 0.500mmol), K_2CO_3 (0.150g, 1.087mmol), NMP (44 mL) and cyclohexane (15 mL) were added to a three-necked 100-mL flask equipped with a mechanical stirrer, a condenser, a nitrogen inlet and a Dean-Stark trap. The reaction bath was heated to 120 ^oC for 6 hours to remove water from the system. After removing cyclohexane, the reaction bath was cooled to 90 ^oC, and 6FPAEB oligomer (4.500 g, 0.500 mmol) was added. The bath temperature was raised to 135 ^oC and kept at this temperature for 48 h. The reaction mixture was precipitated into acetone (1000 mL) affording a fibrous polymer. The product was stirred in acetone for 12 h and in deionized (DI) water at 90 ^oC for 12 hours, and dried in *vacuo* at 120 ^oC for 24 h.

4.2.5 Membranes Casting and Acidification

The 6FPAEB-BPS100 copolymers in salt form were dissolved in DMAc (~7% w/v) and filtered through a 0.45 μm Teflon syringe filter. The filtered solution was then cast onto dry, clean glass substrate and dried for 24 h under an infrared lamp at ~45 ℃. The membranes were treated via 2 methods. In Method 1, the membranes were annealed under vacuum at 220 ℃, which is about 30 ℃ higher than the T_g of the 6FPAEB block. In Method 2, the membranes were further dried in a vacuum oven at 110 ℃ for 24 h. The membranes in the salt form were converted to acid form by boiling in 0.5 M sulfuric acid solution for 2 h, followed by boiling in deionized water for 2 h.

4.2.6 Characterization

^{1}H NMR and ^{19}F NMR analyses were conducted on a Varian INOVA spectrometer operating at 400 MHz. The spectra of BPS100 oligomers and 6FPAEB-BPS100 multiblock copolymers were obtained from a 10% solution (w/v) in a DMSO-d_6 solution at room temperature. The spectra of 6FPAEB hydrophobic oligomers were obtained from a solution in $CDCl_3$. ^{13}C NMR analyses were conducted on a Varian Unity spectrometer, operating at 100.58 mHz with DMSO-d_6 as solvent.

SAXS was performed using a Riguka S-Max 300 3 pinhole SAXS system. X-ray source is the Cu Kα radiation, and the wavelength is 0.154 nm. The sample-to-detector distance is 1600 mm. SAXS two-dimensional images were obtained using a fully integrated 2D multiwire proportional counting gas-filled detector, with an exposure time of 1 hour. All the membranes were characterized in salt form. The measured intensity values were corrected for sample thickness, sample transmission and background scattering.

The bulk morphologies of the membranes were characterized by transmission electron microscopy (TEM). Electron density contrast between hydrophilic and hydrophobic segments within the membrane samples was enhanced by quantitatively exchanging the acidic protons on the sulfonic acid moieties with cesium ion. Acidified membranes were immersed in DI water and titrated with aqueous CsOH solution until the solution became neutral. The cesium stained membranes were then embedded in epoxy and ultramicrotomed into 50–70 nm thin sections with a diamond knife. Transmission electron micrographs were obtained using a Philips EM 420 transmission electron microscope (TEM) operating at an accelerating voltage of 47 kV.

Thermogravimetric analyses (TGA) of the 6FPAEB-BPSH100 membranes were determined by using a TA Instrument TGA Q500. Prior to TGA characterization, all the samples were vacuum-dried and kept in the TGA furnace at 150 ^{o}C for 30 min to remove residual solvent and moisture. The samples were then evaluated over the range of 50-650 ^{o}C at a heating rate of 10 ^{o}C/min under an air atmosphere.

Glass transition temperatures (T_gs) of 6FPAEB-BPS100 membranes (salt from) were determined by differential scanning calorimetry (DSC) with a TA Instruments DSC Q-1000 at a heating rate of 10 ^{o}C/min under a stream of nitrogen. Prior to DSC characterization, all the samples were thermal treated with Method 1.

4.2.7 Intrinsic Viscosities (IVs)

IVs of BPS100 oligomers and 6FPAEB-BPS100 multilblock copolymers were obtained from a size exclusion chromatography (SEC) equipped with a Waters 1515 isocratic HPLC pump, a Waters autosampler, a Waters HR5–HR4–HR3 column set, a Waters 2414 refractive-index detector, and a Viscotek 270 viscometric detector. NMP (containing 0.05 M LiBr) was used as the mobile phase. Intrinsic viscosities of 6FPAEB oligomers were obtained from an Alliance Waters 2690 Separations Module with a Viscotek T60A dual viscosity detector and laser refractometer equipped with a Waters HR 0.5 + HR 2 + HR 3 + HR 4 styragel column set. Tetrahydrofuran was used as the mobile phase at 25 ℃.

4.2.8 Tensile Testing

Uniaxial load tests were performed using an Instron 5500R universal testing machine equipped with a 200-lb load cell at 80 ^{o}C and 10% or 90% relative humidity (RH). Crosshead displacement speed was 5 mm/min and gauge lengths were set to 25 mm. A dogbone die was used to punch specimens 50 mm long with a minimum width of 4 mm. Prior to test, specimens were equilibrated at 10% or 90% RH and 80 ^{o}C for 48 h. All specimens were mounted in manually tightened grips. Approximate tensile moduli for each specimen were calculated based on the stress and elongation values for the specimen at the first data point at or above 2% elongation. All the membranes were tested in salt form.

4.2.9 Measurement of Proton Conductivities

Proton conductivities of the 6FPAEB-BPSH100 membranes under fully hydrated state were determined at 30^{o}C in liquid water. Before the measurement, the memberanes were equilibrated in DI water at 30 ^{o}C for 24 h. The Solartron 1252+1287 Impedance/Gain-Phase Analyzer over the frequency range of 10 Hz to 1 MHz was used for the measurements following the procedure reported in the literature [25]. A humidity-temperature oven (ESPEC, SH240) was used in partially hydrated state proton conductivities measurement of 6FPAEB-BPSH100 membranes. Membranes were equilibrated at the specified RH and temperature for 1 h before each measurement. The conductivity was calculated by the following equation (Equation 4.1):

$$\sigma = \frac{L}{R \cdot S} \quad \text{(Equation 4.1)}$$

Where σ (S/cm) is proton conductivity, L (cm) is the distance between two electrodes, R (Ω) is the resistance of the membrane and S (cm^2) is the surface area that protons transport though the membrane.

4.2.10 Water Uptake and Swelling Ratios

The water uptake of all membranes was determined gravimetrically. First, the membranes were equilibrated in DI water at room temperature for 2 days after acidification. Wet membranes were removed from the DI water, blotted dry to remove surface droplets, and quickly weighed. The membranes were then dried at 120 ^{o}C under vacuum for 24 h and weighed again. The water uptake of the membranes was calculated according to the following equation (Equation 4.2), where W_{dry} and W_{wet} refer to the mass of the dry and wet membrane, respectively.

$$Water\ Uptake\ (\%) = \frac{W_{wet} - W_{dry}}{W_{dry}} \times 100 \quad \text{(Equation 4.2)}$$

The volume swelling ratios of the membranes were determined from the dimensional changes from wet to dry state. Acidified membranes were equilibrated in DI water for 2 days, and dimensions in the wet state were measured. The dried dimensions were obtained after drying the wet membrane at 80 ^{o}C in a convection oven for 2 h.

4.3 Results and Discussion

4.3.1 Synthesis and Characterization of Oligomers and Multiblock Copolymers

Fluorine terminated 6FPAEB hydrophobic oligomers were synthesized by copolymerization of 6F-BPA and excess DFBN monomers, as shown in Figure 4.1. The molecular weight and end group functionality of the oligomers were controlled by

off-setting the molar feed ratios of monomers according to the Carothers equation. In all cases, the molar feed ratios of DFBN over 6F-BPA were greater than 1 to give fluorine telechelic functionality and target number-average molecular weights (M_n) ranging from 7 to 21 kg/mol. Figure 4.2 shows the ^{1}H NMR of 6FPAEB oligomers.

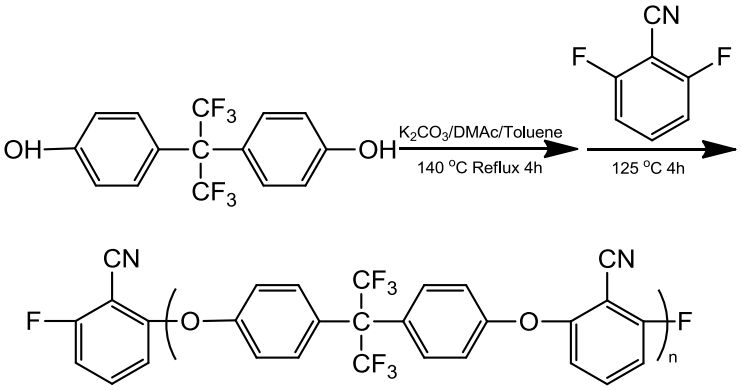

Figure 4. 1. Synthesis of fluorine terminated poly(arylene ether benzonitrile) (6FPAEB) hydrophobic oligomer

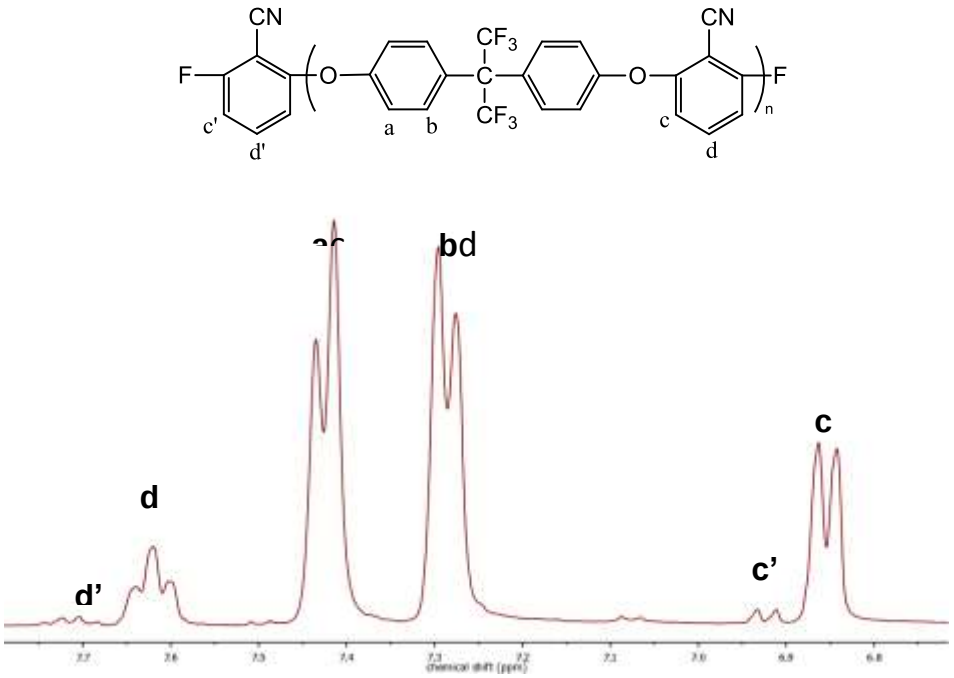

Figure 4. 2. ^{1}H NMR of 6FPAEB 9 kg/mol oligomer

Analysis of a ^{19}F NMR spectrum was used to determine the M_n of the resulting oligomer. Figure 4.3 shows the ^{19}F NMR spectrum of a 6FPAEB-9k oligomer. The peak at -63.4 ppm (integration value 103.8) is attributed to the fluorine in the chain. The peak at -105.9 (integration value 2) is attributed to the end-group aromatic fluorines of the 6FPAEB oligomer. The 2 kinds of fluorine in the 6FPAEB oligomers have a mole ratio of 6n/2, where n is the number of repeat units. Therefore, the number of repeat units can be calculated to obtain the M_n of a 6FPAEB oligomer.

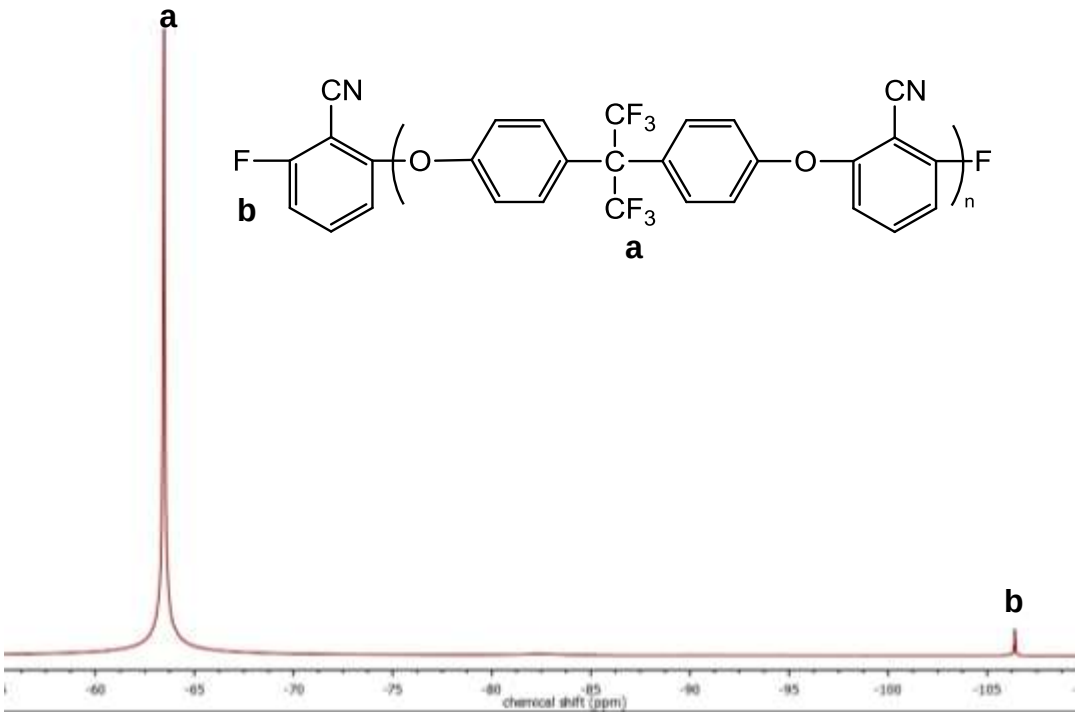

Figure 4. 3. ^{19}F NMR of 6FPAEB 9 kg/mol oligomer

The determined M_ns from ^{19}F NMR, measured M_ns from SEC and intrinsic viscosities (IVs) from SEC of the 6FPAEB hydrophobic oligomers are summarized in Table 4.1. The determined M_ns from ^{19}F NMR and SEC are similar and close to the target ones. In Figure 4.4, the log-log plot of the IVs and the M_ns measured from ^{19}F NMR

exhibits a reasonably linear relationship and confirmed successful control of molecular weight for hydrophobic block series.

Table 4. 1. Molecular weight characterization of 6FPAEB oligomers

Target M_n (kg/mol)	M_n from ^{19}F NMR (g/mol)	M_n from SEC (g/mol)	IV from SEC (dL/g)
5	4950	4800	0.07
7	7200	6900	0.09
10	10100	10300	0.11
12	12500	12000	0.13
15	15400	15200	0.15

* IV values were obtained from SEC in THF at 25 ^{o}C

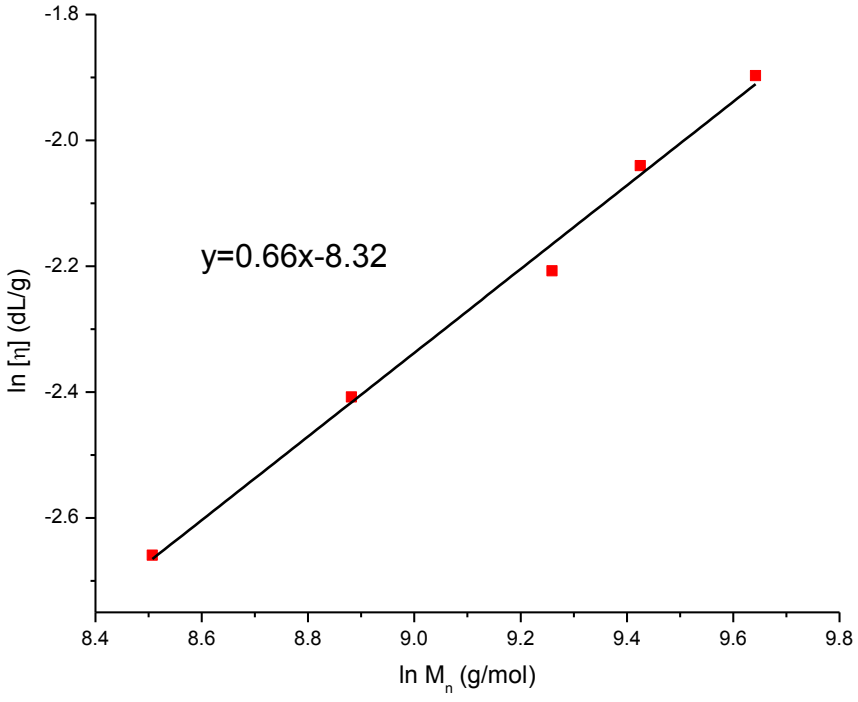

Figure 4. 4. ln η vs. ln M_n plot of 6FPAEB oligomers

Fully disulfonated poly(arylene ether sulfone) (BPS100) hydrophilic oligomers with phenoxide telechelic functionality were synthesized by copolymerization of SDCDPS and excess BP monomers as shown in Figure 4.5.

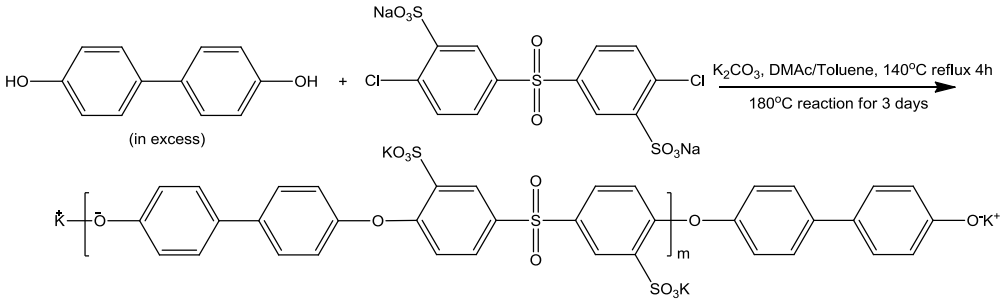

Figure 4. 5. Synthesis of the phenoxide terminated disulfonated poly(arylene ether sulfone) (BPS100) Hydrphilic Oligomers

The M_ns of the hydrophilic oligomers were determined by ^1H NMR, as Figure 4.6 shown. By comparing the integration of the protons (6.80 ppm; integration value 2) next to the phenoxide groups on the end-group and the integration of the protons (8.28 ppm; integration value 15.7) next to the potassium sulfonate group on the SDCDPS moieties, the M_n of each BPSH100 oligomer was determined.

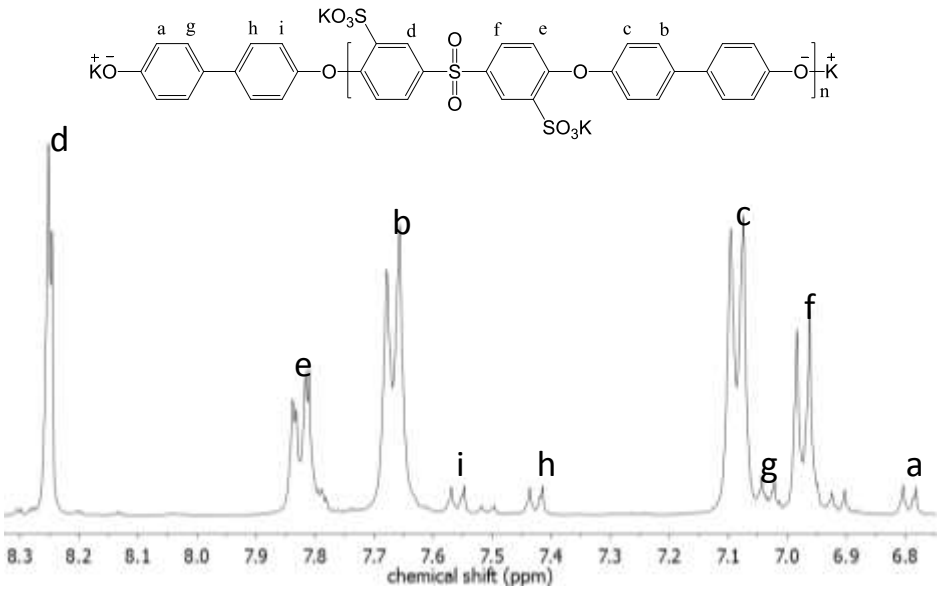

Figure 4. 6. ^{1}H NMR of phenoxide terminated BPS100 Oligomer

The molecular weights measured from ^{1}H NMR and intrinsic viscosities obtained from SEC are summarized in Table 4.2. There is a linear relationship between the logM_ns and logIVs, which indicates that control of the molecular weights for the hydrophilic oligomers is successful, as Figure 4.7 shown.

Table 4. 2. Molecular weight characterization of BPS100 oligomers

Target M_n (kg/mol)	**M_n from ^{1}H NMR (g/mol)**	**IV* (dL/g)**
5	5200	0.13
7	7100	0.18
10	10300	0.23
12	12200	0.28
15	14600	0.32

* Measured by SEC with 0.05M LiBr/NMP as mobile phase at 60 ^{o}C

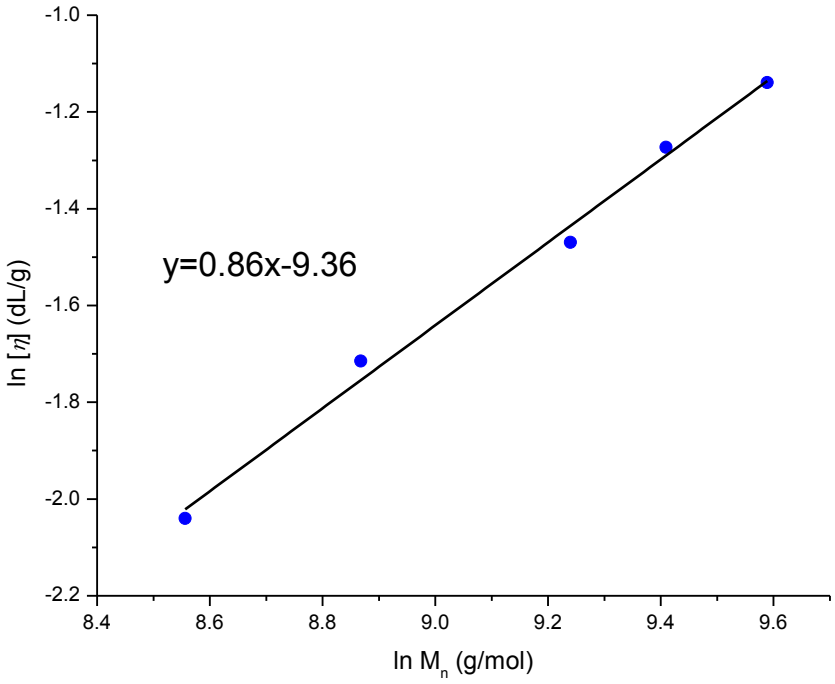

Figure 4. 7. ln η vs. ln M_n plot of BPS100 oligomers

A series of 6FPAEB-BPS100 hydrophobic hydrophilic multiblock copolymers was synthesized via a coupling reaction between phenoxide terminated BPS100 and fluorine terminated 6FPAEB oligomers. The synthesis scheme is shown in Figure 4.8. The multiblock copolymers are identified as 6FPAEB-BPS(H)100 Ak-Bk, where A and B represent the block length of 6FPAEB and BPSH100 respectively, and H represent the acid form of the copolymer.

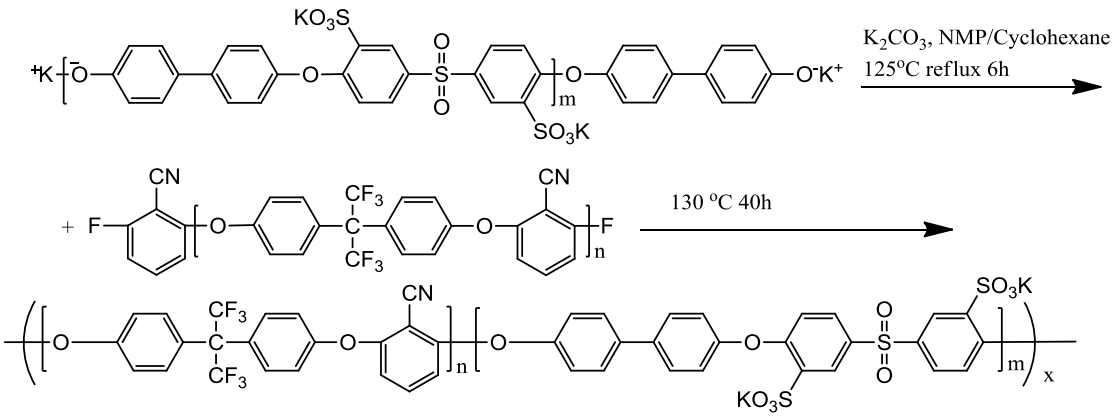

Figure 4. 8. Synthesis of 6FPAEB-BPS100 multiblock copolymers

The completion of the coupling reaction was monitored by ^{1}H NMR spectrum. After 40 h reaction, the ^{1}H NMR spectrum, as Figure 4.9 shown, confirmed the disappearance of the peaks on the phenoxide end group of the hydrophilic oligomer.

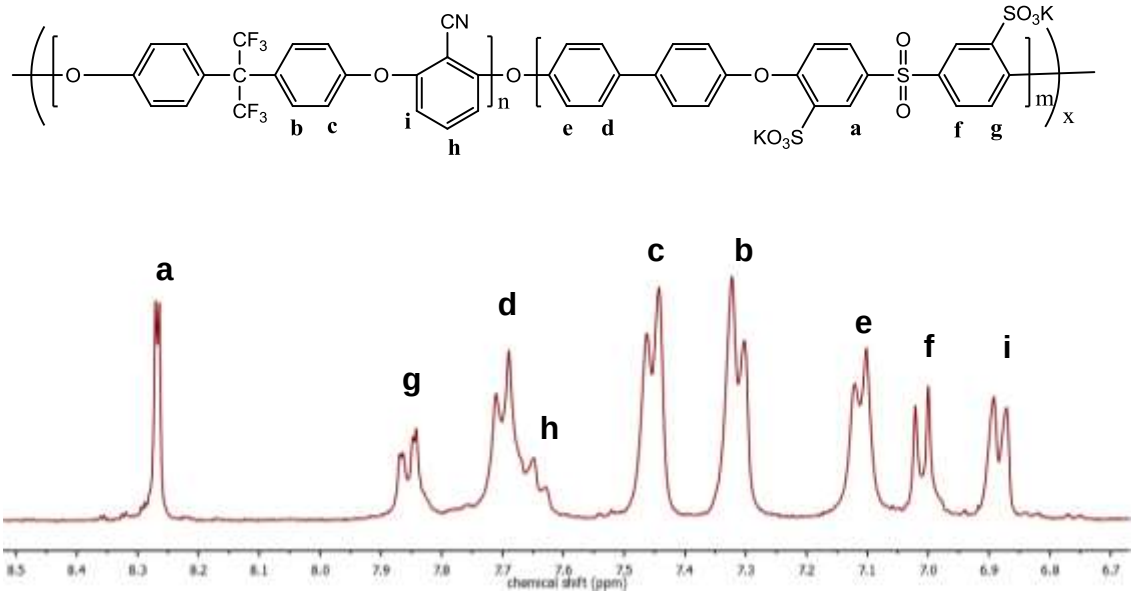

Figure 4. 9. ^{1}H NMR of a 6FPAEB-BPS100 multiblock copolymer

During the coupling reaction, a frequent concern is the possible occurrence of an ether-ether interchange side reaction, which may result in the randomization of the copolymer chain. A random copolymer, 6FPAEB35, with a comparable chemical composition, was synthesized according to a procedure reported elsewhere [26] for comparison. Figure 4.10 is a comparison of the ^{13}C NMR spectra of the 6FPAEB35 random copolymer (bottom) and 6FPAEB-BPS100 15k-15k multiblock copolymer (top). The carbon atoms connected to the oxygen via ether bonds of 6FPAEB35 backbones show multiplet peaks in the spectrum, which suggests a random sequence of the repeat units. In contrast, the carbon atoms connected to the oxygen via ether bonds of 6FPAEB-BPS100 15k-15k multiblock copolymer show sharp single peaks, confirming the ordered sequence in the multiblock copolymer and minimization of the ether-ether interchange side reaction.

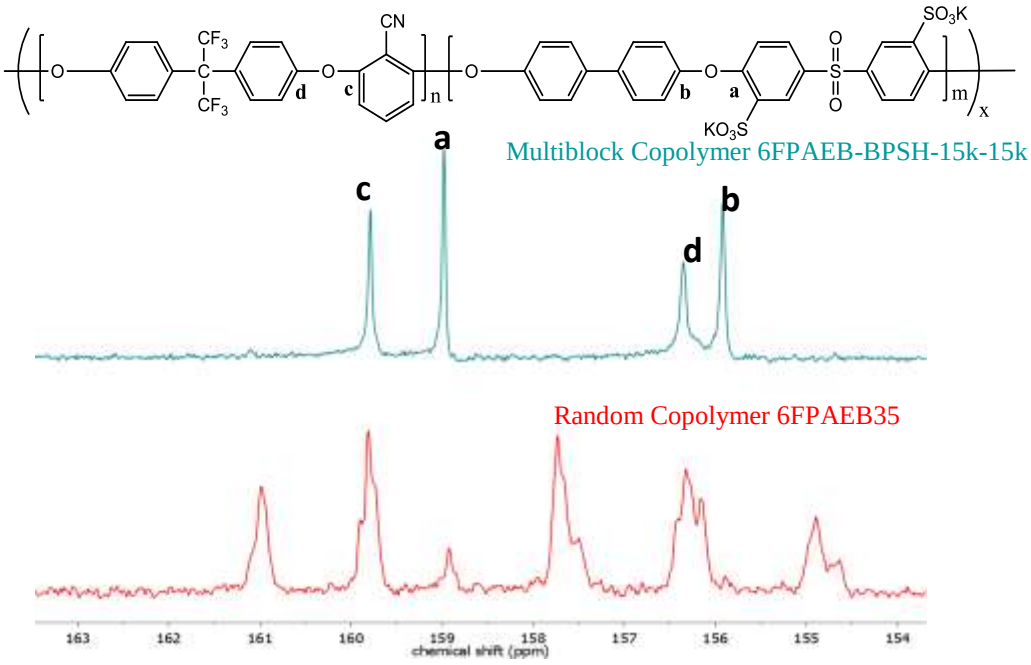

Figure 4. 10. ^{13}C NMR of a 6FPAEB-BPS100 15k-15k multiblock copolymer (top) and a 6FPAEB35 random copolymer (bottom)

4.3.2 Differential Scanning Calorimetry (DSC)

DSC is one important characterization technique utilized for determining the glass transition temperature, $T_{g,}$ and the crystalline melting transition temperature, $T_{m,}$ for polymers. The DSC trace of a 6FPAEB-BPS100 11k-11k multiblock copolymer is shown in Figure 4.11. The curve is taken from the second heating cycle with a 10 ^{o}C/min heating rate to 350 ^{o}C. Two thermal transitions, one at around 190 ^{o}C and the other at 245 ^{o}C, are observed, which can be assigned to the glass transition of the hydrophobic 6FPAEB blocks and that of hydrophilic BPS100 blocks, respectively. The two distinguished T_gs indicate the existence of nanophase separated block structures.

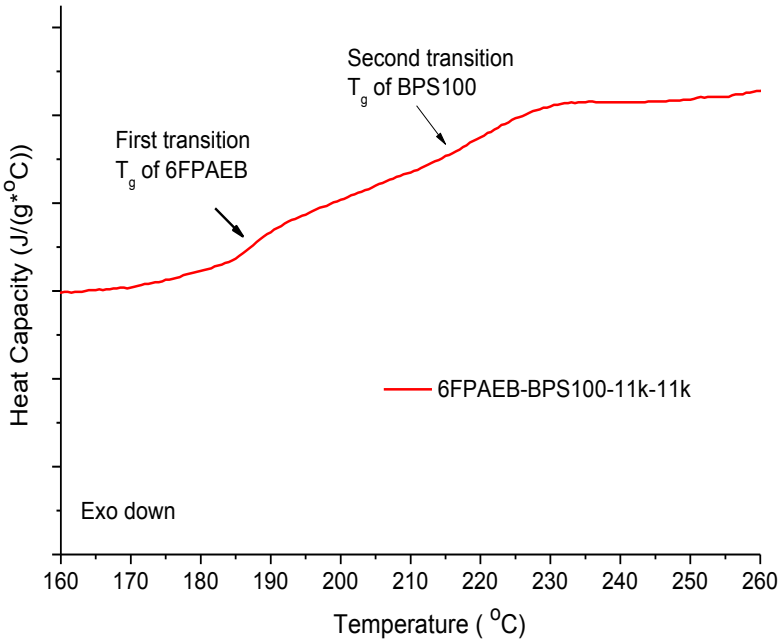

Figure 4. 11. DSC trace of a 6FPAEB-BPS100 11k-11k multiblock copolymer

4.3.3 Thermal Treatment of The 6FPAEB-BPSH100 Membranes

One of the most important critical characteristics for PEM is water management. Lee *et al.* reported the water uptakes of the membranes increased as the increase of the block length of the multiblock copolymers [16]. Although the proton conductivities revealed similar tendencies as water uptake for the membranes, there is still a concern that high water uptake and high swelling ratio of long block length multiblock copolymers may impair the mechanical properties of membranes. To address this dilemma, various thermal treatments were conducted on the salt-form membranes to tailor the morphology development during film formation, aiming at reducing the water sorption without compromising IEC and high proton conductivity. As shown in Table 4.3, the non-annealed membranes (Method 2) showed the typical trend of water uptake increase with longer hydrophilic block lengths. However, upon annealing at 30 ^{o}C higher than the T_g of 6FPAEB block, all the membranes (Method 1) showed significant reduction in water sorption. The reduction in wt% of water sorption was as nearly sixfold after the annealing treatment. Furthermore, the water uptake of the annealed samples showed independence of the block length of copolymers, which seems to suggest that annealing treatment would be a feasible and efficient approach to overcome the loss of mechanical and dimensional stabilities for the membranes with very long hydrophilic blocks under fully hydrated conditions. Generally, the water uptakes of annealed 6FPAEB-BPSH100 series are about 10 wt% lower than those of the annealed 6FK-BPSH100 series in Chapter 3, which may be explained by the higher hexafluoroisopropylidenediphenol moieties and improved hydrophobic properties of 6FPAEB hydrophobic oligomer compared to 6FK hydrophobic oligomer.

Table 4. 3. Effect of annealing on the water uptake of 6FPAEB-BPSH100 multiblock copolymers

	Water Uptake				
6FPAEB-BPSH100	**7K-7K**	**9K-9K**	**11K-11K**	**13K-13K**	**15K-15K**
Method 1	42%	44%	46%	51%	46%
Method 2	85%	93%	150%	270%	330%

Not only the water management but also the stress-strain performance of the 6FPAEB-BPSH100 showed significant improvement after thermal treatment by Method 1. Both 6FPAEB-BPS100 15k-15k membranes, treated by 2 different methods, show better stress-strain performance than the 6FPAEB35 random copolymer membrane at low relative humidity (RH) at 80 ^{o}C, as shown in Figure 4.12 (left). Thermal treatment at 220 ^{o}C increases strength but decreases elongation of 6FPAEB-BPS100 15k-15k membrane. At high RH, the stress of 6FPAEB-BPS100 15k-15k and 6FPAEB35 membranes decreases significantly, but stress-strain performance of the 6FPAEB-BPSH100 15k-15k thermal treated by Method 1 still shows significant improvement compared to 6FPAEB-BPSH100 15k-15k thermal treated by Method 2, as shown in Figure 4.12 (right). The increase in the elongation of 6FPAEB-BPS100 15k-15k and 6FPAEB35 membranes probably is due to the absorbed water works as plasticizer.

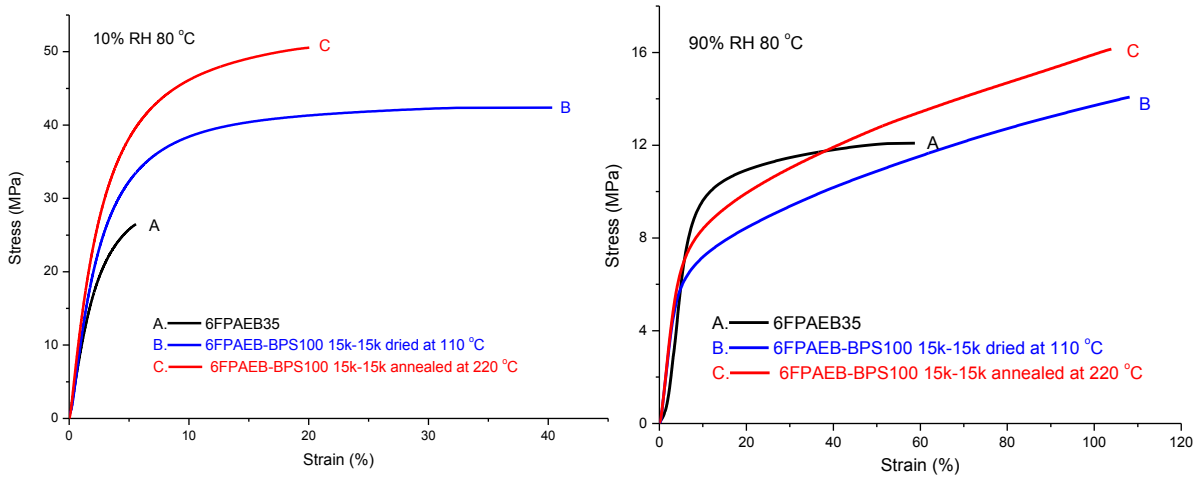

Figure 4. 12. Stress-strain behavior of 6FPAEB-BPS100 15k-15k at 80 °C (left: at 10% RH; right: at 90% RH)

4.3.4 Small Angle X-Ray Scattering (SAXS)

Small angle X-Ray scattering (SAXS) can determine the lamellar structure in semicrystalline polymers, dimensions of phase-separation in block copolymers and heterogeneities in ionomers. Scattered intensity versus the magnitude of the scattering vector *q* profile is often used to represent the patterns of SAXS. The SAXS profiles of the 6FPAEB-BPS100 multiblock copolymer membranes cast with DMAc and thermal treated with Method 1 are presented in Figure 4.13. In the investigated range of scattering wave vectors, the profiles of 6FPAEB-BPS100 multiblock copolymer membranes exhibit scattering maxima, while the SAXS profile of 6FPAEB35 random copolymer membrane is featureless. The observed scattering maxima in the profiles of 6FPAEB-BPS100 series of membranes are attributed to the aggregated nano-phase separated ionic domains. As the block length increases, the scattered intensity also increases, which suggests that the longer blocks induce an enhanced degree of phase separation. The SAXS profiles of

6FPAEB-BPS100 multiblock copolymer membranes also confirm the presence of the ordered periodic microstructures and its dependence on the block length of the oligomers. The morphology information of the long-range ordered periodic microdomain structure in a block copolymer can be obtained from the relative positions of multiple scattering peaks in the SAXS profiles. For a lamellar structure, the SAXS profile shows a series peaks with the q value at q_{max}, $2q_{max}$ $3q_{max}$……where q_{max} is the scattering wave vector of the main scattering maximum. For all of the three 6FPAEB-BPS100 multiblock copolymer membranes, there are 2 peaks that can be clearly observed in each SAXS profile, the first order peak is observed at q_{max} and the second order one is observed at $2q_{max}$, which suggests the presence of the highly ordered lamellar structure. The 2^{nd} order peak of 6FPAEB-BPS100 7k-7k is relatively weaker than those of 11k-11k and 15k-15k, which suggests the short block length, although induces the ionic domain aggregation, prevents the formation of well-order lamellar structure. Enhanced phase separation yields more distinct and ordered ionic domains. It is also observed that as the block length of 6FPAEB-BPS100 multiblock copolymers increases, the main scattering peak shifts to lower q values. This behavior indicates the interdomain distance increases as the block length increases.

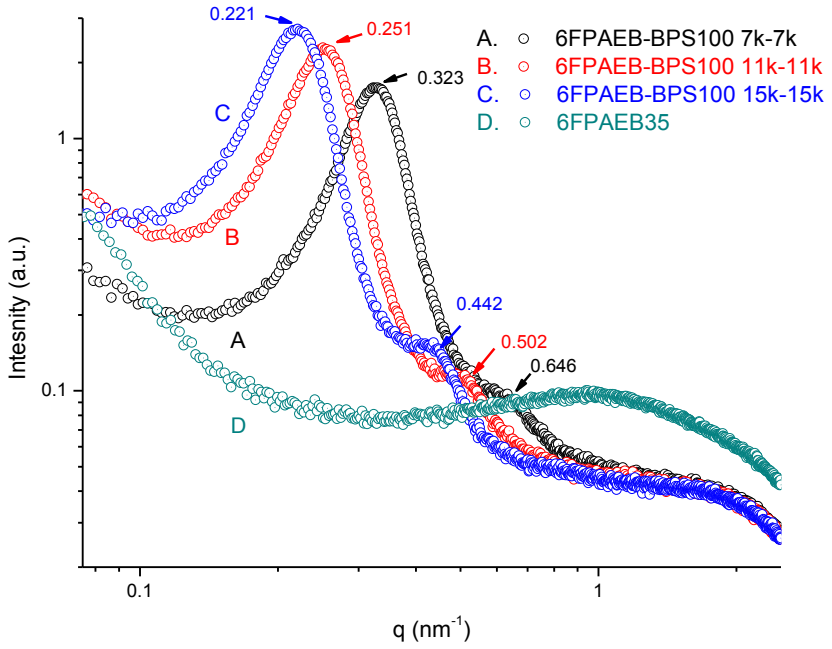

Figure 4. 13. SAXS profiles of 6FPAEB-BPS100 multiblock and 6FPAEB35 random copolymer membranes treated by Method 1

4.3.5 Properties of 6FPAEB-BPSH100 Multiblock Copolymer Membranes

The fundamental properties of the 6FPAEB-BPSH100 multiblock copolymer membranes thermal treated by Method 1 are summarized in Table 4.4, 4.5 and 4.6. A 6FPAEB35 random copolymer and Nafion® 212 were also included as controls in each Table. The intrinsic viscosity (IV) data confirmed 6FPAEB-BPS100 high molecular weight multiblock copolymers were obtained. Tough ductile transparent membranes were also cast from the copolymers.

In Table 4.4 the IEC values of the 6FPAEB-BPSH100 multiblock copolymers with equal block length were well controlled around 1.5 meq/g by adjusting molar charge ratios for the hydrophobic:hydrophilic oligomers at 1.1:1 (Series A). Unlike

polymerization of small molecular monomers, a perfect 1:1 stoichiometry is not necessary to achieve high molecular weight multiblock copolymers. As a general observation, all of the 6FPAEB-BPSH100 mulitblock copolymer membranes showed improved proton conductivity compared with Nafion® 212 control and random copolymer 6FPAEB35H. The dependence of liquid water proton conductivity on the block length was also observed. As the block length increased, improved proton conductivity was observed in liquid water. This observation is in agreement with our studies on other poly(arylene ether sulfone) multiblock copolymer systems.

Table 4. 4. The properties of 6FPAEB-BPSH100 with equal block length and controlled IEC (Series A)

6FPAEB-BPSH100 (1.1:1)	IV (dL/g)[a]	IEC (meq/g)[b]	Water Uptake(wt%)	Proton Conductivity[c] (S/cm)
4k-4k	0.68	1.50	40	0.12
7k-7k	0.61	1.55	42	0.13
9k-9k	0.81	1.53	44	0.14
13k-13k	1.25	1.50	51	0.15
15k-15k	1.01	1.55	46	0.16
Nafion® 212	N/A	1.00	22	0.12
6FPAEB35 (random)	0.62	1.50	32	0.08

a: Measured by SEC with 0.05M LiBr/NMP as mobile phase at 60 ℃
b: Measured from ^{1}H NMR
c: Measured in liquid water at 30℃

The IEC values of 6FPAEB-BPSH100 multiblock copolymers can also be controlled by adjusting the block length of the hydrophobic and hydrophilic oligomers when a 1:1 stoichometry was applied in the coupling reactions. Table 4.5 lists the properties of 6FPAEB-BPSH100 multiblock copolymers with longer hydrophobic blocks than

hydrophilic blocks in a same copolymer (Series B). Like Series A, Series B also exhibits good proton conductivity in fully hydrated state. With the increase of the block length, the proton conductivity of Series B only slightly improves. While longer hydrophilic blocks favor better conductivity performance, an increase in hydrophobic block length tends to lower a membrane's proton transport properties. The hydrophobic block length effect seems to dominate in Series B. The water uptake shows no dependence on the block length after annealing treatment of Series B.

Table 4. 5. The properties of 6FPAEB-BPSH100 with unequal block length and controlled IECs (Series B)

6FPAEB-BPSH100 (1:1)	IV (dL/g)[a]	IEC (meq/g)[b]	Water Uptake (wt%)	Proton Conductivity[c] (S/cm)
5k-4k	0.62	1.58	40	0.11
9k-6k	0.73	1.55	42	0.12
12k-9k	0.84	1.54	49	0.12
13k-10k	0.95	1.50	51	0.13
17k-13k	0.96	1.45	46	0.13
Nafion® 212	N/A	1.00	22	0.12
6FPAEB35 (random)	0.62	1.50	32	0.08

a: Measured by SEC with 0.05M LiBr/NMP as mobile phase at 60 ℃
b: Measured from ^{1}H NMR
c: Measured in liquid water at 30℃

In contrast with series B, a series (Series C) of 6FPAEB-BPSH100 multiblock copolymers with shorter hydrophobic blocks than hydrophilic blocks in a same copolymer were synthesized to achieve higher IEC values, as shown in Table 4.6. The IEC of Series C was controlled around1.9 meq/g, which is higher than that of Series A and Series B. Series C exhibits improved conductivity compared to 6FPAEB35 random

copolymer and Nafion® 212 in fully hydrated state. When the block length of 6FPAEB-BPSH100 increases from 7k-11k to 13k-17k, the proton conductivity also increases from 0.13 S/cm to 0.19 S/cm, which indicates longer block length may induce enhanced co-continuous hydrophilic domains and improve the proton transport. Generally, high IEC Series C absorbed more water than low IEC Series A and Series B. But an interesting phenomenon of Series C is that a reduced water uptake is observed when the hydrophobic and hydrophilic block length increase simultaneously. This phenomenon suggests longer hydrophobic blocks may also promote the enhanced co-continuous phase and tend to lower the membrane's water uptake.

Table 4. 6. The properties of 6FPAEB-BPSH100 with unequal block length and controlled IECs (Series C)

6FPAEB-BPSH100 (1:1)	IV (dL/g)[a]	IEC (meq/g)[b]	Water Uptake (wt%)	Proton Conductivity[c] (S/cm)
7k-11k	0.73	1.95	140	0.13
9k-13k	0.82	1.90	100	0.16
11k-15k	0.86	1.88	80	0.17
13k-17k	0.81	1.92	75	0.19
Nafion® 212	N/A	1.00	22	0.12
6FPAEB35 (random)	0.62	1.50	32	0.08

a: Measured by SEC with 0.05M LiBr/NMP as mobile phase at 60 ℃
b: Measured from ^{1}H NMR
c: Measured in liquid water at 30 ℃

The performance of a 6FPAEB-BPSH100 multiblock copolymer is related to several parameters, such as IEC, hydrophobic and hydrophilic block length, and thermal treatment. Controlling the three parameters independently makes it possible to tailor a copolymer for optimal performance. An increase in IEC would be generally accompanied

by an improved conductivity performance and increased water uptake. Annealing treatment would reduce the water uptake of the membranes and overcome the loss of mechanical and dimensional stabilities. For the copolymers with higher IECs (around 1.9 meq/g), the hydrophilic block length effect seems to dominate, while the hydrophobic block length effect in reducing water uptake is also observed.

4.3.6 Proton Conductivity Performance under Partially Hydrated States

The conductivity performance of a multiblock copolymer under partially-hydrated states is very important for a PEM. Figure 4.14 shows plots of proton conductivity at 80 ^{o}C as a function of relative humidity (RH) for 6FPAEB-BPSH100 9k-9k and 13k-13k. The plot of conductivity of Nafion® 212 membrane is also shown for comparison. In the whole range of RH, the conductivity of 6FPAEB-BPSH100 and Nafion® 212 decrease as the RH decrease. When the RH is lower than 80%, the conductivity of Nafion® 212 decreases more rapidly than that of 6FPAEB-BPSH100. Both 6FPAEB-BPSH100 9k-9k and 13-13k membranes outperform Nafion® 212 when the RH is lower than 80%. The conductivity performance of 6FPAEB-BPSH100 under partially hydrated conditions improves as the block length increases, which suggests longer hydrophilic block length would form enhanced co-continuous phase and facilitate the proton transport. This phenomenon was also observed in the conductivity vs. RH for 6FPAEB-BPSH100 9k-13k and 13k-17k, as shown in Figure 4.15.

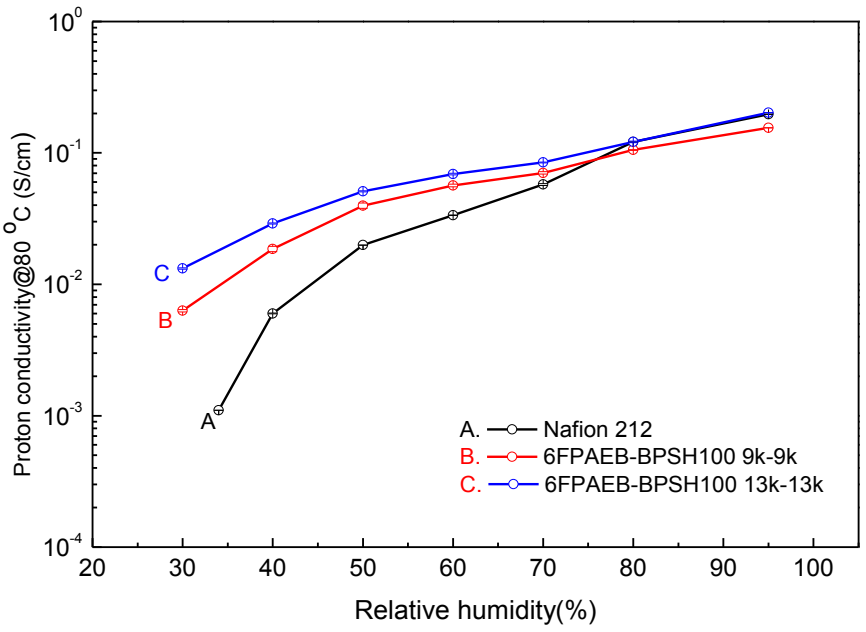

Figure 4. 14. Effect of block length on the proton conductivity of 6FPAEB-BPSH100 multiblock copolymers with controlled IEC at 1.5 meq/g (measured at 80 ℃)

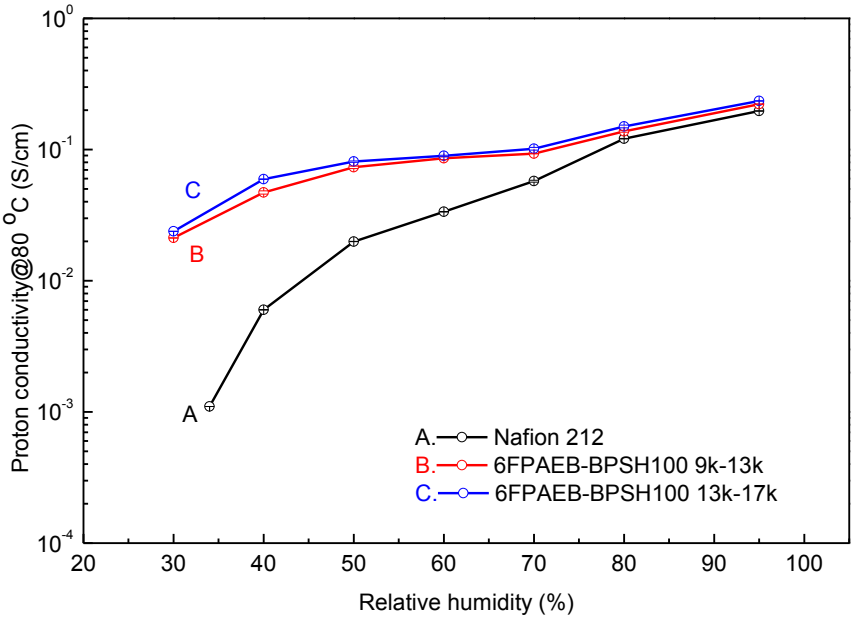

Figure 4. 15. Effect of block length on the proton conductivity of 6FPAEB-BPSH100 multiblock copolymers with controlled IEC at 1.9 meq/g (measured at 80 ℃)

IEC also shows an impact on the conductivity performance of 6FPAEB-BPSH100 membranes under partially hydrated states. Figure 4.16 shows proton conductivity at 80 ^{o}C as a function of RH for 6FPAEB-BPSH100 9k-9k and 9k-13k with the conductivity of Nafion® 212 for comparison. In the full range of RH, the conductivity of 9k-13k outperforms 9k-9k and Nafion®. An increase in IEC facilitates the improvement of conductivity under partially hydrated states and increases the water uptake of the membrane. The comparison 6FPAEB-BPSH100 13k-17k and 13-13k also shows the same tendency in Figure 4.17.

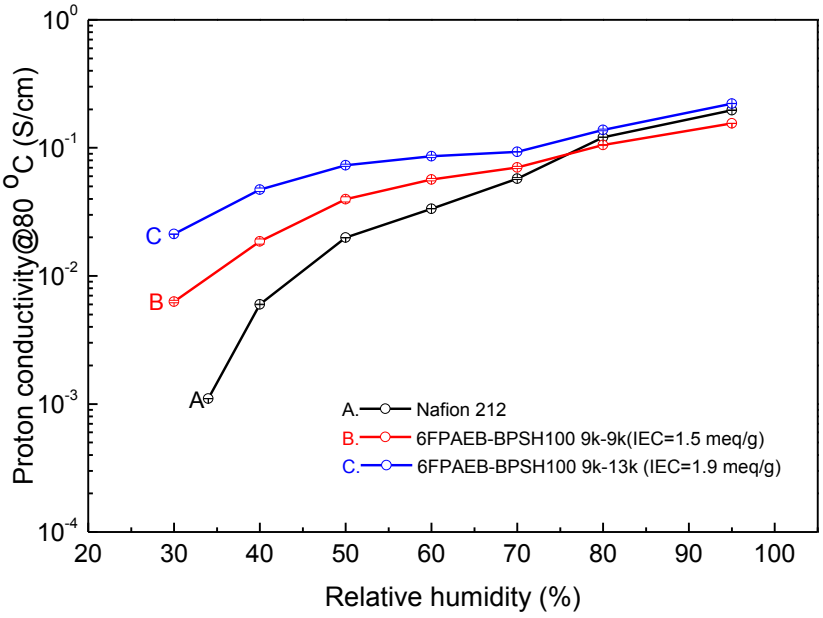

Figure 4. 16. Effect of IEC on proton conductivity of 6FPAEB-BPSH100 multiblock copolymers (measured at 80 ℃)

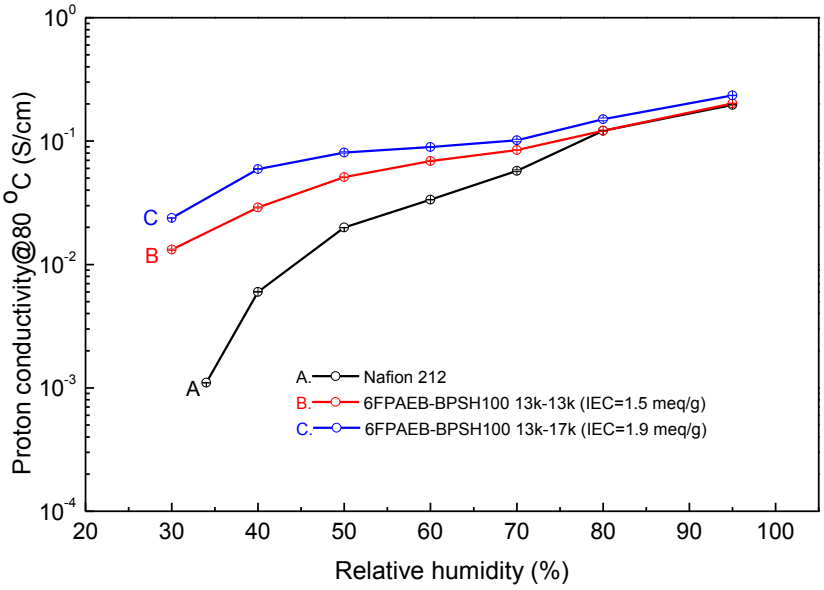

Figure 4. 17. Effect of IEC on proton conductivity of 6FPAEB-BPSH100 multiblock copolymers (measured at 80 ℃)

4.3.7 Transmission Electron Microscopy (TEM) of 6FPAEB-BPSH100 Membranes

It was observed that hydrophilic-hydrophobic mulitblock copolymers exhibited well ordered nanophase separation [20]. The presence of the nanophase separation provides a co-continuous hydrophilic phase and facilitates the proton transport. Figure 4.18 shows the TEM images of the 6FPAEB-BPSH multiblock copolymer membranes with different block lengths treated by Method 1. The bright and dark regions in the images correspond to un-stained hydrophobic domains and cesium stained ion electron-rich hydrophilic domains, respectively. Nanophase separation between hydrophilic and hydrophobic domains was developed in the 6FPAEB-BPSH multiblock copolymer membranes. As the block length increases, 6FPAEB-BPSH100 multiblock copolymer membrane shows more enhanced connectivity of the hydrophilic and hydrophobic domains and more clearly

lamellar structure, which is agree with the data from SAXS profile shown in Figure 4.13. The block length effect on the conductivity performance under partially hydrated states shown in Figure 4.14 and 4.15 can be explained by the observation of the co-continuous better hydrophilic channel formation from TEM.

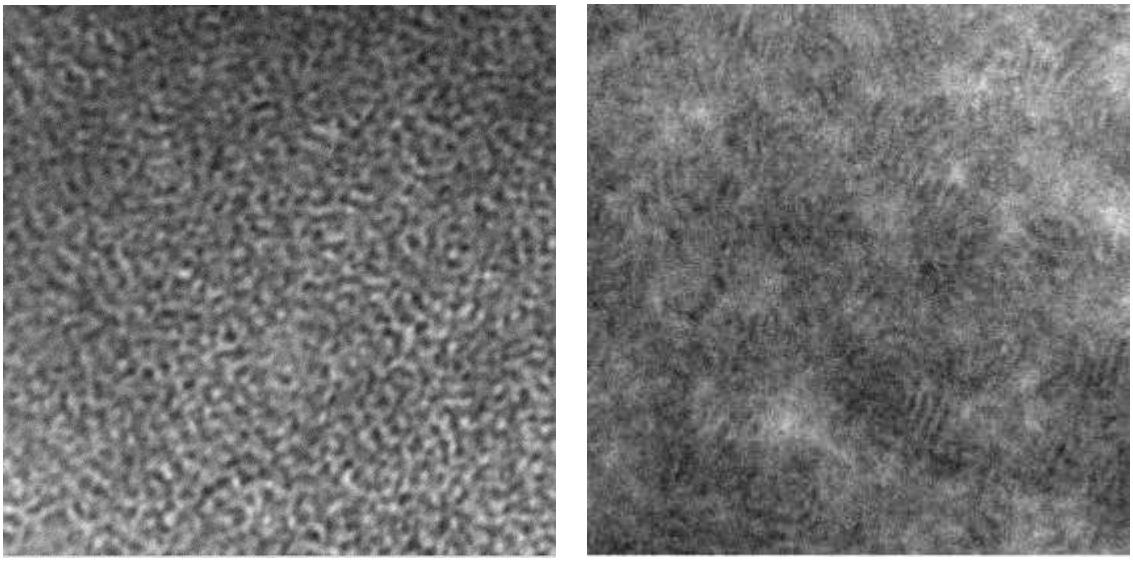

Figure 4. 18. TEM images of 6FPAEB-BPSH multiblock copolymer membranes treated by Method 1 (left: 7K-7K, right: 15K-15K)

4.3.8 Thermogravimetric Analyses (TGA) of 6FPAEB-BPSH100 Membranes

The TGA traces of 6FPAEB-BPSH100 copolymers membranes, whose IECs were fixed at 1.5 meq/g, are shown in Figure 4.19. The TGA trace of a BPSH35 random copolymer is also shown as comparison. The multiblock copolymers generally display a two-step weight loss: desulfonation at ~320 ^{o}C and main chain decomposition at ~500 ^{o}C. All the three block copolymers in Figure 4.19 display very similar weight loss behavior at the first step, which suggests the control of IEC is successful. It is worth noting that the

desulfonation temperature of 6FPAEB-BPSH100 multiblock copolymers is around 320 ^{o}C, which is ~50 ^{o}C higher than BPSH35 random copolymer or the other multiblock copolymers with different chemical structures. The interaction between the nitrile groups and sulfonic acid groups on the main chains may induce the increased temperature of desulfonation and improve the thermooxidative stability of 6FPAEB-BPSH100 multiblock copolymers.

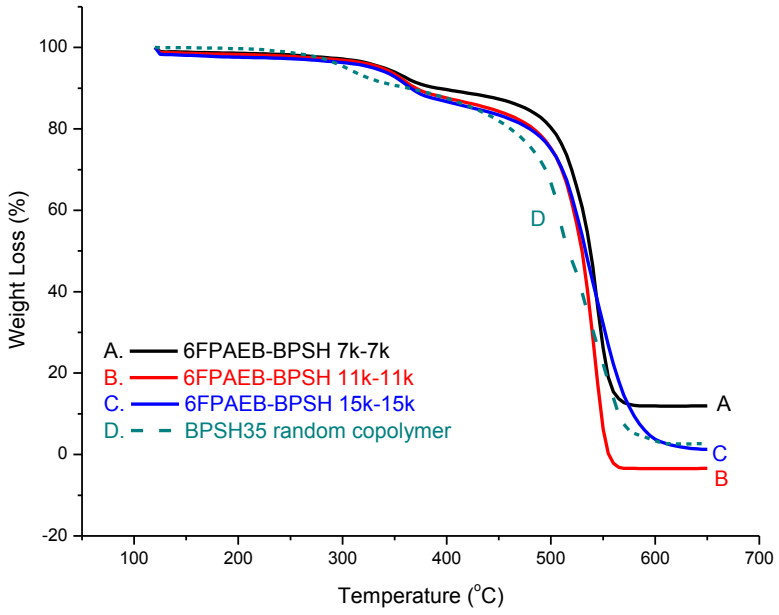

Figure 4. 19. TGA traces of 6FPAEB-BPSH100 multiblock copolymers with controlled IEC at 1.5 meq/g

4.3.9 Swelling-deswelling Properties of Multiblock Copolymers

In the water swollen state, the mechanical strength of a PEM is strongly related to the weight-based water sorption. The volume-based water swelling is relevant to the durability of a membrane electrode assembly (MEA). A significant in-plane swollen

membrane will create considerable stress during the wet-dry cycles and lead to premature failure of the MEA. It has been found that the 6FPAEB-BPSH100 multiblock copolymer membranes exhibit attractive dimensional swelling behavior and make them promising as alternative PEMs.

Figure 4.20 shows the dimensional swelling behavior of 6FPAEB-BPSH100 multiblock copolymers with 6FPAEB35 and Nafion® for comparison. The multiblock copolymers exhibit anisotropic swelling behavior while the 6FPAEB35 and Nafion® 112 show isotropic swelling behavior. As the block length increases, in-plane swelling (x- and y-directions) stays the same or decreases while through-plane (z-direction) swelling increases. This behavior indicates the development of enhanced ordered morphology as block length increases. The low in-plane swelling of 6FPAEB-BPSH100 multiblock copolymer membranes results in much lower stress at the interface and better stability of the MEA to prevent the membrane electrode failure.

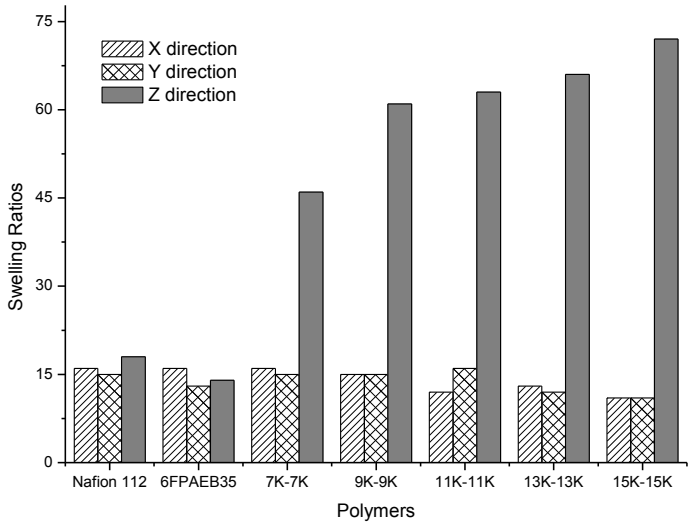

Figure 4. 20. Comparison of dimensional swelling data for 6FPAEB-BPSH100 multiblock, copolymers, BPSH35 and Nafion® 112

4.4 Conclusions

A series of 6FPAEB-BPS100 hydrophobic-hydrophilic multiblock copolymers have been successfully synthesized based on the coupling of a fluorine terminated poly(arylene ether benzonitrile) (6FPAEB) hydrophobic oligomer and a phenoxide terminated disulfonated poly(arylene ether sulfone) (BPS100) hydrophilic oligomer. The regularly sequenced structures of 6FPAEB-BPS100 multiblock copolymers were confirmed by ^{13}C NMR. The ether-ether interchange side reactions had been minimized by utilizing relatively mild reaction temperature. DSC traces of 6FPAEB-BPS100 multiblock copolymers show 2 T_gs and suggest phase separation in copolymers. Intrinsic viscosities of 6FPAEB-BPS100 copolymers confirmed that high molecular weight copolymers were obtained. For non-annealed samples, water uptake of the membranes in acid form increased with the increase of block lengths. However, water uptake was significantly reduced upon annealing at temperature greater than the T_g of 6FPAEB block and the water uptake dependence of block length diminished. The block lengths and IEC of the copolymers are two important parameters to affect the membranes' proton conductivity both in fully and partially hydrated states. Multiblock copolymers with higher block lengths and/or higher IEC showed better performance with regard to proton conductivity, presumably due to their more distinct nanophase separation and better connectivity among the ionic domains, as evidenced by morphology characterizations from TEM and SAXS profiles. The desulfonation temperature of 6FPAEB-BPSH100 series is ~50 ^oC higher than that of BPSH35 and other multiblock copolymer series, which suggests 6FPAEB-BPSH100 multiblock copolymers are more thermooxidatively stable. The anisotropic swell behavior of 6FPAEB-BPSH100 multiblock copolymers results in much

lower stress at the interface and better stability of the MEA to prevent the membrane electrode failure.

4.5 References:

1. Whittingham MS and Zawodzinski T. Chem. Rev. 2004;104(10):4243.
2. Winter M and Brodd RJ. Chem. Rev. 2004;104(10):4245.
3. Hickner MA, Ghassemi H, Kim YS, Einsla BR, and McGrath JE. Chem. Rev. 2004;104(10):4587.
4. Banerjee S and Curtin DE. J. Fluorine Chem. 2004;125(8):1211.
5. Rozière J and Jones DJ. Annual Review of Materials Research 2003;33(1):503.
6. Mauritz KA and Moore RB. Chem. Rev. 2004;104(10):4535.
7. Wang F, Hickner M, Kim YS, Zawodzinski TA, and McGrath JE. J. Membr. Sci. 2002;197(1-2):231.
8. Chikashige Y, Chikyu Y, Miyatake K, and Watanabe M. Macromolecules 2005;38(16):7121.
9. Xing PX, Robertson GP, Guiver MD, Mikhailenko SD, Wang KP, and Kaliaguine S. J. Membr. Sci. 2004;229(1-2):95.
10. Shang XY, Tian SH, Kong LH, and Meng YZ. J. Membr. Sci. 2005;266(1-2):94.
11. Summer MJ, Harrison WL, Weyers RM, Kim YS, McGrath JE, Riffle JS, Brink A, and Brink MH. J. Membr. Sci. 2004;239(2):199.
12. Miyatake K, Zhou H, Matsuo T, Uchida H, and Watanabe M. Macromolecules 2004;37(13):4961.
13. Einsla BR, Kim YS, Hickner MA, Hong YT, Hill ML, Pivovar BS, and McGrath JE. J. Membr. Sci. 2005;255(1-2):141.
14. Asensio JA, Borros S, and Gomez-Romero P. J. Membr. Sci. 2004;241(1):89.
15. Wang F, Hickner M, Ji Q, Harrison W, Mecham J, Zawodzinski TA, and McGrath JE. Macromolecular Symposia 2001;175:387.
16. Lee HS, Roy A, Lane O, Dunn S, and McGrath JE. Polymer 2008;49(3):715.
17. Li YX, Roy A, Badami AS, Hill M, Yang J, Dunn S, and McGrath JE. J. Power Sources 2007;172(1):30.
18. Wang H, Badami AS, Roy A, and McGrath JE. Journal of Polymer Science Part a-Polymer Chemistry 2007;45(2):284.
19. Yu X, Roy A, Dunn S, Badami AS, Yang J, Good AS, and McGrath JE. J. Polym. Sci., Part A: Polym. Chem. 2009;47(4):1038.
20. Lee HS, Badami AS, Roy A, and McGrath JE. J. Polym. Sci., Part A: Polym. Chem. 2007;45(21):4879.
21. Roy A, Hickner MA, Yu X, Li YX, Glass TE, and McGrath JE. J. Polym. Sci., Part B: Polym. Phys. 2006;44(16):2226.
22. Roy A, Lee H-S, and McGrath JE. Polymer 2008;49(23):5037.
23. Wiles KB, de Diego CM, de Abajo J, and McGrath JE. J. Membr. Sci. 2007;294(1-2):22.

24. Sankir M, Bhanu VA, Harrison WL, Ghassemi H, Wiles KB, Glass TE, Brink AE, Brink MH, and McGrath JE. J. Appl. Polym. Sci. 2006;100(6):4595.
25. Springer TE, Zawodzinski TA, Wilson MS, and Gottesfeld S. J. Electrochem. Soc. 1996;143(2):587.
26. Sankir M, Kim YS, Pivovar BS, and McGrath JE. J. Membr. Sci. 2007;299(1-2):8.

Chapter 5: Synthesis and Characterization of Multiblock Partially Fluorinated Hydrophobic Poly(arylene ether sulfone) Hydrophilic Disulfonated Poly(arylene ether sulfone) Copolymers for Proton Exchange Membranes

Yu Chen, Chang Hyun Lee, Desmond VanHouten, Ozma Lane, Myoungbae Lee, Mingqiang Zhang, Robert B. Moore and James E. McGrath*

Macromolecular Science and Engineering Program, Macromolecules and Interfaces Institute, Virginia Polytechnic Institute and State University, Blacksburg, Virginia 24061

Abstract

A series of multiblock copolymers (6FBPS0-BPS100), based on alternating segments of phenoxide terminated fully disulfonated poly(arylene ether sulfone) (BPS100) and fluorine-terminated poly(arylene ether sulfone) (6FBPS0) were synthesized via coupling reaction. 6FPBPS0-BPS100 multiblock copolymers with various block length and fixed ion exchange capacity (IEC) were prepared for a comparative study. By utilizing mild reaction conditions, the ether-ether interchange reactions were avoided, preventing the randomization of the copolymers. Tough ductile transparent membranes were cast from the block copolymers. Membrane properties of these multiblock copolymers were characterized with regard to intrinsic viscosity, thermal stabilities, morphology, water uptake, and proton conductivity. The results were compared to those of Nafion® and random copolymer 6F40BP60. The block length dependence on nanophase separated morphology, confirmed by transmission electron microscopy (TEM) and small angle X-Ray scattering (SAXS), accounts for enhanced proton conductivity at reduced relative humidity (RH) with longer block length.

Keyword: partially fluorinated polymers; hydrophobic-hydrophilic multiblock copolymers; proton exchange membranes

5.1 Introduction

Polymer electrolyte membrane fuel cells (PEMFCs) have attracted substantial attention as future power sources for automobiles, portable and stationary applications due to their high power density, excellent energy conversion efficiency, quiet operation and zero pollution emission [1]. Proton exchange membranes (PEMs) in PEMFCs play critical role as transporting protons and barrier the fuel from anodes to cathodes [2, 3]. As a successful PEM material, there are some requirements such as high proton conductivity, good mechanical strength, high oxidative and hydrolytic stability, low fuel and oxidant permeability, ease of fabrication, and excellent water management under low relative humidity (RH) cycling [4, 5]. Perfluorosulfonic acid polymers (PFSAs), such as Nafion® manufactured by DuPont, are the most promising and state-of-the-art PEM materials due to their good chemical stability, excellent mechanical properties and high proton conductivity [6]. However, PFSA materials have several drawbacks such as decreased conductivity performance at evaluated temperature (>80 ^{o}C), high methanol permeability and high cost.

Recently significant effort has been devoted to develop sulfonated aromatic statistical copolymers such as sulfonated poly(arylene ether sulfone)s (BPSHs), poly(ether ether ketone)s (SPEEKs), poly(arylene ether nitrile)s (SPAEBs), polyimides (SPIs) and polybenzimidazoles as alternatives for PEM materials [7-14]. Even though the proton conductivity of some sulfonated aromatic statistical copolymer membranes was comparable to Nafion® under fully hydrated conditions, this parameter decreases remarkably at lower relative humidity (RH). An increase in ion exchange capacity of the copolymers (IEC) may help to resolve this problem, but the high IEC copolymers are

found to swell excessively and lose mechanical strength when the percolation limit is reached [15]. The proton conductivity performance, water management and dimension stability of sulfonated aromatic copolymer membranes are challenges researchers are investigating means to overcome by careful design of chemical structure and morphology.

Sulfonated aromatic multiblock copolymers will nanophase separate into co-continuous hydrophilic and hydrophobic phases [16] and enhance the formation of proton transporting channel; thus the proton conductivity significantly improved especially under partially hydrated states. Wholly aromatic hydrophilic-hydrophobic multiblock copolymers based on fully sulfonated poly(arylene ether sulfone) (BPS100) hydrophilic blocks and different types of hydrophobic blocks have been intensively investigated as new PEM materials by the McGrath group [16-28]. Significant improvements in proton conductivity, water management and dimension stability have been found in those multiblock copolymer systems.

Lee et al. synthesized and characterized a series of BPS100-BPS0 non-fluorinated multiblock copolymers [20], Yu et al. synthesized and characterized a series of BisSF-BPSH fluorinated multiblock copolymers [25], both series of multiblock copolymers achieved satisfied proton conductivity in fully and partially hydrated states. Nakabayashi etc al. [29] reported synthesis and characterization of several sulonated multiblock poly(ether sulfone) copolymers by using decafluorobiphenyl (DFBP) as chain extender, but experienced difficulties with maintaining precise control of the block length and sequence.

In this chapter, we report on the synthesis and characterization of partially

fluorinated hydrophobic poly(arylene ether sulfone)-hydrophilic sulfonated poly(arylene ether sulfone) (6FBPS0-BPSH100) multiblock copolymers. A series of 6FBPS0-BPSH100 multiblock copolymers were directly synthesized based on fluorine-terminated partially fluorinated hydrophobic poly(arylene ether sulfone) (6FBPS0) telechelic oligomers and phenoxide-terminated hydrophilic sulfonated poly(arylene ether sulfone) telechelic oligomers (BPSH100) via coupling reactions. ^{13}C NMR confirmed that the mild coupling conditions minimized possible ether-ether exchange reactions. The multiblock 6FBPS0-BPSH100 copolymer membranes have been proved to outperform the 6F40BP60H random copolymer and Nafion® 212 both under fully and partially hydrated conditions.

5.2 Experimental

5.2.1 Materials.

4-Fluorophenyl sulfone (DFDPS) was purchased from Aldrich and use as received. 4, 4′-hexafluoroisopropylidenediphenol (6F-BPA), received from Ciba, was sublimated then recrystallized twice from toluene. Monomer grade 4,4′-biphenol (BP) were provided by Eastman Chemical Company, and dried under vacuum at 100 ^{o}C prior to use. 3,3'-Disulfonated-4,4'-dichlorodiphenylsulfone (SDCDPS) was synthesized from DCDPS and purified according to a procedure reported elsewhere [30]. *N*-Methyl-2-pyrrolidinone (NMP), *N*,*N*-dimethylacetamide (DMAc), cyclohexane, and toluene were purchased from Aldrich and distilled over calcium hydride before use. Potassium carbonate was purchased from Aldrich and dried under vacuum at 180 ^{o}C prior to use. Acetone and methanol were purchased from Fisher Scientific and used without further purification.

5.2.2 Synthesis of The 6FBPS0 Hydrophobic Oligomer

A typical polymerization procedure for the hydrophobic 10,000g/mol 6FBPS0 oligomer is as follows: 6F-BPA (3.500 g, 10.41 mmol) was added to a three-neck 100mL round bottom flask equipped with a mechanical stirrer, a condenser, a nitrogen inlet and a Dean-Stark trap. DMAc (24 mL) was added to the flask and the mixture was stirred to obtain a clear solution. Then K_2CO_3 (1.655 g, 11.96 mmol) was added, followed by toluene (12 mL). The reaction bath was first set to 140 ^oC and kept at this temperature for 4 h to dehydrate the system. The bath temperature was cooled to 160 ^oC to remove most of the toluene. The reaction was cooled to 80 ^oC and DFBPS (2.797g, 11.00mmol) was added. The bath temperature was raised to 135 ^oC for 10 hours, then cooled to room temperature and filtered to remove the salt, and precipitated into methanol (1000 mL). The oligomer was stirred overnight in methanol and then dried in *vacuo* at 110 ^oC for at least 48 h.

5.2.3 Synthesis of The BPS100 Hydrophilic Oligomer

A sample synthesis of 10,000 g/mol BPS100 is as follows: A three neck round bottom flask, equipped with a mechanical stirrer, a condenser, a nitrogen inlet and a Dean-Stark trap, was charged with BP (1.590 g, 8.54 mmol), SDCDPS (4.435 g, 9.03 mmol), and DMAc (28 mL). The mixture was stirred until dissolved, then K_2CO_3 (1. 36 g, 9.85 mmol) and toluene (14 mL) were added. The reaction bath was heated to 145 ^oC for 4 h in order to azeotropically remove water from the system. The bath temperature was slowly raised to 180 ^oC by the controlled removal of toluene. The reaction was allowed to proceed at 180 ^oC for 72 h. The mixture was cooled to room temperature and filtered to

remove the salt, then coagulated in acetone (1000 mL). The precipitated oligomer was stirred overnight in acetone and then dried in *vacuo* at 160 ^{o}C for 48 h.

5.2.4 Synthesis of The Multiblock Copolymer

A typical coupling reaction was conducted as follows: BPS100 (5.000g, 0.500mmol), K_2CO_3 (0.150g, 1.087mmol), NMP (44 mL) and cyclohexane (15 mL) were added to a three-necked 100-mL flask equipped with a mechanical stirrer, a condenser, a nitrogen inlet and a Dean-Stark trap. The reaction bath was heated to 120 ^{o}C for 6 hours to remove water from the system. After removing cyclohexane, the reaction bath was cooled to 90 ^{o}C, and 6FBPS0 oligomer (5.000 g, 0.500 mmol) was added. The bath temperature was raised to 145 ^{o}C and kept at this temperature for 48 h. The reaction mixture was precipitated into acetone (1000 mL) affording a fibrous polymer. The product was stirred in acetone for 12 h and in deionized (DI) water at 90 ^{o}C for 12 hours, and dried in *vacuo* at 120 ^{o}C for 24 h.

5.2.5 Membranes Cast and Acidification

The 6FBPS0-BPS100 copolymers in salt form were dissolved in DMAc (~7% w/v) and filtered through a 0.45 μm Teflon syringe filter. The filtered solution was then cast onto dry, clean glass substrate and dried for 24 h under an infrared lamp at ~45 ℃. The membranes were treated via 2 methods. In Method 1, the membranes were annealed under vacuum at 220 ℃ which is about 30 ℃ higher than the T_g of 6FBPS0 blocks. In Method 2, the membranes were further dried in a vacuum oven at 110 ℃ for 24 h. The membranes in the salt form were converted to acid form by boiling in 0.5 M sulfuric acid

solution for 2 h, followed by boiling in deionized water for 2 h.

5.2.6 Characterization

^{1}H NMR and ^{19}F NMR analyses were conducted on a Varian INOVA spectrometer operating at 400 MHz. The spectra of BPS100 oligomers and 6FBPS0-BPS100 multiblock copolymers were obtained from a 10% solution (w/v) in a DMSO-d_6 solution at room temperature. The spectra of 6FBPS0 hydrophobic oligomers were obtained from a solution in $CDCl_3$. ^{13}C NMR analyses were conducted on a Varian Unity spectrometer, operating at 100.58 mHz with DMSO-d_6 as solvent.

SAXS was performed using a Riguka S-Max 300 3 pinhole SAXS system. X-ray source is the Cu Kα radiation, and the wavelength is 0.154 nm. The sample-to-detector distance is 1600 mm. SAXS two-dimensional images were obtained using a fully integrated 2D multiwire proportional counting gas-filled detector, with an exposure time of 1 hour. All he membranes were characterized in salt form. The measured intensity values were corrected for sample thickness, sample transmission and background scattering.

The bulk morphologies of the membranes were characterized by transmission electron microscopy (TEM). Electron density contrast between hydrophilic and hydrophobic segments within the membrane samples was enhanced by quantitatively exchanging the acidic protons on the sulfonic acid moieties with cesium ion. Acidified membranes were immersed in DI water and were titrated with aqueous CsOH solution until the solution became neutral. The cesium stained membranes were then embedded in epoxy and ultramicrotomed into 50–70 nm thin sections with a diamond knife.

Transmission electron micrographs were obtained using a Philips EM 420 transmission electron microscope (TEM) operating at an accelerating voltage of 47 kV.

Thermogravimetric analyses (TGA) of the 6FBPS0-BPSH100 (acid form) membranes were determined by using a TA Instrument TGA Q500. Prior to TGA characterization, all the samples were vacuum-dried and kept in the TGA furnace at 150 ^{o}C for 30 min to remove residual solvent and moisture. The samples were then evaluated over the range of 50-650 ^{o}C at a heating rate of 10 ^{o}C/min under an air atmosphere.

Glass transition temperatures (T_gs) of 6FBPS0-BPS100 membranes (salt from) were determined by differential scanning calorimetry (DSC) with a TA Instruments DSC Q-1000 at a heating rate of 10 ^{o}C/min under nitrogen. Prior to DSC characterization, all the samples were thermal treated with Method 1.

Dynamic mechanical analysis (DMA) of 6FBPS0-BPS100 (salt form) was performed using a TA Instruments 2890 Dynamic Mechanical Analyzer. Salt-form rectangular membrane films measuring 0.35 mm x 4 mm x 25 mm were used for the test. Multi-frequency tension tests were conducted on the membranes, with an amplitude of 25 μm and a pre-load force of 0.025 N in a nitrogen atmosphere.

5.2.7 Intrinsic viscosities (IVs)

Intrinsic viscosities of BPS100 oligomers and 6FBPS0-BPS100 multilblock copolymers were obtained from a size exclusion chromatography (SEC) equipped with a Waters 1515 isocratic HPLC pump, a Waters autosampler, a Waters HR5–HR4–HR3 column set, a Waters 2414 refractive-index detector, and a Viscotek 270 viscometric detector. NMP (containing 0.05 M LiBr) was used as the mobile phase. Intrinsic

viscosities of 6FBPS0 oligomers were obtained from an Alliance Waters 2690 Separations Module with a Viscotek T60A dual viscosity detector and laser refractometer equipped with a Waters HR 0.5 + HR 2 + HR 3 + HR 4 styragel column set. Chloroform was used as the mobile phase at 30 ℃

5.2.8 Tensile Testing

Uniaxial load tests were performed using an Instron 5500R universal testing machine equipped with a 200-lb load cell at room temperature and 40-50% relative humidity (RH). Crosshead displacement speed was 5 mm/min and gauge lengths were set to 25 mm. A dogbone die was used to punch specimens 50 mm long with a minimum width of 4 mm. Prior to test, specimens were dried under vacuum at 110 ^{o}C for at least 24 h and then equilibrated at 44% RH and 30 ^{o}C for 48 h. All specimens were mounted in manually tightened grips. Approximate tensile moduli for each specimen were calculated based on the stress and elongation values for the specimen at the first data point at or above 2% elongation. All the membranes were tested in salt form.

5.2.9 Measurement of Proton Conductivities

Proton conductivities of the 6FBPS0-BPSH100 membranes under fully hydrated state were determined at 30^{o}C in liquid water. Before the measurement, the memberanes were equilibrated in DI water at 30 ^{o}C for 24h. The A Solartron 1252+1287 Impedance/Gain-Phase Analyzer over the frequency range of 10 Hz to 1 MHz was used for the measurements following the procedure reported in the literature[31]. A humidity-temperature oven (ESPEC, SH240) was used in partially hydrated state proton conductivities measurement of 6FBPS0-BPSH100 membranes. Membranes were

equilibrated at the specified RH and temperature for 1 h before each measurement. The conductivity was calculated by the following equation (Equation 5.1):

$$\sigma = \frac{L}{R \cdot S} \quad \text{(Equation 5.1)}$$

Where σ (S/cm) is proton conductivity, L (cm) is the distance between two electrodes, R (Ω) is the resistance of the membrane and S (cm^2) is the surface area that protons transport though the membrane.

5.2.10 Water Uptake and Swelling Ratios

The water uptake of all membranes was determined gravimetrically. First, the membranes were equilibrated in DI water at room temperature for 2 days after acidification. Wet membranes were removed from the DI water, blotted dry to remove surface droplets, and quickly weighed. The membranes were then dried at 120 ^{o}C under vacuum for 24 h and weighed again. The water uptake of the membranes was calculated according to the following equation (Equation 5.2), where W_{dry} and W_{wet} refer to the mass of the dry and wet membrane, respectively.

$$Water\ Uptake\ (\%) = \frac{W_{wet} - W_{dry}}{W_{dry}} \times 100 \quad \text{(Equation 5.2)}$$

The volume swelling ratios of the membranes were determined from the dimensional changes from wet to dry state. Membranes were equilibrated in DI water, and dimensions in the wet state were measured. The dried dimensions were obtained after drying the wet membrane at 80 ^{o}C in a convection oven for 2 h.

5.3 Results and Discussion

5.3.1 Synthesis and Characterization of Oligomers and Multiblock Copolymers

Figure 5.1 shows the synthesis of fluorine terminated 6FBPS0 hydrophobic oligomers via copolymerization of 6F-BPA and an excess of DFDPS monomer. The molecular weight and end group functionality of the oligomers were precisely controlled by off-setting the molar feed ratios of monomers according to the Carothers equation. The molar feed ratio of DFDPS to 6F-BPA was greater than 1 to give fluorine telechelic functionality and provide target number-average molecular weights ranging from 4 to 17 kg/mol. Figure 5.2 shows the ^{1}H NMR of a 6FBPS0 oligomer.

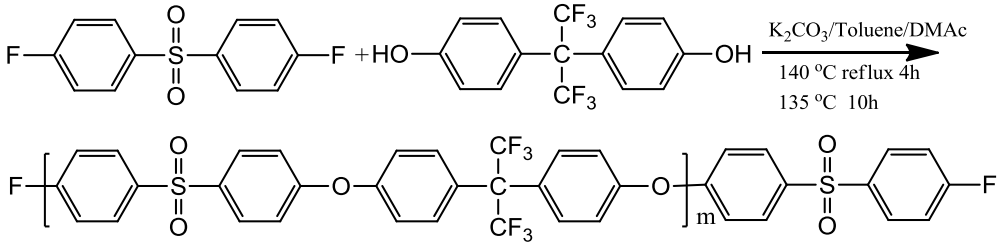

Figure 5. 1. Synthesis of fluorine terminated poly(arylene ether sulfone) (6FBPS0) hydrophobic oligomer

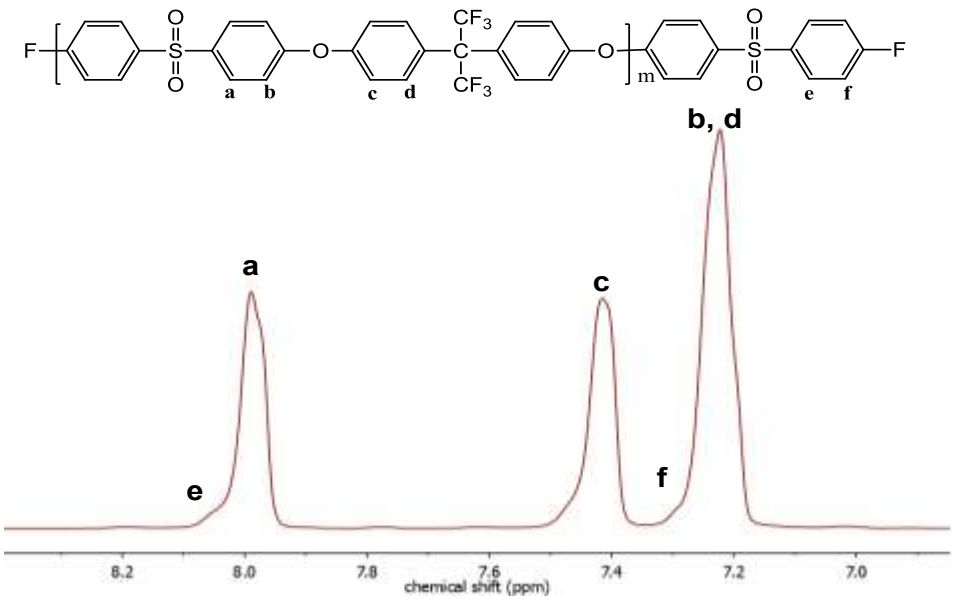

Figure 5. 2. ^{1}H NMR of a 6FBPS0 10 kg/mol oligomer

It is hard to calculate the number average molecular weight (M_n) of 6FBPS0 from ^{1}H NMR due to overlap of the signal of the end group protons and that of the protons on the main chain. Analysis of ^{19}F NMR spectra of 6FBPS0 oligomers is an efficient method for determination of the M_n. Figure 5.3 shows the ^{19}F NMR spectrum of a 6FBPS0-10k oligomer. The peak at -63.5 ppm (integration value 110.2) is attributed to the fluorine atoms in the chain. The peak at -104.9 ppm (integration value 2.0) is attributed to the end-group aromatic fluorines atoms of the 6FBPS0 oligomer. The 2 types of fluorine atoms in the 6FBPS0 oligomers have a mole ratio of 6n/2, where n is the number of the repeat unit. Therefore, the number of repeat units can be calculated to obtain the M_ns of 6FBPS0 oligomers.

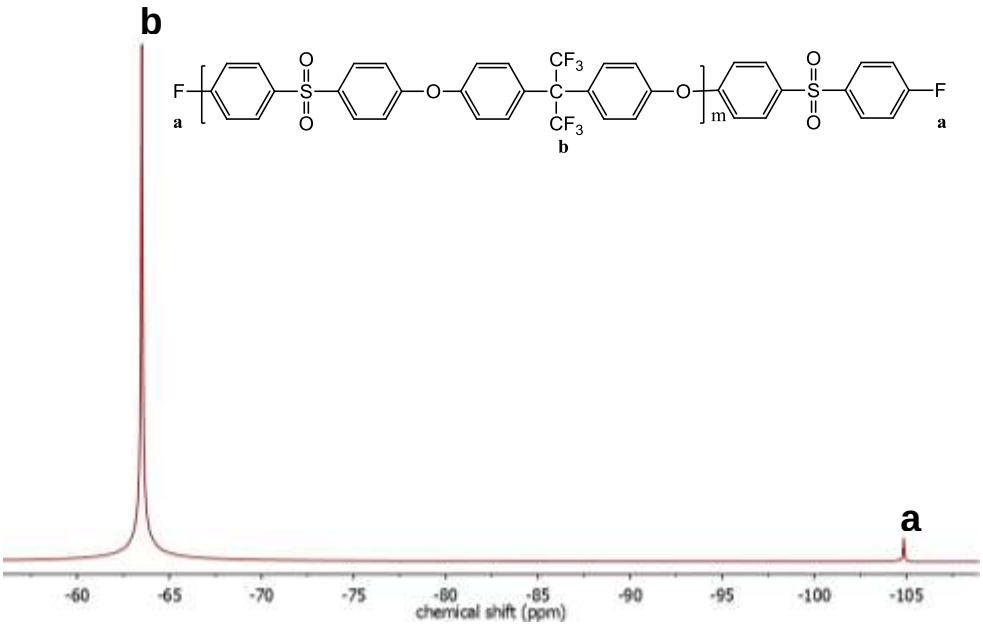

Figure 5. 3. ^{19}F NMR of a 6FBPS0 10kg/mol oligomer

The M_n measured from ^{19}F NMR and intrinsic viscosity (IV) obtained from SEC are summarized in Table 5.1. An increase in IV was observed when the M_n of 6FBPS0 increased. There is a linear relationship between the logM_n and logIV, indicating that control of the molecular weights for the hydrophobic oligomers was successful, as shown in Figure 5.4.

Table 5. 1. Molecular weight characterization of 6FBPS0 oligomers

Target M_n (kg/mol)	M_n from ^{19}F NMR (g/mol)	IV* (dL/g)
6	5800	0.09
8	7700	0.10
10	10400	0.12
12	11700	0.13
14	14100	0.14

* IV values were obtained from SEC in chloroform at 25 ^{o}C

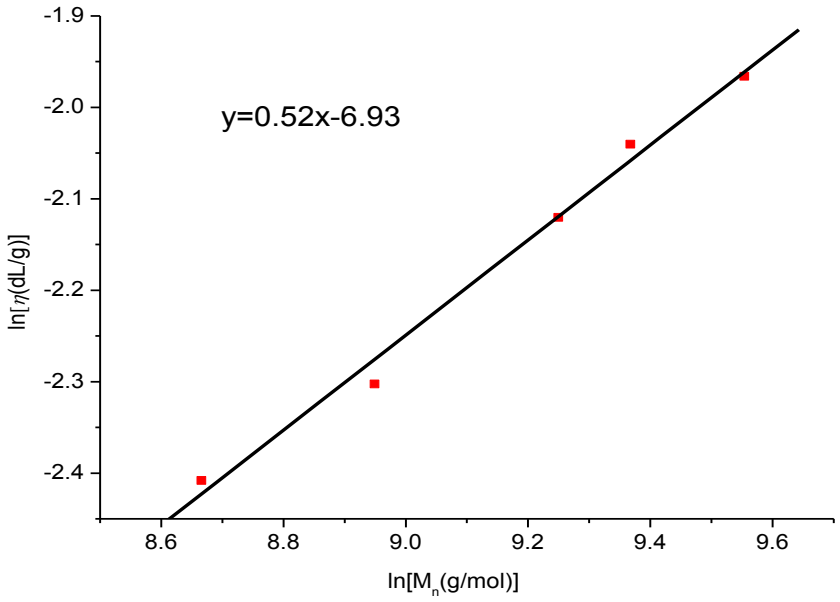

Figure 5. 4. ln η vs. ln M_n plot of 6FBPS0 oligomers

Phenoxide terminated fully disulfonated poly(arylene ether sulfone) (BPS100) hydrophilic oligomers were synthesized by copolymerization of SDCDPS and excess BP monomers, as shown in Figure 5.5. The molecular weight and end group functionality of the oligomers were precisely controlled by off-setting the molar feeding ratios of monomers according to the Carothers equation.

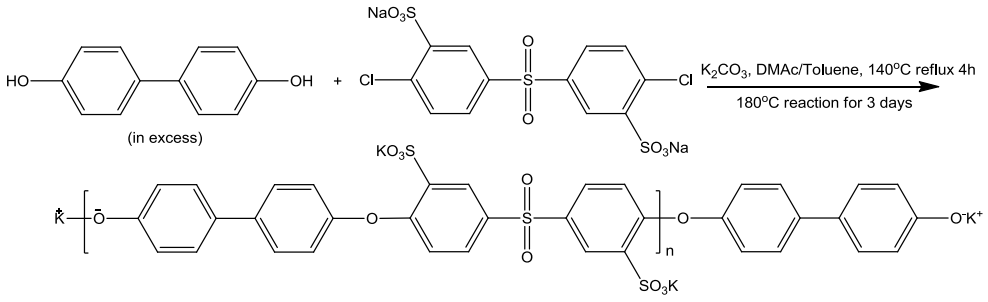

Figure 5. 5. Synthesis of the phenoxide terminated disulfonated poly(arylene ether sulfone) (BPS100) hydrphilic oligomers

The M_ns of the hydrophilic oligomers were determined by ^{1}H NMR. Figure 5.6 shows the spectrum of BPS100, where protons from the terminal BP moieties were assigned to four small peaks at 6.80, 7.05, 7.40, and 7.55 ppm, while the peaks at 7.10 and 7.65 were assigned to the protons of the BP moieties in the middle of BPS100 oligomer backbone. By comparing the integrations of the protons on the end-group BP (peak a) and of the protons on the SDCDPS moieties (peak d), the M_n of each BPS100 oligomer was determined.

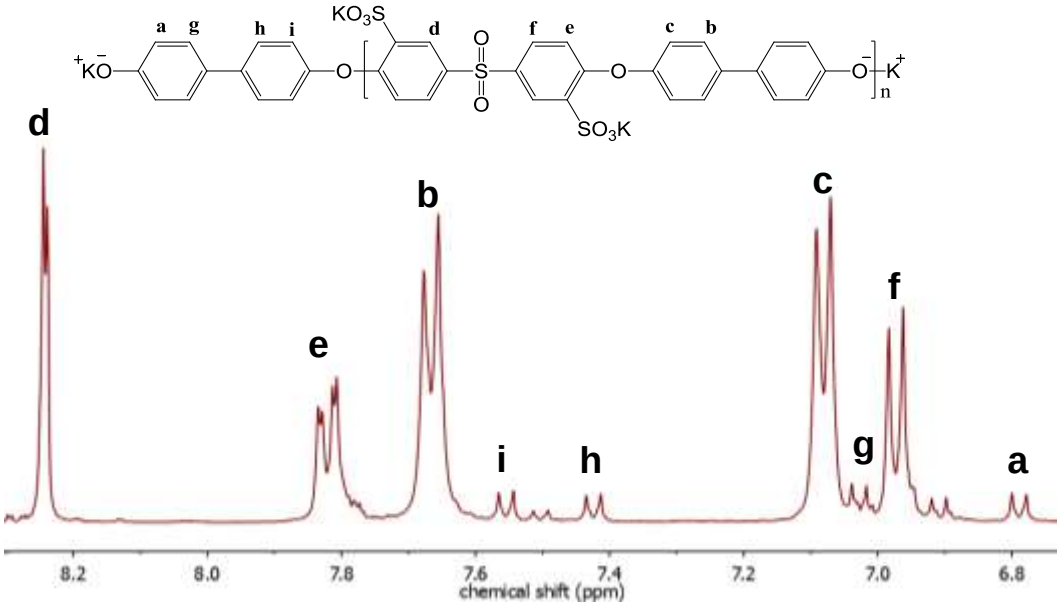

Figure 5. 6. ^{1}H NMR of a phenoxide terminated BPS100 oligomer

Table 5.2 shows the summary of the molecular weights measured from ^{1}H NMR and intrinsic viscosities obtained from SEC. An increase in IV was observed when the M_n of BPS100 increased. A linear relationship between the logM_n and logIV was observed, which indicates that control of the molecular weights for the hydrophilic oligomers was successful, as shown in Figure 5.7.

Table 5. 2. Molecular weight characterization of BPS100 oligomers

Target M_n (kg/mol)	M_n from ^1H NMR (g/mol)	IV* (dL/g)
6	6000	0.15
8	8100	0.20
10	10300	0.25
12	12200	0.27
14	14200	0.31

* Measured by SEC with 0.05M LiBr/NMP as mobile phase at 60 ^oC

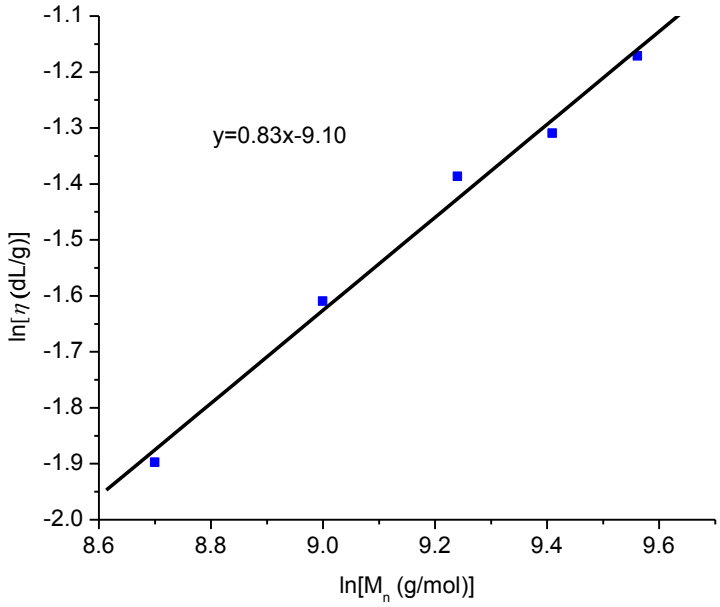

Figure 5. 7. ln η vs. ln M_n plot of BPS100 oligomers

As shown in Figure 5.8, a series of partially fluorinated sulfonated poly(arylene ether sulfone) multiblock coupolymers (6FBPS0-BPS100) were successfully synthesized via coupling reaction. The stoichiometry of the coupling reaction was based on a 1.1:1 molar ratio of the hydrophobic (6FBPS0)/hydrophilic (BPS100) oligomers to control the

ion exchange capacity (IEC) value at 1.5 meq/g. Although the feed ratio of the oligomers is generally higher than 1:1, all the multiblock copolymers yield high intrinsic viscosities and can be cast into tough membranes. The multiblock copolymers are identified as 6FBPS0-BPS(H)100 Ak-Bk, where A and B represent the block length of 6FBPS0 and BPS (H)100, respectively and H represent the acid form of the copolymer.

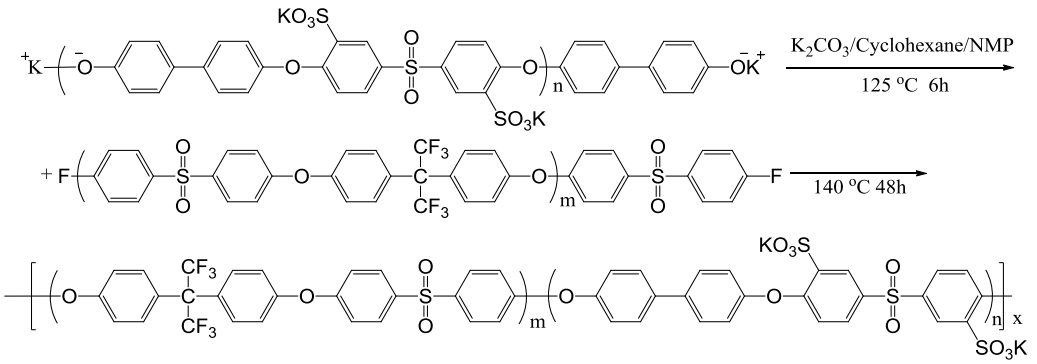

Figure 5. 8. Synthesis of 6FBPS0-BPS100 multiblock copolymers via coupling reaction

The completion of the coupling reaction was monitored by ^{1}H NMR spectrum. After 48 h of reaction time the ^{1}H NMR spectrum, as Figure 5.9 shown, confirmed the disappearance of the peaks on the phenoxide end group of the hydrophilic oligomer.

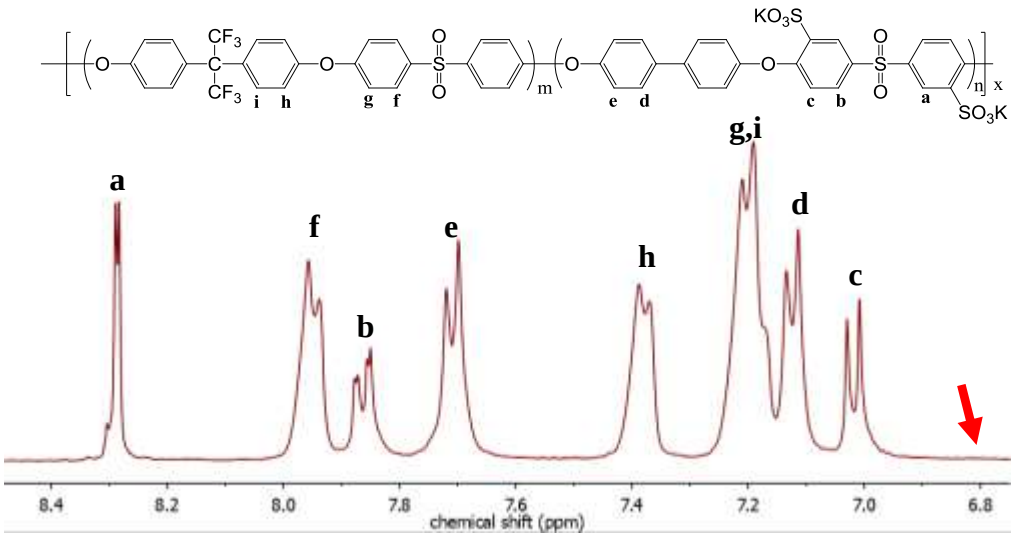

Figure 5. 9. ^{1}H NMR of 6FBPS0-BPS100 multiblock copolymer

In this coupling reaction, the ether–ether chain interchange side reaction is a concern, which may result in a randomized chain structure. The comparison of the ^{13}C NMR spectra of the 6F60BP40 random copolymer (bottom) and 6FBPS0-BPS100 10k-10k multiblock copolymer (top) is shown in Figure 5.10. The spectrum of 6F60BP40 shows multiplet peaks, which indicates a random sequence of each moiety on the main chain. In contrast, the spectrum of 6FBPS0-BPS100 10k-10k shows only narrow sharp single peaks, confirming the presence of long range ordered hydrophobic and hydrophilic segments and the apparent avoidance of any ether-ether chain interchange side reaction.

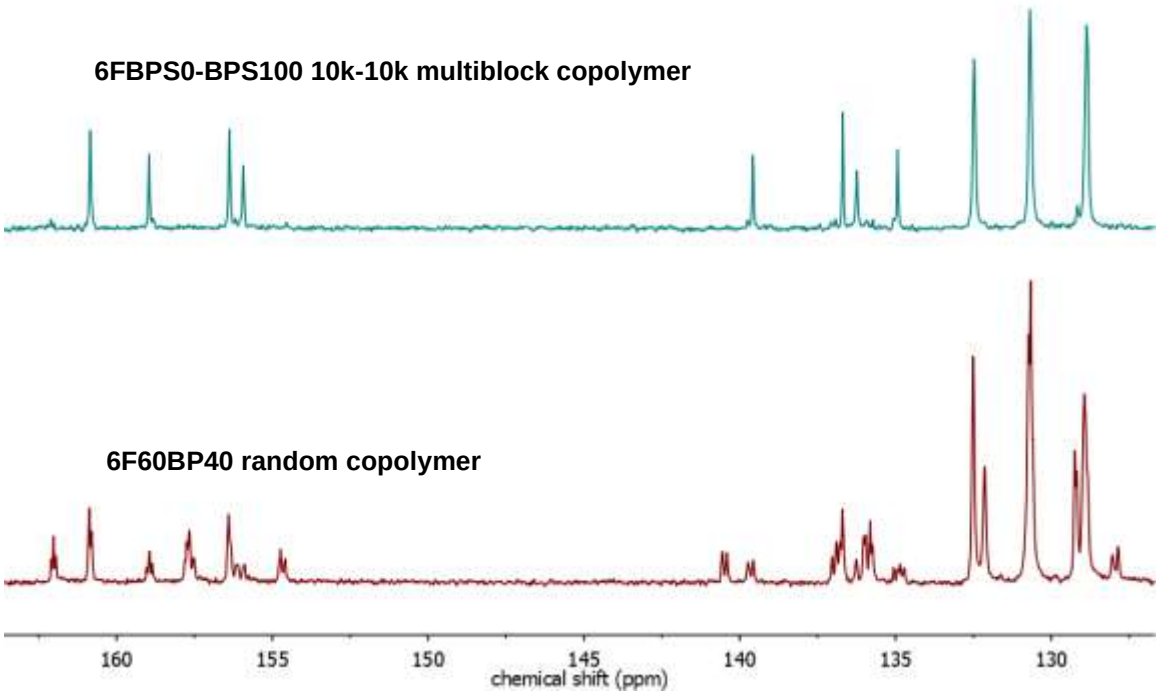

Figure 5. 10. ^{13}C NMR of 6FBPS0-BPS100 10k-10k multiblock copolymer (top) and 6F60BP40 random copolymer (bottom)

5.3.2 Thermal Treatment of The 6FBPS0-BPSH100 Membranes

Water management is one of the most important critical properties for a PEM. Lee *et al.* reported the water uptakes of the membranes increased with the block length of the multiblock copolymers [20]. High water uptake and swelling ratios of longer block length multiblock copolymers may lower the mechanical strength of the membranes and reduce the durability on MEAs. To overcome this drawback, we adopted various thermal treatments on the salt-form membranes in order to tailor the morphology development during film formation, aiming at reducing the water sorption without compromising IEC and high proton conductivity. After acidification, the non-annealed membranes showed

the typical trend of water uptake increasing with the increase of hydrophilic block length. However, as can be seen in Table 5.3, upon annealing at 30 ^{o}C above the T_g of the 6FBPS0 block, water sorption was significantly reduced for all acidified membranes. Furthermore, the water uptake of the annealed samples showed independence of the block length of copolymers, which seems to suggest that annealing treatment would be a feasible and efficient approach to overcome the loss of mechanical and dimensional stabilities for the membranes with very long hydrophilic blocks under fully hydrated conditions.

Table 5. 3. Effect of annealing on the water uptake of 6FBPS0-BPSH100 multiblock copolymers

6FBPS0-BPSH100*	**Water Uptake**				
	6K-6K	**8K-8K**	**10K-10K**	**12K-12K**	**15K-15K**
Method 1	48%	55%	55%	58%	60%
Method 2	44%	95%	185%	250%	340%

*all membranes are in acid form

5.3.3 Differential Scanning Calorimetry (DSC)

DSC is one important characterization technique utilized for determining the glass transition temperature (T_g) and the crystalline melting transition temperature (T_m) for polymers. The DSC trace of a 6FBPS0-BPS100 13k-13k multiblock copolymer is shown in Figure 5.11. The copolymer was tested in the salt form because the acid-form copolymer membranes are known to be thermally and oxidatively unstable above 250 ^{o}C. The curve is taken from the second heating cycle with a 10 ^{o}C/min heating rate to 350 ^{o}C. A sharp transition at 205 ^{o}C can be assigned to the T_g of 6FBPS0 blocks. Another very

broad transition, covering a temperature range of 250-300 ^{o}C, was linked to the relaxation of the BPS100 ionic blocks. The observation of the clear T_g for fluorinated blocks indicates the existence of nanophase separated block structures.

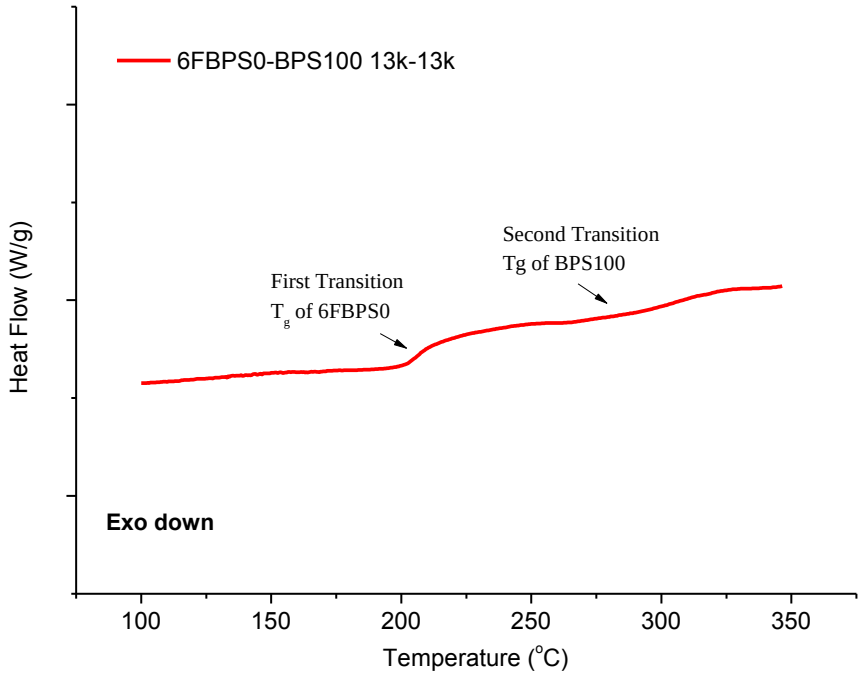

Figure 5. 11. DSC trace of a 6FBPS0-BPS100 13k-13k multiblock copolymer

5.3.4 Dynamic Mechanical Analysis (DMA) of 6FBPS0-BPS100 Multiblock Copolymer Membranes

DMA can be used to determine the glass transition temperature of the polymer and the transitions induced by other molecular motions. Figure 5.12 shows the DMA plots of 6FBPS0-BPS100 multiblock copolymers with a BPS32 as control. DMA analyses were performed on copolymers in the salt form since the acid form copolymer membranes are thermally and oxidatively unstable above about 250 ^{o}C. A distinct transition was observed between 210 and 220 ^{o}C from the DMA for all of the 6FBPS0-BPS100 multiblock

copolymers, which was attributed to chain relaxation in 6FBPS0 hydrophobic block. In contrast, no significant transition was observed from the DMA plot for BPS32 random copolymer.

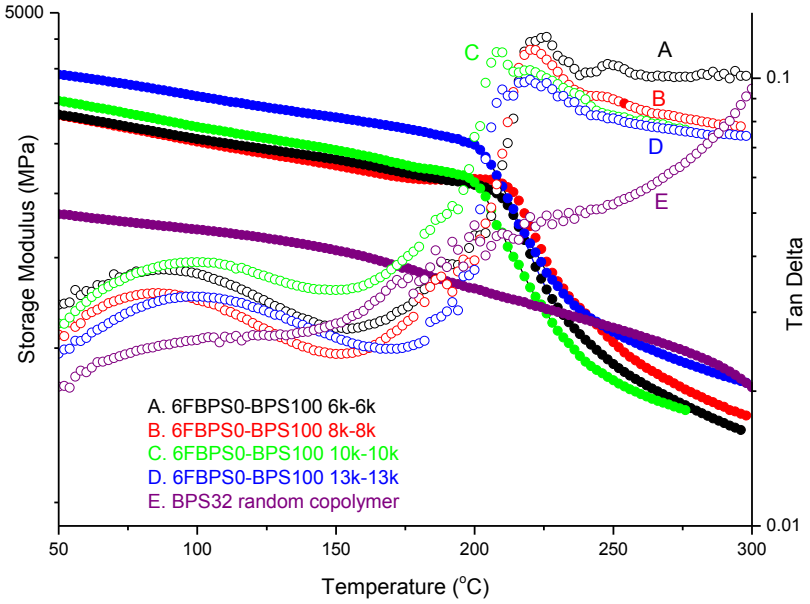

Figure 5. 12. DMA plots for 6FBPS0-BPS100 multiblock copolymers with a BPS32 as control; the closed symbols represent the storage modulus and the open symbols represent the tan δ

5.3.5 Small Angle X-Ray Scattering (SAXS)

SAXS has been wildly used in determination the size and the spatial arrangement of the micro structure in nano-scale for block copolymers. Scattered intensity versus the magnitude of the scattering vector *q* profile is often used to represent the patterns of SAXS. Figure 5.13 shows the SAXS profiles of the 6FBPS0-BPS100 multiblock copolymers with various block lengths cast from DMAc and thermally treated with

Method 1. Scattering maxima are observed in the profiles of 6FBPS0-BPS100 multiblock copolymers, while the profile of the 6F40BP60 random copolymer is featureless. The observed scattering maxima in the SAXS profiles of 6FBPS0-BPS100 multiblock copolymers are attributed to the aggregated ionic domains. The scattered intensity of 6FBPS0-BPS100 copolymers enhances with an increase in block length, suggesting the longer hydrophilic block facilities an enhanced degree of phase separation. The SAXS profiles of 6FBPS0-BPS100 multiblock copolymers also confirm the presence of the ordered periodic microstructures and the dependence of ordered periodic microstructures on the block length of the oligomers. The morphology of the long-range ordered periodic microdomain structure in a block copolymer can be determined from the q values of higher-order peaks relative to the first-order peak for interparticle scattering, because such material exhibits different arrays depending on the dominant shape of its microdomain structure. For a lamellar structure, the SAXS profile shows a series peaks with the q value at q_{max}, $2q_{max}$ $3q_{max}$……where q_{max} is the scattering vector of the main scattering maximum. For the 6FBPS0-BPS100 10k-10k and 15k-15k multiblock copolymers, there are 2 peaks can be clearly observed in each SAXS profile, the first order peak is at q_{max} and the second order one is at 2 q_{max}, which suggests the presence of the highly ordered lamellar structure. The 2^{nd} order peak of 6FBPS0-BPS100 5k-5k cannot be observed, which suggests the short block length, although induces the ionic domain aggregation, prevents the formation of well-order lamellar structure. It is also observed that the main scattering peak shifts to the lower q values as the block length increases of 6FBPS0-BPS100 series. This behavior indicates that as the block length increases, the interdomain distance increases, and further leads to the increasing of the

cluster size and probabililty of proton transport enhancement.

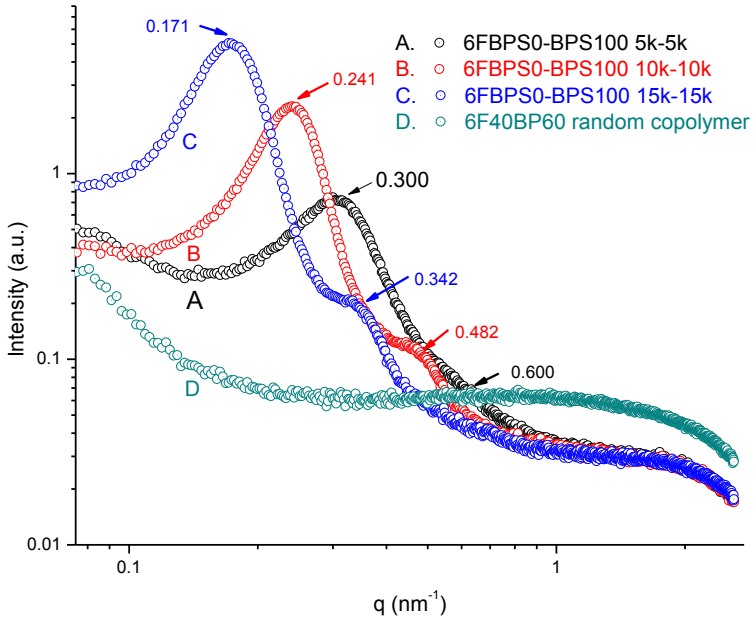

Figure 5. 13. SAXS profiles of 6FBPS0-BPS100 multiblock copolymer and 6F40BP60 random copolymer membranes treated by Method 1

5.3.6 Transmission Electron Microscopy (TEM) of 6FPAEB-BPSH100 Membranes

Ordered nanophase separation and the dependence of the nanophase separation on the block length were observed in the hydrophobic-hydrophilic multiblock copolymers [18, 32]. The presence of the nanophase separation provides co-continuous hydrophilic phase channels across the membrane. As the block length of 6FBPS0-BPS100 multiblock copolymers increases, the co-continuous hydrophilic domains increase and facility better proton transport. Figure 5.14 shows the TEM images of the 6FBPS0-BPS100 multiblock copolymer membranes with different block lengths. The bright and dark regions in the

images correspond to non-stained hydrophobic domains and cesium stained ion electron-rich hydrophilic domains, respectively. It was clearly indicated that the nanophase separation between hydrophilic and hydrophobic domains was observed in the 6FBPS0-BPSH multiblock copolymer membranes. Furthermore, as the block length increase, enhanced degree of phase separation and more clearly lamellar structure were observed, which is agree with the data from SAXS profile shown in Figure 5.13. The block length effect on the conductivity performance under partially hydrated states shown in Figure 5.16 can be supported by the observed improvement in co-continuous hydrophilic channel formation from TEM.

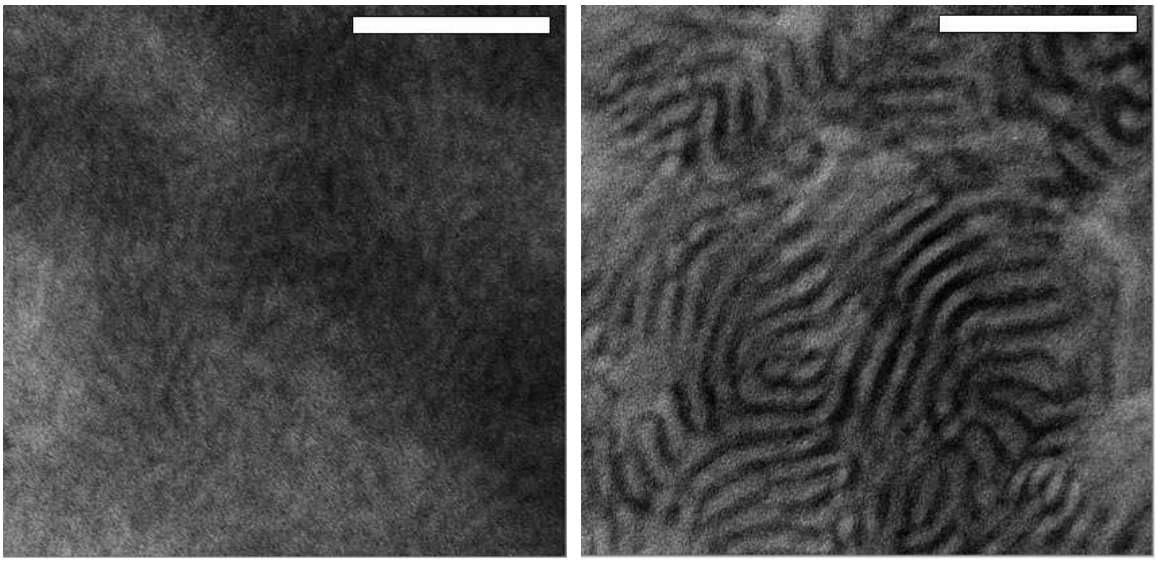

Figure 5. 14. TEM images of 6FBPS0-BPSH100 multiblock copolymer membranes (left: 6FBPS0-BPSH100 10K-10K, right: 6FBPS0-BPSH100 15K-15K); the scale is 100nm

5.3.7 Tensile Testing

The tensile properties of 6FBPS0-BPS100 multiblock copolymer membranes were determined and shown in Table 5.4 and Figure 5.15 with a BPS 32 random copolymer as

a control. All the 6FBPS0-BPS100 membranes have a tensile strength near 50 MPa, which is about 20 MPa lower than that of BPS 32 random copolymer. This difference may indicate that the 6FBPS0-BPS100 multiblock copolymers have relatively lower molecular weights than the BPS32 random copolymer. In addition, all of the 6FBPS0-BPS100 multiblock copolymer membranes show better elongation performance than the BPS32 random copolymer, which may be explained by the influence of softer co-continuous 6FBPS0 domains.

Table 5. 4. Tensile properties of 6FBPS0-BPS100 multiblock copolymers

Samples	Tensile Modulus (MPa)	Tensile Strength (MPa)	Elongation (%)
6FBPS0-BPS100 6k-6k	1590 ±70	46 ±1	27 ±9
6FBPS0-BPS100 8k-8k	1610 ±20	48+1	52 ±10
6FBPS0-BPS100 10k-10k	1750 ±70	52 ±3	55 ±25
BPS32 (random)	1900 ±60	70 ±7	23 ±20

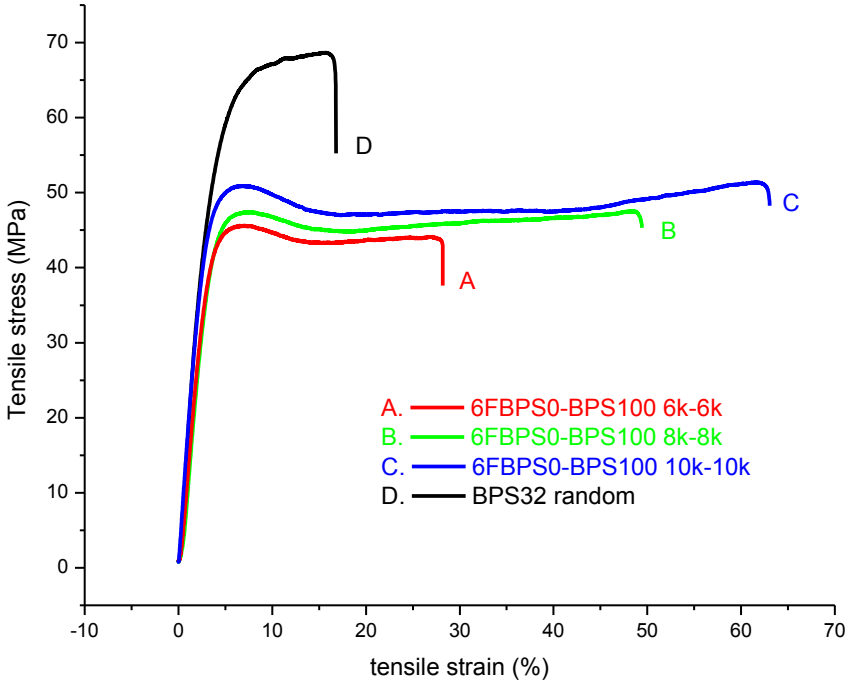

Figure 5. 15. Stress-strain curves of 6FBPS0-BPS100 multiblock copolymers with a BPS32 random copolymer as control

5.3.8 Properties of 6FBPS0-BPSH100 Multiblock Copolymer Membranes

The fundamental properties of the 6FBPS0-BPSH100 multiblock copolymer membranes thermal treated by Method 1 are summarized in Table 5.5. A 6F40BP60 random copolymer and Nafion® 212 were also included as controls. The intrinsic viscosity (IV) data confirmed high molecular weight 6FBPS0-BPS100 multiblock copolymers were obtained.

The stoichiometry of the coupling reaction was based on a 1.1:1 molar ratio of the hydrophobic(6FBPS0)/hydrophilic (BPS100) oligomers to control the IEC value at 1.5 meq/g. A perfect 1:1 stoichiometry is not necessary to achieve high molecular weight

multiblock copolymers. Superior proton conductivity was observed for all 6FBPS0-BPSH100 multiblock copolymer membranes compared to Nafion® 212 and random copolymer 6F40BP60H. The dependence of proton conductivity in fully hydrated state on the block length was also observed. Improved proton conductivity was observed as the block length increased. This observation is in agreement with our studies on other poly(arylene ether sulfone) multiblock copolymer systems.

Table 5. 5. The properties of 6FBPS0-BPSH100 with equal block length and controlled IEC

6FBPS0-BPSH100 (1.1:1)	IV (dL/g)[a]	IEC(meq/g)[b]	Water Uptake (wt%)	Proton Conductivity[c] (S/cm)
4k-4k	0.68	1.55	40	0.14
6k-6k	0.82	1.53	48	0.17
8k-8k	0.83	1.50	55	0.17
10k-10k	1.05	1.55	55	0.18
12k-12k	1.17	1.60	58	0.19
15k-15k	1.25	1.56	60	0.20
Nafion® 212	N/A	1.00	22	0.12
6F40BP60	0.62	1.50	32	0.08

a: Measured by SEC with 0.05M LiBr/NMP as mobile phase at 60 ℃
b: Measured from ^{1}H NMR
c: Measured in liquid water at 30℃

The operation conditions for a PEMFC frequently include partially hydrated states, so proton exchange membranes that have high proton conductivity under low relative humidity (RH) are desirable. Figure 5.16 shows proton conductivity at 80 ^{o}C as a function of relative humidity (RH) for 6FBPS0-BPSH100 6k-6k, 10k-10k and 15k-15k, where the conductivities of Nafion® 212 membrane are also shown for comparison.

Across the entire RH range, 6FBPS0-BPSH100 block copolymers outperformed Nafion® 212. The performance of the multiblock copolymers under partially hydrated state improved with increasing block length. This performance improvement is related to the formation of long, co-continuous hydrophilic domains in the copolymer with longer block length. Protons can be transported along with the sulfonic acid groups and water molecules through the enhanced co-continuous hydrophilic channels. The enhanced nano-phase separated co-continuous hydrophilic domain morphology, as confirmed by SAXS, lowers the morphological barrier for proton transport and improves the proton transport at low RH.

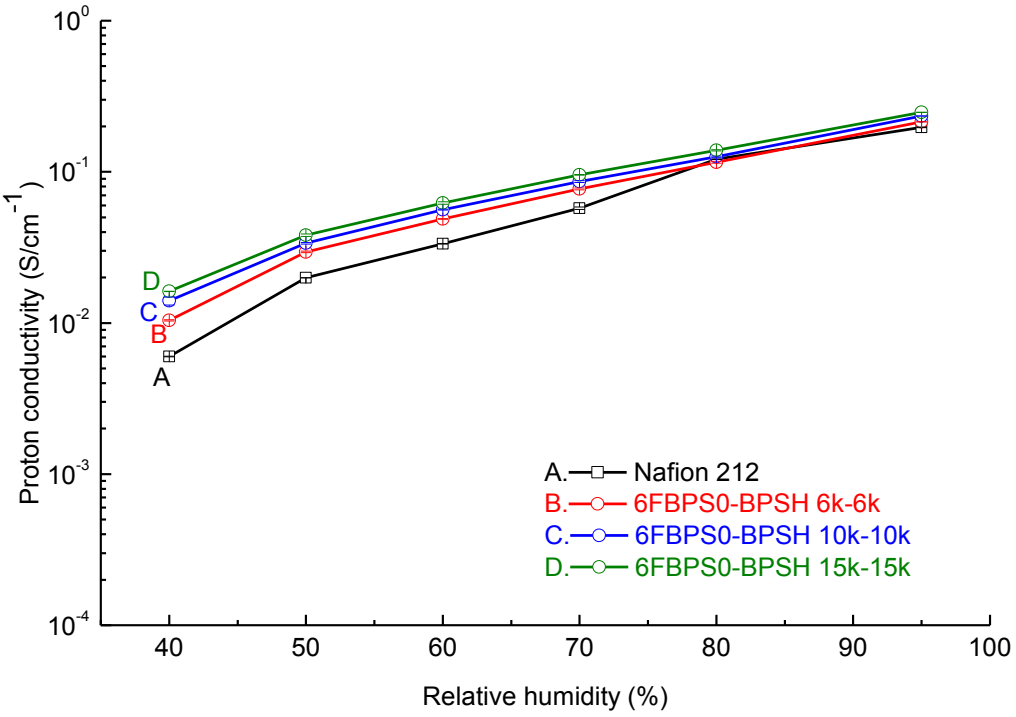

Figure 5. 16. Effect of block length on the proton conductivity of 6FBPS0-BPSH 100 multiblock copolymers (measured at 80 ℃)

5.3.9 Thermogravimetric Analyses (TGA) of 6FPAEB-BPSH100 Membranes

The thermal and thermo-oxidative stability as a function of weight loss of this series of 6FBPS0-BPSH100 multiblock copolymers (acid form) was investigated by TGA, as shown in Figure 5.17. All copolymers exhibit a two-stage degradation profile. The initial weight loss was observed at 270 ^{o}C and attributed to the decomposition of the sulfonic acid groups on the BPSH100 blocks. The second weight loss was observed at 450 ^{o}C and assigned to the decomposition of polymer main chains. All the copolymers showed very similar weight loss behavior at the first step, which suggests the control of IEC is successful.

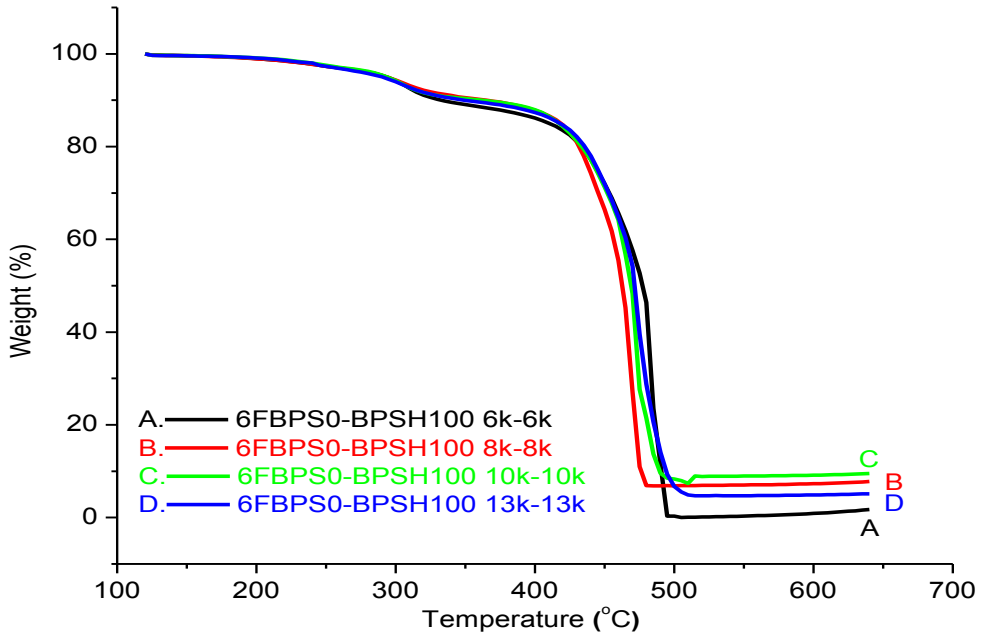

Figure 5. 17. TGA traces of 6FBPS0-BPSH100 multiblock copolymers with controlled IEC at 1.5 meq/g

5.3.10 Swelling-deswelling Properties of 6FBPS0-BPSH100 Multiblock Copolymers

The mechanical strength of a PEM is strongly related to the weight-based water sorption in the fully hydrated state. The volume-based water swelling, which directly influences the dimensional changes of a PEM, is relevant to the durability of a membrane electrode assembly (MEA). When a membrane shows a significant in-plane swelling, considerable stress is created during the wet-dry cycles, destroying the membrane-electrode interfaces and leading to premature failure of the MEA. It has been found that the 6FBPS0-BPSH100 multiblock copolymer membranes exhibit attractive dimension swelling behavior and make them promising as alternative PEMs.

The dimension swelling behaviors of 6FBPS0-BPSH100 multiblock copolymers with 6F40BP60H and Nafion® as comparison are shown in Figure 5.18. The multiblock copolymers exhibit anisotropic swelling behavior and the 6F40BP60H and Nafion® 112 show isotropic swelling behavior. For multiblock copolymer membranes, in-plane swelling (x- and y-directions) stays the same or decreases slightly while through-plane (z-direction) swelling increases with block length. This behavior indicates the development of enhanced ordered morphology as block length increases. The low in-plane swelling of 6FBPS0-BPSH100 multiblock copolymer membranes may lead to much lower interface stress and improved MEA stability to prevent membrane electrode failure.

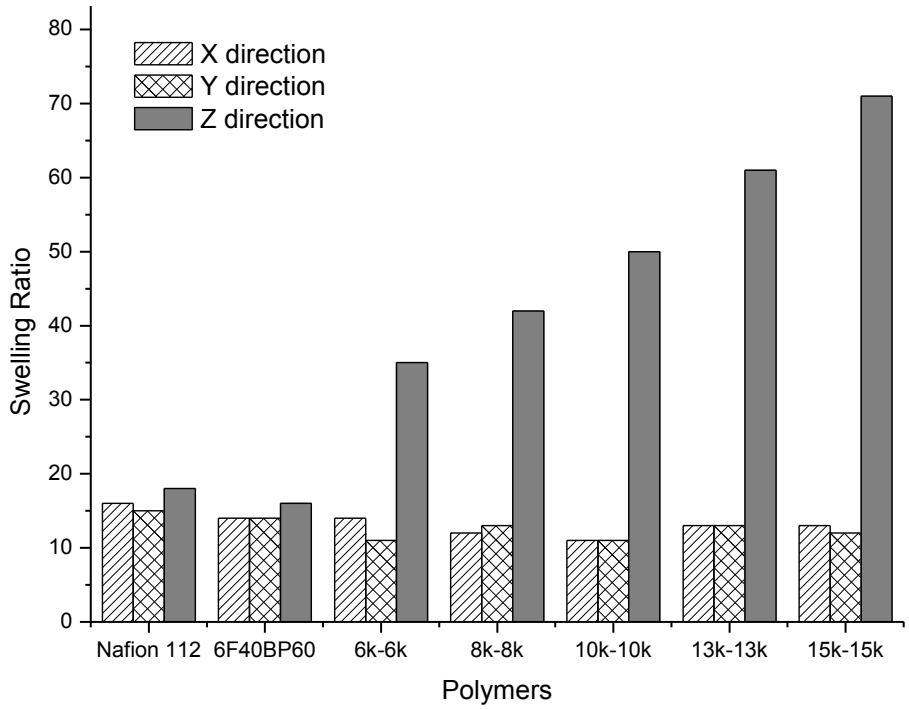

Figure 5. 18. Comparison of dimensional swelling data for 6FBPS0-BPSH100 multiblock, copolymers, 6F40BP60H and Nafion® 112

5.4 Conclusions

A series of 6FBPS0-BPS100 hydrophobic-hydrophilic multiblock copolymers have been successfully synthesized based on the coupling of a fluorine terminated poly(arylene ether sulfone) (6FBPS0) hydrophobic oligomer and a phenoxide terminated disulfonated poly(arylene ether sulfone) (BPS100) hydrophilic oligomer. Intrinsic viscosities of 6FPAEB-BPS100 copolymers confirmed that high molecular weight copolymers were obtained. The regularly sequenced structure of 6FBPS0-BPS100 multiblock copolymers was confirmed by ^{13}C NMR. The ether-ether interchange side reactions were avoided by utilization of relatively mild reaction temperatures. DSC and DMA traces of

6FBPS0-BPS100 multiblock copolymers confirm the presence of 2 thermal transitions and suggest phase separation in copolymers. Water uptake was significantly reduced upon annealing at temperature greater than the T_g of the 6FBPS0 block and the water uptake dependence on block length diminished entirely. Multiblock copolymers with higher block lengths showed improved performance with regard to proton conductivity, presumably due to their more distinct nanophase separation and better connectivity among the ionic domains, as evidenced by morphology characterizations from TEM and SAXS profiles. TGA traces confirm the 6FBPS0-BSH100 multiblock copolymer membranes are thermooxidatively stable up to 270 ^{o}C. The anisotropic swelling behavior of 6FBPS0-BPSH100 multiblock copolymers should result in much lower stress at the interface and better stability of the MEA to prevent membrane electrode failure.

5.5 References:

1. Carrette L, Friedrich KA, and Stimming U. Fuel Cells 2001;1(1):5.
2. Whittingham MS and Zawodzinski T. Chem. Rev. 2004;104(10):4243.
3. Winter M and Brodd RJ. Chem. Rev. 2004;104(10):4245.
4. Hickner MA, Ghassemi H, Kim YS, Einsla BR, and McGrath JE. Chem. Rev. 2004;104(10):4587.
5. Kerres JA. J. Membr. Sci. 2001;185(1):3.
6. Mauritz KA and Moore RB. Chem. Rev. 2004;104(10):4535.
7. Wang F, Hickner M, Kim YS, Zawodzinski TA, and McGrath JE. J. Membr. Sci. 2002;197(1-2):231.
8. Chikashige Y, Chikyu Y, Miyatake K, and Watanabe M. Macromolecules 2005;38(16):7121.
9. Xing PX, Robertson GP, Guiver MD, Mikhailenko SD, Wang KP, and Kaliaguine S. J. Membr. Sci. 2004;229(1-2):95.
10. Shang XY, Tian SH, Kong LH, and Meng YZ. J. Membr. Sci. 2005;266(1-2):94.
11. Summer MJ, Harrison WL, Weyers RM, Kim YS, McGrath JE, Riffle JS, Brink A, and Brink MH. J. Membr. Sci. 2004;239(2):199.
12. Miyatake K, Zhou H, Matsuo T, Uchida H, and Watanabe M. Macromolecules 2004;37(13):4961.
13. Einsla BR, Kim YS, Hickner MA, Hong YT, Hill ML, Pivovar BS, and McGrath

JE. J. Membr. Sci. 2005;255(1-2):141.
14. Asensio JA, Borros S, and Gomez-Romero P. J. Membr. Sci. 2004;241(1):89.
15. Kim YS, Hickner MA, Dong L, Pivovar BS, and McGrath JE. J. Membr. Sci. 2004;243(1-2):317.
16. Badami AS, Roy A, Lee H-S, Li Y, and McGrath JE. J. Membr. Sci. 2009;328(1-2):156.
17. Li YX, Roy A, Badami AS, Hill M, Yang J, Dunn S, and McGrath JE. J. Power Sources 2007;172(1):30.
18. Lee HS, Badami AS, Roy A, and McGrath JE. J. Polym. Sci., Part A: Polym. Chem. 2007;45(21):4879.
19. Lee HS, Roy A, Badami AS, and McGrath JE. Macromolecular Research 2007;15(2):160.
20. Lee HS, Roy A, Lane O, Dunn S, and McGrath JE. Polymer 2008;49(3):715.
21. Lee H-S, Roy A, Lane O, Lee M, and McGrath JE. J. Polym. Sci., Part A: Polym. Chem. 2010;48(1):214.
22. Lee H-S, Roy A, Lane O, and McGrath JE. Polymer 2008;49(25):5387.
23. Badami AS, Lane O, Lee H-S, Roy A, and McGrath JE. J. Membr. Sci. 2009;333(1-2):1.
24. Wang H, Badami AS, Roy A, and McGrath JE. Journal of Polymer Science Part a-Polymer Chemistry 2007;45(2):284.
25. Yu X, Roy A, Dunn S, Badami AS, Yang J, Good AS, and McGrath JE. J. Polym. Sci., Part A: Polym. Chem. 2009;47(4):1038.
26. Yu X, Roy A, Dunn S, Yang J, and McGrath JE. Macromolecular Symposia 2006;245-246(1):439.
27. Ghassemi H, McGrath JE, and Zawodzinski TA. Polymer 2006;47(11):4132.
28. Ghassemi H, Ndip G, and McGrath JE. Polymer 2004;45(17):5855.
29. Nakabayashi K, Matsumoto K, and Ueda M. J. Polym. Sci., Part A: Polym. Chem. 2008;46(12):3947.
30. Sankir M, Bhanu VA, Harrison WL, Ghassemi H, Wiles KB, Glass TE, Brink AE, Brink MH, and McGrath JE. J. Appl. Polym. Sci. 2006;100(6):4595.
31. Springer TE, Zawodzinski TA, Wilson MS, and Gottesfeld S. J. Electrochem. Soc. 1996;143(2):587.
32. Lee M, Park JK, Lee H-S, Lane O, Moore RB, McGrath JE, and Baird DG. Polymer 2009;50(25):6129.

Chapter 6: Semi-crystalline Hydrophobic-Hydrophilic Multiblock Copolymers Based on Poly(arylene ether sulfone) via Low-Temperature Coupling Reactions for Proton Exchange Membranes

Yu Chen, Chang Hyun Lee, James E. McGrath*

Macromolecular Science and Engineering Program, Macromolecules and Interfaces Institute, Virginia Polytechnic Institute and State University, Blacksburg, Virginia 24061

Abstract

Multiblock copolymers based on alternating segments of telechelic phenoxide terminated hydrophilic fully disulfonated poly(arylene ether sulfone) (BPS100) and decafluorobiphenyl (DFBP) terminated hydrophobic poly(arylene ether ketimine) (PEEKt), were synthesized from the hydrophilic and ketemine-protected amorphous hydrophobic telechelic oligomers by nucleophilic coupling reactions. After film formation from DMSO, the copolymer was acidified, which converted the ketimine to semi-crystalline ketone segments and the sulfonate salts to desulfonic acids. A semi-crystalline phase having a T_m of 325 ^oC was confirmed. The multiblock copolymers membranes were tough, ductile and solvent resistant after hydrolysis. The fundamental properties as proton exchange membranes (PEMs) were explored. Enhanced conductivities under fully hydrated and reduced humidity conditions were observed when compared with Nafion® and a BPSH40 random copolymer with a similar ion exchange capacity (IEC). These multiblock copolymers exhibited anisotropic swelling behavior, whereas the random copolymers were isotropic.

Keywords: semi-crystalline, hydrophobic-hydrophilic multiblock copolymers, proton exchange membranes

6.1 Introduction

Proton exchange membrane fuel cells (PEMFCs) have been extensively studied as potential alternative power sources for electric vehicles, portable and residential power sources because of their high power density, excellent energy conversion efficiency, quiet operation and zero pollution emission. Proton exchange membranes (PEMs), the key component of PEMFCs, are responsible for transporting the protons from anode to cathode [1, 2]. There are several critical requirements for a successful PEM material, such as high proton conductivity, good mechanical strength, high oxidative and hydrolytic stability, low fuel and oxidant permeability, ease of fabrication, and excellent water management under low relative humidity (RH) cycling [3, 4]. Currently, perfluorinated sulfonic acid containing ionomers (PFSAs), such as Nafion® manufactured by DuPont, are widely used as PEM materials due to their good chemical stability, excellent mechanical properties and high proton conductivity [5]. However, there are several major drawbacks of these materials, such as high cost, high methanol permeability, low ceiling operation temperature (<80 ℃) [6].

A number of sulfonated aromatic statistical copolymers, such as sulfonated poly(arylene ether sulfone)s (BPSHs), poly(ether ether ketone)s (SPEEKs), poly(arylene ether nitrile)s (SPAEBs), polyimides (SPIs) and polybenzimidazoles have been developed as potential alternatives to Nafion® [7-14]. Although some of the sulfonated statistical copolymers achieved reasonable proton conductivity under fully hydrated states [15], only limited conductivity performance was observed under partially hydrated states. Further improvement of membrane properties, especially the conductivity performance under partially hydrated states, is a primary goal for researchers.

The sulfonated multiblock copolymer membranes exhibited hydrophilic/hydrophobic nanophase separated morphologies in the presence of water [16]. This nanophase separation permitted the formation of co-continuous hydrophilic domains and significantly enhanced proton transport under partially hydrated conditions [17, 18]. Wholly aromatic hydrophilic-hydrophobic multiblock copolymers based on fully sulfonated poly(arylene ether sulfone) (BPS100) hydrophilic blocks and different types of hydrophobic blocks have been introduced as new PEM materials by McGrath's group [16, 19-30].

In this paper we first report the synthesis and characterization of semi-crystalline hydrophobic poly(ether ether ketone)-hydrophilic disulfonated poly(arylene ether sulfone) (PEEK-BPSH100) multiblock copolymers. However, due to their semi-crystalline structure, PEEK blocks are insoluble in most organic solvents at relative lower reaction temperature, which prevent the coupling reaction between PEEK and BPS100. In order to facilitate the synthesis and processing, removable bulky ketimine was introduced to synthesize amorphous PEEKt pre-oligomers [31-33]. The synthesis procedure first involves synthesis of hydrophobic poly(ether ether ketimine)-hydrophilic sulfonated poly(arylene ether sulfone) (PEEKt-BPS100) multiblock pre-copolymers via coupling reactions between phenoxide terminated hydrophilic BPS100 and decafluorobiphenyl (DFBP) end-capped hydrophobic PEEKt blocks. The highly reactive perfluorinated end groups of the PEEKt blocks allowed for a low reaction temperature in the coupling reaction to minimize the possibility of ether-ether interchange reaction and made it possible to achieve high yields and molecular weights of the multiblock copolymers. Amorphous PEEKt-BPS100 copolymers were then simultaneously hydrolyzed and

acidified to produce semi-crystalline PEEK-BPSH100. The proton conductivity, water uptake and other membrane properties of the acidified semi-crystalline PEEK-BPSH100 membranes were evaluated.

6.2 Experiments

6.2.1 Materials

4,4'-Difluorobenzophenone (DFK), was purchased from TCI America, and purified by recrystallization from ethanol. Decafluorobiphenyl (DFBP) was purchased from Aldrich and used as received. Hydroquinone was purchased from Aldrich, and dried under vacuum at 100 ^{o}C. 4, 4′-hexafluoroisopropylidenediphenol (6F-BPA), received from Ciba, was sublimated and then recrystallized twice from toluene. Monomer grade 4,4'-dichlorodiphenylsulfone (DCDPS) and 4,4′-biphenol (BP) were provided by Solvay Advanced Polymers and Eastman Chemical Company, respectively, and dried under vacuum at 120 ^{o}C prior to use. 3,3'-Disulfonated-4,4'-dichlorodiphenylsulfone (SDCDPS) was synthesized from DCDPS and purified according to a procedure reported elsewhere [34]. Aniline was purchased from Aldrich and purified by vacuum distillation from calcium hydride. N-Methyl-2-pyrrolidinone (NMP), N,N-dimethylacetamide (DMAc), cyclohexane, and toluene were purchased from Aldrich and distilled from calcium hydride before use. The 3 Å molecular sieves and potassium carbonate were purchased from Aldrich and dried under vacuum at 180 ^{o}C prior to use. Dimethyl sulfoxide (DMSO), chloroform, acetone, methanol and 2-propanol (IPA) were purchased from Fisher Scientific and used without further purification.

6.2.2 Synthesis of N- Phenyl(4,4' - difluorodiphenyl) ketimine (DFKt)

DFK (60 g, 0.275 mol) and aniline (40 mL 0.44 mol) were added to a two-necked round-bottom flask equipped with a nitrogen inlet, Dean-Stark trap and a condenser. Toluene (250 mL), along with 150 g of 3 Å molecular sieves were added into the flask. The reaction bath was heated to 140 ^{o}C to let toluene reflux over 24 h until 100% conversion to ketimine had occurred as confirmed by ^{1}H NMR. Toluene and excess aniline were then removed by rotary evaporation. The ketimine product was recrystallized 2 times from toluene to give 40.0 g (50% yield) of a yellow crystalline solid with a melting point of 113-115 ^{o}C.

6.2.3 Synthesis of Amorphous Phenoxide Terminated Poly(ether ether ketimine) Hydrophobic Oligomer (PEEKt)

A series of amorphous fluorine terminated poly(ether ether ketimine) oligomers (PEEKt) was synthesized with different molecular weights by offsetting the stoichiometry according to the Carothers equation. A sample synthesis of 9,000 g/mol PEEKt oligomer is as follows. A 100-mL three-necked round-bottom flask, equipped with a mechanical stirrer, a nitrogen inlet, a condenser and a Dean-Stark trap was charged with 5.6421 g (0.0192 mol) of DFKt, 2.2064 g (0.0200 mol) of hydroquinone and 40 mL of NMP. The mixture was stirred until dissolved, and then 3.33 g (0.0241 mol) of potassium carbonate and 20 mL of toluene were added. The reaction bath was heated to 145 ^{o}C for 4 h in order to azeotropically remove water from the system. The bath temperature was slowly raised to 170 ^{o}C by the controlled removal of toluene. The reaction was allowed to proceed at 170 ^{o}C for 24 h. The mixture was cooled to room

temperature and filtered to remove most of the salt, then coagulated in 1 L of methanol. The precipitated oligomer was stirred in methanol for 24 h and then dried under vacuum at 140 ^{o}C for 48 h.

6.2.4 End-capping of Phenoxide Terminated PEEKt Hydrophobic Oligomer with DFBP

Phenoxide-terminated PEEKt oligomers were end-capped with DFPB via a nuclephilic aromatic substitution mechanism. A sample end-capping reaction of 7,000 g/mol PEEKt oligomer is as follows. A 100-mL three-necked round-bottom flask, equipped with a mechanical stirrer, a nitrogen inlet, a Dean-Stark trap, and a condenser was charged with 7.000 g (1 mmol) of Phenoxide terminated DFKt oligomer, 0.5528 g (4 mmol) and 70 mL DMAc. The mixture was stirred until dissolved, and then 3.33 g (0.0241 mol) of potassium carbonate and 25 mL of toluene were added. The reaction bath was heated to 145 ^{o}C in order to azeotropically remove water from the system. After 4 h, toluene was removed. The reaction temperature was set at 105 ^{o}C, then 2.0067 g (6 mmol) DFBP was added into the flask. The reaction was allowed to proceed at 105 ^{o}C for 24 h. The mixture was cooled to room temperature and filtered to remove most of the salt, then coagulated in 1 L of methanol. The precipitated oligomer was stirred in methanol for 24 h and then dried under vacuum at 140 ^{o}C for 48 h.

6.2.5 Synthesis of Phenoxide Terminated Disulfonated Hydrophilic Oligomer (BPS100)

A series of phenoxide terminated fully disulfonated hydrophilic oligomers (BPS100) was synthesized with different molecular weights by offsetting the stoichiometry according to the Carothers equation. A sample synthesis of 7,000 g/mol BPS100 is as

follows. A 100-mL three-necked round-bottom flask, equipped with a mechanical stirrer, a nitrogen inlet, a Dean-Stark trap, and a condenser was charged with 4.0230 g (0.0216 mol) of BP, 9.8020 g (0.0200 mol) of SDCDPS, and 70 mL DMAc. The mixture was stirred until dissolved, and then 3.50 g (0.0254 mol) of potassium carbonate and 35 mL toluene were added. The reaction bath was heated to 145 ^{o}C for 4 h in order to azeotropically remove water from the system. The bath temperature was slowly raised to 180 ^{o}C by the controlled removal of toluene. The reaction was allowed to proceed at 180 ^{o}C for 72 h. The mixture was cooled to room temperature and filtered to remove most of the salt, then coagulated in 2 L of acetone. The precipitated oligomer was stirred in acetone for 24 h and then dried under vacuum at 140 ^{o}C for 48 h.

6.2.6 Synthesis of Amorphous Hydrophobic-Hydrophilic Multiblock Copolymers (PEEKt-BPS100)

A typical coupling reaction was conducted as follows: 5.00 g (0.667 mmol) of BPS100, 0.25 g (1.81 mmol) of potassium carbonate, 80 mL of NMP and 30 mL of cyclohexane were added to a 250-mL three-necked flask equipped with a mechanical stirrer, a nitrogen inlet, a Dean-Stark trap and a condenser. The reaction bath was heated to 125 ^{o}C for 6 h to dehydrate the system. After removing cyclohexane, the reaction temperature was lower to 105 ^{o}C, 6.50 g (0.5 mmol) of DFBP end-capped PEEKt oligomer was added. The coupling reaction was allowed for 24h. The reaction mixture was filtered and precipitated into 1 L IPA. The copolymer was purified in a Soxhlet extractor with methanol for 24 h and with chloroform for another 24 h. The copolymer was dried at 140 ^{o}C under vacuum for 24 h.

6.2.7 Film Casting, Hydrolysis and Acidification

The PEEKt-BPS100 copolymers in the salt form were dissolved in NMP or DMSO (7% w/v) and filtered through 0.45 mm PTFE syringe filters. The solutions were then cast onto clean glass substrates. The films were dried for 24 h with an infrared lamp at 45-55 ^{o}C. The residual solvent was removed by drying in a vacuum oven at 190 ^{o}C for 24 h. The amorphous PEEKt-BPS100 membranes were converted to semi-crystalline acid form PEEK-BPSH100 in 1 M hydrochloric acid solution at 100 ^{o}C for 24 h, followed by boiling in deionized water for 2 h.

6.2.8 Characterization

^{1}H NMR and ^{19}F NMR analyses were conducted on a Varian INOVA spectrometer operating at 400 MHz. The spectra of BPS100 oligomers and 6FK-BPS100 multiblock copolymers were obtained from a 10% solution (w/v) in a DMSO-d_6 solution at room temperature. The spectra of DFBP end-capped PEEKt hydrophobic oligomers were obtained from a solution in $CDCl_3$. ^{13}C NMR analyses were conducted on a Varian Unity spectrometer, operating at 100.58 mHz with DMSO-d_6 as solvent.

Absorbance mode FTIR spectra of thin films were obtained using a Bruker Tensor 27 spectrophotometer in a wave number range from 600-4000 cm^{-1}.

Intrinsic viscosities of PEEKt, DFBP end-capped PEEKt, BPS100 oligomers and PEEKt-BPS100 multilblock copolymers were obtained from a size exclusion chromatography (SEC) equipped with a Waters 1515 isocratic HPLC pump, a Waters autosampler, a Waters HR5–HR4–HR3 column set, a Waters 2414 refractive-index detector, and a Viscotek 270 viscometric detector. NMP (containing 0.05 M LiBr) was

used as the mobile phase [35].

Thermogravimetric analyses (TGA) of the PEEK-BPSH100 membranes were determined with a TA Instrument TGA Q500. Prior to TGA characterization, all the samples were vacuum-dried and kept in the TGA furnace at 150 ^{o}C for 30 min to remove residual solvent and moisture. The samples were then evaluated over the range of 50-650 ^{o}C at a heating rate of 10 ^{o}C/min under an air atmosphere. Glass transition temperatures (T_gs) and melting exothermos were determined by differential scanning calorimetry (DSC) with a TA Instruments DSC Q-1000 at a heating rate of 10 ^{o}C/min under a stream of nitrogen.

6.2.9 Determine of Proton Conductivity

The ohmic resistance (R, Ω) of the PEM membrane was measured using a homemade test cell [36] via four-point probe alternating current (a.c.) impedance spectroscopy in the frequency range from 3 MHz to 10 Hz under two different conditions (liquid water at 30 ℃ and relative humidity (RH) from 30 to 95% at 80 ℃). The resistance value of each membrane was obtained by averaging at least five measurements to guarantee the water equilibration of the membranes at certain temperature and humidity. The whole wiring system for measuring the ohmic resistance was shielded from the platinum electrodes to the potentiometer (a combined system of an electrochemical interface, Solartron 1287, and an impedance/gain-phase analyzer, Solartron 1252A) to avoid electromagnetic noise. The proton conductivity (σ, S cm^{-1}) was obtained from the following equation (Equation 6.1):

$$\sigma = \frac{L}{R \cdot S} \quad \text{(Equation 6.1)}$$

Where σ (S/cm) is proton conductivity, L (cm) is the distance between two electrodes, R (Ω) is the resistance of the membrane and S (cm^2) is the surface area that protons transport though the membrane. For measurements of proton conductivity in liquid water, each membrane was fully hydrated by soaking in DI water at room temperature for 24 h. For determining proton conductivity under partially hydrated conditions, membranes were equilibrated in a humidity-temperature controlled oven (ESPEC, SH-240) at a certain relative humidity (RH) level and 80 ℃ for at least 40 minutes before each measurement.

6.2.10 Determine of The Water Uptake and Dimension Swelling

The water uptake of all membranes was determined gravimetrically. The acidified PEEK-BPSH100 membranes were equilibrated in DI water at room temperature for 2 days. Wet membranes were removed from the DI water, blotted dry to remove surface droplets, and quickly weighed. The membranes were then dried at 120 ^{o}C under vacuum for 24 h and weighed again. The water uptake of the membranes was calculated according to the following equation (Equation 6.2), where W_{dry} and W_{wet} refer to the mass of the dry and wet membrane, respectively.

$$Water\ Uptake\ (\%) = \frac{W_{wet} - W_{dry}}{W_{dry}} \times 100 \quad \text{(Equation 6.2)}$$

The volume swelling ratios of the membranes were determined from the dimensional changes from wet to dry state. Membranes were equilibrated in DI water, and dimensions in the wet state were measured. The dried dimensions were obtained after drying the wet membrane at 80 ^{o}C in a convection oven for 2 h.

6.3 Results and Discussion

6.3.1 Synthesis of N-Phenyl(4,4'-difluorodiphenyl) ketimine (DFKt)

The synthesis of DFKt monomer is a nucleophilic substitution reaction as shown in Figure 6.1. An excess amount of aniline and longer reaction time were needed to ensure the full conversion of DFK to DFKt.

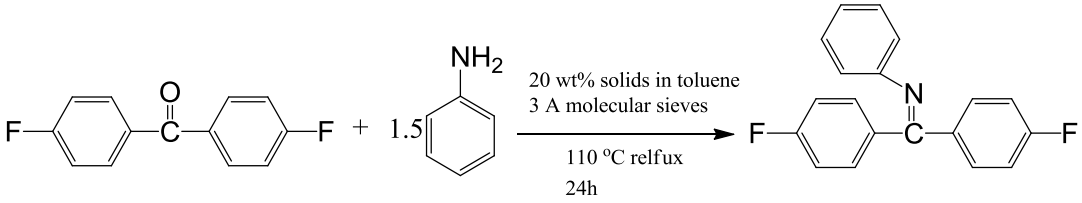

Figure 6. 1. Synthesis of N-phenyl(4,4'-difluorodiphenyl) ketimine (DFKt) monomer

Figure 6.2 shows the ^{1}H NMR of N-phenyl(4,4'-difluorodiphenyl) ketimine (DFKt) Monomer, the peaks in the spectrum can be properly assigned as the protons in the DFKt molecule. The high purity of DFKt was confirmed due to the lack of other signals indicating the presence of impurities.

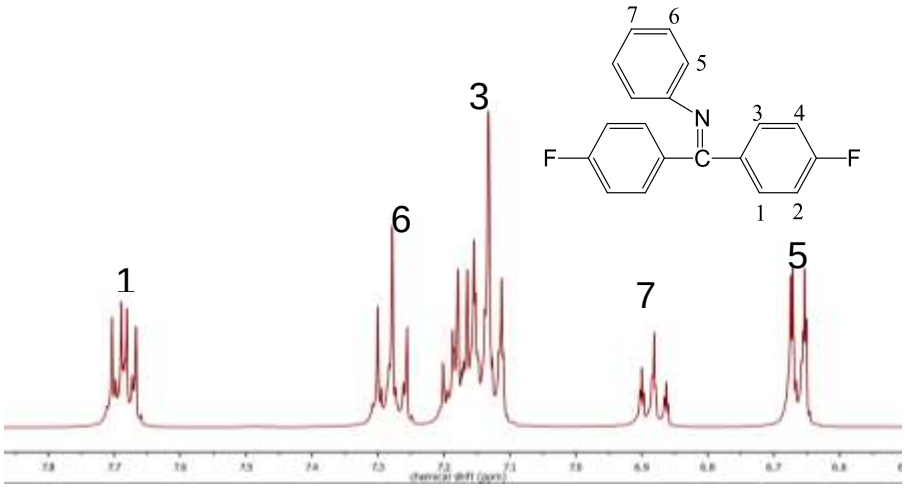

Figure 6. 2. ^{1}H NMR of N-phenyl(4,4'-difluorodiphenyl) ketimine (DFKt) monomer

6.3.2 Synthesis of Phenoxide Terminated PEEKt Oligomers

Phenoxide-terminated amorphous PEEKt hydrophobic oligomers were synthesized by copolymerization of DFKt and excess hydroquinone monomers as shown in Figure 6.3. The molecular weight and end group functionality of the oligomers were precisely controlled by off-setting the molar feeding ratios of monomers according to Carothers equation. In all cases, the molar feed ratios of HQ over DFKt were larger than 1 to give phenoxide telechelic functionality and target number-average molecular weights ranging from 4 to 21 kg/mol. Unfortunately, due the overlap of the proton signals in the ^{1}H NMR spectrum, it is not possible to use the integrations of ^{1}H NMR spectra to calculate the number average molecular weight (M_n).

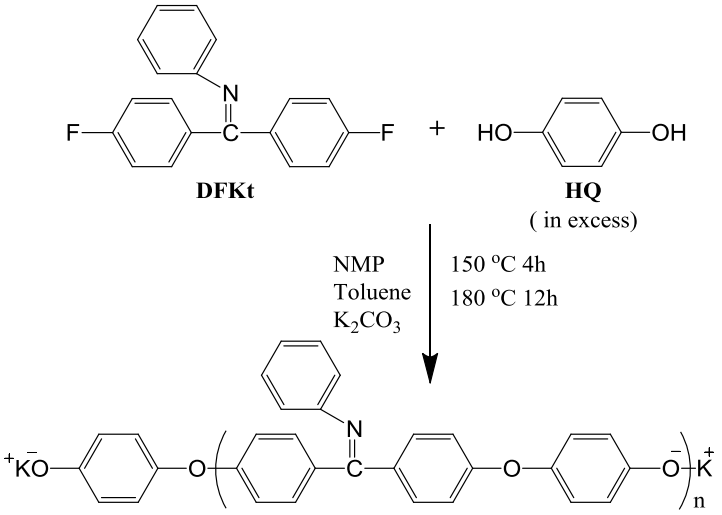

Figure 6. 3. Synthesis of amorphous phenoxide terminated poly(ether ether ketimine) oligomer (PEEKt)

6.3.3 Synthesis and Characterization of DFBP End-capped PEEKt Oligomers

Because the PEEKt and BPS100 oligomers possess the same phenoxide telechelic

functionality, it is necessary to modify one of the oligomers to halide terminated to facility the coupling reactions for producing multiblock copolymers. Phenoxide terminated PEEKt oligomers were end-capped with DFPB to achieve fluorine-terminated PEEKt, as shown in Figure 6.4. A large excess (6 times the amount of PEEKt) of DFBP was added to prevent the inter-oligomer coupling reaction of PEEKt oligomers. Due to the high reactivity of DFBP, a mild reaction temperature (105 ^{o}C) and relatively short reaction time (~12 h) were sufficient to afford the fluorine-terminated PEEKt. Figure 6.5 shows the ^{1}H NMR spectra before (Figure 6.5, top) and after (Figure, 6.5. bottom) end-capping of PEEKt with DFBP. Although there are no significant changes in the sharpness and chemical shift position of the peaks, after DFBP end-capping, one peak overlapped at 6.75 ppm in the spectrum of phenoxide terminated PEEKt, disappeared. This partially overlapping peak should be assigned to the protons on the HQ moieties locate at the ends of the oligomers. The disappearance of the peak suggests the phenoxide end groups react with DFBP.

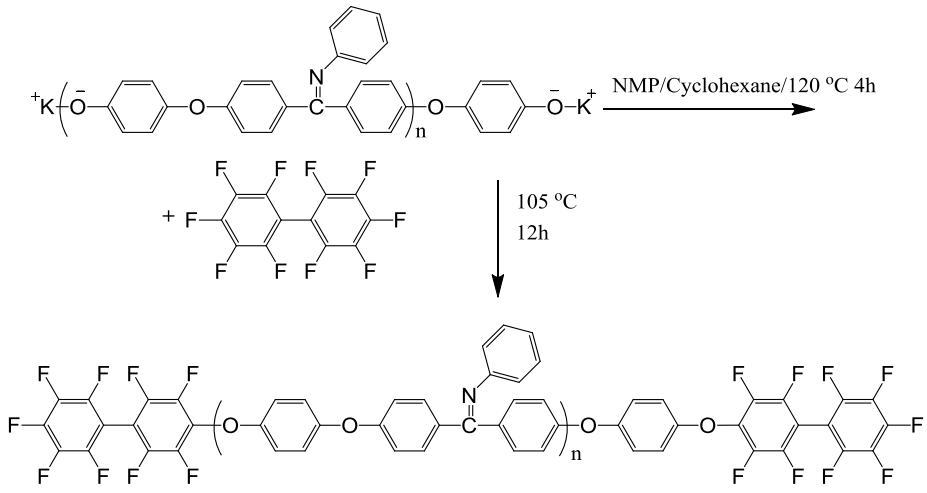

Figure 6. 4. End-capping of PEEKt oligomer with DFBP

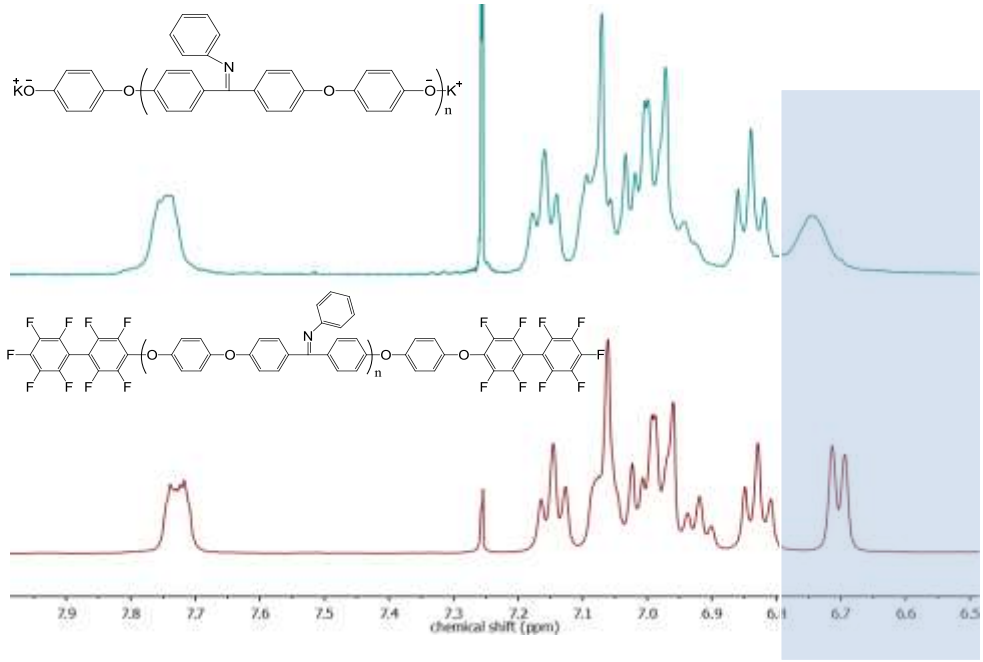

Figure 6. 5. ^{1}H NMR of PEEKt oligomers before (top) and after (bottom) end-capping with DFBP

The measurement of the M_ns of PEEKt oligomers is very important in the synthesis of multiblock copolymers with proper block lengths and IECs. Analysis of a ^{19}F NMR spectrum can be utilized to determine the M_n of the fluorine-terminated oligomer with a small amount 6F-BPA added as a reference. By comparing the respective integrations of the fluorine groups of a quantitative amount of PEEKt oligomer and 6F-BPA, the M_n of the oligomer is determined. Figure 6.6 shows a ^{19}F NMR spectrum of precisely weighed DFBP end-capped PEEKt-9k oligomer and 6F-BPA. The peak at -64.2 ppm is attributed to the fluorine in the 6F-BPA. Five peaks at -137.3, -137.9, -149.9,-152.9 and -160.3ppm are attributed to the fluorines on the end-capping DFBP. The M_n of the DFBP end-capped PEEKt can be calculated with the following equation (Equation 6.3), where W_{PEEKt} and $W_{6F\text{-}BPA}$ are the weights of PEEKt sample and 6F-BPA reference, MW of

6F-BPA is 336.23 g/mol. I_b, I_c and I_f are the integrations of corresponding fluorines in Figure 6.6. The calculated M_n of PEEK includes the molecular weight of end-capping groups.

$$\frac{\frac{W_{PEEKt}}{Mn\ of PEEKt}}{\frac{W_{6f-BPA}}{MW\ of\ 6F-BPA}\times 6} = \frac{(I_b+I_c)/8}{I_f} \quad (\text{.....Equation 6.3})$$

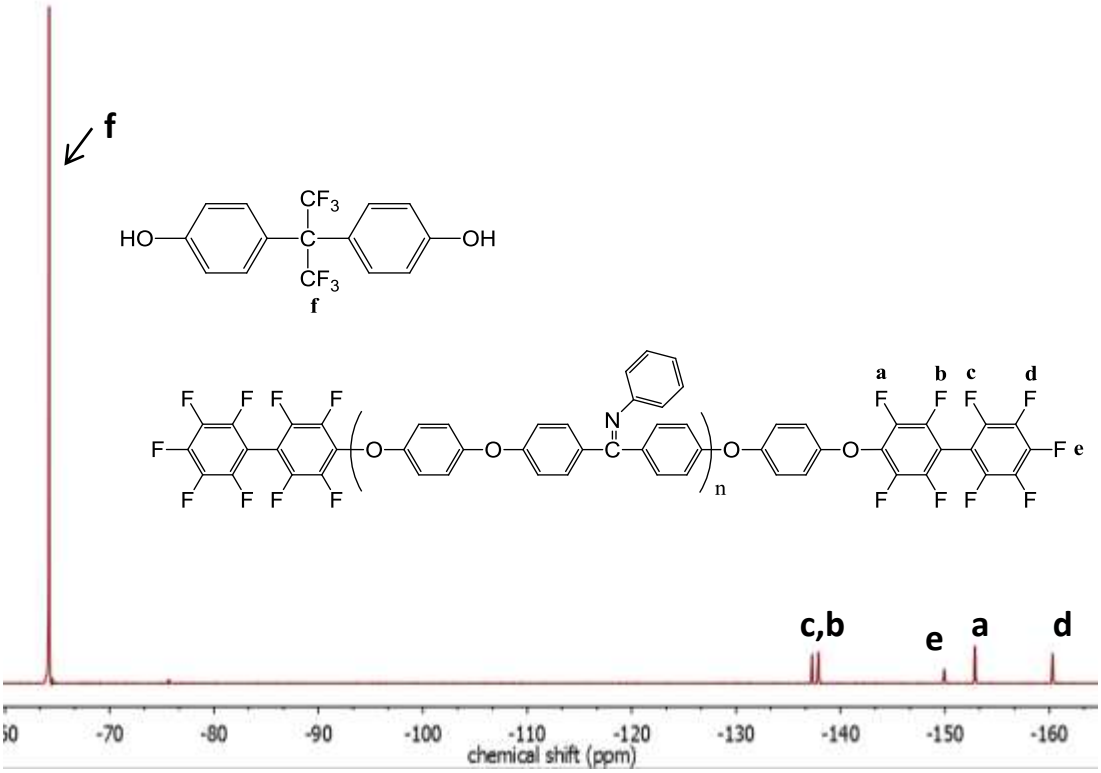

Figure 6. 6 ^{19}F NMR of DFBP end-capped PEEKt with 6F-BPA as a reference

The intrinsic viscosities of PEEKt before and after DFBP end-capping as well as the M_n calculated from ^{19}F NMR are listed in Table 6.1. After end-capping with DFBP, the intrinsic viscosities of PEEKt only increased slightly, the slight increases in intrinsic viscosities before and after the DFBP end-capping reaction are due to chain length extension by the end-capping reagent DFBP, rather than the inter-oligomer coupling

reactions.

Table 6. 1. Intrinsic viscosities of PEEKt before and after DFBP end-capping

Target M_n (g/mol)	**Hydrophobic Blocks**		
	M_n[a](g/mol) (measured from ^{19}F NMR)	IV[b] (dL/g) (Before end-capping)	IV[c] (dL/g) (after end-capping)
7k	7300	0.16	0.17
9k	9200	0.20	0.24
14k	14500	0.27	0.29
17k	17400	0.31	0.38
21k	20800	0.36	0.42

a. M_n were calculated from Equation 6.3
b. Measured by SEC with 0.05M LiBr/NMP as mobile phase at 60 ^oC
c. Measured by SEC with 0.05M LiBr/NMP as mobile phase at 60 ^oC

6.3.4 Synthesis and Characterization of Phenoxide Terminated BPS100 Oligomers

Phenoxide-terminated fully disulfonated poly(arylene ether sulfone) hydrophilic oligomers (BPS100) were synthesized via a nucleophilic aromatic substitution reaction. A small amount of excess BP monomer was used to control the telechelic functionality and molecular weight, as shown in Figure 6.7.

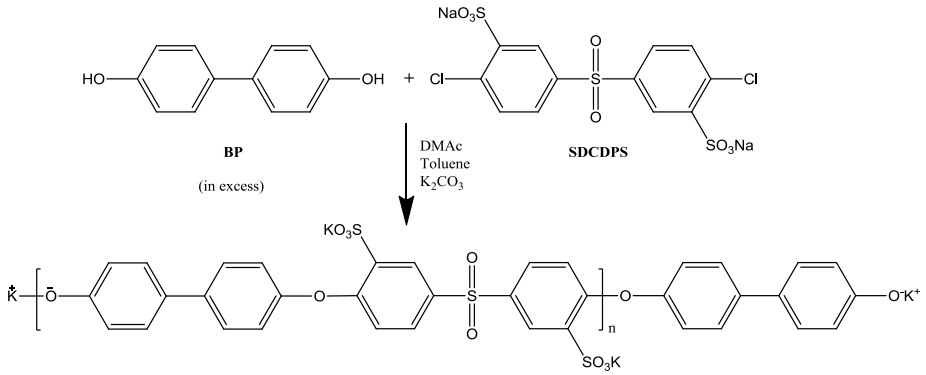

Figure 6. 7. Synthesis of phenoxide terminated fully disulfonated hydrophilic oligomer (BPS100)

The M_ns of the hydrophilic oligomers can be determined by ^1H NMR. Figure 6.8 shows the ^1H NMR spectrum of BPS100, Protons from the terminal BP moieties were assigned to four small peaks at 6.80, 7.05, 7.40, and 7.55 ppm, while the peaks at 7.10 and 7.65 were assigned to the protons of the BP moieties in the middle of BPS100 oligomer backbone. By comparing the integrations of the protons on the end-group BP and of the protons on the SDCDPS moieties, the M_n of each BPS100 oligomer was determined.

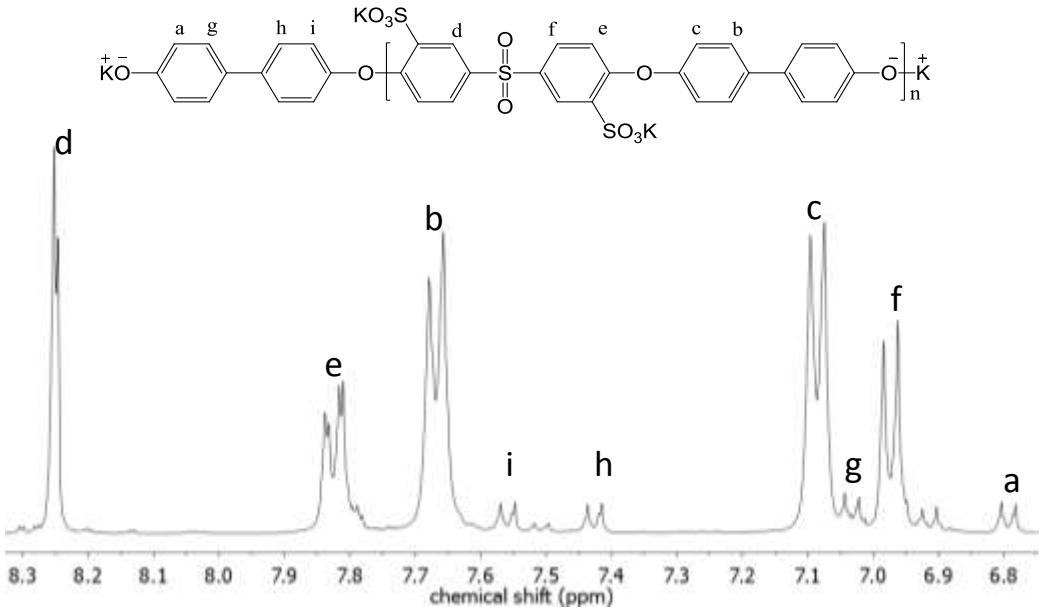

Figure 6. 8. ^1H NMR of phenoxide terminated BPS100 oligomer

The molecular weights and intrinsic viscosities obtained from SEC are summarized in Table 6.2. An increase in IV was observed when the M_n of BPS100 increased. There is a linear relationship between the log number average molecular weights and log intrinsic viscosities, which indicates that control of the molecular weights for the hydrophilic

oligomers was successful, as shown in Figure 6.9.

Table 6. 2. Characterization of hydrophilic (BPS100) oligomers

Target M_n	**Hydrophilic Blocks**	
(g/mol)	M_n[a] (g/mol)	IV[b] (dL/g)
5000	5200	0.13
7000	7100	0.18
9000	9100	0.20
13000	13700	0.28
15000	14600	0.32

a: Measured by ^{1}H NMR
b: Measured by SEC with 0.05M LiBr/NMP as mobile phase at 60 ^{o}C

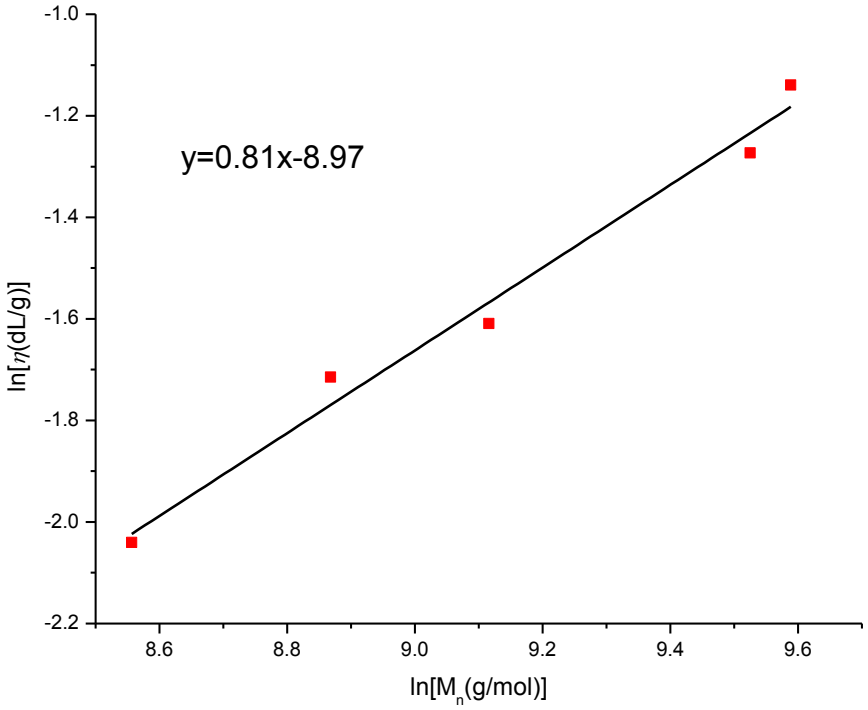

Figure 6. 9. ln η vs. ln M_n plot of BPS100 oligomers

6.3.5 Synthesis and Characterization of PEEKt-BPS100 Multiblock Copolymers

A series of amorphous hydrophobic hydrophilic multiblock copolymers was synthesized via a coupling reaction between phenoxide terminated BPS100 and DFBP end-capped PEEKt oligomers, as Figure 6.10 shown. The stoichiometry of the reactions was set as 1:1. The intrinsic viscosity (IV) data confirmed high molecular weight PEEKt-BPS100 multiblock copolymers were obtained.

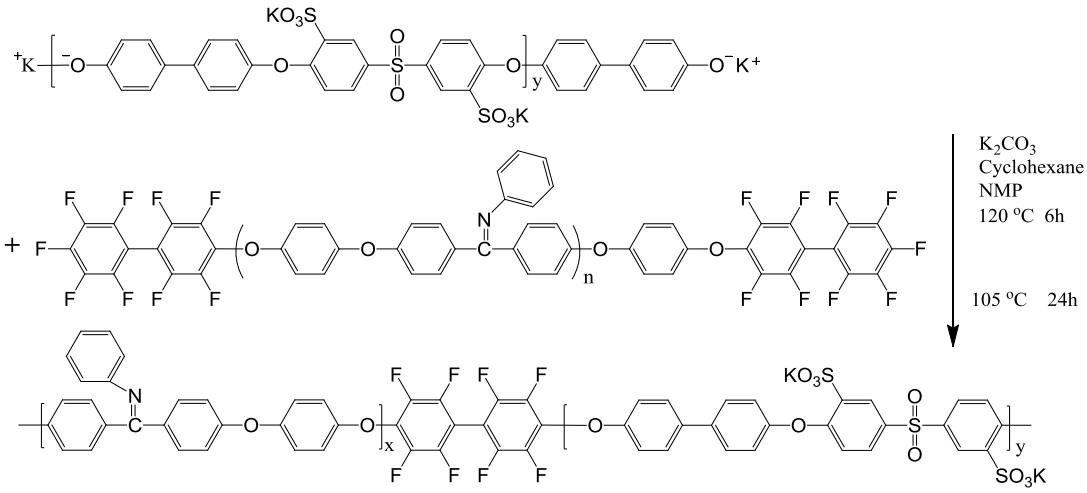

Figure 6. 10. Synthesis of PEEKt-BPS100 multiblock copolymers

Figure 6.11 shows the ^{1}H NMR of a PEEKt-BPS100 multiblock copolymer. It is difficult to monitor the degree of the coupling reaction from the disappearance of the phenoxide end group peaks of BPS100 (peak **a** in Figure 6.8) as described in the literature [21]. At this chemical shift position on ^{1}H NMR spectrum of PEEKt-BPS100, there are overlapping peaks from the protons of SDCDPS and DFKt moieties (peaks **c** and peak **k**).

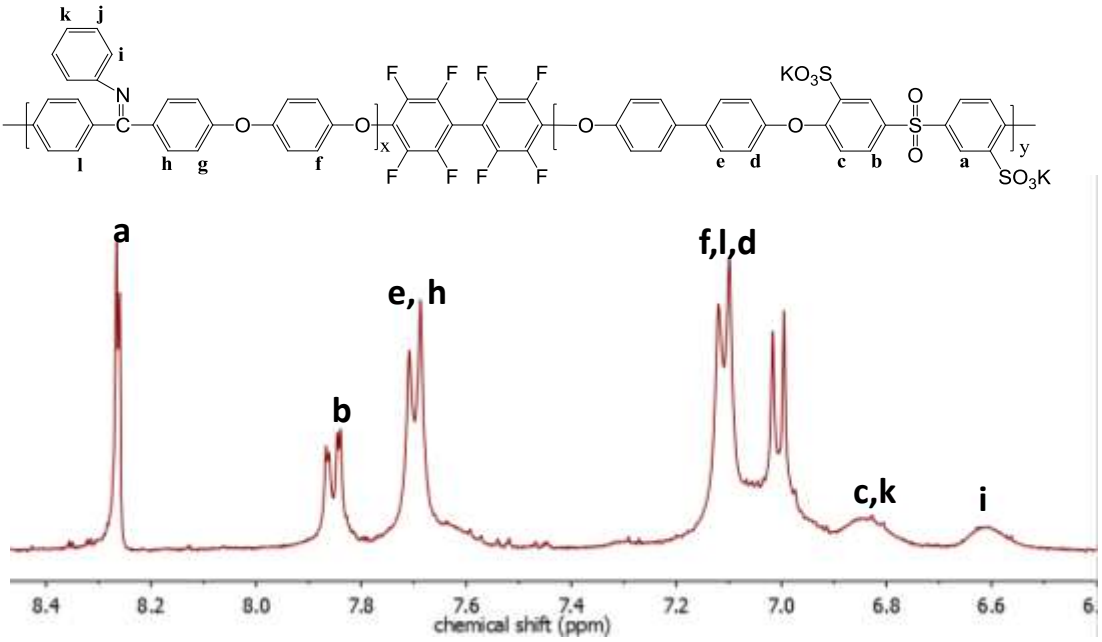

Figure 6. 11. ^{1}H NMR of PEEKt-BPS100 9k-7k multiblock copolymer

Because of the high reactivity of DFBP moieties, the coupling reaction can be accomplished at a relatively low temperature and short reaction time to minimize the possible ether-ether interchange side reactions. Figure 6.12 shows the ^{13}C NMR of PEEKt-BPS100 9k-7k. In the chemical shift range of 150-170 ppm, the peaks can be properly assigned to the carbons on the backbone of the PEEKt-BPS100 polymer. The two peaks at 156.3 ppm and 158.8ppm, which are assigned to the carbons on the each end of the ether bond in BPS100 blocks (Figure 6.12 peak **b** and **a**), are still sharp and narrow. This phenomenon suggests the multiblock copolymer maintains an ordered sequence and confirms the minimization of the ether-ether interchange side reactions.

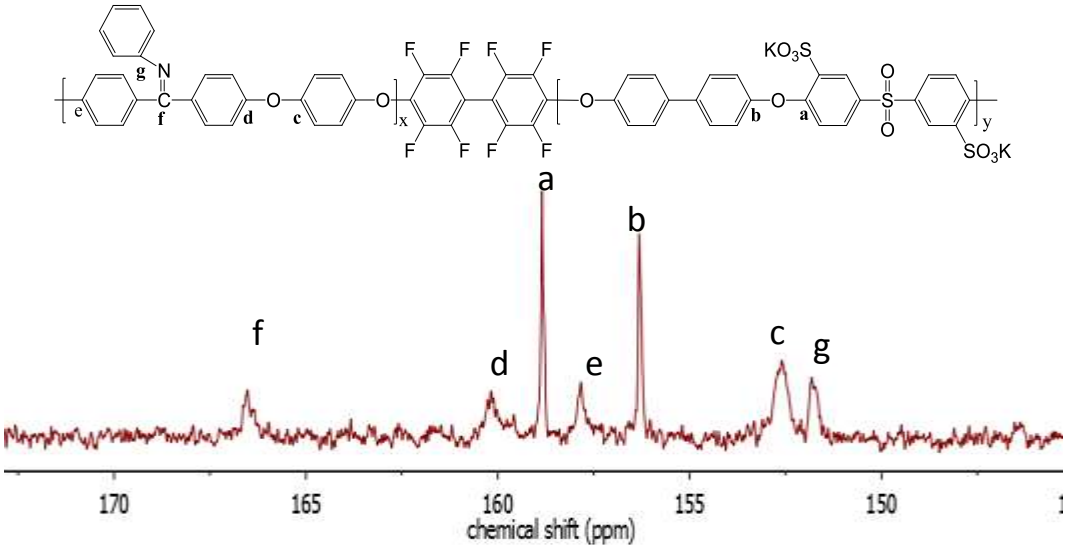

Figure 6. 12. ^{13}C NMR of PEEKt-BPS100 9k-7k multiblock copolymer

6.3.6 Film Casting, Hydrolysis and Acidification

The PEEKt-BPS100 multiblock copolymer membranes were cast from NMP and DMSO solutions. Membranes were boiled in aqueous 0.5M hydrochloric acid (HCl) then 0.5M sulfuric acid (H_2SO_4) solutions to hydrolyze the amorphous PEEKt blocks to semi-crystalline PEEK blocks and to simultaneously acidify the BPS100 blocks to BPSH100 blocks, as Figure 6.13 shown. The reason of using 0.5M HCl is the produced aniline chloride is more easily to dissolve in water and removed from the membrane. After acidification, the cleavage of the ketimine groups caused a change in the molecular weight of the hydrophobic blocks (e.g. PEEKt-BPS100 9k-7k to PEEK-BPSH 7k-7k). After this procedure, the high crystallinity of PEEK blocks prevents the PEEK-BPSH100 from dissolution in any polar organic solvent, such as DMSO, DMAc or NMP.

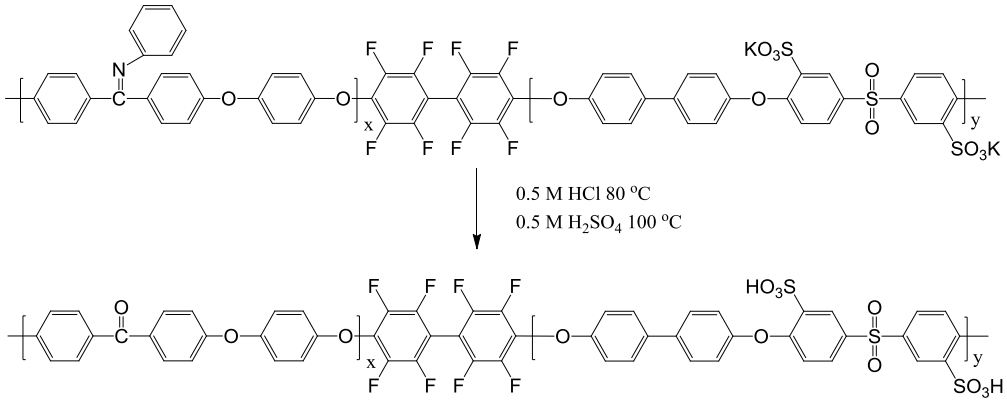

Figure 6. 13. Hydrolysis and acidification to convert amorphous PEEKt-BPS100 to semi-crystalline PEEK-BPSH100

Fourier transform infrared (FT-IR) spectroscopy is a powerful tool used to characterize the functional groups in a material. The hydrolysis and acidification of the PEEKt-BPS100 to PEEK-BPSH100 membranes can be determined by FT-IR. Figure 6.14 shows the FT-IR spectra of a PEEKt-BPS100 16k-13k membrane before and after acidification. The absorption bands at 1247, 1095 and 1029 cm^{-1} can be assigned to asymmetric and symmetric O=S=O stretching vibrations of sulfonic groups. The absorption band assigned to the S–O stretching of sulfonic group shifts from 696 cm^{-1} to 686 cm^{-1} after acidification. This absorption band shift suggests the acidification of potassium sulfonic groups to sulfonic acid groups.

A representative FT-IR spectrum of PEEKt-BPS100 16k-13k (Figure 6.14, top) exhibits a large peak at 1590 cm^{-1}, which can be assigned as a C=N stretching vibration. The decease of the C=N stretching peak and the appearance of the C=O stretching peak at 1650 cm^{-1} in PEEK-BPSH100 13k-13k spectrum (Figure 6.14, bottom) confirm the hydrolysis of PEEKt-BPS100 to PEEK-BPSH100.

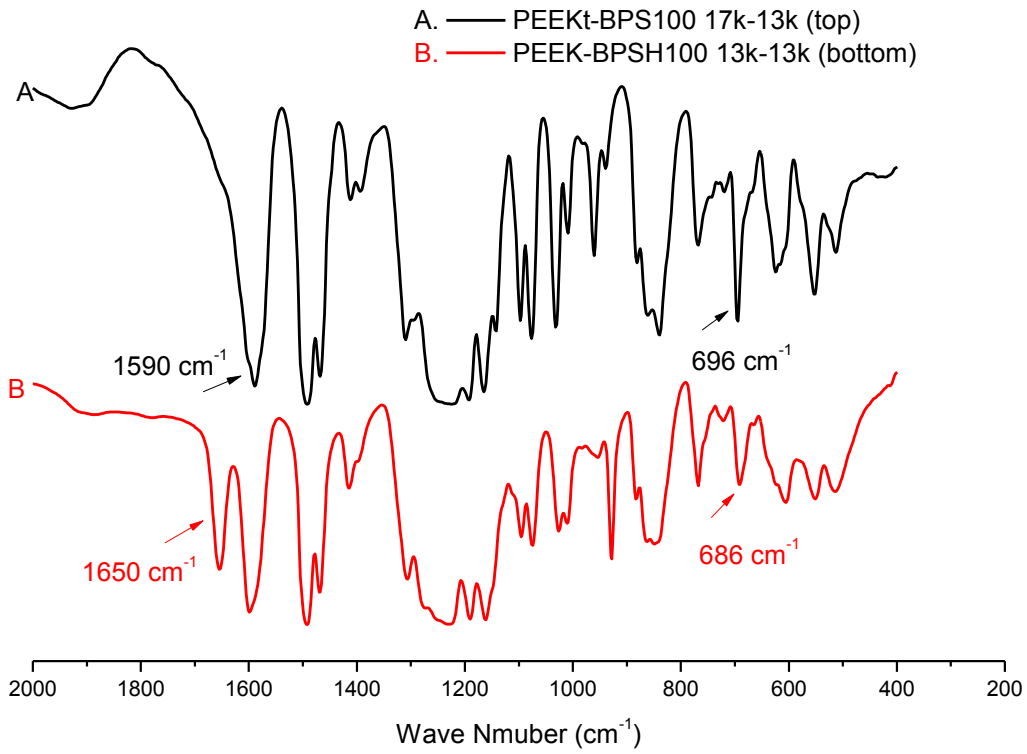

Figure 6. 14. IR Spectra of PEEKt-BPS10016k-13k (before hydrolysis) (top) and PEEK-BPSH100-13k-13k (after hydrolysis) (bottom)

6.3.7 Thermal Properties Characterization

DSC is one important characterization technique to determine the glass transition temperature T_g and the crystalline melting transition temperature T_m for polymers. Two thermal transitions, one at around 165 ^oC and the other at 245 ^oC were observed in the DSC trace of PEEKt-BPS100 17k-13k as Figure 6.15 shown. These 2 thermal transitions can be assigned to the glass transition of the hydrophobic PEEKt blocks and that of hydrophilic BPS100 blocks, respectively. No melting endotherm transition was observed due to the PEEKt-BPS100 series copolymers are amorphous.

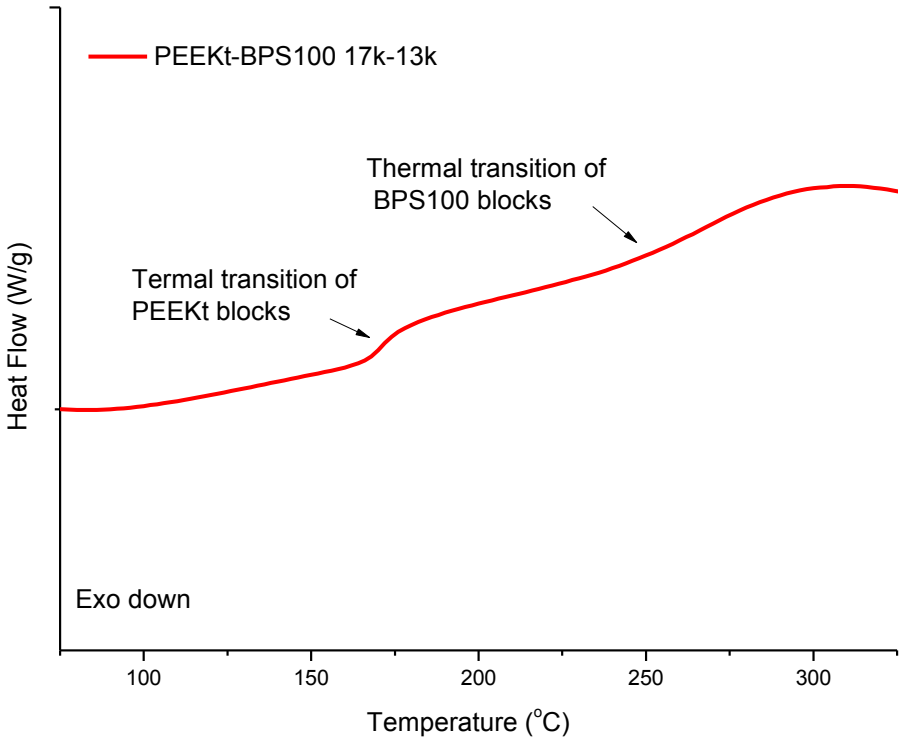

Figure 6. 15. DSC thermogram of PEEKt-BPS100 17k-13k

Amorphous PEEKt-BPS100 17k-13k was hydrolyzed and acidified to semi-crystalline PEEK-BPSH100 13k-13k in diluted sulfuric acid solution. The DSC trace of PEEK-BPSH100 13k-13k is shown in Figure 6.16. A very broad thermal transition from 140 ^{o}C to 250 ^{o}C was observed. This very broad thermal transition indicates the decreased T_g of BPSH100 blocks after acidification partially overlaps with the T_g of PEEK blocks. A melting endotherm at 340 ^{o}C was observed and attributed to the presence of semi-crystalline domains in the PEEK-BPSH100 13k-13k membrane.

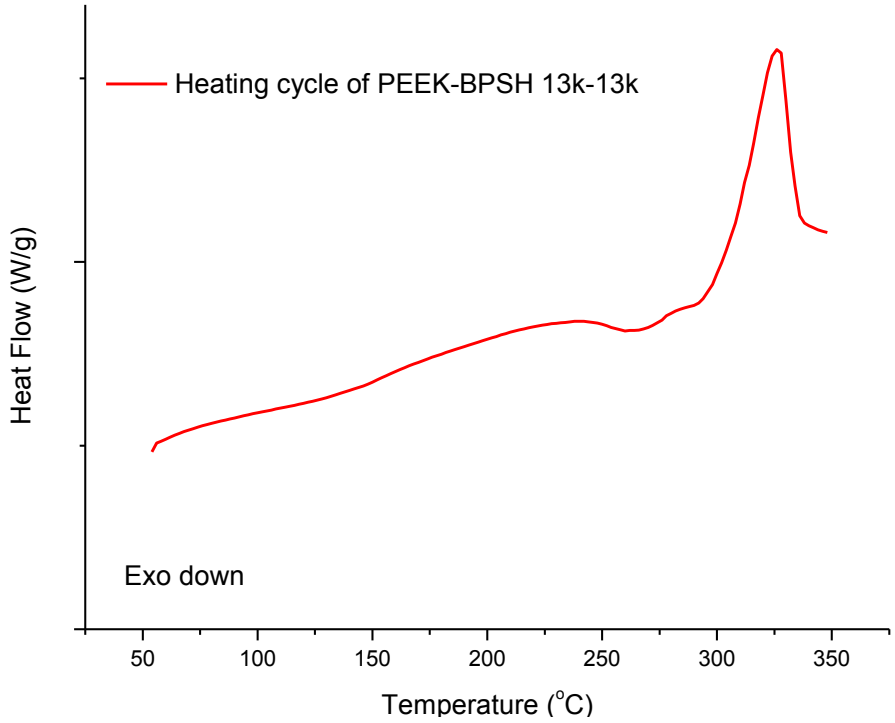

Figure 6. 16. DSC thermogram of PEEK-BPSH100 13k-13k

Thermal and oxidative stability of the PEEK-BPSH100 multiblock copolymers were investigated by TGA, as shown in Figure 6.17. The TGA was conducted in an air atmosphere to assess the oxidative stability of the copolymers. Such copolymers displayed a two-step weight loss. The first was observed at 270 ^{o}C and assigned to the desulfonation of BPSH100 blocks. The second degradation began at 450 ^{o}C, which was led by the decomposition of the copolymer backbones. The block lengths in the copolymers in this study did not affect the thermal and oxidative stability. All the copolymers showed very similar weight loss behavior indicating the control of IEC (or degree of sulfonation) is successful.

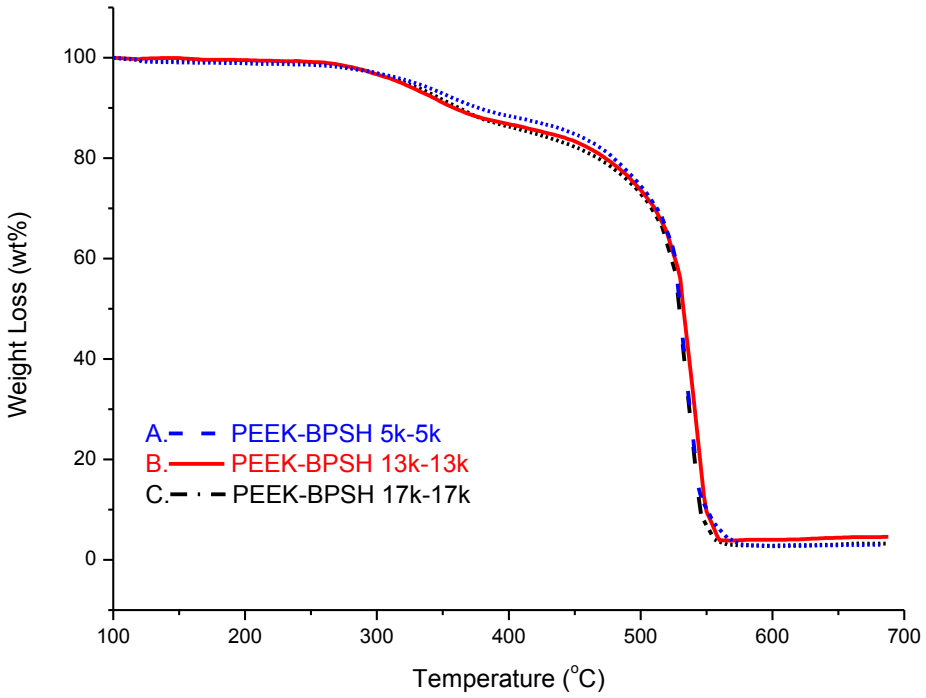

Figure 6. 17. TGA thermograms of PEEK-BPSH100 multiblock copolymers

6.3.8 Characterization of The Membrane Properties of PEEK-BPSH100

Tough, ductile, transparent PEEKt-BPS100 membranes were cast from NMP and DMSO, as Table 6.3 shown. After hydrolysis and acidification, the PEEK-BPSH100 multiblock copolymer membranes turn to light yellow and do not dissolve in normal organic solvents such as NMP and DMSO, due to the high crystallinity of the PEEK blocks. The water uptake of PEEK-BPSH100 block copolymers increases with the increase in block length, which is consistent with other reported block copolymers [21].

Table 6. 3. Properties of PEEK-BPSH100 multiblock copolymers

PEEKt-BPS100	PEEK-BPSH100	Yield (%)	IV (dL/g) [a]	IEC (meq/g) [b]	Water uptake (%)
7k-5k	5k-5k	84	0.83	1.60	47
12k-9k	9k-9k	88	0.96	1.65	50
17k-13k	13k-13k	85	1.10	1.70	53
21k-17k	17k-17k	91	1.13	1.70	85
Nafion® 112		N/A	N/A	0.90	22
BPSH40		95	0.85	1.52	50

a: Measured by SEC with 0.05M LiBr/NMP as mobile phase at 60 ^{O}C, in PEEKt-BPS100 state
b: Measured from ^{1}H NMR
c: Measured from DMSO cast membranes, acid form in liquid water at 30 ^{O}C

The proton conductivity of the PEEK-BPSH100 multiblock copolymer membranes were measured in liquid water at 30 ^{o}C as shown in Figure 6.18. A BPS40 random copolymer and Nafion® 212 were also included as controls. The dependence of proton conductivity performance of PEM membranes on solvent selectivity has been reported [34]. Two solvents, NMP and DMSO, were evaluated as casting solvents for PEEKt-BPS100 block copolymers. NMP is a good solvent for both PEEKt and BPS100 oligomers. DMSO, which dissolves BPS100 oligomers well, is not a good solvent for PEEKt oligomers. After acidification, the PEEK-BPSH100 block copolymer membranes cast from NMP solution become opaque in the fully hydrated state, while those cast from DMSO still maintain their transparency. As the block length increases, the proton conductivity of the PEEK-BPSH100 block copolymer membranes cast from NMP decreases rapidly. In contrast, the proton conductivity slightly increases with the increase in block length for PEEK-BPSH100 block copolymer membranes cast from DMSO. The solvent selection shows a more significant impact in the higher block length copolymers.

The proton conductivity values of the NMP and DMSO cast PEEK-BPSH100 5k-5k membranes only show a slight difference. When the block length of PEEK-BPSH100 increases to 17k-17k, the proton conductivity of the membrane cast from DMSO almost doubles compared to that of the membrane cast from NMP.

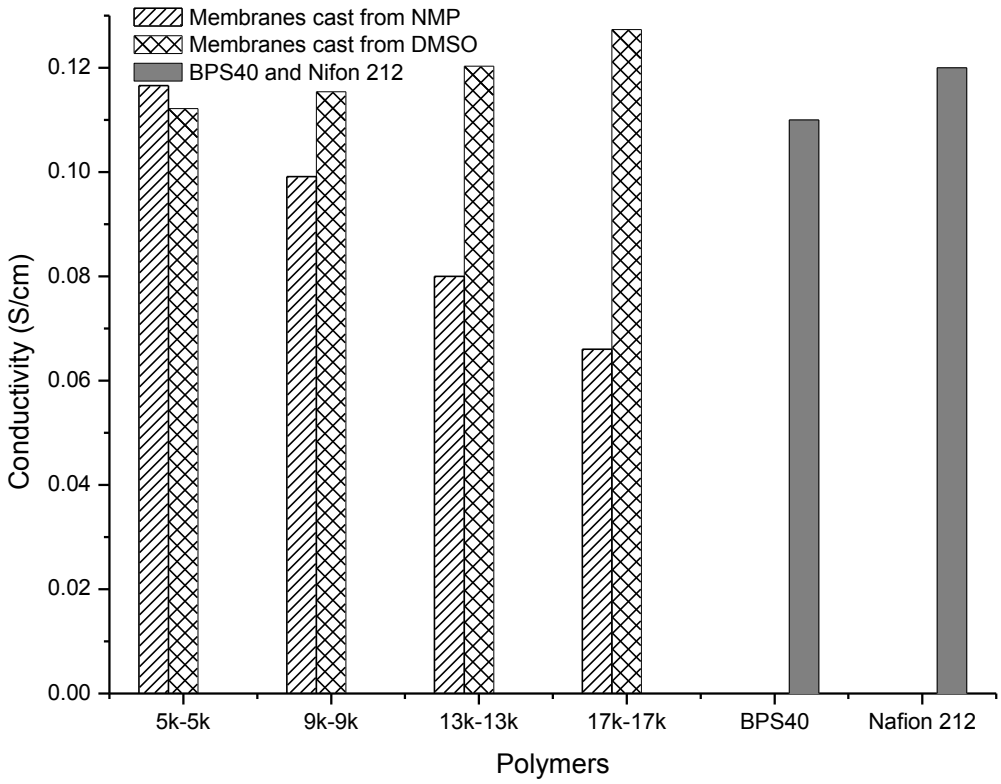

Figure 6. 18. Proton conductivity of PEEK-BPSH100 multiblock copolymer membranes cast from NMP and DMSO solution.

The proton conductivity of PEEK-BPSH100 17k-17k cast from a DMSO solution as a function of relative humidity (RH) at 80 ^{o}C was measured and is displayed in Figure 6.19. The proton conductivity of the randomly copolymerized BPSH40 dropped significantly at lower RH levels as expected. Sufficient water molecules provide proton

transport under fully hydrated states. However, the scattered hydrophilic domains in the random copolymer cannot form the broader channels of sulfonic acid groups to facilitate proton transport under partially hydrated conditions. In contrast, under partially hydrated states, protons can be transported along with the sulfonic acid groups and water molecules through the long, co-continuous channels in multiblock copolymers.

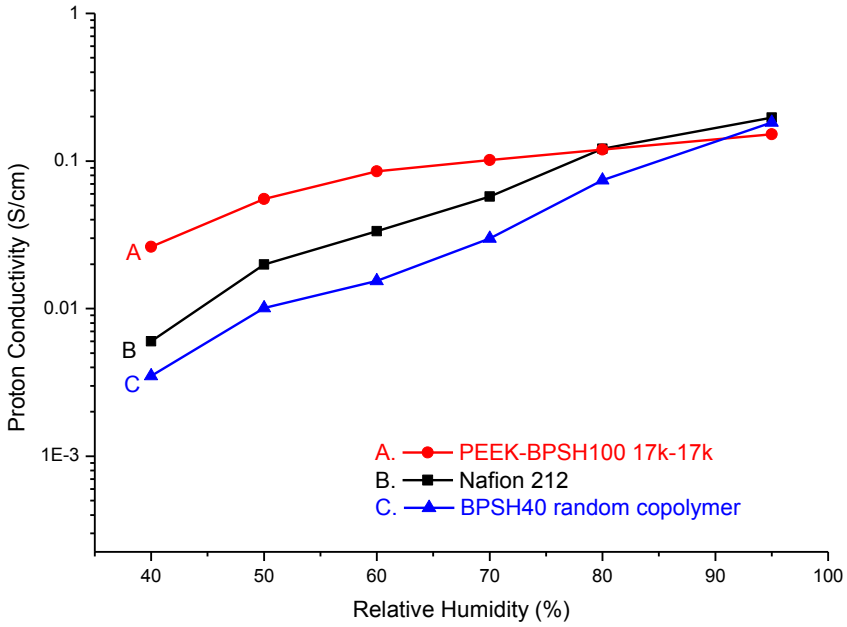

Figure 6. 19. Proton conductivity vs. RH of PEEK-BPSH 100 17k-17k multiblock copolymers with Nafion® and BPSH40 as references (measured at 80 ℃)

6.3.9 Swelling-Deswelling Behavior of PEEK-BPSH100 Multiblock Copolymer

The compatibility between proton exchange membrane (PEM) and electrodes is always a major concern in the real operation conditions for a membrane electrode assembly (MEA). When a proton exchange membrane shows a significant in-plane swelling, during the wet-dry cycles, considerable stress is created at the interface between

the membrane and electrodes. The high stress could destroy the compatibility of membrane and electrode, leading to premature failure of the MEA.

The dimension swelling behaviors of PEEK-BPSH100 multiblock copolymers with BPSH35 and Nafion® as comparison is shown in Figure 6.20. The BPSH35 and Nafion® 112 membranes show isotropic swelling behavior. In contrast, PEEK-BPSH100 multiblock copolymer membranes exhibit anisotropic swelling behavior. For PEEK-BPSH100 membranes, in-plane swelling (x- and y-directions) decreases while through-plane (z-direction) swelling increases as the block length increases. This behavior indicates the development of enhanced ordered morphology as block length increases. The low in-plane swelling of PEEK-BPSH100 multiblock copolymer membranes may induce a much lower interface stress and better MEA stability to prevent the membrane electrode failure.

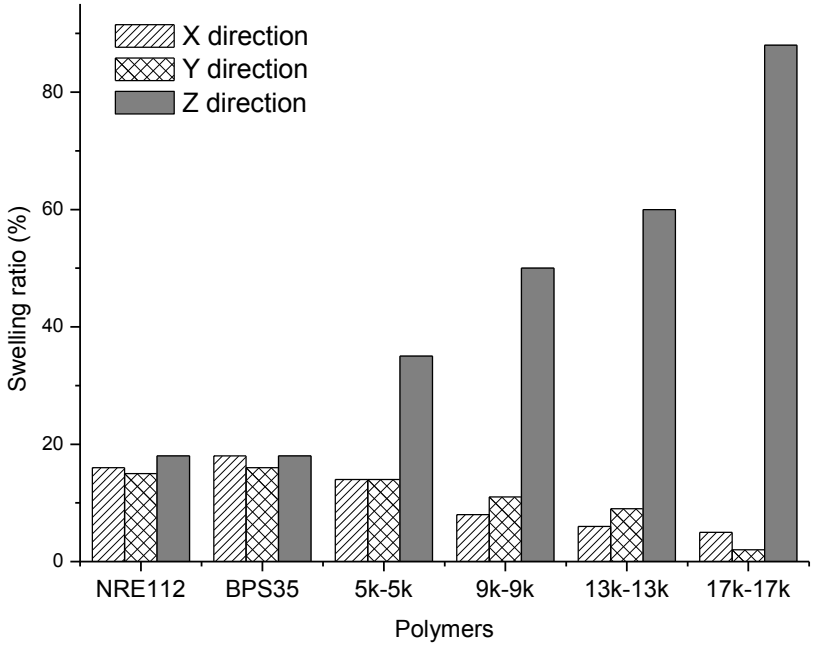

Figure 6. 20. Comparison of dimensional swelling data for PEEK-BPSH100 multiblock, copolymers, BPSH35 and Nafion® 112

6.4 Conclusions

Multiblock semi-crystalline hydrophobic poly(ether ether ketone)-hydrophilic disulfonated poly(arylene ether sulfone) (PEEK-BPSH100) copolymers were developed and characterized. PEEK-BPSH100 multiblock copolymers were successfully synthesized by hydrolysis of multiblock PEEKt-BPS100 pre-copolymers. FT-IR spectrum confirmed the hydrolysis of PEEKt-BPS100 to PEEK-BPSH100. DSC traces showed a melting endotherm, confirming the presence of semi-crystalline domains in the PEEK-BPSH100. The proton conductivities of the multiblock semi-crystalline PEEK-BPSH100 copolymers were comparable or higher than that of Nafion® and BPSH 40 random copolymer. PEEK-BPSH100 17k-17k shows better conductivity performance under low RH, presumably due to its more distinct nanophase separation and better connectivity among the ionic domains, supports the existence of well connected proton transport channels in the PEEK-BPSH100 membranes. The anisotropic swell behavior of PEEK-BPSH100 multiblock copolymers may result in much lower stress at the interface and improve the compatibility between membrane and electrode.

6.5 References:

1. Winter M and Brodd RJ. Chem. Rev. 2004;104(10):4245.
2. Whittingham MS and Zawodzinski T. Chem. Rev. 2004;104(10):4243.
3. Hickner MA, Ghassemi H, Kim YS, Einsla BR, and McGrath JE. Chem. Rev. 2004;104(10):4587.
4. Kerres JA. J. Membr. Sci. 2001;185(1):3.
5. Mauritz KA and Moore RB. Chem. Rev. 2004;104(10):4535.
6. Rozière J and Jones DJ. Annual Review of Materials Research 2003;33.
7. Wang F, Hickner M, Kim YS, Zawodzinski TA, and McGrath JE. J. Membr. Sci. 2002;197(1-2):231.
8. Chikashige Y, Chikyu Y, Miyatake K, and Watanabe M. Macromolecules

2005;38(16):7121.
9. Xing PX, Robertson GP, Guiver MD, Mikhailenko SD, Wang KP, and Kaliaguine S. J. Membr. Sci. 2004;229(1-2):95.
10. Shang XY, Tian SH, Kong LH, and Meng YZ. J. Membr. Sci. 2005;266(1-2):94.
11. Summer MJ, Harrison WL, Weyers RM, Kim YS, McGrath JE, Riffle JS, Brink A, and Brink MH. J. Membr. Sci. 2004;239(2):199.
12. Miyatake K, Zhou H, Matsuo T, Uchida H, and Watanabe M. Macromolecules 2004;37(13):4961.
13. Einsla BR, Kim YS, Hickner MA, Hong YT, Hill ML, Pivovar BS, and McGrath JE. J. Membr. Sci. 2005;255(1-2):141.
14. Asensio JA, Borros S, and Gomez-Romero P. J. Membr. Sci. 2004;241(1):89.
15. Wang F, Hickner M, Ji Q, Harrison W, Mecham J, Zawodzinski TA, and McGrath JE. Macromolecular Symposia 2001;175:387.
16. Lee HS, Badami AS, Roy A, and McGrath JE. J. Polym. Sci., Part A: Polym. Chem. 2007;45(21):4879.
17. Roy A, Hickner MA, Yu X, Li YX, Glass TE, and McGrath JE. J. Polym. Sci., Part B: Polym. Phys. 2006;44(16):2226.
18. Roy A, Lee H-S, and McGrath JE. Polymer 2008;49(23):5037.
19. Li YX, Roy A, Badami AS, Hill M, Yang J, Dunn S, and McGrath JE. J. Power Sources 2007;172(1):30.
20. Lee HS, Roy A, Badami AS, and McGrath JE. Macromolecular Research 2007;15(2):160.
21. Lee HS, Roy A, Lane O, Dunn S, and McGrath JE. Polymer 2008;49(3):715.
22. Lee H-S, Roy A, Lane O, Lee M, and McGrath JE. J. Polym. Sci., Part A: Polym. Chem. 2010;48(1):214.
23. Lee H-S, Roy A, Lane O, and McGrath JE. Polymer 2008;49(25):5387.
24. Badami AS, Roy A, Lee H-S, Li Y, and McGrath JE. J. Membr. Sci. 2009;328(1-2):156.
25. Badami AS, Lane O, Lee H-S, Roy A, and McGrath JE. J. Membr. Sci. 2009;333(1-2):1.
26. Wang H, Badami AS, Roy A, and McGrath JE. Journal of Polymer Science Part a-Polymer Chemistry 2007;45(2):284.
27. Yu X, Roy A, Dunn S, Badami AS, Yang J, Good AS, and McGrath JE. J. Polym. Sci., Part A: Polym. Chem. 2009;47(4):1038.
28. Yu X, Roy A, Dunn S, Yang J, and McGrath JE. Macromolecular Symposia 2006;245-246(1):439.
29. Ghassemi H, McGrath JE, and Zawodzinski TA. Polymer 2006;47(11):4132.
30. Ghassemi H, Ndip G, and McGrath JE. Polymer 2004;45(17):5855.
31. Lindfors BE, Mani RS, Mcgrath JE, and Mohanty DK. Makromolekulare Chemie-Rapid Communications 1991;12(6):337.
32. Brink AE, Gutzeit S, Lin T, Marand H, Lyon K, Hua T, Davis R, and Riffle JS. Polymer 1993;34(4):825.
33. Bourgeois Y, Devaux J, Legras R, and Parsons IW. Polymer 1996;37(14):3171.
34. Sankir M, Bhanu VA, Harrison WL, Ghassemi H, Wiles KB, Glass TE, Brink AE, Brink MH, and McGrath JE. J. Appl. Polym. Sci. 2006;100(6):4595.
35. Yang J, Li Y, Roy A, and McGrath JE. Polymer 2008;49(24):5300.

36. Lee CH, Park HB, Lee YM, and Lee RD. Industrial & Engineering Chemistry Research 2005;44(20):7617.
37. Lee M, Park JK, Lee H-S, Lane O, Moore RB, McGrath JE, and Baird DG. Polymer 2009;50(25):6129.

Chapter 7: Future Research

Common requirements critical to all high-performance polymer electrolyte membrane fuel cells (PEMFCs) include: (1) high proton conductivity; (2) low electronic conductivity; (3) low permeability to fuel and oxidants; (4) low water transport through diffusion and electro-osmosis; (5) oxidative and hydrolytic stabilities; (6) good mechanical properties both in the dry and hydrated states; (7) low cost; and (8) ability to be fabricated into membrane-electrode assemblies (MEA) [1].

Partially fluorinated hydrophobic-disulfonated hydrophilic multiblock copolymers have demonstrated excellent conductivity both in fully and partially hydrated states. The mechanical properties and water absorption have been significantly improved by annealing the polymer membranes above the T_g of partially fluorinated hydrophobic blocks. Further research in assessing the performance of partially fluorinated hydrophobic-disulfonated hydrophilic multiblock copolymer membranes as alternative PEMs is to evaluate the permeability to fuel and oxidants of the membranes, the fabrication of membranes into MEAs and the fuel cell operation performance. Some preliminary measurements of direct methanol fuel cell (DMFC) operation performance of 6FPAEB-BPSH100 were conducted in Los Alamos National Lab (LANL) in conjunction with Dr. Kim, as shown in Figure 7.1. Both 6FPAEB-BPSH100 7k-7k and 15k-15k copolymers show significant improvement compared to Nafion® 117 in DMFC operation. The DMFC operation performance of 6FPAEB-BPSH100 7k-7k shows a slight improvement over that of 15k-15k, which is probably due to the thinner 7k-7k membrane. To investigate the influence of block length on the DMFC operation performance, a film continuous casting device would be applied to control the uniform thickness of

6FPAEB-BPSH100 membranes with various block lengths. Across the entire range of operation power densities, the high frequency resistances (HFR) of both copolymers are much lower than that of Nafion®, which indicates the 6FPAEB-BPSH100 series multiblock copolymers show better compatibility with Nafion-bonded electrodes even than Nafion® 117 itself.

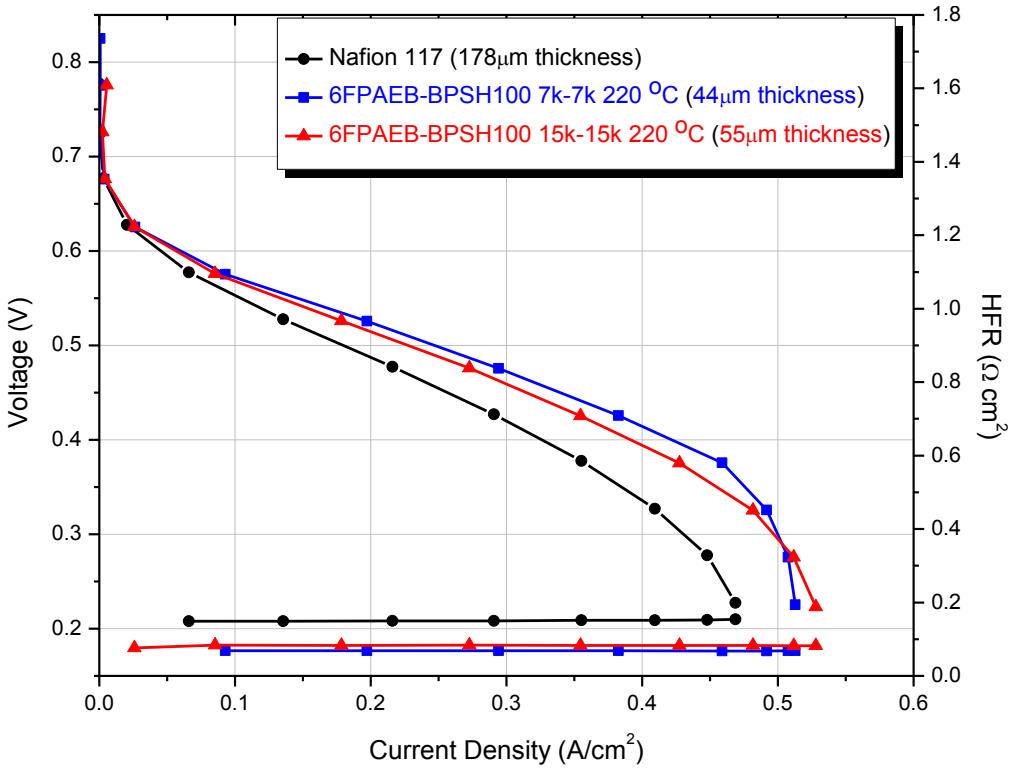

Figure 7. 1. Voltage vs. current density curves of 6FPAEB-BPSH100 7k-7k, 15k-15k and Nafion® 117; anode: PtRu black (6.9 mg/cm^2), cathode: Pt black (5.4 mg/cm^2), MeOH 0.5M, cell temperature 80^{o}C

Table 7.1 shows the methanol permeability of both 6FPAEB-BPSH100 7k-7k and 15k-15k membranes are much lower than that of Nafion® 117. The methanol permeability of 6FPAEB-BPSH100 15k-15k membrane is slightly higher than that of

7k-7k, because of the larger hydrophilic domains in 15k-15k membrane. Although the methanol limiting current of Nafion® 117 is lower than those of 6FPAEB-BPSH100 7k-7k and 15k-15k, considering the much higher thickness of Nafion® 117, 6FPAEB-BPSH100 series multiblock copolymer membranes actually outperform Nafion® 117 in methanol crossover.

Table 7. 1. Some membrane properties of 6FPAEB-BPSH100 and Nafion® 117

Polymer	Membrane thickness (μm)	Methanol limiting current (mA/cm^2)	Methanol permeability (cm^2/S)
Nafion® 117	178	72	4.61×10^{-6}
6FPAEB-BPSH100 7k-7k	44	110	1.54×10^{-6}
6FPAEB-BPSH100 15k-15k	55	90	1.82×10^{-6}

Disulfonated poly(arylene ether sulfone) random copolymers BPSxx, where xx represents the degree of sulfonation (DS), have been shown to have high chlorine tolerance across a broad pH range (4-10). Salt rejection and water permeability for BPSxx membrane were correlated with DS. High DS BPSxx copolymer (BPS40) displayed higher fluxes and lower salt rejection than copolymers with lower DS (BPS20) [2]. However, water flux and salt rejection were also influenced by the chemical structure of the copolymer and whether the copolymer was in salt or acid form.

Sulfonated aromatic multiblock copolymers nanophase separated into co-continuous hydrophilic and hydrophobic phases [3]. This hydrophilic ionic block could provide high water flux while the hydrophobic block supplies mechanical stability to the system,

which could be advantageous in the applications as reverse osmosis (RO) membrane. Some preliminary measurements of RO membrane operation performance of 6FBPS0-BPSH100 13k-13k were conducted in UT-Austin in conjunction with Professor Freeman, as shown in Table 7.2.

Table 7. 2. Reverse osmosis membrane properties of 6FBPS0-BPS100

	Unit	**13k-13k, 120 ^{o}C[a]**	**13k-13k, 210 ^{o}C[b]**
Pure water permeability	[L μm/ (m^2 h bar)]	0.722	0.591
NaCl rejection	[%]	95.0	96.0
Water permeability at 1 μm film	[m/(sPa)]	2.06×10^{-12}	1.69×10^{-12}
Salt permeability at 1 μm film	[m/s]	2.88×10^{-7}	1.91×10^{-7}
Ion exchange capacity	[meqv./g]	1.5	1.5
Water uptake	[wt.%]	24.6	17.9

[a]Dried under IR lamp at 50-60 ^{o}C for 24 h then vacuum dried at 120 ^{o}C for 24h
[b]Dried under IR lamp at 50-60 ^{o}C for 24 h then vacuum annealed at 210 ^{o}C for 24h

After annealing at 210 ^{o}C for 24h, 6FBPS0-BPS100 13k-13k multiblock copolymer membrane displayed an improvement in salt rejection but a decrease in water permeability. Salt rejection and water permeability can be altered by changing the block length or the IEC of 6FBPS0-BPS100 multiblock copolymers.

References*:*

1. Hickner MA, Ghassemi H, Kim YS, Einsla BR, and McGrath JE. Chem. Rev. 2004;104(10):4587.
2. Park HB, Freeman BD, Zhang Z-B, Sankir M, and McGrath JE. Angew. Chem. 2008;120(32):6108.
3. Badami AS, Roy A, Lee H-S, Li Y, and McGrath JE. J. Membr. Sci. 2009;328(1-2):156.